The novel role of the neuropeptides Orexin and QRFP and their involvement in Alzheimer's disease

A thesis submitted for the degree of Doctor of Philosophy
by

Julie Davies

Division of Biosciences

School of Health Science and Social Care

May 2014

Declaration

I hereby declare that the research presented in this thesis is my own work, except where otherwise specified, and has not been submitted for any other degree.

Julie Davies

Abstract

Alzheimer's disease (AD) is a neurodegenerative disease which affects over 500,000 people in the UK. Worldwide 44 million people are affected by AD and other dementias. Most cases occur over the age of 65 and is characterised by gradual and increasing loss of cognitive function and behavioural abnormalities. The main causes are a build-up of the toxic protein amyloid-β (Aβ) and hyperphosphorylation of the microtubule stabilising protein: tau, leading to neurofibrillary tangles (NFT). These two hallmarks of disease result in neuronal damage and cell death causing associated symptoms and eventually death.

Orexins (OX) are neuropeptides which function to regulate the sleep-wake cycle and feeding behaviour. They are produced from a prepro-orexin (PPO) molecule and cleaved into two isoforms: orexin-A (OXA) and orexin-B (OXB). OXA and OXB are the ligands for two G-protein coupled receptors (GPCR): orexin receptor 1 (OX1R) and orexin receptor 2 (OX2R). 50-80,000 OX producing neurons project to many areas of the brain including the lateral hypothalamus (LHA), locus coeruleus (LC), tuberomammillary nucleus (TMN), paraventricular nucleus (PVN) and raphe nuclei and from these areas regulate feeding and appetite and the sleep wake cycle through their receptors. QRFP is a newly discovered neuropeptide which exerts similar orexigenic activity including the control of feeding behaviour. It is the ligand for the GPCR GPR103, both of which are widely expressed in the brain and also in the retina, testes, thyroid, pituitary and prostate. GPR103 also shares 48 and 47% protein sequence homology with OX1R and OX2R respectively. It is in these tissues where it can exert other physiological functions including regulation of feeding, control of the gonadotropic axis and bone formation. The exact expression and signalling characteristics and physiological actions of QRFP/GPR103 are still poorly understood.

It is through the physiological functions of the orexigenic system and the clinical symptoms observed in AD which suggests a possible link between the two. For example, in AD one of the main reasons for institutionalisation is the severely dysregulated sleep pattern that is experienced by sufferers. They experience increased nocturnal activity and early awakenings as well as hypersomnia and excessive daytime sleepiness; all of which is beyond what someone of the same age

experiences. As well as this AD patients suffer from significant weight loss and a significant negative correlation has been identified between progression of disease and appetite. All of this points towards an involvement of the orexigenic system in AD. AD patients have been found to have a 40% loss of immunoreactive OX neurons and have severe reductions in circulating OXA. This led us to believe that the OX system is of vital importance in AD and could be targeted to ameliorate symptoms. Studies have implicated OX and OXR in memory processes, appetite regulation, and severe disturbances of the sleep-wake cycle all of which are phenotypes of AD. Given that they play a key role in energy homeostasis and physiological behaviour, we hypothesise that OXs and their receptors are implicated in the pathophysiology of AD. Therefore, in this study we will investigate the detailed expression and signalling characteristics of OXR and GPR103 *in vitro* and in clinical samples

In this study we neuronally differentiated two human neuroblastoma cell lines: IMR32 and SH-SY5Y. Neuronally acquired phenotype was confirmed through increased neurite length, increased expression of key neuronal proteins and increases in microtubule-associated protein tau (*MAPT*), neurogenin1 (*NG1*) and neuron-specific enolase *(NSE*) as well as a reduction in the neuronal marker of immaturity; nestin (*NES*). OXR and GPR103 were confirmed in both cell lines after differentiation at mRNA and protein level and were shown to be fully functional through phosphorylation of extracellular signal-regulated kinases 1/2 (ERK1/2). We also identified possible cross talk of GPR103 with the OXR though addition of selective OXR antagonists, which blocked QRFP induced ERK1/2 phosphorylation. We show for the first time that addition of $A\beta^{42}$ and zinc sulphate to mimic AD *in vitro,* results in a significant reduction of OX1R and GPR103 in the cell lines SH-SY5Y and we have performed the first comprehensive study in clinical AD patients which demonstrate a loss of *OX1R*, *OX2R* and *GPR103* at mRNA and protein level compared to age matched controls in the hippocampus. We performed microarray analysis which identified many genes and pathways regulated by the OXA, OXB and QRFP; including corticotropin-releasing hormone receptor (*CRHR1*), regulated in development and DNA damage responses 1 (*REDD1*), erythropoietin (*EPO*), Bcl-2-like protein 1 (*BCL2L11*), myb proto-oncogene protein (*c-myb*), vasoactive intestinal peptide (*VIP*), endothelin 1 (*EDN1*) as well as the nuclear factor kappa-light-chain-enhancer of activated B cells (NF-KB) and hypoxia-inducible factor-1α (HIF-1α)

pathways. These genes are all implicated in neuroprotection, particularly in AD. This represents the first comprehensive gene expression data in a neuroblastoma cell line for these orexigenic proteins.

Collectively these data suggest a potential role of the orexigenic system in neuroprotection and a functional loss of the receptors in AD patients which could confer a loss of neuroprotection through the orexigenic system. Pharmacological intervention directed at the orexigenic system may prove to be an attractive avenue towards the discovery of novel therapeutics for diseases such as AD and improving neuroprotective signalling pathways.

Acknowledgments

I would like to express my eternal gratitude to Dr. Manos Karteris; for his supervision, advice and guidance. Without his faith in me when I had none I would not have made it this far. Thank you for putting up with me!

I would also like to thank Dr. Amanda Harvey for giving me wonderful opportunities and guidance, Dr. Chris Eskiw for giving me the courage I needed to push through and Dr. Mat Themis for his constant and unrelenting help even when he had better things to do. Christine Newton and Alison Marriott have shown me infinite kindness and were always willing to go above and beyond to help. My colleagues and friends at Brunel are the people who understand all the difficulties and provided me with such emotional support and much laughter; Sara, Karly, Alpa, George, Sheba, Pickles, Helen, Amanda, Punam, Azadeh and even though she wasn't here physically she was most certainly here in spirit; Seda. Sara; thank you for always staying late with me and telling me to shut up when I was being ridiculous! Koarly; thanks for the vanilla coke and pictures of cats that always cheered me up to no end. I would like to say a special thank you to Phil and Chris, who before I even started this journey; had faith in me. Your kindness will not be forgotten.

To my family; words do not exist to describe my gratitude. You have supported me in every way. What you have all done for me extends far beyond what anyone could expect. I love you all so much from the bottom of my heart.

My wonderful sister Elise; you are the most beautiful human being I have ever met. Although you couldn't always understand, you tried your best to make me smile and forget my worries. You helped me in so many ways and you always, always believed in me. Elise, you always made things seem a little easier. To my wonderful parents Fran and Warren and my step parents Amanda and Peter. Firstly I would like to apologise for having been a 25 year old student. You believed in me and gave me so much love. You are the most supporting family anyone could wish for. I consider myself privileged to have you as my parents (and step parents!). My English Nan; Lynne, who was always ready to cook me dinner and fill me with caffeine and do her utmost to make me laugh. My French grandparents; Nadine and Lucien. Although you are so far away, you always felt so close and knowing that you were always thinking of me gave me a tremendous amount of hope and confidence that everything would be fine.

Finally I would like to thank my boyfriend Ed, thank you for your love and your patience and not getting angry with me when I lost the plot. And thank you for getting me all the animals! Even though they all bite me and run away from me, I love them very much. Well sometimes.

Table of Contents

List of Figures

List of Tables

List of abbreviations

ACE	Angiotensin-converting enzyme
dNTP	Deoxyribonucleotide
8-OHG	8-hydroxydeoxyguanosine
ACh	Acetylcholine
AChE1	Acetylcholinesterase
AD	Alzheimer's disease
ADAM10	A disintegrin and metalloproteinase domain-containing protein 10
AICD	APP intracellular cytoplasmic domain
ALX3	ALX homeobox 3
APLP1	Amyloid-like protein 1
APLP2	Amyloid precursor-like protein 2
APOE	Apolipoprotein E
APP	Amyloid precursor protein
APS	Ammonium persulfate
(A-T)	Adenine-Thymine
ATP	Adenosine triphosphate
Aβ	Amyloid-beta
BACE1	Beta-secretase 1
BAT	Brown adipose tissue
BBB	Blood–brain barrier
BIM	Bcl-2-like protein 11
BrdU	Bromodeoxyuridine
BRET	Bioluminescence resonance energy transfer
BTK	Bruton's tyrosine kinase
CA	Cornu ammonis
cAMP	Cyclic adenosine monophosphate
CB1	Cannabinoid receptor type 1
CCS	Copper chaperone for superoxide dismutase
cdk5	Cell division protein kinase 5
LOAD	Late-onset Alzheimer's disease
LRP1	Low density lipoprotein receptor-related protein 1
MAPK	Mitogen-activated protein kinase
MAPK14	Mitogen-activated protein kinase 14
MAPT	Microtubule-associated protein tau
MEF2C	Myocyte-specific enhancer factor 2C
MEK	Mitogen-activated protein kinase
MIQE	Minimum information for publication of quantitative real-time PCR experiments
MMP-2	Matrix metalloproteinase-2
MMP-9	Matrix metalloproteinase-9
mRNA	Messenger ribonucleic acid
mTOR	Mammalian target of rapamycin
MYCN	N-myc proto-oncogene protein
NADH	Nicotinamide adenine dinucleotide
NF-KB	Nuclear factor kappa-light-chain-enhancer of activated B cells
NCAM2	Neural cell adhesion molecule 2 precursor
NCOA7	Nuclear receptor coactivator 7
NES	Nestin
NG1	Neurogenin-1
NFT	Neurofibrillary tangle
NIK	NF-kappa-B-inducing kinase
NMDA	N-methyl-D-aspartate
NMDAR	N-methyl-D-aspartate receptor
NO	Nitric oxide
NPFF	Neuropeptide FF
NPY	Neuropeptide Y
NSE	Neuron-specific enolase
NTC	Non-template control
OD	Optical densitometry

cKO	Conditional knock out	**OX**	Orexin
cDNA	Complementary DNA	**OX1R**	Orexin receptor 1
ChAT	Choline acetyltransferase	**OX2R**	Orexin receptor 2
CHO	Chinese hamster ovary	**OXA**	Orexin A
CNS	Central nervous system	**OXB**	Orexin B
CO_2	Carbon dioxide	**PBS**	Phosphate buffered saline
CRE	Camp response elements	**PDGFR-β**	Platelet-derived growth factor receptor
CREB	Camp response element-binding protein	**PDGF-β**	Platelet-derived growth factor
CRH	Corticotropin-releasing hormone	**PEN-2**	Presenilin enhancer 2
CRHR1	Corticotropin-releasing hormone receptor	**p-ERK1/2**	Phosphorylated extracellular signal-regulated kinases
CSF	Cerebrospinal fluid	**PFA**	Paraformaldehyde
Ct	Cycle threshold	**PHF**	Paired helical filaments
CTF	C-terminal fragment	**PIP2**	Phosphatidylinositol 4,5-bisphosphate
DAB	3,3'-diaminobenzidine	**PKA**	Protein kinase A
DAG	Diacylglycerol	**PKC**	Protein kinase C
DAPI	4',6-diamidino-2-phenylindole	**PLC**	Phospholipase C
DG	Dentate gyrus	**PLP**	Pyridoxal phosphate
DMSO	Dimethyl sulfoxide	**POMC**	Pro-opiomelanocortin
DNA	Deoxyribonucleic acid	**PP2A**	Protein phosphatase 2
DPX	Di-N-butyle phthalate in xylene	**PPO**	Prepro-orexin
DTT	Dithiothreitol	**PrRP**	Prolactin-releasing peptide
EC	Entorhinal cortex	**PS1**	Presenilin 1
ECL	Enhanced chemiluminescence	**PS2**	Presenilin 2
EIF4A2	Eukaryotic initiation factor 4A-II	**RNA**	Ribonucleic acid
EMEM	Eagle's minimal essential medium	**PTGER1**	Prostaglandin E receptor 1
EPO	Erythropoietin	**PVN**	Paraventricular nucleus
EOAD	Early onset Alzheimer's disease	**qPCR**	Quantitative real-time polymerase chain rection
EOFAD	Early-onset familial Alzheimer's disease	**RA**	Retinoic acid
ER	Endoplasmic reticulum	**RAGE**	Receptor for advanced glycation end products
ERK	Extracellular signal-regulated kinases	**RASGRP1**	RAS guanyl-releasing protein 1
FBS	Fetal bovine serum	**REM**	Rapid eye movement
FGFR4	Fibroblast growth factor receptor 4	**RIN**	RNA integrity number
FITC	Fluorescein isothiocyanate	**ROS**	Reactive oxygen species

FSH	Follicle-stimulating hormone	**RPM**	Revolutions per minute
FTD	Frontotemporal dementia	**RQ**	Relative quantity
GAP	Gtpase-activating protein	**SAPK/JNK**	Stress-activated protein kinase/c-Jun kinase
GAPDH	Glyceraldehyde 3-phosphate dehydrogenase	**SB**	SB-334867
GC	Guanine-cytosine	**SDHA**	Succinate dehydrogenase complex
GDP	Guanosine diphosphate	**SDS-PAGE**	Sodium dodecyl sulfate polyacrylamide gel electrophoresis
GEF	Guanine nucleotide exchange factor	**siRNA**	Small interfering RNA
GHSR	Growth hormone secretagogue receptor	**SIRT1**	Sirtuin 1
GIRK	G protein-coupled inwardly-rectifying potassium channel	**SNP**	Single-nucleotide polymorphism
GNG13	Guanine nucleotide-binding protein subunit gamma-13	**SUB**	Subiculum
GnRH	Gonadotropin-releasing hormone	**SYK**	Spleen tyrosine kinase
GO	Gene ontology	**TACE**	ADAM metallopeptidase domain 17
GPCR	G protein-coupled receptors	**TBE**	Tris/borate/edta
G-protein	Guanosine nucleotide-binding protein	**TCS**	TCS OX229
GRIN1	Glutamate [NMDA] receptor subunit zeta-1	**TEMED**	Tetramethylethylenediamine
GSK-3β	Glycogen synthase kinase 3	**t-ERK1/2**	Total extracellular signal-regulated kinases
GTP	Guanosine triphosphate	**Tm**	Melting temperature
GWAS	Genome-wide association study	**TMD**	Transmembrane domain
ddH2O	Double-distilled water	**TMN**	Tuberomamillary nucleus
HEK	Human embryonic kidney	**TNFAIP3**	Tumour necrosis factor alpha-induced protein 3
IDE	Insulin-degrading enzyme	**TNF-α**	Tumour necrosis factor alpha-induced protein 3
IGF-1	Insulin-like growth factor 1	**TRITC**	Tetramethylrhodamine
IHC	Immunohistochemistry	**TrkB**	Tyrosine kinase receptor
IL-1β	Interleukin-1 beta	**TSC1**	Tuberous sclerosis 1
IMS	Industrial methylated spirit	**VDCC**	Voltage-dependent calcium channels
IP3	Inositol trisphosphate	**VGCC**	Voltage-gated calcium channel
IP3R	Inositol trisphosphate receptor	**VIP**	Vasoactive intestinal peptide
ISF	Interstitial fluid	**VMH**	Ventromedial hypothalamus
kbp	Kilo-base pair	**VTA**	Ventral tegmental area
KEGG	Kyoto encyclopedia of genes and genomes	**ZF**	Zona fasciculata
KO	Knock out	**ZG**	Zona glomerulosa
LC	Locus coeruleus	**ZR**	Zona reticularis

LHA	Lateral hypothalamic area	**α7nAChR**	Alpha-7 nicotinic acetylcholine receptor

1

Chapter 1

General introduction

1.1 History of Alzheimer's disease

In 1901 Alois Alzheimer identified a patient Auguste Deter as having abnormal behavioural symptoms including; short-term memory loss, delusions, disorientation and disruptive behaviour (Ramirez-Bermudez 2012). Auguste died in 1906 and Alois identified amyloid β (Aβ) plaques and neurofibrillary tangles (NFT) in her brain and presented these findings later that year and termed the disease presenile dementia. In 1910 the disease was reclassified as Alzheimer's disease (AD) after the clinician who first identified and described the disease (Zilka, Novak 2006).

1.2 Clinical and pathological features

1.2.1 Epidemiology

Currently over 800,000 people in the UK suffer from dementia with more than 60% of these cases attributable to AD and 44 million people are affected worldwide (Alzheimer's Disease International). Two thirds of those afflicted with AD are female and it results in 60,000 deaths in the UK each year (Alzheimer's Disease International). Most cases of AD are sporadic and occur after the age of 65, however some occur at a much younger age of between 30-65 and can be familial. These patients have the same presentation, however familial AD has an earlier onset with symptoms and pathology which can be more severe (Bird 1993, Bird 2008).

1.2.2 Pathology

Diagnosis of the disease is dependent upon a neuropathological assessment. It is generally harder to diagnose a living patient; however upon death autopsy examination

allows the gold standard of AD diagnosis. Diagnosis includes observing clinical indicators, cerebral cortical atrophy, microscopy of Aβ plaques and NFTs. Death of a patient with AD is usually as a result of exhaustion, malnutrition or pneumonia, with duration of disease ranging from 1-25 years but averaging 8-10 years (Bird 2008).

AD is characterized by gradual and increasing loss of cognitive function accompanied by behavioural abnormalities. Symptoms include progressive memory loss, personality changes, confusion, loss of language skills and motor ability, severe sleep disturbances, depression, delusions, hallucinations, aggressive behaviour, weight loss, impaired judgment and orientation and death (Blennow, de Leon & Zetterberg 2006). These symptoms correlate with the specific areas of brain degeneration and as the disease progresses so too does neurodegeneration and consequently symptoms. Post-mortem (PM) studies of AD brains show synaptic and neuronal loss, oxidative damage, active inflammatory cells, amyloid plaques, NFT accumulation and synaptic degeneration (Medeiros, Baglietto-Vargas & Laferla 2010).

The two components; amyloid plaques and NFTs, are the primary characteristics of the disease. Aβ is a physiologically normal protein which under non-diseased circumstances works to control synaptic plasticity and performs a variety of other functions (Pearson, Peers 2006; Lesne et al. 2005). In a disease situation Aβ processing results in an extra two amino acids which culminates in depositions known as amyloid plaques and eventually neuronal cell death (Carrillo-Mora, Luna & Colin-Barenque 2014). NFTs are comprised mainly of the microtubule associated tau protein which becomes hyperphosphorylated. Phosphorylation of this protein results in inadequate binding of tau to microtubules, thus causing microtubule destabilisation and having detrimental ramifications for cellular transport and neuronal viability (Gendreau, Hall 2013; Sisodia 1999).

1.3 Genetics of AD

1.3.1 Early onset AD (EOAD)

The genetic background of AD is heterogeneous and complex. AD is generally divided into 2 categories, one with an onset below 65 years of age: early onset AD (EOAD) and

one with an onset after 65 years: late onset AD (LOAD) (Borovecki et al. 2010). Of the 5-10% of AD cases which are EOAD, about 60% of these have multiple cases within their families and of these 13% are inherited by way of an autosomal dominant trait which affects at least 3 generations; however some cases of EOAD without any family history have been reported. Inherited instances of AD are known as early onset familial AD (EOFAD) (Bagyinszky et al. 2014; Brickell et al. 2006). Those afflicted have Mendelian transmission and it is attributable to 3 possible gene mutations, all involved in the production of Aβ. Mutations affect either the amyloid precursor protein (*APP*) gene found on chromosome 21q21.3, the presenilin 1 (*PSEN1*) gene on chromosome 14q24.3 or the presenilin 2 (*PSEN2*) gene on chromosome 1q31-42 (Sisodia 2007). Mutations in the *APP* gene contributes to 10-15% of EOFAD cases, *PSEN2* gene mutations account for less than 5% of cases and *PSEN1* for 70-80% of cases. Mutations in these genes result in aberrant production of Aβ leading to dementia (Table 1.1) (Bird 1993; Cruts, Theuns & Van Broeckhoven 2012).

Gene (Protein)	Chromosomal location	Mode of inheritance	Relevance to AD pathogenesis
APP (Aβ precursor protein)	21q21.3	Autosomal dominant	Increase in Aβ ($Aβ^{42}$/ $Aβ^{40}$ ratio); mutations close to γ-secretase site
PSEN1 (presenilin 1)	14q24.3	Autosomal dominant	Increase in Aβ ($Aβ^{42}$/ $Aβ^{40}$ratio); essential for γ-secretase activity
PSEN2 (presenilin 2)	1q31-42	Autosomal dominant	Increase in Aβ (Aβ42/ $Aβ^{40}$ratio); essential for γ-secretase activity (?)
APOE (apolipoprotein E, E4-allele)	19q13.32	Complex (risk increases)	Increase in Aβ aggregation; decreased Aβ clearance (?); involved in γ-secretase activity (?)

Table 1.1: Overview of the candidate AD genes and their relevance to pathogenesis. Adapted from: (Sisodia 2007)

1.3.2 Late onset AD (LOAD)

The most prominent genetic risk factor for sporadic AD is the apolipoprotein E (*ApoE4*) allele. There are 3 isoforms of this allele: *ApoE2*, *ApoE3* and *ApoE4*. Circa 20-25% of the population have one or two *E4* alleles, however approximately 50-65% of those with AD have at least one *ApoE4* allele (Meyer et al. 1998; Blacker et al. 1997). Those who are *ApoE4* homozygous can develop AD up to 10 years earlier than those lacking the allele. On the other hand the much rarer *E2* allele seems to confer a protective effect (Strittmatter, Roses 1996). Nevertheless *E4* is an associated risk factor and not a cause; AD can still develop without this contributing factor being present.

1.4 APP and Aβ

1.4.1 APP

APP is a protein, whose gene in humans is located on chromosome 21 and consists of 18 exons spanning circa 300 kilo-base pair (kbp) (Bergsdorf et al. 2000). The APP family comprises of three homologues in vertebrates: *APP*, APP-like protein 1(*APLP1*) and APP-like protein 2 (*APLP2*) (De Strooper, Annaert 2000). All three of these genes encode type 1 membrane proteins which pass once through the membrane, with their N-terminus exposed to extracellular space, a large extracellular domain and short cytoplasmic regions all undergoing similar processing. However only *APP* contains the sequence for the Aβ protein (Sisodia 2007; Tharp, Sarkar 2013). APP is expressed in neuronal cells and extra neuronal tissues, depending on the isoform of APP (Nalivaeva, Turner 2013). APP is a membrane glycoprotein and alternative splicing of the messenger ribonucleic acid (mRNA) is known to give rise to three major isoforms encoding proteins of 695, 751 and 770 amino acids (Lamb et al. 1993). The 695 isoform is the predominant variant in the neurons and is the isoform which contributes to Aβ generation (Gralle, Ferreira 2007). APP^{751} and APP^{770} unlike APP^{695} contain exon 7 which encodes a serine protease inhibitor or Kunitz protease inhibitor. Only small amounts of these isoforms are expressed in the brain and APP^{751} is the predominant APP isoform elsewhere. Aβ is encoded by exons 16 and 17 of the *APP* gene and can potentially be generated by any of these isoforms (Figure 1.1) (Ling, Morgan &

Kalsheker 2003). In the human brain the ratio of *APP* mRNA is approximately $APP^{770}/APP^{751}/APP^{695}$ = 1:10:20 (Nalivaeva, Turner 2013).

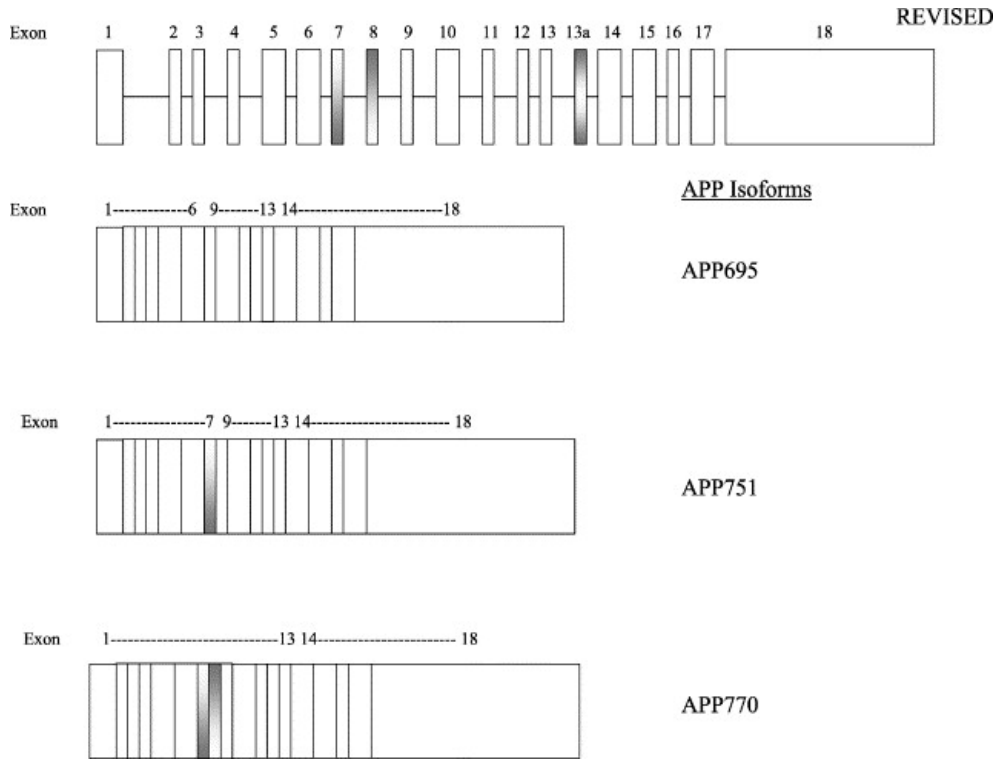

Figure 1.1: APP and its three main isoforms. Human APP has 18 exons and alternative splicing gives rise to three isoforms. Aβ is comprised of exons 16 and 17 (Ling, Morgan & Kalsheker 2003).

Full length APP undergoes proteolytic cleavage by either an amyloidogenic or non-amyloidogenic pathway, depending on the secretase activity. α-secretase cleaves APP through the non-amyloidogenic pathway and β-secretase through the amyloidogenic pathway (Nalivaeva, Turner 2013). These secretases cleave the protein within the luminal domain, causing a large part of the ectodomain to be removed and thus generates membrane bound α or β, C terminal fragments (CTF). The main neuronal β-secretase is a transmembrane aspartyl protease known as BACE1. This cleaves APP

within its ectodomain, leading to the N-terminus of Aβ. This creates a 99 amino acid CTF and cleavage by the γ-secretase leads to generation of a 50 amino acid cytoplasmic polypeptide known as APP intracellular domain (AICD) (Sisodia 2007; Edbauer et al. 2003). The non-amyloidogenic pathway accounts for 90% of APP processing and APP is cleaved within the Aβ region (at Lys16-Leu17) and not only does α-secretase stop the formation of the amyloidogenic protein but the large ectodomain released from APP has been shown to have a neuroprotective and memory enhancing function (Furukawa et al., 1996; Nalivaeva, Turner 2013; Allinson et al. 2003). α-secretases include tumour necrosis factor-α-converting enzyme (TACE) and a disintegrin and metalloproteinase domain-containing protein 10 (ADAM10) as well as other metalloproteases (Caescu, Jeschke & Turk 2009). Once the N terminal of the protein has been generated through α or β secretase activity, the remaining part of APP can now be cleaved. This is brought about by an intramembranous cleavage of α or β CTFs by γ-secretase activity, which liberates the p3 (3kDa) protein from the α CTF and Aβ (4kDa) is released into the extracellular space from the β CTF (Sisodia 2007; Edbauer et al. 2003).

γ-secretase is composed of presenilin 1 and 2 (PS1 and PS2) nicastrin, anterior pharynx defective 1 (APH-1) and presenilin enhancer 2 (PEN2) proteins. PS are the catalytic subunits of the secretase, with a pair of conserved aspartic acid residues in the 6^{th} and 7^{th} transmembrane domains being crucial for functionality. APH-1 and PEN2 stabilise the complex and nicastrin recruits APP CTFs to the secretase site (Figure 1.2) (Kawasumi et al. 2004; LaFerla 2002; Edbauer et al. 2003). The major catalytic sites of γ-secretase activity in Aβ are at amino acid positions 40 and 42, and thus can result in the production of two forms of Aβ. More than 90% of Aβ cleavage results in $Aβ^{40}$ and $Aβ^{42}$ accounts for less than 10%. Mutations of APP near the γ-secretase site result in a favourable cleavage at the 42^{nd} position rather than the 40^{th}, increasing the ratio of $Aβ^{42}$. This $Aβ^{42}$ protein forms aggregates in the brain and contributes to amyloid plaques associated with AD (Sisodia 2007).

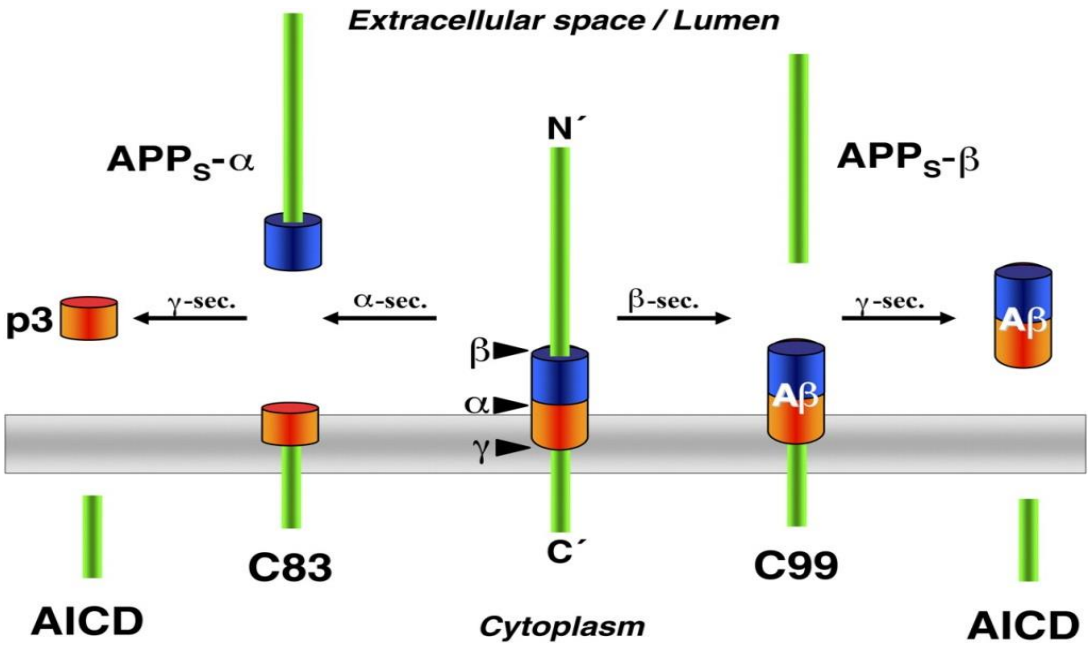

Figure 1.2: Cleavage of APP to generate Aβ. In non-amyloidogenic splicing, APPs extracellular domain is cleaved near to the transmembrane domain by an α-secretase, which is released into the extracellular space. The remaining part of the protein (c38) is cleaved by γ-secretase to form the peptide p3. In amyloidogenic processing, the APP is cleaved by a β-secretase, creating β-APP (C99). Cleavage by γ-secretase creates either a 40 or 42 amino acid form. The 42 amino acid form is the main constituent of amyloid plaques (Kaether, Haass 2004).

1.4.2 Normal physiological role of Aβ

Although Aβ is implicated in disease it also exhibits normal physiological functions, although its exact role is still unclear. In rodent and human neuronal cell cultures inhibition of γ- or β-secretase as well as inhibition of Aβ with an antibody lead to neuronal toxicity and cell death, however introduction of Aβ restored cell viability suggesting a vital role of Aβ in maintaining neuronal viability (Plant et al. 2003). Aβ production increases with increased communication between neurons and interestingly the areas which have the highest metabolic activity within the brain are the most susceptible to Aβ accumulation in AD, increased Aβ then depresses excitatory synapses and leads to a reduction in neuronal activity (Cirrito et al. 2008; Ting et al. 2007). This neuronal activity dependent modulation of Aβ could function as a negative feedback mechanism to prevent over-activity of neurons and be beneficial in a non-diseased state

(Kamenetz et al. 2003). Aβ has also been implicated in memory formation and synaptic plasticity (Senechal, Larmet & Dev 2006; Doyle et al. 1990; Huber et al. 1993). In rats, Aβ antibodies injected before a learning exercise, severely disrupted memory formation and treatment with Aβ after learning exercises significantly enhanced retention of memories, suggesting an important role of Aβ in memory formation (Garcia-Osta, Alberini 2009). In TgAPP mice, which over expresses APP there is enhanced plasticity compared to non-transgenic mice and in rat hippocampal slices APP was shown to modulate neuronal plasticity (Ma et al. 2007; Ishida et al. 1997). Hence Aβ may play a vital role in memory formation and neuroplasticity.

1.4.3 Aβ in AD and the amyloid cascade hypothesis

AD is complex and involves many disease mechanisms and there is no consensus on what the originating factor is. There are three main hypotheses as to what initiates AD: the amyloid cascade hypothesis, the tau hypothesis and the cholinergic hypothesis (Mudher, Lovestone 2002; Francis et al. 1999). The amyloid cascade hypothesis is popular due to mutations in the *APP*, *PS1* and *PS2* genes leading to EOFAD (Sisodia 2007). It is of note that in those with trisomy 21 by the age of 40 will all have developed AD neuropathology due to *APP*s location on chromosome 21 (Geller, Potter 1999). The amyloid cascade hypothesis postulates that it is the production of toxic Aβ which initiates AD and subsequently leads to NFTs and progression of AD (Mohandas, Rajmohan & Raghunath 2009; Mudher, Lovestone 2002). The mechanisms which lead to $A\beta^{42}$ being fibrillogenic and resulting in aggregation are not clear. It is thought it may be as a result of $A\beta^{42}$ having two extra amino acids: isoleucine and alanine, which make the protein more hydrophobic and transition from a monomeric form to β-sheets (Kim, Hecht 2006).

Aβ mediated neuronal toxicity is arbitrated by several mechanisms. It is a very potent mediator of oxidative stress damage. Receptor for advanced glycation end products (RAGE) is a member of the immunoglobulin superfamily of cell surface markers which binds advance glycation end products and is highly expressed in the hippocampus and cerebellum (Yan et al. 1996). Aβ can bind to RAGE which results in oxidative stress and subsequently apoptosis (Yan et al. 1996; Daffu et al. 2013). Aβ can also cause

neuronal damage through generation of free radicals and reactive oxygen species (ROS). Production of free radicals and ROS in the brain during AD is increased in humans and contributes to neurotoxicity, with antioxidants having been shown to protect against this toxicity (Manczak et al. 2010; Zandi et al. 2004; Smith et al. 2010; Sonnen et al. 2008). This is of particular importance because the brain is susceptible to oxidative damage due to a low glutathione content which is an antioxidant, high polyunsaturated fat content of neuronal membranes (which have a propensity to form free radicals and causes membrane disintegration) and the substantial requirement of oxygen for the brain (Christen 2000; Hazel, Williams 1990). Free radicals cause cell death and are capable of modifying deoxyribonucleic acid (DNA) and are thought to modify up to 10,000 bases every day (Christen 2000). Mitochondrial dysfunction may also play an important role in the pathology of AD. Aβ has been found to accumulate in mitochondrial membranes of AD patients, which can interact with mitochondrial matrix proteins causing dysfunction, fragmentation and decreased mitochondrial fusion leading to cell death as well as the mitochondria being particularly susceptible to ROS (Lustbader et al. 2004; Reddy, Beal 2008; Caspersen et al. 2005; Murphy 2009).

Aβ in the brain is regulated through a balance of production and clearance and chronic imbalance of this may propagate Aβ accumulation (Sommer 2002). An increase in Aβ production generally occurs in EOFAD where there are genetic mutations of the genes controlling Aβ production. However the majority of AD cases do not experience elevated Aβ production and AD may be as a result of inefficient clearance across the blood brain barrier (BBB) or selective processing of APP to form $A\beta^{42}$ (Sommer 2002; Deane, Zlokovic 2007). The low density lipoprotein receptor-related protein-1 (LRP1) is the main receptor thought to be responsible for Aβ clearance through the BBB (Cirrito et al. 2005; Qosa et al. 2012). Anti-LRP1 antibodies significantly inhibit Aβ clearance from the brain and rifampicin (which induces LRP1) drastically increases Aβ clearance (Qosa et al. 2012). Another mechanism for clearing Aβ from the brain is the production and turnover of cerebrospinal fluid (CSF) to transport it from the brain interstitial fluid (ISF) (Silverberg et al. 2003). However it is thought this only accounts for a small amount of Aβ clearing and that the majority is cleared through transport of the BBB by LRP1 (Shibata et al. 2000). There are several mechanisms thought to

contribute to Aβ degradation including neprilysin, insulin-degrading enzyme (IDE), matrix metalloproteinase 2 (MMP-2), matrix metalloproteinase 9 (MMP-9) and angiotensin-converting enzyme (ACE). Neprilysin is a zinc metallopeptidase located on neuronal cells (Nalivaeva et al. 2012). Neprilysin knock out (KO) mice were shown to have increased Aβ levels and a neprilysin inhibitor led to increased Aβ in mice and was shown to degrade not only monomeric forms of the protein but also the toxic oligomers (Iwata et al. 2000; Iwata et al. 2001; Kanemitsu, Tomiyama & Mori 2003). Neprilysin levels are also shown to decrease with age in the hippocampus and are markedly decreased in AD (Caccamo et al. 2005; Carpentier et al. 2002).

1.5 γ-Secretase and its components

γ-secretase is an intramembranous cleaving protease comprised of APH1, PEN2, nicastrin and PS1/2. This protease cleaves within the transmembrane domain (TMD) of over 100 transmembrane 1 proteins and is important in not only APP processing but also cleaves and releases the cytoplasmic domains of other transmembrane proteins (Haapasalo, Kovacs 2011; Kopan, Ilagan 2004). In APP, γ-secretase cleaves the transmembrane protein which results in the cytoplasmic intracellular domain and a secreted peptide (Takami et al. 2009).

1.5.1 Presenilin

The presenilin proteins were first discovered through the genetic linkage identified in AD. The genes *PSEN1* and *PSEN2* encode the presenilin proteins: PS1 and PS2 respectively. They are multi-pass transmembrane proteins that function as a part of the γ-secretase complex cleaving APP through the amyloidogenic pathway (Figure 1.3) (Parks, Curtis 2007). PS1 and PS2 share 62% homology and contain the active site of the γ-secretase, formed by 2 aspartic acid residues at TM6 and TM7 in the transmembrane domain. In PS1 they are D257 and D385 and for PS2: D263 and D366 (Walker et al. 2005).

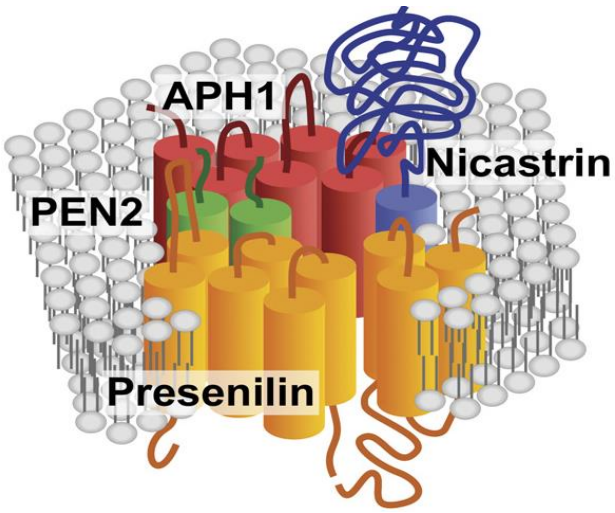

Figure 1.3: The γ-secretase complex. The core consists of 4 components: presenilin, nicastrin, APH1 and PEN2. Presenilin supplies the catalytic activity by encoding a nine-pass transmembrane aspartyl protease. All four components are needed for adequate γ-secretase activity. Although the contribution of the other components has not yet been fully elucidated, it is known that all parts are required for functioning of the complex (Parks, Curtis 2007).

Mutations in the presenilin genes as well as *APP* enhance Aβ production and contribute to AD development. The *PSEN1* gene which encodes the PS1 protein is located on chromosome 14q24.3 and the *PSEN2* gene which encodes the PS2 protein is found on chromosome 1q42.2. They each have 10 coding exons which have tissue specific alternative splicing (Tandon, Fraser 2002). Currently *PSEN1* has approximately 197 known mutations identified in EOFAD which may contribute to pathology and there are 31 identified mutations in the *PSEN2* gene (Cruts, Theuns & Van Broeckhoven 2012; Walker et al. 2005; Lessard, Wagner & Koo 2010). Mutations in *PSEN1* account for up to 80% of EOFAD cases (Cruts, Theuns & Van Broeckhoven 2012). The *PSEN1* gene encodes the 42-43kDa PS1 protein and is cleaved between 260-319 amino acids, which in 58% of identified EOFAD cases is where the mutation occurs (Thinakaran et al. 1996). In yeast which lacks endogenous γ-secretase; human γ-secretase was reconstituted and PS1 microsomes experience much higher activity than PS2 microsomes and this also occurs in a blastocyst derived cell line (Lai et al. 2003; Yagishita, Futai & Ishiura 2008). However not all of the PS1 expressed was active in

APP processing and in fact PS1 and PS2 both produce similar levels of Aβ (Yagishita, Futai & Ishiura 2008; Yonemura et al. 2011).

In mouse conditional knock out (cKO) models of *PSEN1* and *PSEN2* ($PS^{-/-}$), hippocampal learning and memory is severely disrupted and leads to a reduction in long term potentiation and N-methyl-D-aspartic acid (NMDAR) synaptic responses. These responses all occur before neuropathology becomes detectable. This demonstrates the importance of PS in synaptic plasticity (Saura et al. 2004). In AD Transgenic mice lacking the *PSEN1* gene there was an increase in α and β secretase cleaved CFTs generated by APP cleavage, with no change in the actual secretion of APP (De Strooper et al. 1998). This advocates that with no apparent increase in APP production and absence of PS1 α and β secretase processing of APP continues, however production of Aβ is limited due to malfunctioning γ-secretase activity. With mutated *PSEN1* there is a toxic gain of function and mutated PS leads to increased production of the amyloidogenic $A\beta^{42}$; often at the expense of the non-toxic $A\beta^{40}$ (Saura et al. 2004). Of the *PSEN1* mutations, many occur throughout the sequence and not necessarily in functional domains, which explains why there is partial loss of function rather than total loss, confirmed by the finding that $PS^{-/-}$ mice are not viable (De Strooper et al. 1998). $PS^{-/-}$ mice develop an age dependent synaptic, dendritic and neuronal degeneration including astrogliosis and hyperphosphorylation of tau showing that PS is indeed critical for neuronal endurance (De Strooper et al. 1998). The *PSEN1* KO mice cause a lethal phenotype, however *PSEN2* KOs cause no obvious aberrant phenotype and experience normal Aβ secretion suggesting it is PS1 that is essential for catalytic activity (Walker et al. 2005).

1.5.2 Other components of γ-secretase

All well as PS, γ-secretase is also comprised of nicastrin, PEN2 and APH1. Nicastrin is a protease which is not catalytically active, but is thought to be essential in recruitment of proteins into the γ-secretase complex and thus acts as a receptor for γ-secretase substrates (Shah et al. 2005). Nicastrin also maintains stability of the other proteins in the complex and in an embryonic fibroblast cell line small interfering RNA (siRNA) targeted against nicastrin resulted in a significant reduction of APH-1, PEN-2, and PS1,

suggesting an important role in nicastrin maintaining γ-secretase complex integrity (Zhang et al. 2005). A more novel role for nicastrin has been suggested in its regulation of neprilysin; the protein responsible for Aβ degradation. In a nicastrin deficient fibroblast cell line neprilysin mRNA expression and activity was significantly reduced and when cells were transfected with nicastrin the neprilysin activity was restored, suggesting that nicastrin is responsible for neprilysin stability and subsequent Aβ clearing (Pardossi-Piquard et al. 2006). PEN2 is a protein which forms one of the regulatory components of the γ-secretase complex. PEN2 down regulation by siRNA causes a reduction in *PSEN1* expression, impairs nicastrin maturation and consequently results in defunct γ-secretase formation (Luo et al. 2003). Its main function appears to be in γ-secretase stability and subsequent protein processing (Francis et al. 2002). APH1 also forms part of the γ-secretase complex and a transmembrane GXXXG motif in APH1 is essential for assembly and maturation of the whole γ-secretase complex (Hu, Fortini 2003).

1.6 Tau protein

Tau is a protein produced by the microtubule associated protein tau gene (*MAPT*) located on chromosome 17q21 (Medeiros, Baglietto-Vargas & Laferla 2010). Tau is highly soluble and exists as an unfolded protein. Its primary function is to associate with tubulin and encourage its congregation into microtubules in the axons, thus stabilising the structure and allowing axonal transport (Conde, Caceres 2009). Microtubules form part of the cytoskeleton and are linear filaments, comprised of α and β tubulin heterodimers (Desai, Mitchison 1997). One microtubule consists of 10-15 filaments that form a 24nm wide hollow cylinder (Conde, Caceres 2009; Tucker et al. 1985). Microtubules form bundles in axons and dendrites and are important for their growth and maintenance which provides structural integrity to these regions (Conde, Caceres 2009). Tau co-polymerises with microtubules through cycles of assembly and disassembly of microtubule bundles and this association increases microtubule rigidity in the axons (Felgner et al. 1997). In the neurons the microtubules provide structure for the axonal shaft and allow extension and elongation (Stiess, Bradke 2010). Tau is not thought to be essential for axonal stability as KO models in mice showed no major defects in brain morphology, however the microtubule density in axons was reduced

and it is thought that other microtubule stabilising proteins compensate for absence of tau (Harada et al. 1994). Several other mechanisms for tau have been identified, but they seem to play a much lesser role, including phosphorylated tau which can stabilise β-catenin (Medeiros, Baglietto-Vargas & Laferla 2010).

The tau gene is over 100kbp and has 16 exons. It has a guanine-cytosine (GC) rich 5' region, followed by a single untranslated exon. Upstream of this exon are many sequences which contain binding sites for transcription factors. Expression of tau is largely confined to neurons, with 6 isoforms of tau in the human adult brain as a result of differential splicing (Figure 1.4) (Avila et al. 2004; Ballatore, Lee & Trojanowski 2007).

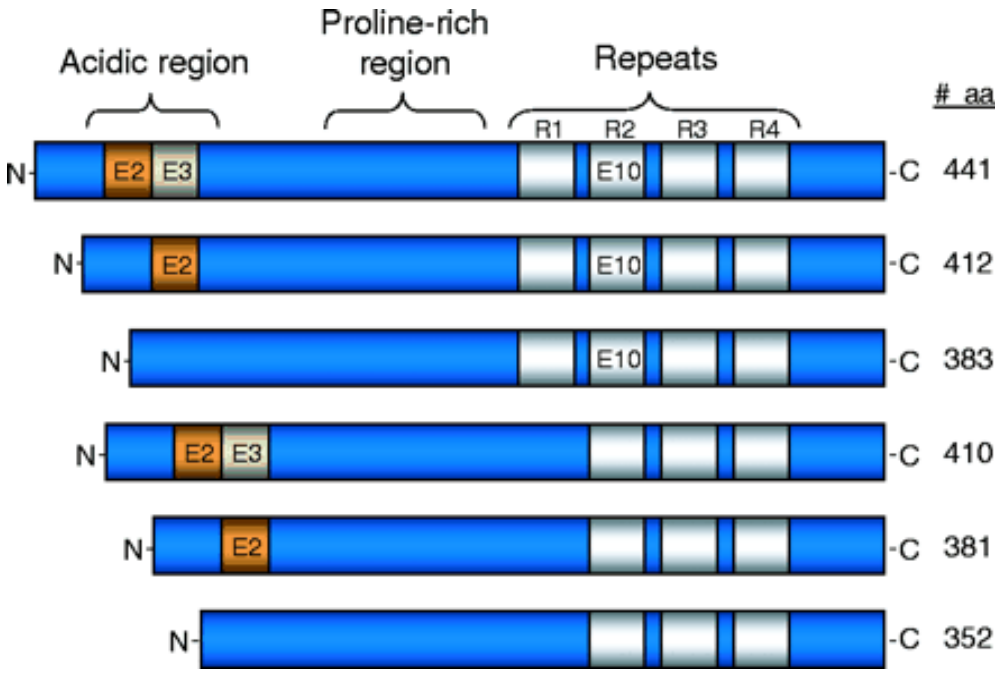

Figure 1.4: The six main isoforms of tau. The different isoforms are created through differential splicing of exons 2, 3 and 10. Exon 10 dictates whether tau will have a second microtubule binding repeat, allowing an extra microtubule binding domain. In the fetal brain only the 352 amino acid version is present. In AD the proline rich region becomes hyperphosphorylated (Johnson, Stoothoff 2004).

Tau can be divided into domains. Firstly 2 domains: one known as the projection domain containing the amino terminal and the other is known as the microtubule

binding domain containing the carboxyl terminal (Hirokawa, Shiomura & Okabe 1988). This projection domain can be further sub-divided into 2 regions: the amino terminal with many of the acidic residues and the proline rich region (Ballatore, Lee & Trojanowski 2007). The microtubule binding domain has 3 (R3) or 4 (R4) sequences of 31-32 amino acid residue repeats and the 6 isoforms differ in how many repeats they have and by the presence or absence of one or two 29 or 58 amino acid repeats in the N-terminal region (Ballatore, Lee & Trojanowski 2007; Kar et al. 2003; Gong, Iqbal 2008). The isoforms range from 352 to 441 amino acids and differ in these repeats as a result of differential splicing (Kolarova et al. 2012). These R3/R4 sequences have an 18 amino acid portion which contains the tubulin binding ability and the other 13/14 amino acid sequences allows binding to microtubules to promote assembly (Avila et al. 2004). In developing neurons, tau phosphorylation can influence its cellular distribution. When the proline rich region of tau is phosphorylated, it can be found mainly at the somatodendritic compartment, but when dephosphorylated it can be found in the distal part of the axon (Avila et al. 2004). In many instances phosphorylation of tau regulates its binding to microtubules or the membrane (Avila et al. 2004). The phosphorylation of tau at serine/threonine residues detaches it from microtubules and dephosphorylation of tau by phosphatases restores its affinity to bind to microtubules (Ballatore, Lee & Trojanowski 2007).

1.6.1 Tau in AD and the tau hypothesis

Another hypothesis for the initiation of AD is the tau hypothesis. This theory suggests that AD is initiated through hyperphosphorylated tau and subsequent aggregation of these proteins into NFTs which then leads to other AD associated pathologies including Aβ plaques (Mudher, Lovestone 2002). Support for this theory was strengthened due to NFTs occupying neurons and resulting in cell death and also due to NFT accumulation correlating with symptom progression, which was not seen with Aβ plaques (Nagy et al. 1995; Lace et al. 2009). However it has also been shown that circulating Aβ is elevated in early AD which does positively correlate with cognitive decline in early disease and this elevation occurred before any increases in tau pathology which suggests that tau pathology is not the initiating factor for AD (Naslund et al. 2000). The most compelling argument against the tau hypothesis is the discovery that mutations in *MAPT* in patients

with frontotemporal dementia (FTD) have tau pathology but no Aβ aggregation, whereas mutations in *APP* result in AD and tau pathology (Heutink 2000; Engler et al. 2008).

In normal tau, several serine and threonine residues are phosphorylated and in the normal brain tau has 2-3 moles of phosphate per mole of tau; however in the AD brain phosphate is 3 fold higher (Kopke et al. 1993). The phosphorylation state of tau is due to the regulation of the kinases and phosphatases that can act upon it. The main tau kinases and phosphatases include glycogen-synthase kinase-3β (GSK-3β), cyclin-dependent protein kinase 5 (cdk5), protein kinase A (PKA) and protein phosphatase 2 (PP2A) (Gong, Iqbal 2008; Kopke et al. 1993). The reasons for abnormal tau hyperphosphorylation in AD are not fully understood. PP2A has been shown to be reduced in expression and activity in AD resulting in an inability to correctly dephosphorylate tau (Liu et al. 2005; Gong et al. 1995; Gong et al. 1993). PP2A demonstrates broad substrate specificity and also dephosphorylates β-tubulin and β-catenin which are also shown to be hyperphosphorylated in AD and down-regulation of PP2A may have an important part to play in tau pathology in AD (Gong, Iqbal 2008; Vijayan et al. 2001).

In AD, the main pathology that arrives from tau dysfunction is NFTs. NFTs are comprised of hyperphosphorylated tau, which become misfolded and form aggregates (Figure 1.5). In AD there are over 40 potential hyperphosphorylation sites which have been shown to occur (Hanger et al. 2007). Tau in NFTs form paired helical filaments (PHF) and straight filaments (Armstrong 2009; Crowther 1991). PHF and straight filaments are comprised of tau, with PHF consisting of two strands twisted around each other and straight filaments not observing this contortion and accounting for only 5% of NFT composition (Crowther 1991; Friedhoff et al. 2000). All six of the tau isoforms have been reported to be present in PHF (Alonso et al. 2001). This loss of tau leads to microtubule instability and reduced axonal transport which may lead to neuronal damage (Brunden, Trojanowski & Lee 2009). Early tau deposits are pretangles and do not in fact exhibit the pleated β sheets that aggregates do and are therefore intermediate. These early pretangles may cause axonal defects, synapse loss and neuroinflammation (Ballatore, Lee & Trojanowski 2007). The loss of tau and NFT deposition leads to

disruption of the cytoskeleton and neurite extension, further leading to disturbance of axonal transport and synaptic dysfunction and thus neurodegeneration. Mice administered with paclitaxel (a microtubule stabilising protein) had reduced degeneration as a result of their tauopathies (Zhang et al. 2005). Due to the large area occupied by the tangles there may be physical disruption to surrounding cells which also affects axonal transport. Tangles may also appropriate other major proteins and aggravate the aggregates (Ballatore, Lee & Trojanowski 2007).

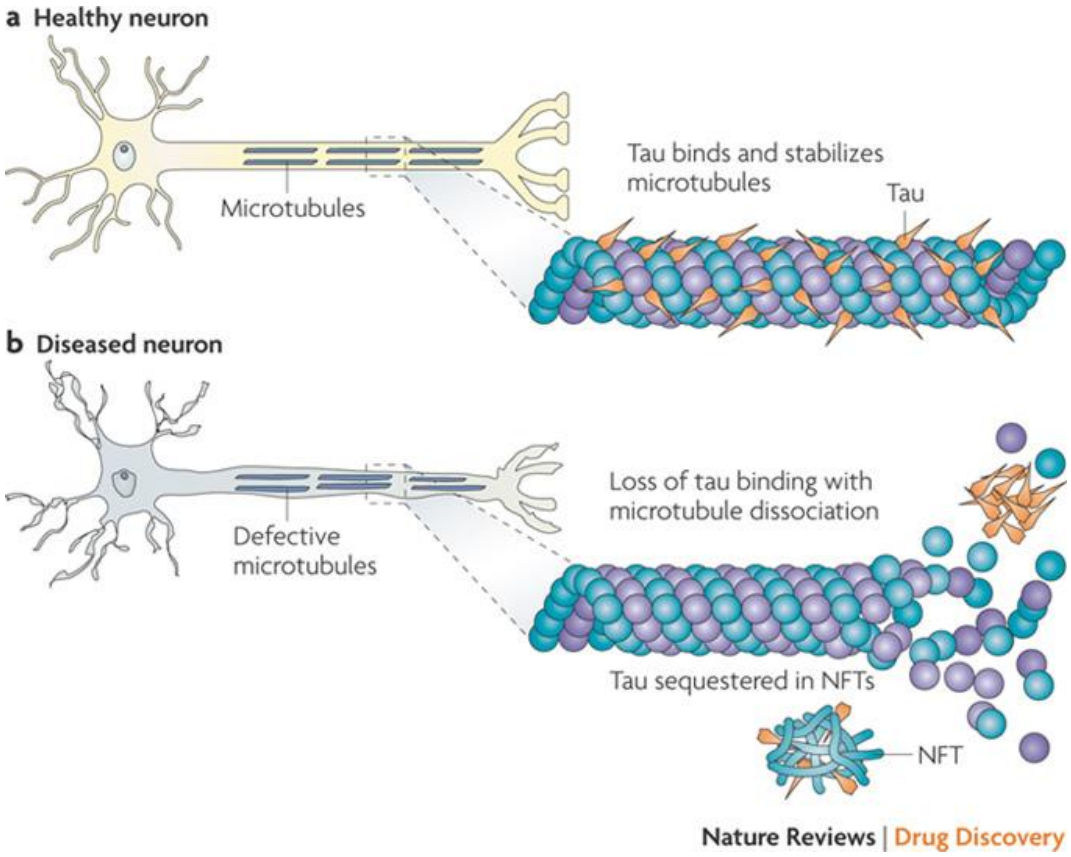

Figure 1.5: Tau hyperphosphorylation. A) Tau normally stabilises microtubules in neurons. B) In AD tau becomes hyperphosphorylated, which reduces binding of tau to microtubules and allows tau to be sequestered into NFTs. This reduction in tau leads to microtubule instability and reduced axonal transport (Brunden, Trojanowski & Lee 2009).

1.7 The cholinergic hypothesis

The cholinergic hypothesis is the third main theory of the origin of AD. It proposes that the degeneration of cholinergic neurons in the basal forebrain and subsequent reduction

in cholinergic signalling significantly contributes to degeneration of cognitive function observed in AD (Francis et al. 1999). The development of this theory was as a result of significant reductions in AD patients of choline acetyltransferase (ChAT); the enzyme responsible for the synthesis of the neurotransmitter acetylcholine (ACh) (Perry et al. 1977; Bowen et al. 1976). The discovery that in AD there was reduced ACh release and loss of cholinergic neurons further supported the idea that it is a loss of cholinergic activity which contributes to AD (Rylett, Ball & Colhoun 1983; Whitehouse et al. 1982). However this theory is perhaps the least popular of the three. Recent studies have found that in clinical trials using acetylcholinesterase inhibitors (AChEI), which prevent the breakdown of ACh, there is limited efficacy in treating AD with any observed effects being transient and patients still experienced cognitive decline over time as well as studies in rats showing that reductions in ACh do not contribute to memory deficits (Doody et al. 2001; Mohs et al. 2001; Winblad et al. 2001; Parent, Baxter 2004). However cholinergic loss is an early occurrence in AD and may not be causative but may affect the brains ability to compensate for an accrual of risk factors associated with increasing age (Geula et al. 2008; Craig, Hong & McDonald 2011).

1.8 GPCRs

GPCRs also known as seven-transmembrane domain receptors are the largest superfamily of membrane receptors. GPCRs include receptors for neuropeptides, chemokines and calcium ions as well as a plethora of other targets. GPCRs have been extensively studied and as such constitute around 50% of therapeutic drug targets even though only 10% of GPCRs are used as targets (Pierce, Premont & Lefkowitz 2002; Lundstrom 2009; Kroeze, Sheffler & Roth 2003).

1.8.1 GPCR structure

GPCRs exhibit seven hydrophobic transmembrane (TM) helices which are linked though intra and extracellular loops and are serpentine like. They are ordered as a cylinder with TM1 neighbouring TM7 and the complex is stabilised by hydrogen bonds. They possess an extracellular amino terminus and an intracellular carboxyl terminus. The most variable part of the GPCR is the carboxyl terminus, the intracellular loop spanning TM5 and TM6 and the amino terminus, all of which gives each GPCR

specificity (Kobilka 2007; Fredriksson et al. 2003). There are over 800 GPCRs classed into five groups: rhodopsin, adhesion, frizzled/taste, glutamate and secretin families (Fredriksson et al. 2003).

1.8.2 G protein cycle

GPCRs function through activation of a guanine nucleotide-binding protein (G-protein). G-proteins are heterotrimeric and comprised of α, β, and γ subunits. When the receptor is not active the Gα protein is bound to guanosine diphosphate (GDP) and upon receptor activation this GDP is substituted for a guanosine triphosphate (GTP) instigating dissociation of the G-protein from the GPCR. The Gα now has a low affinity for the Gβγ complex due to a conformational change and Gβγ is released and dissociates from the Gα subunit and downstream effects can now commence (Smrcka 2008; Wess 1997). Gα also exhibits guanosine triphosphatase (GTPase) activity and this acts to hydrolyse GTP to GDP to allow increased affinity of Gα to Gβγ and allow re-association of the whole G-protein complex (Figure 1.6) (Smrcka 2008; Wess 1997).

1.8.3 Types of G-protein

G-proteins are categorised into four main families according to the Gα protein: $G\alpha_s$ ($G\alpha_s$, $G\alpha_{olf}$), $G\alpha_i$ ($G\alpha_t$, $G\alpha_{i1}$, $G\alpha_{i2}$, $G\alpha_{i3}$, $G\alpha_{o1}$, $G\alpha_{o2}$, $G_{\alpha\zeta}$), $G\alpha_{q/11}$ ($G\alpha_q$, $G\alpha_{11}$, $G\alpha_{14}$, $G\alpha_{15}$, $G\alpha_{16}$), and $G\alpha_{12/13}$, ($G\alpha_{12}$, $G\alpha_{13}$). Each G-protein signals through a distinct pathway (Moreira 2014).

1.8.3.1 $G\alpha_s$

$G\alpha_s$ stimulates adenylyl cyclase (AC) which leads to the catalysis of adenosine triphosphate (ATP) to cyclic adenosine monophosphate (cAMP). cAMP can then phosphorylate and subsequently activate the cAMP dependent protein: protein kinase A (PKA) and other downstream effectors which then initiates a number of downstream effects (Pierce, Premont & Lefkowitz 2002).

1.8.3.2 $G\alpha_q$

$G\alpha_q$ subunits are capable of activating phospholipase C (PLC). Once active PLC can cleave phosphatidylinositol 4,5-bisphosphate (PIP2) into diacylglycerol (DAG) and

inositol 1,4,5-triphosphate (IP_3) (Jalili, Takeishi & Walsh 1999). As well as being a precursor for IP_3 and DAG, PIP2 also regulates ion channels, actin cytoskeleton remodelling and vesicle trafficking (Thapa, Anderson 2012). DAG can activate protein kinase C (PKC) which has many effects including contributing to cellular proliferation and differentiation and protein translocation to membranes (van Blitterswijk, Houssa 2000). IP_3 causes increases in intracellular calcium through binding to its receptors in the endoplasmic reticulum (ER) and allows intracellular calcium stores to be released which then facilitates activation of calcium channels in the plasma membrane leading to calcium influx (Neves, Ram & Iyengar 2002).

1.8.3.3 $G\alpha_i$

$G\alpha_i$ functions to inhibit AC and thus cAMP (Taussig, Iniguez-Lluhi & Gilman 1993). It can however also activate PLC through cross talk with $G\alpha_q$ which can lead to cellular regulation through the secondary messengers IP_3 and DAG (Jalili, Takeishi & Walsh 1999; Chan et al. 2000). $G\alpha_i$ is abundantly expressed in the brain and plays a particularly important role in activation of G protein-coupled inwardly-rectifying potassium channels (GIRK). These GIRKs allow potassium efflux causing membrane hyperpolarisation which results in neuronal excitation (Wettschureck, Offermanns 2005).

1.8.3.4 $G\alpha_{12/13}$

$G\alpha_{12/13}$ only contains two members: G_{12} and G_{13}. These proteins can activate guanine nucleotide exchange factors (GEF) which subsequently activate GTPases (Aittaleb, Boguth & Tesmer 2010). GEFs activate GTPases by facilitating the transfer of GDP to GTP. Receptors for ACh, serotonin, somatostatin and dopamine are known to couple to these G-proteins (Siehler 2009).

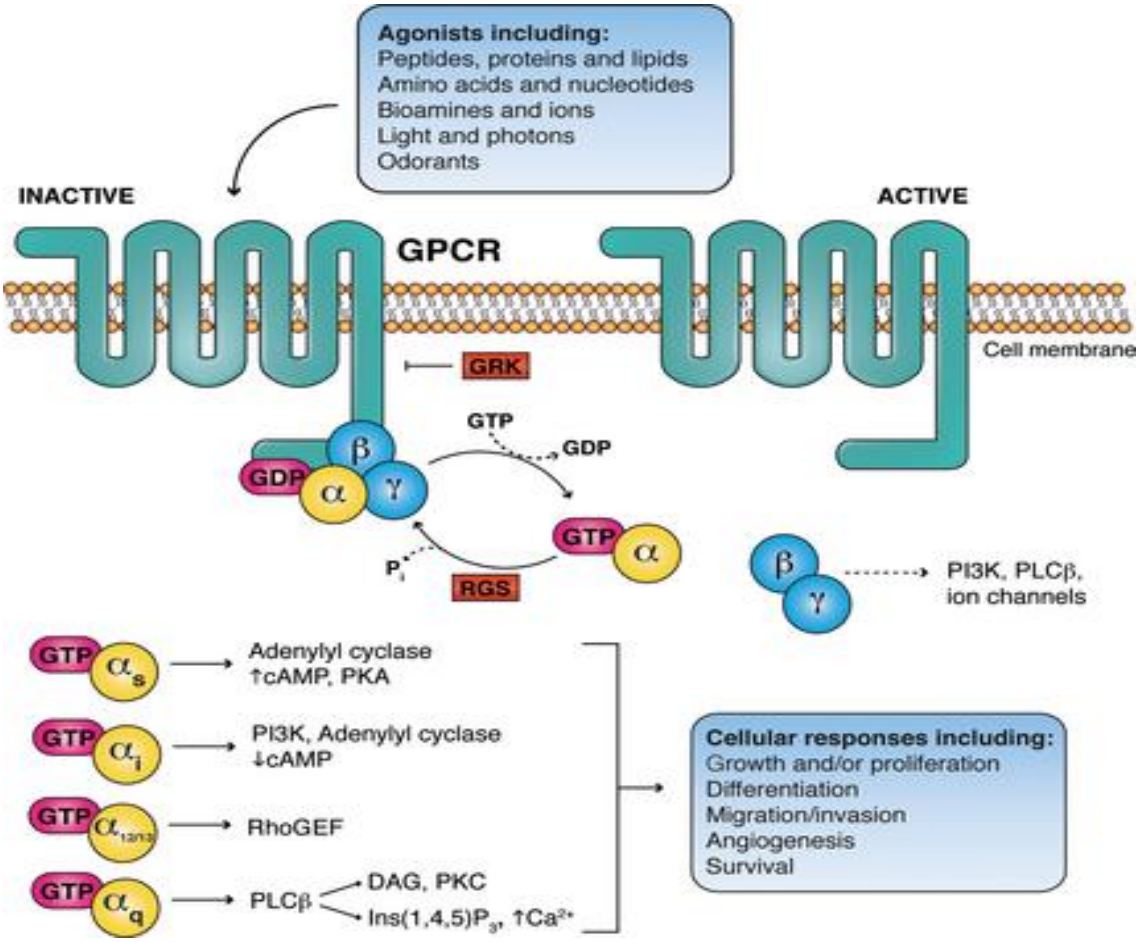

Figure 1.6: GPCR structure and cycle. Activation of GPCRs through agonists causes conformational change and allows the exchange of GDP for GTP in the Gα subunit. GTP binding causes dissociation of the G protein complex and GTP-bound Gα then interacts with downstream signalling effectors to activate secondary messengers deepening on the type of Gα subunit (George, Hannan & Thomas 2013).

1.9 Orexin

1.9.1. Prepro-orexin

Orexin (OX) or hypocretin are neuropeptides which function largely to regulate the sleep-wake cycle and feeding behaviour (Johren et al. 2001). OXs are produced from the cleavage of a 130 amino acid precursor protein also known as prepro-orexin (PPO) to form two distinct proteins from one precursor molecule. Initially the 33 amino acid N-terminal is cleaved, forming pro-orexin; this is then cleaved by prohormone

convertases giving rise to one molecule each of orexin-A (OXA) and orexin-B (OXB) (Figure 1.7) (Spinazzi et al. 2006). The first 33 amino acids of the sequence have the characteristics of a secretory signal; a hydrophobic core with residues attached to small polar side chains (von Heijne 1986; Sakurai et al. 1999). Ala33-Gln34 form the residues for cleavage to produce OXA. The Gln33 is possibly enzymatically cyclised into the N-terminal pyroglutamyl residue by transamidation (Sakurai et al. 1999). The last residue of OXA is followed by Gly67, which is believed to act as a donor for C-terminal amidation (von Heijne 1986). Subsequent to this donor site is a pair of basic residues Lys68-Arg69 which form a recognition site for prohormone convertases which cleave here to generate OXB and allow separation of the two proteins and Met96 is followed by Gly-Arg-Arg, constituting the C-terminal amidation of OXB (Sakurai et al. 1998). PPO shares 83% homology between rats and humans. It is located at chromosome 17q21 and contains two exons and one intron (Sakurai et al. 1998).

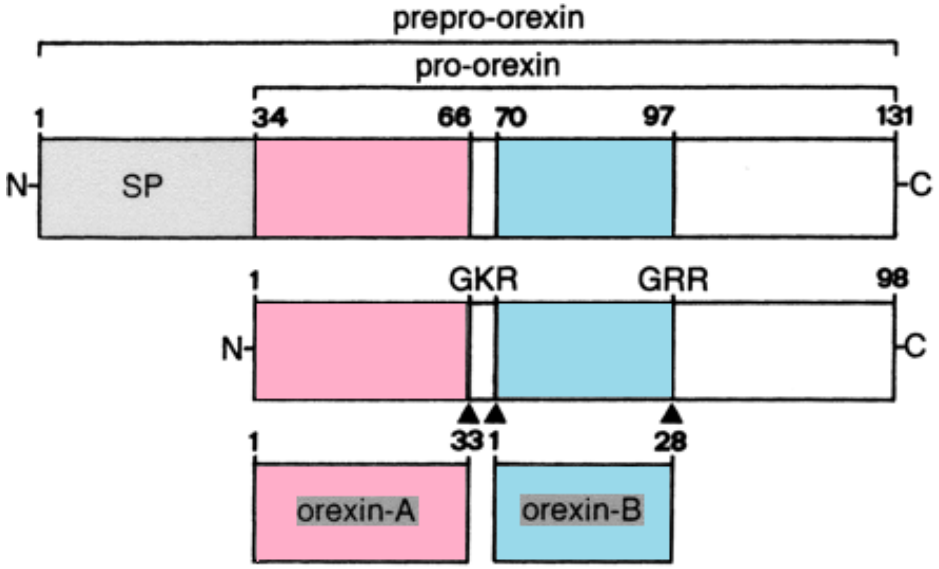

Figure 1.7: Prepro-orexin cleavage. First the signal peptide is cleaved, followed by cleavage by prohormone convertases at sites with basic amino acid residues to produce OXA (33 amino acids) and OXB (28 amino acids) (Spinazzi et al. 2006).

It is thought that due to its position at 17q21, the PPO gene may be involved in a group of diseases known as chromosome 17 linked dementia. This includes disinhibition-dementia-parkinsonism-amyotrophy complex which was mapped to position 17q21-22

(Wilhelmsen et al. 1994). People with this disease normally exhibit symptoms of behavioural disturbances, frontal lobe dementia and parkinsonism. Interestingly those afflicted by the disease exhibit increased feeding and crave and horde sweets; symptoms suggestive of OX involvement (Sakurai et al. 1998; Wilhelmsen et al. 1994). Because OXs mechanism of action is to regulate feeding behaviour and the sleep wake cycle; the expression of PPO is largely limited to the lateral hypothalamus (LHA), but has also been found to be expressed in the epididymis, penis and adrenal gland (Sakurai et al. 1998; Karteris, Chen & Randeva 2004; Peyron et al. 1998). However 50-80,000 orexin producing neurons project throughout the brain but are concentrated in areas such as the LHA, locus coeruleus (LC), tuberomammillary nucleus (TMN) and raphe nuclei and from these areas result in regulation of feeding, appetite and the sleep wake cycle (Sakurai 2007).

1.9.2 OXA and OXB

OXs were first discovered in 1998, simultaneously by Sakurai and deLecea (Sakurai et al. 1998; de Lecea et al. 1998). They were initially identified as neuropeptides which were similar to secretin and were isolated from a rat lateral hypothalamus using PCR subtraction cloning and identified as OXs or hypocretins (Sakurai et al. 1998; de Lecea et al. 1998; Ebrahim et al. 2002; Gautvik et al. 1996).

OXs as previously described are cleaved from PPO to yield the 33 amino acid OXA and 28 amino acid OXB. OXA is circa 3.5kDa and has a pyroglutamyl residue at the N-terminus and a C-terminal amidation (Spinazzi et al. 2006). The pyroglutamyl residue functions as a protective mechanism to prevent cleavage by aminopeptidases. There are two intrachain disulfide bridges between adjacent cysteines at positions 6 and 12 and also 7 and 14 (Lee et al. 1999). Its sequence is well persevered amongst mammals, with OXA being identical in humans, pigs, rats and mice (Spinazzi et al. 2006). OXB is roughly 2.9kDa with a C-terminal amidation and is highly preserved in mammals with only 2 amino acid substitutions at positions 2 and 18, causing it to differ in humans compared to pigs, rats and mice. OXB is linear peptide that possibly forms two alpha helices (Lee et al. 1999). The C-terminals of OXA and OXB are very similar (Figure 1.8) (Spinazzi et al. 2006). The two proteins show 46% primary structure homology,

which is not surprising considering one prepro-protein is cleaved to produce two molecules as opposed to differential splicing (Zawilska, Urbanska & Sokolowska 2013). The OXs are packaged into dense core vesicles and are thought to be synaptically released and function as neurotransmitters (de Lecea et al. 1998). OXA induces longer lasting effects than OXB and this is most likely due to the post translational modifications experienced by OXA including N-terminal pyroglutamyl cyclisation (Sakurai et al. 1998; Scammell, Winrow 2011). OXA has a markedly higher liposolubility than OXB which allows it to penetrate the BBB with greater ease by simple diffusion, giving it potential as a therapeutic target (Kastin, Akerstrom 1999). OXA was also shown to be much more stable in the blood than OXB, perhaps explaining the longer lasting effects of OXA as opposed to OXB (Kastin, Akerstrom 1999).

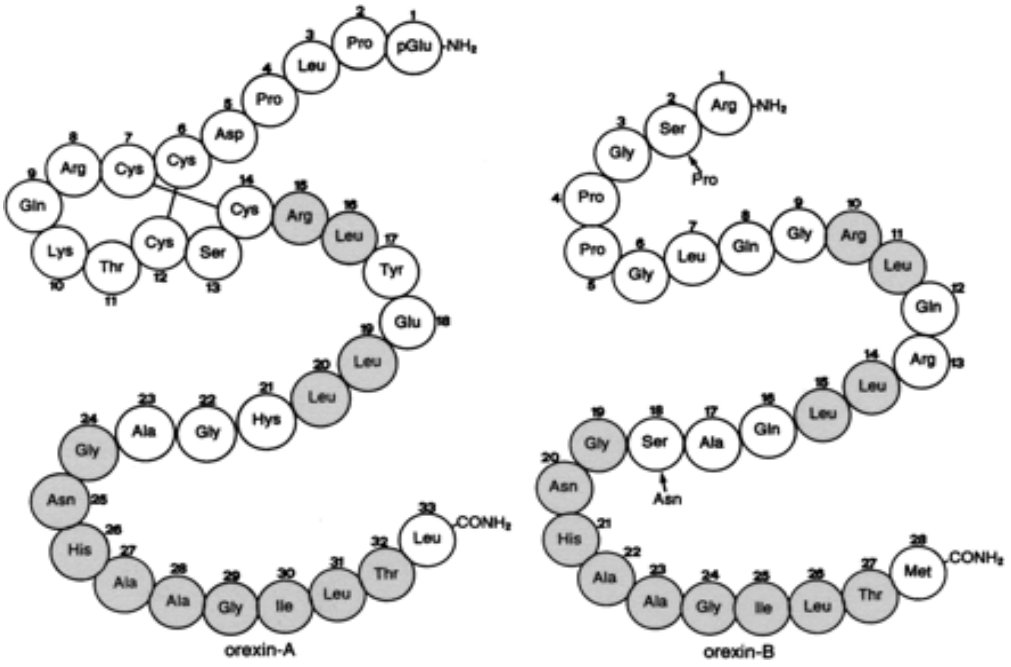

Figure 1.8: Structure of OXA and OXB. The amino acid sequence of human OXs. Arrows indicate the amino acid substitutions at positions 2 and 18 in OXB that differ between humans and rats, pigs and mice. Identical amino acids between the two proteins are shaded (Spinazzi et al. 2006).

OXs were initially found to be involved in appetite, due to the discovery of their production in the LHA which is known to be a regulatory area of feeding, supported by the fact that lesions occurring in this area dramatically reduce food intake (Bernardis, Bellinger 1996). Further study showed that neurons positive for OX were projected throughout the brain suggesting a more widespread and complex role (Figure 1.9) (Hungs, Mignot 2001).

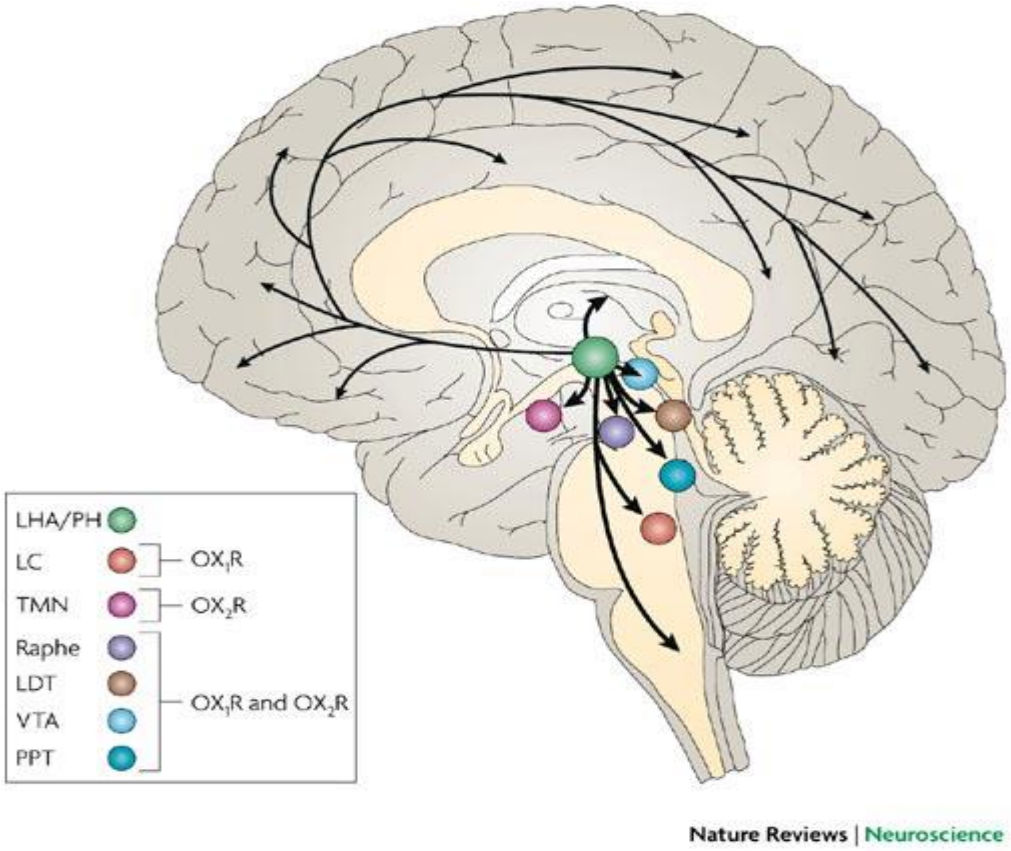

Figure 1.9: Orexinergic neuron projections in the brain. This image demonstrates the predicted orexinergic projections throughout the human brain. Circles represent dense receptor expression and projections. OX neurons starting at the LHA and posterior hypothalamus regulate the sleep wake cycle and maintain arousal by sending excitatory signals projecting to the central nervous system (CNS). There are particularly dense projections to the monoaminergic and cholinergic nuclei in the brain stem and hypothalamic regions, LC, TMN, raphe nuclei and laterodorsal/pedunculopontine tegmental nuclei. The ventral tegmental area (VTA) is linked to the reward system (Sakurai 2007).

1.9.3 Orexin receptors

OXA and OXB bind to two different receptors: orexin receptor 1 (OX1R) and orexin receptor 2 (OX2R); both of which are GPCRs. OX1R is 425 amino acids and OX2R is 444 amino acids, sharing 64% sequence identity. Both receptors are strongly conserved amongst mammals and have 94% homology between human and rats (Sakurai et al. 1998). OXs have different affinities for the receptors; OX1R binds OXA with very high affinity (IC50 20nM in a competitive binding assay) but it exhibits a much lower affinity for OXB of 420nM (Sakurai et al. 1998). OX2R shows less discrimination between the OXs and they both have similarly high affinities of IC50 38nM (OXA) and 36nM (OXB) (Sakurai et al. 1998; Scammell, Winrow 2011).

1.9.3.1 Expression and distribution of orexin receptors

The most intense areas of OX producing neurons are around the paraventricular nucleus (PVN), arcuate nucleus and TMN. OX2R is predominantly expressed in the PVN, cerebral cortex and nucleus accumbens. OX1R is highly expressed in the hippocampal formation, dorsal raphe and LC (Figure 1.10) (Trivedi et al. 1998). They are co-expressed in the ventromedial hypothalamic nucleus (VMH), posterior hypothalamus (PH), dorsomedial nucleus, hippocampal formation, thalamic nuclei and subthalamic nuclei (Lu et al. 2000). These areas of dense orexinergic neurons fire rapidly during wakefulness, at a much slower rate during non-rapid eye movement (REM) and not at all in REM (Lee, Hassani & Jones 2005). It is believed that OX exerts its effects on wakefulness by acting upon histaminergic neurons through OX2R. When injected with OX rats experience prolonged periods of wakefulness and this is less pronounced when the histamine H1 receptor antagonist pyrilamine is also administered (Sakurai 2007; Yamanaka et al. 2002). Other areas of OXR expression include the testes and adrenal glands, however only small amounts of OXR expression are found here (Karteris, Chen & Randeva 2004; Scammell, Winrow 2011; Blanco et al. 2002). Due to the low level expression of these receptors outside of the brain any antagonists are not likely to cause any obvious effects outside of the brain.

1.9.3.2 Orexin receptor signalling

OXs cause neurons in the brain to experience changes in membrane potential which causes slow and long-lasting depolarisation resulting in either firing of the neurons or an increased firing rate, making them excitatory. This membrane depolarisation is as a result of closure of potassium channels which are normally active in a resting state, activation of a sodium-calcium exchanger and the activation of cation channels (Ivanov, Aston-Jones 2000; Brown et al. 2001; Eriksson et al. 2001; Burdakov, Liss & Ashcroft 2003; Hwang, Chen & Dun 2001; Yang, Ferguson 2002). OX1R and OX2R both result in the release of calcium from intracellular stores and chelation of calcium prevents OX depolarisations (Burdakov, Liss & Ashcroft 2003). This depolarisation can be mediated through activation of voltage-gated calcium channels (VGCC) (Kohlmeier et al. 2008; Van Den Pol et al. 2001).

As OXRs are GPCRs they use G-proteins to mediate signal transduction. Both receptors have been shown to be promiscuous in their signalling characteristics and have been shown to couple to three of the four available G-proteins; Gq, Gi/o and Gs. Coupling can vary based on cell type for example in the rat brain stem OXRs couple to Gi/o and in the rat hypothalamus to Gs and Gq (Kukkonen 2013; Kukkonen, Leonard 2014; Bernard, Lydic & Baghdoyan 2002; Bernard, Lydic & Baghdoyan 2003). Due to the difficulty for direct measurement of G-protein activation and selective G protein inhibition, conclusive data on OXR G-protein coupling is still unclear (Kukkonen, Leonard 2004; Kukkonen 2014). GTP-azidoaniline binds to G proteins when a receptor is activated which can then be identified using antibodies. Using this technique OX2R has been shown to differentially couple to Gq, Gi/o and Gs proteins in the adrenal gland (Karteris et al. 2001; Karteris et al. 2005).

AC is a common downstream effector of GPCR signalling and OXRs have been shown to regulate this effector molecule (Kukkonen, Leonard 2014; Karteris et al. 2005; Randeva et al. 2001; Tang et al. 2008). OX1R can couple to Gs which stimulates AC and cAMP production or Gq to activate PKC (Holmqvist et al. 2005; Kawabe et al. 1994). However OXRs have also been shown to inhibit AC potentially due to coupling to Gi as this inhibition is ablated by pertussis toxin and some other reports suggest that

there are no changes in cAMP after OX addition (Holmqvist et al. 2005; Magga et al. 2006). It is likely that the differences in G-protein coupling are dependent on cell type as these different G-protein coupling mechanisms were observed in different cell lines: Chinese hamster ovary (CHO) and human embryonic kidney (HEK) respectively.

OXRs initiate increases in intracellular calcium in many cell types including CHO, HEK and neuro-2a (Sakurai et al. 1998; Magga et al. 2006; Holmqvist, Akerman & Kukkonen 2002). This activation occurs through activation of PLC potentially through Gq coupling. PLC is a family of cytosolic phosphoinositide specific enzymes whose main target is PIP2. Cleavage by PLC generates DAG and IP_3, IP_3 then binds ER IP_3 receptors and facilitates the release of calcium into the cytosol (Kukkonen, Leonard 2014; Konieczny, Keebler & Taylor 2012). This depletion of calcium causes the membrane to allow a calcium influx to replace the diminished stores and this can regulate calcium responsive ion channels, enzymes and proteins. This depolarisation also activates VGCCs. OX1R and OX2R strongly activate PLC in several different cell types including CHO, HEK and the neuronal neuro-2a cell line (Holmqvist, Akerman & Kukkonen 2002; Lund et al. 2000; Putula, Kukkonen 2012). However it is not known whether the downstream effects of this elevated PLC is to increase calcium or to elevate DAG for potential PKC elevation (Kukkonen, Leonard 2014).

1.9.4 Physiological effects of orexins

Due to the wide reaching nature of OXs not only in the brain but also in peripheral tissues, it has a wide range of physiological functions (Karteris, Chen & Randeva 2004; Sakurai 2007; Kukkonen, Leonard 2014; Karteris et al. 2005).

1.9.4.1 Energy homeostasis

When Sakurai first identified OX its involvement in feeding was noted; particularly that OXA administration increased food intake in rats (Sakurai et al. 1998). This was confirmed by the administration of an OX1R antagonist which blocked OXA simulated increases in feeding in genetically obese mice (Haynes et al. 2002). This may be due to the dense projections of OX neurons in the arcuate nucleus, which when activated release neuropeptide Y (NPY) and the inhibitor of food intake: pro-opiomelanocortin

(POMC) is inhibited (Muroya et al. 2004; Yamanaka et al. 2003). This ability of OX to activate NPY and inhibit POMC may cause feeding stimulation. OX is also linked to glucose regulation. When blood glucose is decreased OX expression increases, potentially to stimulate appetite and when blood glucose is high OX production is decreased to reduce feeding behaviour (Tsuneki, Wada & Sasaoka 2012; Sakurai 2006).

1.9.4.2 Sleep-wake cycle and arousal

Many OX neurons are found in areas of the brain which regulate the sleep-wake cycle, indicating an important role of OX in its regulation. Narcolepsy is a fairly common disorder affecting 1 in 2000 adults with an onset between 15-30 years of age (Ebrahim et al. 2003). It is a disorder of sleep which manifests itself with four main symptoms; excessive daytime sleepiness, uncontrollable bouts of sleep during the day, cataplexy and sleep paralysis during wakefulness accompanied by hypnagogic hallucinations which would otherwise normally occur at the onset of sleep (Scammell, Winrow 2011; Ebrahim et al. 2003). All of these attributing symptoms make it difficult for an individual to stay awake during the day and the extent of this disability is dependent upon the severity of the condition.

The link between sleep and OX was initially discovered after Chemelli produced PPO KO mice to observe its effect on appetite, as it was believed this was its primary function. To which it was later discovered that the mice were experiencing severe sleepiness and cataplexy (Chemelli et al. 1999). This lead to OX2R KO mice, which experienced narcolepsy like symptoms and although OX1R KO mice did experience disrupted sleep, the effects were less severe than in OX2R KO mice (Chemelli et al. 1999; De la Herran-Arita et al. 2011; Willie et al. 2003). Estabrooke discovered in rats that OX neurons had more Fos reactivity during periods of wakefulness which became reduced during periods of non-REM or REM sleep. This was supported by staining of brain sections for OX, which showed intense staining of sections from rats who experienced induced wakefulness compared to those who had induced sleep (Estabrooke et al. 2001). OX infusion in mice increased wakefulness and a dual OXR antagonist promoted sleep, thus supporting this mechanism (Kang et al. 2009). Mignot showed that in those with narcolepsy there were vastly reduced levels of circulating CSF OX, possibly as a result of autoimmune destruction of OX producing neurons

which were also vastly reduced, indeed one study showed that 7 out of 9 individuals with narcolepsy had undetectable levels of OX (Hungs, Mignot 2001; Nishino et al. 2000; Mahlios, De la Herran-Arita & Mignot 2013). However, narcolepsy which was first identified in dogs is as a result of mutation of OX2R not autoimmune destruction of OX producing neurons (Lin et al. 1999).

1.9.4.3 Reward system

OX neurons project to the VTA and nucleus accumbens, both areas which have been implicated in the reward system and drug addiction (Sharf, Sarhan & Dileone 2010). Fos activation of OX neurons in mice was higher in those given food and drug rewards as well as activation of hypothalamic OX neurons increasing drug-seeking behaviour in these mice; this effect was blocked with an OXA antagonist (Harris, Wimmer & Aston-Jones 2005). An OX1R antagonist administered to rats with an alcohol-preference ablated an olfactory cue-induced reinstatement of alcohol seeking behaviour and they also exhibited increased expression of PPO mRNA (Lawrence et al. 2006; Anderson et al. 2014). In addition an OX1R antagonist reduced the relapse of alcohol-preferring rats (Dhaher et al. 2010). This suggests that OX can increase reward seeking behaviour.

1.9.4.4 Other physiological function of OXs

Brown adipose tissue (BAT) plays a vital role in regulating body temperature as it is found in hibernating mammals and infant humans and functions to generate body heat (Gilsanz, Hu & Kajimura 2013; Cannon, Nedergaard 2004). OXR KO mice experience obesity even though they show less feeding behaviour and it is thought this occurs as a result of impaired thermogenesis in BAT due to inability of brown preadipocytes to differentiate in the absence of OX. Inactivation of BAT as a consequence of OX absence does not allow energy dissipation in response to a high calorie diet and reduces energy expenditure resulting in obesity (Sellayah, Bharaj & Sikder 2011). OX administration in rats has also been shown to increase blood pressure and heart rate (Shirasaka et al. 1999; Smith, Connolly & Ferguson 2002).

1.9.5 Orexin and AD

Several studies have demonstrated abhorrent circadian rhythms as well as disrupted sleep-wake cycles in patients with AD (van Someren et al. 1996). In fact behavioural

and sleep disturbance are one of the most common reasons for institutionalisation of AD patients (Bianchetti et al. 1995; Pollak, Perlick 1991; Harper et al. 2001). This dysregulated sleep-wake cycle is also marked by increased nocturnal activity and early awakenings as well as hypersomnia or excessive daytime sleepiness and exceeds what is seen in elderly patient controls regarding frequency and duration (Harper et al. 2001). Patients who experienced these symptoms to a greater extent also had increased severity of AD, including greater memory problems and impaired cognition (McCurry et al. 1999; Moe et al. 1995). These symptoms appear to be specific to AD and are not observed in other dementias (Harper et al. 2001). A strong link between AD and OX was first shown in 2007 when a group identified that in those with AD there was lower circulating OXA (Friedman et al. 2007). In 2009 Kang examined the effects of OX on Aβ accumulation in mice brains under different circumstances. They used Tg2576 human *APP* transgenic mice and wild-type mice. Using these models they found that ISF Aβ levels had diurnal variation, with higher levels during periods of dark compared to light. Upon further investigation it was revealed that Aβ levels corresponded to the time spent awake rather than the time of day (Kang et al. 2009). Mice who were sleep deprived through an OXA infusion exhibited increased Aβ levels which were higher than during normal sleep patterns (Kang et al. 2009). After this sleep deprivation mice slept for a longer period and had an instant reduction in ISF Aβ. Following this, a dual OXR antagonist was administered and this abolished the diurnal variation of Aβ and reduced time spent awake by circa 10% and removal of the antagonist restored it (Kang et al. 2009). In mice that underwent chronic sleep deprivation, Aβ plaque formation compared to age matched controls was considerably more pronounced and treatment with the antagonist vastly reduced plaque formation compared to age matched controls (Kang et al. 2009). This study however did not examine receptor levels in the AD mice and as this is an artificial system with regards to chronic OX infusion it may not be an appropriate model. The mouse models used only exhibit the Aβ pathology of AD, so results do not take into account when all the dynamics of AD are present. This study was performed over a very short time frame so any effects could have been transient and were not long lasting; this makes it difficult to draw any reasonable conclusions as to whether the OX system is actually neurodegenerative. One recent study did not find any correlation between OX levels or tau and $A\beta^{42}$ in the CSF suggesting that OXs do

not directly regulate burden of disease (Schmidt et al. 2013). Other evidence also suggests a link between OX and AD. In one study which monitored behavioural symptoms in AD there was a significant negative correlation with appetite and dementia; with disease progression, appetite decreased suggesting a reduction in OX signalling (Fernandez et al. 2010). AD patients also exhibit a 40% reduction in orexigenic neurons and severe reductions in circulating OX levels (Fronczek et al. 2011). However a reduction in the OX signalling system is also observed with increasing age. In rats with increased age there is a reduction in responsiveness to OXA and they experience a reduction of innervation to cholinergic neurons as well as reductions in PPO expression and circulating OXs (Stanley, Fadel 2012; Kessler et al. 2011). Aged rats also display fewer OX immunoreactive neurons than younger controls (Sawai et al. 2010).

There is increasing evidence of an important role of OX in learning and memory processes. OXB infusion in rats improved accuracy and attention processes and OX1R antagonists impaired performance in an attention task, combined this suggests an important role of OXs in cognition (Lambe et al. 2005; Boschen, Fadel & Burk 2009). OXA administration in sleep deprived rhesus monkeys improved their performance in tasks but did not have any effect on non-sleep deprived monkeys suggesting OX is capable of improving symptoms as opposed to improvement of basal performance (Deadwyler et al. 2007). OX1R antagonist infusion of the cornu ammonis 1 (CA1) of the hippocampus impaired spatial learning and memory (Akbari et al. 2008; Akbari, Naghdi & Motamedi 2006).

This data suggests that the OX system can improve cognitive function in a sub-optimal system especially with regards to memory and learning, so the implication that augmentation of the OX system worsens the burden of AD in mice is contradictory. The reduction of OX in AD in humans may partially contribute to cognitive and behavioural symptoms of AD.

1.10 GPR103

RFamide peptides are a family of peptides that contain an Arg-Phe-NH_2 motif at their C-terminal. Five groups of RFamide have been identified: neuropeptide FF (NPFF),

prolactin-releasing peptide (PrRP), gonadotropin-inhibitory hormone (GnIH), kisspeptin and the 26RFa group or GPR103 receptor with its ligand QRFP (Ukena et al. 2011). The 26RFa group was originally identified in a frog brain (Chartrel et al. 2003). The peptide in its longest form is a 43 amino acid termed QRFP, but due to several processing sites of the peptide a 26 (26RFa), 6 ($26RFa_{20-26}$) and 9 (9RFa) amino acid form can also be generated (Figure 1.10) (Bruzzone et al. 2006; Takayasu et al. 2006; Chartrel et al. 2011). The 9RFa appears to be a very poor agonist of the receptor and may not be biologically important (Jiang et al. 2003; do Rego et al. 2006). Fragments of the N-terminal and central region of the peptide result in no physiological changes in mice, suggesting it is the C-terminal domain which is of physiological importance (do Rego et al. 2006). 26RFa is strongly conserved between species with a similarity that varies between 77-85% between mammals and amphibians (Chartrel et al. 2011). The previously identified orphan GPCR: GPR103 was identified as being the receptor for this ligand (Jiang et al. 2003; Fukusumi et al. 2003). GPR103 is a GPCR that shares 38% TM homology with the receptor NPFF2, initially suggesting that the ligand for GPR103 may be an RFamide peptide making 26RFa and QRFP good candidates as GPR103 ligands (Chartrel et al. 2011; Lee et al. 2001). GPR103 also shares 48, and 47% protein sequence homology with OX1R and OX2R respectively (Jiang et al. 2003). It was later revealed that 26RFa binds to GPR103 with high affinity and that upon 26RFa stimulation flag-tagged GPR103 in CHO was internalised (Jiang et al. 2003; Chartrel et al. 2011; Fukusumi et al. 2003). 26RFa and QRFP were both found to increase intracellular calcium concentration as a result of cAMP reduction in CHO and HEK cells suggesting a coupling to the $G_{i/o}$ G-proteins and QRFP has been found to have a higher affinity for GPR103 than 26RFa (Chartrel et al. 2011; Fukusumi et al. 2003).

In humans the *QRFP* gene has been found to be expressed in the VMH and PVN (Bruzzone et al. 2006). Outside of the human brain QRFP is expressed in the highest quantities in the retina, bones, heart, kidney, testes, thyroid, pituitary and prostate (Jiang et al. 2003; Baribault et al. 2006).

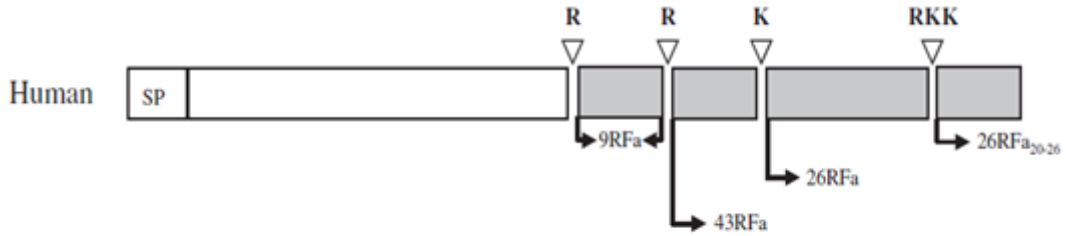

Figure 1.10: 26RFa precursor. R and K represent arginine and lysine cleavage sites which produce 9RFa, 43RFa, 26RFa or $26RFa_{20-26}$ fragments from the precursor protein. [Adapted from (Chartrel et al. 2011)]

1.10.1 Physiological function of QRFP

1.10.1.1 Feeding behaviour

Due to intense expression of QRFP expressing neurons in the hypothalamus including the VMH, hypothalamic area and arcuate nucleus, it was suggested that it was involved in feeding behaviour. QRFP administration in mice resulted in a dose dependent increase in feeding and QRFP was increased in the hypothalamus of starved mice with the 43 amino acid version being more potent than 26RFa (Chartrel et al. 2003; Takayasu et al. 2006; do Rego et al. 2006; Moriya et al. 2006). In mice which received injections of QRFP for 13 days there was increased body weight, fat mass, plasma glucose, insulin and cholesterol and in genetically obese mice QRFP mRNA is increased (Takayasu et al. 2006; Moriya et al. 2006). QRFP administration leads to increased NPY and decreased POMC in the arcuate nucleus and leads to an increase in food intake in mice; which is very similar to the effects exerted by OX (Muroya et al. 2004; Lectez et al. 2009). GPR103 is also expressed by the NPY neurons of the arcuate nucleus but not of the POMC neurons. This suggests that QRFP indirectly decreases POMC though stimulation of NPY neurons, which was confirmed by NPY antagonists abolishing the inhibitory effect of QRFP on the POMC neurons and thus resulting in decreased feeding (Lectez et al. 2009).

1.10.1.2 Control of the gonadotropic axis

The administration of QRFP results in an increase in the gonadotropins; luteinising hormone (LH) and follicle stimulating hormone (FSH) (Navarro et al. 2006; Patel et al.

2008). QRFP also increases gonadotropin releasing hormone (GnRH) and it is thought that QRFP regulates the hypothalamic-pituitary-gonadal axis by activating GnRH secreting neurons (Chartrel et al. 2011; Patel et al. 2008). As QRFP is expressed in the testes it is possible that it also directly regulates the hypothalamic-pituitary-gonadal axis at the gonadal level (Jiang et al. 2003).

1.10.1.3 Bone formation

GPR103 deficient mice are viable but suffer from osteopenia (Baribault et al. 2006). They endure a reduction in bone density as well as thinning of the osteochondral growth plate, thickening of trabecular branches and a reduction in osteoclasts; all of which is suggestive of inhibition of osteochondral bone formation (Baribault et al. 2006). The hypothalamic nuclei which GPR103 uses to control feeding are also important in bone formation and modelling with obesity having been shown to protect from osteoporosis (Chartrel et al. 2011; Ducy et al. 2000). The osteoporosis-prone mouse strain; SAMP6, was sequenced and four single-nucleotide polymorphisms (SNPs) in QRFP were found which were not found in the controls. One of these SNPs is located in the promoter region of QRFP which produces a neuron-restrictive silencing factor binding site. This acts as a repressor which decreases gene expression in tissues outside of the brain and these mice exhibit lower expression of the QRFP transcript (Zhang et al. 2007).

1.10.1.4 Other functions of QRFP

In rats there is high GPR103 expression in the adrenal cortex (Fukusumi et al. 2003). However administration of QRFP does not appear to exert any effects on corticosteroids but may regulate adrenal steroidogenesis (Chartrel et al. 2011; Fukusumi et al. 2003; Ramanjaneya et al. 2013). QRFP has also been implicated in nociception. Administration of QRFP reduced agitation behaviours caused by paw formalin injection which may suggest an analgesic effect of QRFP (Yamamoto, Miyazaki & Yamada 2009). Central administration of QRFP resulted in increased arterial blood pressure and heart rates in mice and increased stress levels based on grooming behaviour (Takayasu et al. 2006).

2

Chapter 2

Methods and materials

2.1 Cell lines and culture

Two neuroblastoma cell lines used were; IMR32, obtained from the Health Protection Agency and SH-SY5Y, a gift from Dr. Mattia Calissano, UCL. The Holten LaminAir Class II Haeraus Instrument hood was thoroughly cleaned with trigene and 70% industrial methylated spirit (IMS) before usage, where all work requiring sterile conditions was performed. All equipment used was sterile and cleaned with 70% IMS before use in the flow hood.

IMR32 cells were cultured in Eagles minimum essential media (EMEM) (Sigma-Aldrich) supplemented with 10% fetal bovine serum (FBS) (Sigma-Aldrich), 1% non-essential amino acids (Gibco), 1% 200mM L-glutamine (Gibco) and 1% penicillin/streptomycin (Gibco). SH-SY5Y cells were cultured in a ratio of 1:1 of EMEM and Hams F12 media (Sigma-Aldrich), supplemented with 10% FBS, 1% non-essential amino acids, 1% 200mM L-glutamine and 1% penicillin/streptomycin. Both cell lines were maintained in 75cm^2 non treated culture flasks (Nunc) under standard tissue culture conditions at 37ºC and 5% carbon dioxide (CO_2). Cells reached confluence after 48-72 hours and were subcultured by splitting the cells in a 1:6 ratio. Seeding densities were not performed for general tissue culture, but were seeded at specific densities for experiments. Cells were washed with 1x phosphate buffered saline (PBS) (Gibco) and were detached with 2.5ml TrypleExpress (Life Technologies) through incubation for several minutes. 2.5ml of media was added to the flask once cells were visibly detached and this suspension was centrifuged for 5

minutes at 1,500 revolutions per minute (RPM) in a Heraeus 1.0 centrifuge. The supernatant was removed and the pellet was resuspended in a known volume of media and distributed evenly among new flasks containing 19ml of fresh pre-warmed media. The flasks were then placed in the incubator and not disturbed for at least 4 hours to allow cell adherement.

2.2 Thawing of cryopreserved cells

To thaw cells for culturing complete media was warmed in a 37°C water bath for 30 minutes prior to thawing. 19ml of media was then aliquoted into a 75cm^2 flask and placed in a 37°C, 5% CO_2 incubator. Vials were taken from liquid nitrogen on dry ice and cells were thawed in a 37ºC water bath. When the vials had defrosted, they were resuspended in the pre-warmed flask and placed in the incubator. Cells were left for at least 4 hours without being disturbed in the incubator.

2.3 Cryopreservation of cell lines

Cryopreservation of cells was performed to maintain the cell lines. This was achieved by aspirating the culture medium from the flask of confluent cells and washing with 1x PBS warmed to 37°C. Cells were then detached for several minutes at 37°C with TrypleExpress after which 2.5ml of media was added. This suspension was placed into a 50ml centrifuge tube and spun for 5 minutes at 1,500 RPM, after which the supernatant was removed leaving the pellet. Freezing media was made up with dimethyl sulfoxide (DMSO) (Sigma-Aldrich), FBS and complete media; as described in table 2.1. This was then added to the pellet of cells, resuspended and placed into a 1.6ml cryovial (Fisher Scientific). Cells were placed into a Nalgene Mr. Frosty (Sigma-Aldrich), containing isopropanol to allow slow cooling and avoid crystal formation. This was stored at -80°C overnight then transferred to liquid nitrogen.

Reagent	Volume/75cm^2 flask
DMSO	100µl
FBS	400µl
Media	500µl

Table 2.1: Requirements for freezing down one confluent 75cm^2 flask of cells

2.4 Cell counts

Cell counts were performed to enable consistency of experiments. Detachment of cells as previously described was completed. Cells were centrifuged for 5 minutes at 1,500 RPM and resuspended in 5ml of 37°C warmed media. 5µl of this suspension was pipetted under the coverslip of a haemocytometer to fill the chamber. The number of cells within one large square of the haemocytometer were counted and the number of cells in the total suspension was calculated using the formula below.

$$\left(\frac{\text{Number of cells counted}}{\text{Number of large squares counted}} \text{ X media added (ml)} \right) \text{X } 10^4 = \text{Number of cells in suspension}$$

To calculate how many cells were in the total suspension the following calculation was used:

$$\frac{\text{Number of cells in suspension}}{5000\mu l} = \text{Number of cells/µl}$$

This was then used to decide how much of the suspension was needed to obtain the required cell seeding density:

$$\frac{\text{Seeding density required}}{\text{Number of cells / µl}} = \text{Volume of cell suspension to add to new flask (µl)}$$

2.5 Cell differentiation

Both cells lines were differentiated to acquire a more neuronal phenotype. This was achieved by using two different agents. IMR32 cells were treated for 20 days with 10µM 5-bromo-2'-deoxyuridine (BrdU) (Sigma-Aldrich). Due to the time needed to differentiate these cells and their fast growing nature, they were subcultured on the following days: 0, 2, 4, 6, 8, 12, 16 and 20 and cell counts and microscopy images were performed. SH-SY5Y cells were differentiated for 6 days with 10µM retinoic acid (RA) (Sigma-Aldrich). Differentiation was more rapid and cells were subcultured on days 0, 2, 4 and 6, with cell counts and microscopy images taken on these days. Both cell lines were seeded at $1x10^6$ cells.

2.6 RNA extraction from cells

RNA was extracted so as to observe changes in gene transcript levels under different experimental situations. RNA was extracted using the Sigma GenElute mRNA Miniprep Kit according to manufacturer's instructions. Briefly, all equipment and work surfaces were cleaned with 70% IMS and RNAse AWAY (Sigma-Aldrich). RNA extraction was performed on cells attached to a $75cm^2$ flask or a 6 well plate. Firstly cells were briefly washed with 1x PBS. For a $75cm^2$ flask 2ml of a lysis solution with 20µl of β-mercaptoethanol was added to the cells and for a 6 well plate 250µl of lysis solution and 2.5µl β-mercaptoethanol. The flask was gently rocked then left for 2 minutes to ensure lysis of all cells. 700µl of the cell lysate was transferred to a GenElute filtration column at a time and the column was centrifuged at 12,000 RPM for 2 minutes to allow removal of cellular debris. An equal volume of 70% ethanol was added to the cell lysate and vortexed. 700µl of the lysate/ethanol mixture was added to a GenElute binding column at a time. Columns were then centrifuged for 15 seconds at 12,000 RPM. The column binds RNA, so the column was kept but flow through was discarded. 500µl of wash solution 1 was added to the column and centrifuged at 12,000 RPM for 15 seconds. After placing the binding column into a fresh collection tube, 500µl of wash solution 2 was added and spun at 12,000 RPM for 15 seconds and flow through was discarded and the column kept. This wash step was repeated. To ensure no ethanol remained the columns were put

through a further drying stage and centrifuged for 2 minutes and flow through was discarded. Binding columns were transferred to fresh collection tubes. 50µl of elution solution was added and centrifuged at 12,000 RPM for 1 minute. 0.5µl of the RNAse inhibitor: SUPERase In (Ambion) was added to each sample to prevent RNA degradation. To remove residual DNA the RNA was treated with DNase I (Sigma-Aldrich). Samples were treated with 5µl of 10x reaction buffer and 5µl of DNase I and gently mixed and incubated for 15 minutes at room temperature. 5µl of stop solution was added to inactivate DNase I and the samples were incubated at 70ºC for 10 minutes.

RNA concentration was read at 230, 260 and 280nm using the NanoDrop spectrophotometer (NanoDrop 2000C, Thermo scientific), using 1µl per sample. Optical density readings of A260/A280 and A260/A230 were used to measure protein and carbohydrate contamination respectively and were expected to be between 1.8-2.0.

2.7 RNA extraction from human hippocampal samples

Before performing RNA extraction, human hippocampal samples which were snap frozen, were thawed on ice and transferred to sterile eppendorf tubes containing lysis buffer. Samples were then homogenised using the TissueLyser II (Qiagen). Proteinase K (Sigma-Aldrich) was added to each sample after homogenisation and incubated at 55ºC for 10 minutes. The previously mentioned RNA extraction steps were then followed.

2.8 cDNA synthesis

Complimentary DNA (cDNA) synthesis was performed to create a double stranded copy of the extracted mRNA to observe gene transcript levels in a given sample.

The amount of RNA needed was calculated using the following equation:

$$\frac{\text{Total cDNA required}}{\text{RNA concentration}} = \text{RNA required}$$

A SuperScript II reverse transcriptase kit (Sigma-Aldrich) was used according to the manufacturers' protocol. Briefly the required amount of RNA was made up to 10 µl with nuclease free water. Then a mastermix (Table 2.2) was made of deoxyribonucleotide triphosphate (dNTP) and random primers for the total number of samples and 2µl was added to each sample. This was heated at 65°C for 5 minutes on a heat block followed by quick chilling on ice. Another mastermix (Table 2.2) was made comprising the 5x first strand buffer, dithiothreitol (DTT) and nuclease free water; 7 µl was added to each sample and left at room temperature for 2 minutes. 1 µl of superscript II was subsequently added to each sample and incubated for 50 minutes at 42°C, after which the temperature was increased to 72°C for 15 minutes. Samples were then stored at -20°C.

Reagent	Quantity per reaction (20µl)
Random Primers (Sigma-Aldrich)	1µl
dNTP (Sigma-Aldrich)	1µl
5x First strand buffer (Sigma-Aldrich)	4µl
DTT (Sigma-Aldrich)	2µl
Nuclease-free water (Ambion)	1µl
Superscript II (Sigma-Aldrich)	1µl

Table 2.2: Requirements for one 20µl reaction of cDNA synthesis.

2.9 Real-time polymerase chain reaction (qPCR)

qPCR was performed to observe changes in gene transcript levels in mRNA extracted from cells or tissue. Mastermixes were made up for each primer set (Table 2.3) using Precision 2x real-time PCR Mastermix with SYBR green (PrimerDesign). Mastermixes were vortexed and 19 µl was pipetted into each corresponding well of a

96 well MicroAmp fast optical qPCR plate (Applied Biosystems). 1 µl of cDNA was added to the appropriate wells and for non-template controls (NTC) cDNA was replaced with water. The plate was then sealed using MicroAmp optical adhesive film (Applied Biosystems). Each sample for each gene was performed in triplicate. The plate was briefly centrifuged at 1,000 RPM to ensure thorough mixing and the plate was run on the ABI 7900HT fast real time PCR system (Applied Biosystems) using the illustrated program (Figure 2.1)

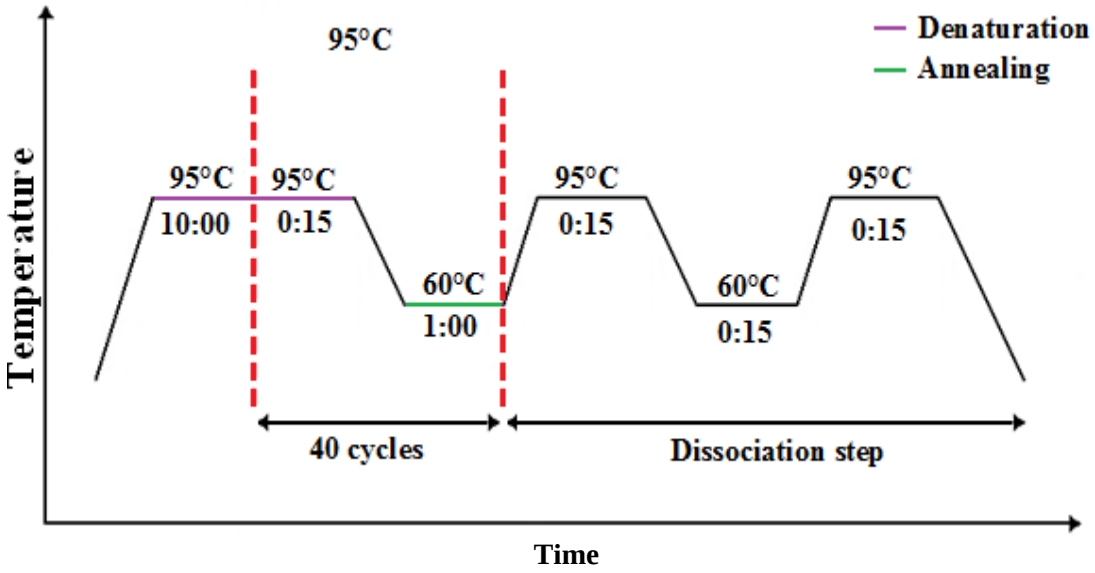

Figure 2.1: Schematic representation of qPCR program and cycles

Reagent	Quantity per reaction (20µl)
Mastermix with SYBR green (PrimerDesign)	10 µl
Nuclease-free water (Ambion)	8 µl
Forward and reverse primer mix (PrimerDesign)	1µl
cDNA	1µl

Table 2.3: Requirements for one 20µl qPCR reaction.

qPCR is measured by either relative or absolute quantification. Absolute quantification determines expression levels by comparing results to a known quantity using a standard curve, whereas relative quantification provides a comparison of the gene of interest with a selected housekeeping gene. An amplification curve is generated which is a graph plotted with the number of cycles against the fluorescence intensity (Figure 2.2). As the cycle number increases the amount of double stranded DNA also increases and fluoresces as the SYBR green molecule binds to the minor groove of DNA. A cycle threshold (Ct) is produced on the basis of the amplification range with a lower Ct indicating increased amplification. SYBR green can result in non-specific binding to primer dimer complexes. Therefore a dissociation curve is produced and provides a graph of the melting temperature (Tm) of the DNA versus the fluorescence intensity (Figure 2.2). This allows analysis of whether it is indeed only one product which has been amplified indicating specificity or multiple products due to primer-dimers (User Bulletin #2, ABI PRISM 7700 Sequence Detection System). A list of all primers used are indicated in table 2.4, however as primers for housekeeping genes were used in commercial kits by PrimerDesign, the sequences were not available to us.

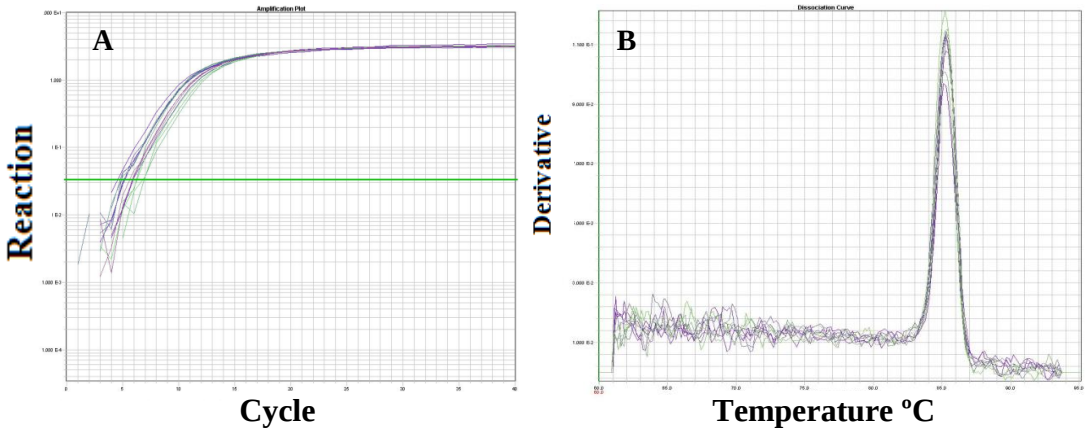

Figure 2.2: Representations of data produced by qPCR. A. Amplification plot and B. Dissociation curve.

Gene	Primer sequence 5'→3'	Forward/Reverse	Amplicon size (bp)
OX1R	CACACGGCTCTTCTCAGTCT	F	204
	GCCAGGTAGGTGACAATAAAGA	R	
OX2R	GCTAAAGAGAGTATTTGGGATGTTT	F	261
	TATAAATAATTGGATTCGCAGCACTA	R	
GPR103	CGCCTCCCTTCCTCTACTCT	F	141
	GAGATCGAGTCTCCCAGTGC	R	
NSE	ATGCGACTAGGTGCAGAGGT	F	133
	GCTCCAAGGCTTCACTGTTC	R	
NES	AACAGCGACGGAGGTCTCTA	F	220
	TTCTCTTGTCCGCAGACTT	R	
NG1	ACGCCCTGTTTCATTCCTTAC	F	81
	CCATCTATTGCCTGCTGACTAG	R	
MAPT	TTTGGTGGTGGTTAGAGATATGC	F	72
	CCGAGGTGCGTGAAGAAATG	R	
CSTF2T	GCACAACCGGAATCATGTCG	F	299
	TTCACTGGCAGCATTGTCCA	R	
DAB2IP	AAAAGGAGGAACCCAGACGC	F	135
	TTTCTTGAGGCGACTCGTAGG	R	
GPR148	GCTCCCATACCTGTACCTGC	F	90
	GTAAAGATGGCCTGGTGCCT	R	
KRT23	CTCCCACAGCAAAGGCCATA	F	130
	GAAGCTGTGTCCGGAGTTCA	R	
OSBPL7	GAGCCAGGCTATGGGAACAT	F	154
	AGATGGGCAGAAGGGCAGTG	R	
PYCRL	TATGTCACTTTCAAGCTCTGGGT	F	271
	ATCACTATGGCCCCTTCCTGG	R	
ZFP42	TTACGTTTGGGAGGAGGTGG	F	229
	ACATTTGTTTCAGCTCAGCGAT	R	
ZP1	CTGGAGAAGGATGGGCGTTT	F	90
	CAGAGTAGCGTCTTGTGCCA	R	

Table 2.4: Primers with forward and reverse sequences used in qPCR.

The following equations (User Bulletin #2, ABI PRISM 7700 Sequence Detection System) were used to analyse the data obtained from performing qPCR:

For cells: $\Delta Ct = Ct_{(\text{gene of interest})} - Ct_{(\text{housekeeping gene})}$

$$\Delta\Delta Ct = \Delta Ct_{(\text{sample})} - \Delta Ct_{(\text{calibrator})}$$

$$\text{Relative quantity (RQ)} = 2^{-\Delta\Delta Ct}$$

For clinical samples: $\Delta Ct = Ct_{(\text{gene of interest})} - Ct_{(\text{housekeeping gene})}$

$$\text{Arbitrary value: } 2^{-\Delta Ct}$$

2.10 Gel electrophoresis

Gel electrophoresis was performed to check the validity of qPCR results. Samples were run on a 1.5% agarose gel. To make the gel; 1.5g of agarose (Fisher-Scientific) was added to 100ml of 1x tris/borate/EDTA (TBE) (89mM Tris-borate, 2mM EDTA, pH 8.3) buffer. This was heated in the microwave for about 2 minutes or until the mixture became clear. Once cooled to circa 55°C, 5µl of ethidium bromide (Sigma-Aldrich) was added and the agarose was then poured into a casting tray and left to cool for 30 minutes. The gel was placed into an electrophoretic tank and submerged in TBE buffer. 3µl of loading dye (Invitrogen) was added to each sample. 7µl of 1kbp DNA ladder (Invitrogen) was added to the first well and 15µl of sample to each well, with a negative control in the last well. The gel was run at 80V and 400mA for approximately 30-45 minutes depending on migration. The gels were imaged using a UVP GDAS 1200 (Gel Documentation Analysis System) under ultraviolet light.

2.11 Cell treatments and protein lysate extraction

Differentiated cells were seeded into 6 well plates and seeded at $1x10^5$. They were starved for 4 hours prior to treatment using media without any FBS. Cells were treated with; 100nM OXA (Tocris Bioscience), 100nM OXB (Tocris Bioscience), 100nM QRFP (Phoenix pharmaceuticals) 10µM SB-334867 (Tocris Bioscience), 10µM TCS-OX229 (Tocris Bioscience), 100nM zinc sulphate (Sigma-Aldrich) or 5ng/ml $A\beta^{1-42}$ (GL Biochem). Cells were incubated with these compounds for the

specified time. Laemmli buffer (Table 2.5) was premade and 200 µl was added to each well. The surface of the plate was scratched with a pipette tip to disrupt cells and heated at 100°C for 10 minutes. This was then aliquoted into tubes and stored at -80°C until ready for use.

Reagent	Quantity
Glycerol	2ml
1M Tris HCL pH 6.7	1ml
β-Mercaptoethanol	0.5ml
10% SDS	4ml
Water	2.5ml
Bromophenol blue	Add for colour

Table 2.5: Recipe for laemmli buffer

2.12 Sodium dodecyl sulfate polyacrylamide gel electrophoresis (SDS-PAGE) and western blotting

All recipes were made up according to the list at the bottom of this section. 10% resolving gels were poured between two glass plates, with 1ml of isopropanol on top of the gel to ensure even gels and was left for 30 minutes at room temperature to set. The isopropanol was washed out with double distilled water (ddH_2O) and the stacking gel was poured on top of the resolving gel, with a 12 well comb inserted into the gel. This was left at room temperature for 30 minutes. Gels were placed into a cassette and loaded into a running tank. 1L of 1x SDS-PAGE running buffer was poured into the tank. Samples were boiled on a heat block for 5 minutes at 100ºC. Protein lysates were then loaded into the wells along with 5µl of PageRuler Plus

Prestained Protein Ladder (Thermo Scientific). The gels were run at 300V and 40mA per gel for 1 hour.

Nitrocellulose membrane (Hybond-C, GE Healthcare) was cut to match the size of the gel and placed in transfer buffer for 5 minutes. The gel was removed from the glass plates and transfer cassettes were set up with the gel, membrane and filter paper either side. The transfer cassettes were then placed in a Biorad Transblot tank, filled with wet-transfer buffer and an ice pack in the tank. Gels were then run at 300V and 400mA for 1 hour. After transfer, membranes were placed in a plastic tray and covered with 20ml blocking buffer and incubated at room temperature for 1 hour. Membranes were then briefly washed in 1x TBS-tween20 (50 mM Tris-Cl, 150 mM NaCl, pH 7.6). Appropriate antibodies were then diluted (Table 2.6) and each membrane was sealed in a plastic pouch with 2.5ml of antibody. These were then incubated at 4°C overnight.

The following day membranes were washed in 1x TBS-tween20, three times for 10 minutes. The secondary antibody was made up in antibody diluent accordingly (Table 2.6). The membranes were placed into plastic pouches and sealed with 3.5ml of secondary antibody and incubated for 1 hour at room temperature.

The enhanced chemiluminescence (ECL) development method was used to visualise the protein bands. Solution A and solution B were prepared and protected from light. In a dark room, solutions A and B were mixed together and applied to the membranes (with a total of 10ml per membrane) and left for 5 minutes. The membranes were inserted into a plastic pocket in a developing cassette with a sheet of Hyperfilm ECL (GE healthcare) and exposed for varying periods of time. These films were then passed through the Curix 60 AGFA developing machine and proteins were visualised on the films.

Primary antibody	Dilution	Details	Secondary antibody	Dilution
Phospho p44/42 MAPK	1:1000	Polyclonal anti-rabbit, Cell Signalling (4377B)	Anti-Goat, peroxidase produced in rabbit, Sigma (A5420)	1:2000
Total 44/42 MAPK	1:1000	Polyclonal anti-rabbit, NEB (9102)	Anti-Goat, peroxidase produced in rabbit, Sigma (A5420)	1:2000
$A\beta^{1-42}$	1:1000	Monoclonal anti-rabbit, Cell Signalling (8243p)	Anti-rabbit IgG peroxidase produced in goat, Sigma (A0545)	1:2000
Phosphorylated Tau (S214)	1:500	Monoclonal anti-rabbit, Abcam (ab10891)	Anti-rabbit IgG peroxidase produced in goat, Sigma (A0545)	1:2000
Tau	1:1000	Monoclonal anti-mouse, Cell Signalling (4019p)	Anti-mouse IgG peroxidase produced in rabbit, Dako (P0260)	1:2000

Table 2.6: Primary and secondary antibodies used in Western blot.

A list of reagents recipes used in SDS-PAGE- western blotting:

- **10% Resolving gel**

7.9ml ddh_2O, 6.7ml 30% acrylamide/bis-acrylamide solution (National Diagnostics), 5ml 1.5M tris base (pH8.8), 200µl 10% SDS , 200µl 10% ammonium persulfate (APS), 8µl tetramethylethylenediamine (TEMED)

- **5% stacking gel**

6.8ml ddh_2O, 1.7ml 30% acrylamide/bis-acrylamide solution, 1.25ml 1M tris base (pH6.8), 100µl 10% SDS, 100µl 10% APS, 10µl TEMED

- **1x SDS PAGE running buffer**

14.4g glycine, 3.02g tris base, 1g SDS, 1L ddH_2O

- **Wet-Transfer buffer**

2.41g tris base, 11.25g glycine, 800ml ddH_2O, 200ml methanol

- **1x TBS tween 20**

1L 1x TBS, 1ml tween20

- **5% Blocking buffer**

5g non-fat milk powder (Marvel), 100ml 1x TBS-tween 20

- **Antibody diluent**

1g BSA (Fisher Scientific), 20ml 1xTBS-tween20

- **ECL solutions:**

Solution A

5ml tris pH 8.0, 22µl coumaric acid (Fisher scientific), 50µl luminol (Fisher scientific)

- **Solution B**

5ml tris pH 8.0, 3µl 30% hydrogen peroxide

2.13 Indirect immunofluorescence

Immunofluorescence was used to observe the location and intensity of proteins within a cell. Antibodies were used which targeted specific proteins of interest.

Cells were grown on coverslips with a seeding density of $1x10^5$. When ready they were washed with 2ml of PBS to remove cellular debris, which was then aspirated. They were fixed for 10 minutes in 2ml 4% paraformaldehyde (PFA). Cells were rinsed three times for 5 minutes in PBS. 0.2% tween20 in PBS (Sigma-Aldrich) was used to permeabilise the cells, after which they were rinsed again for 5 minutes, three times in PBS. Using forceps, coverslips were blotted on paper towels and placed on damp filter paper. Cells were blocked in 75µl of 10% donkey serum (Sigma-Aldrich), diluted in PBS and left for an hour at room temperature to block. Antibodies were made up according to table 2.7 and diluted in 1.5% donkey serum in PBS. 75µl of primary antibody was added to corresponding coverslips and incubated

at room temperature for 1 hour. Secondary antibodies were made up according to table 2.7 with 1.5% donkey serum and 75µl of antibody was added to each coverslip and incubated at room temperature for a further 1 hour. Coverslips were washed for 5 minutes, three times with PBS and then washed in a beaker of water. One drop of VectaShield with 4',6-diamidino-2-phenylindole (DAPI) (Vectorlabs) was added to each Superfrost slide (Fisher Scientific) and coverslips were blotted dry and mounted on slides upside down and placed in the fridge protected from light until microscopic analysis.

Primary antibody	Dilution	Details	Secondary antibody	Dilution
OX1R	1:75	Polyclonal anti-goat, SantaCruz Biosciences (sc-8073)	Alexa Fluor 488, Chicken anti-Goat, Invitrogen (A21467)	1:2000
OX2R	1:75	Polyclonal anti-goat, SantaCruz Biosciences (sc-8074)	Alexa Fluor 488, Chicken anti-Goat, Invitrogen (A21467)	1:2000
GPR103	1:75	Polyclonal anti-rabbit, SantaCruz Biosciences (sc-48187)	Alexa Fluor 568, donkey anti-rabbit, Invitrogen (A10042)	1:2000
Pan Neuronal Marker	1:75	Monoclonal anti-mouse, Millipore (MAB2300)	Alexa Fluor 488, rabbit anti-mouse, Invitrogen (P36930)	1:2000

Table 2.7: Primary and secondary antibodies used in immunofluorescence

2.14 Immunohistochemistry (IHC) using 3,3'-diaminobenzidine (DAB) staining

Paraffin embedded slides were deparaffinised in Histoclear (National Diagnostics) for three, 5 minute washes. Slides were then rehydrated in ethanol for 3 minutes each using the following gradients; Histoclear: ethanol (1:1), 100%, 95%, 70%, 50% and ddH_2O. For antigen retrieval, sodium citrate (2.94g sodium citrate tribasic dehydrate, 0.5ml tween20, 1L ddH_2O, pH6) was heated to boiling point in the microwave, slides were then incubated with this heated buffer in the microwave for 20 minutes, just below boiling point. Slides were cooled in water for 5 minutes and washed twice for 5 minutes in 1xTBS-0.25% triton X (Fisher Scientific). Slides were blocked for 1 hour at room temperature in 1% donkey serum. After blocking, slides were drained and 100µl of appropriate primary antibody was diluted in TBS and added to the slides (Table 2.8). Parafilm (Sigma-Aldrich) was placed on top of the slides to prevent dehydration and these were incubated at 4°C overnight. The following day slides were washed three times for 5 minutes in TBS and then incubated with 0.3% hydrogen peroxide (Fisher Scientific) in TBS for 30 minutes to prevent any endogenous hydrogen peroxide activity. Slides underwent a further three, 5 minute washes, after which the appropriate secondary antibody was diluted in TBS and 100µl added to each slide and incubated for 1 hour at room temperature. After secondary antibody incubation, slides were washed in TBS for three, 5 minute washes. DAB (VectorLabs) reagent was made up by adding 2 drops of buffer solution to 5ml ddH_2O, 4 drops of DAB solution and 2 drops of hydrogen peroxide. Slides were incubated for 2-10 minutes, whilst colour change was observed. After the reaction had occurred slides were washed for 5 minutes in ddH_2O. Slides were then counterstained with Mayers' hematoxylin (Fisher Scientific) for 30 seconds, which was washed off and slides were then stained with 0.1% sodium bicarbonate for 30 seconds to achieve a blue stain. Slides were then dehydrated in gradients of ethanol using: 50%, 70%, 95%, 100%, Histoclear: ethanol (1:1) and Histoclear. 100µl of di-N-butyl phthalate in xylene (DPX) mounting medium (Fisher Scientific) was added to each slide then mounted onto a coverslip. These were allowed to dry for at least 1 hour before observation.

Primary antibody	Dilution	Details	Secondary antibody	Dilution
OX1R	1:75	Polyclonal anti-goat, SantaCruz Biosciences (sc-8073)	Anti-goat, peroxidase produced in rabbit, Sigma (A5420)	1:200
OX2R	1:75	Polyclonal anti-goat, SantaCruz Biosciences (sc-8074)	Anti-goat, peroxidase produced in rabbit, Sigma (A5420)	1:200
GPR103	1:75	Polyclonal anti-rabbit, SantaCruz Biosciences (sc-48187)	Anti-rabbit IgG peroxidase produced in goat, Sigma (A0545)	1:200
Pan Neuronal Marker	1:75	Monoclonal anti-mouse, Millipore (MAB2300)	Anti-mouse IgG peroxidase produced in rabbit, Dako (P0260)	1:200
$A\beta^{1-40}$	1:75	Monoclonal anti-rabbit, Cell Signalling (7672s)	Anti-rabbit IgG peroxidase produced in goat, Sigma (A0545)	1:200
$A\beta^{1-42}$	1:75	Monoclonal anti-rabbit, Cell Signalling (8243p)	Anti-rabbit IgG peroxidase produced in goat, Sigma (A0545)	1:200
Phosphorylated Tau (S214)	1:75	Monoclonal anti-rabbit, Abcam (ab10891)	Anti-rabbit IgG peroxidase produced in goat, Sigma (A0545)	1:200
Tau	1:75	Monoclonal anti-mouse, Cell Signalling (4019p)	Anti-mouse IgG peroxidase produced in rabbit, Dako (P0260)	1:200

Table 2.8: Primary and secondary antibodies used in IHC

2.15 Microarray

RNA was extracted using an RNeasy mini kit (Qiagen) according to manufacturer's instructions. Briefly, 350µl of the RLT buffer was added to each sample and vortexed. This was then pipetted into a QIAshredder spin column and centrifuged for 2 minutes at 12,000 RPM. 600µl of 100% ethanol was added to the cell lysate and mixed by vigorous pipetting. 700µl of each sample was added to an RNeasy mini spin column in a 2ml collection tube and centrifuged for 15 seconds at 10,000 RPM and flow through was discarded. This step was repeated until all the sample had been run through the column. 700µl of RW1 buffer was added to the column and centrifuged for 15 seconds at 12,000 RPM and flow through was discarded. 500µl of RPE buffer was added to each spin column and centrifuged again for 15 seconds at 10,000 RPM. Flow though was discarded and this step was repeated again and centrifuged for 2 minutes. The RNeasy column was placed into a new collection tube and centrifuged for 2 minutes at 10,000 RPM to further dry the column. The column was then placed in a new 2ml collection tube and 50µl of RNase free water was added and the column and spun for 1 minute at 10,000 RPM. RNA was then analysed on a 2100 expert Agilent bioanalyser, to confirm that all samples had an RNA yield greater than 30µg and RNA integrity number (RIN) values above 9. Whole transcriptome amplification was performed using a WTA2-transplex complete whole transcriptome amplification kit (Sigma-Aldrich) according to manufacturer's instructions with optimised volumes. Briefly, 100ng of each sample was added to 0.5µl of library synthesis solution and nuclease free water up to 3.32µl was added. Samples were mixed and incubated in a PTC-225 Pelter Thermal Cycler for 5 minutes at 70°C. For each sample the following was added: 0.5µl library synthesis buffer, 0.78µl nuclease free water and 0.4µl library synthesis enzyme. These samples were incubated in the thermocycler using the following incubations:

- 18°C for 10 minutes
- 25°C for 10 minutes
- 37°C for 30 minutes
- 42°C for 10 minutes
- 70°C for 20 minutes
- 4°C hold

Samples were briefly centrifuged at 5,000 RPM to consolidate samples. To each of these samples; 60.2µl of nuclease free water, 7.5µl of amplification mix, 1.5µl WTA dNTP mix and 0.975µl of amplification enzyme was added. This was then incubated in a thermocycler using the following incubations:

- 94°C for 2 minutes
- 94°C for 30 seconds
- 70°C for 5 minutes

} 20 cycles

- 4°C hold

An RNaseA clean-up was then performed to remove any residual RNA from the newly formed cDNA (Qiagen). 1µl of 4mg/ml RNase A solution was added to each sample and gently mixed. Samples were incubated at 37°C for 10 minutes. 163µl of phenol:chloroform:isoamyl alcohol at pH8 was added to each sample and vortexed. This was then added to phase lock tubes (5 Prime) and centrifuged at 12,000 RPM for 5 minutes, after which the upper aqueous phase was transferred to a new 1.5ml tube. cDNA precipitation was then performed. 0.1 volumes of the sample in ammonium acetate was added to each sample and mixed by inversion. 3.5µl of 5mg/ml glycogen was added and again mixed by inversion. 200µl of ice cold ethanol was added and centrifuged at 12,000 RPM for 20 minutes. The supernatant was removed and 500µl of ice cold 80% ethanol was used to dissolve the pellet which was then centrifuged again at 12,000 RPM for 5 minutes, after which the supernatant was removed. This step was repeated once more. The pellet was dried in a DNA vacuum concentrator: CentriVap DNA Centrifugal Concentrator System 220V (Labconco), and the samples were rehydrated in 20µl of nuclease free water. Samples were analysed on the NanoDrop to confirm that 260/280 and 260/230 absorbance readings were above 1.8 and that concentration was more than 100ng/µl. Samples were then analysed on the bioanalyser to check fragment size.

Samples were labelled with Cy3 dye, using a Cy3 labelling kit (Nimblegen). Into a 0.2ml PCR tube; 0.5µg of cDNA, 20µl of Cy3 random nonamers and water up to 40µl was added. The samples were denatured in a thermocycler for 10 minutes at 98°C then quick chilled for 2 minutes on ice. 5µl dNTP mix, 4µl nuclease free water and 1µl of klenow fragment was added to each sample and pipetted up and down

thoroughly. This was then incubated in the thermocycler at 37°C for 2 hours. Once finished 10.75µl of stop solution was added. To elute the samples 55µl of isopropanol was added at room temperature and protected from sunlight for 10 minutes. This was centrifuged at 12,000 RPM for 10 minutes at 4°C and then the supernatant was discarded. The pellet was rinsed with 500µl of 80% ice cold ethanol and centrifuged at 12,000 RPM for 10 minutes, after which the supernatant was removed. Samples were dried in a DNA vacuum concentrator on a low heat until dry. Pellets were then rehydrated in 25µl of water and vortexed for 30 seconds or until the pellet was rehydrated. Samples were again analysed on the NanoDrop to check concentration and quality. Samples were aliquoted into 4µg total concentration and contents were dried in a DNA vacuum concentrator.

The next step was to hybridise the cDNA to the array and wash the array. The Roche Nimblegen Hybridization System 4 was set to 42°C and left for 3 hours to stabilise. Samples were resuspended in 3.3µl of sample tracking control solution to confirm the sample identity. Samples were vortexed and to each sample the following was added; 6.1µl 2x hybridisation buffer, 2.42µl hybridisation component A and 0.2µl alignment oligo. Samples were vortexed and incubated at 95°C for 5 minutes in the thermocycler, then at 42°C for 5 minutes. Using a precision mixer alignment tool slides were combined with a HX12 mixer. The mixer-slide assembly was heated at 42°C for 5 minutes, and then placed in the slide bay of the hybridisation system. 6µl of sample was added to each appropriate port for the 12 samples. The slides were then mixed in the hybridisation system for 10 minutes and samples were hybridised at 42°C for 16 hours. Following this the slide was washed using a wash buffer kit (Nimblegen). Wash I was made up of 243ml ddH_2O, 27ml of 10x wash buffer I and 27µl 1M DTT. Then another wash I, II and III was made up using 24.3ml ddh_2O, 2.7ml 10x wash buffer I, II or III and 2.7µl of 1M DTT. The first wash I solution was heated to 42°C and the mixer-slide was placed into a mixer disassembly tool in the wash solution and the mixer was removed from the slide. The slide was then washed for 2 minutes in new wash I solution with gentle agitation. The slide was drained and blotted and added to wash solution II for 1 minute with vigorous constant agitation, then transferred to wash solution III for 15 seconds with vigorous constant agitation.

The slide was then spin dried in a Nimblegen microarray dryer for 30 seconds. The array was now ready for scanning.

Dr. Ryan Pink from Oxford Brookes University then scanned the Nimblegen array slide at 3µM on an InnoScan 700 microarray scanner using Mapix version 5.1 software. The TIFF images were then aligned to their Nimblegen design files and converted into probe intensity values using the Nimblegen DEVA software. The data was Loess normalised for array variation of Cy3 using R statistical program. This was quintile normalised across array variation using DNAstar (ArrayStar). The log2 intensity values were formatted using excel.

2.16 Statistical analysis

All data sets were analysed using the Levene's test to test for equal or unequal variance. If the variance was deemed to be unequal and the data was unpaired the Mann-Whitney-U test was performed. If variance was equal and the data was unpaired, then the unpaired students T test was performed. For paired data, if there was equal variance the paired students T test was used. For unequal variance with paired data, the Wilcoxon signed-rank test was performed.

3

Chapter 3

Differentiation and validation of two human neuroblastoma cell lines

3.1 Introduction

IMR32 and SH-SY5Y are human neuroblastoma cell lines which resemble immature neuroblasts in cell culture. IMR32 is a cell line established from an abdominal mass of brain tissue origin in a 13 month old male. The adherent culture is a mixture of two morphologically distinct cell types. The predominant cell is neuroblastic (N-type) and is a small neuroblast like cell which grows in dense collections. The other cell type is a large fibroblast like cell which grows in small quantities in comparison to the N-type cell (Tumilowicz et al. 1970).

SH-SY5Y is a clone of SK-N-SH cells derived from a bone marrow biopsy of neuroepithelial origin from a 4 year old female with neuroblastoma. The SH-SY5Y cell line contains 2 distinct phenotypes: N-type and substrate adherent (S-type) cells. The majority of the culture comprises N-type cells and there are only a small number of S-type cells (Encinas et al. 2000; Biedler, Helson & Spengler 1973). IMR32 and SH-SY5Y have been extensively used as neuronal models and appear to express numerous functional GPCRs including OXRs (Nasman et al. 2006; Chen, Randeva 2010).

These cell lines are at an early differentiation stage and consequently do not display the morphology, inhibited cell division and neuronal markers that are seen with mature neurons (Xie, Hu & Li 2010). As a consequence these cell lines are limited in

studying the mechanisms which occur in mature neurons. It was therefore necessary to differentiate these cell lines using specific differentiating agents to create a neuronal model that exhibits more *in vivo* like characteristics. Differentiation is required to encourage the expression of phenotypic properties characteristic of a mature neuron *in vivo*. This process is irreversible and results in termination of DNA synthesis (Scheibe, Ginty & Wagner 1991). After differentiation it is necessary to validate this model using a wide array of techniques to corroborate differentiation.

3.2 Objectives

Due to extensive work previously performed in IMR32 and SH-SY5Y combined with comprehensive use of these cell lines in previous AD and OXR research it was decided these would be the most appropriate cell lines to use (Nasman et al. 2006; Chen, Randeva 2010; Esmaeili-Mahani et al. 2013). Differentiation using BrdU for IMR32 and RA for SH-SY5Y is necessary to initiate cellular differentiation (Kurata et al. 1993; Korecka et al. 2013). RA causes upregulation of key genes known to be involved in differentiation and neuronal development including; neural cell adhesion molecule 2 (*NCAM2*), tropomyosin receptor kinase B (*TrkB*) as well as transcription factors required for differentiation including: nuclear receptor coactivator 7 (*NCOA7*) and aristaless-like homeobox 3 (*ALX3*) (Korecka et al. 2013; Encinas et al. 2000). During differentiation the N-type cells develop long processes, however the S-type cells do not undergo morphological change and the proportion of N-type cells to S-type cells increases during differentiation (Encinas et al. 2000). IMR32 differentiation is induced by BrdU, through mechanisms which are less clear. Validation of the models was achieved by monitoring cellular proliferation and neurite extension, a Pan Neuronal marker antibody to assess the expression of key neuronal proteins and qPCR to confirm the presence of crucial neuronal genes.

3.3 Results

3.3.1 Morphological changes and cell counts to monitor growth of differentiated cell lines

10µM BrdU was used to differentiate IMR32 for 20 days to acquire a neuronal phenotype (Nasman et al. 2006). SH-SY5Y cells were treated with 10µM RA for 6 days (Encinas et al. 2000; Cheung et al. 2009). Morphological changes and cell numbers for both cell lines were monitored during the differentiation process using microscopy and cell counts.

IMR32 cells were passaged at days: 0, 2, 4, 6, 8, 12, 16 and 20 to prevent over-confluence and were seeded at $1x10^6$ cells. Cell counts were performed as 3 independent experiments.

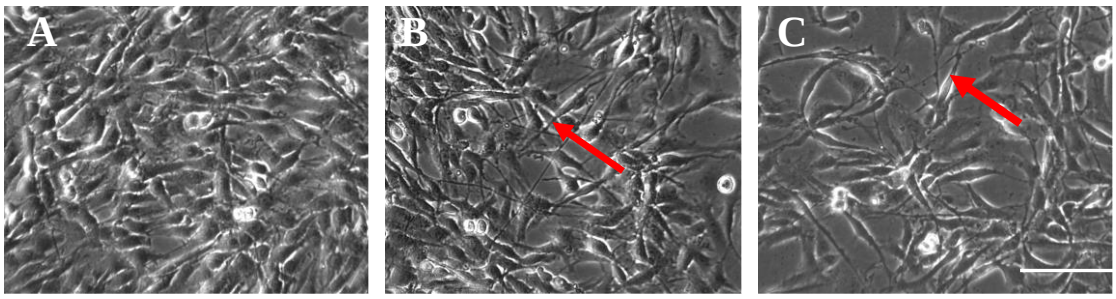

Figure 3.1: Representative images of IMR32 differentiation achieved through treatment with 10µM BrdU, which induces a more neuronal phenotype with neurite extensions and reduced confluence. x20 maginifcation. Bars = 100µm.

A) undifferentiated cells. **B**) 6 days 10µM BrdU. **C**) 20 days 10µM BrdU.

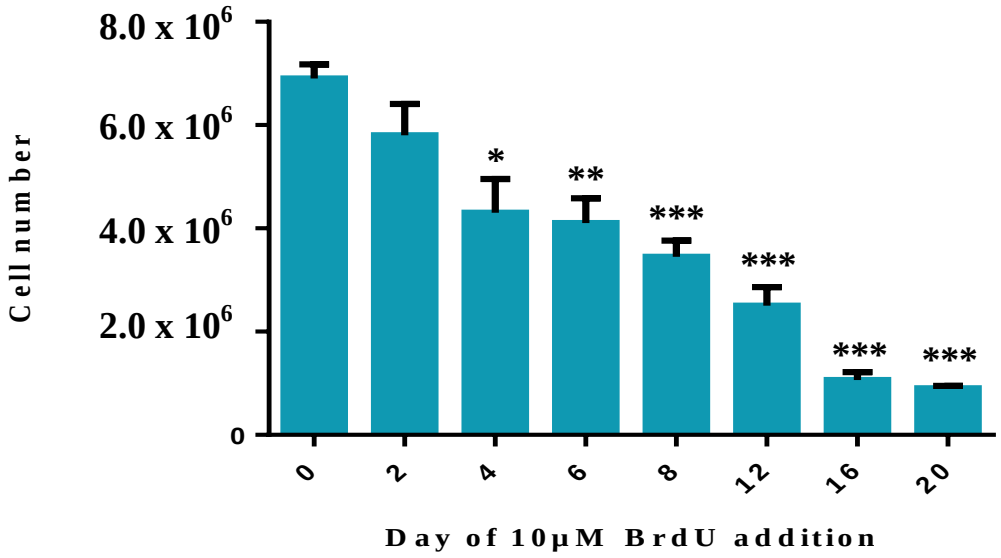

Figure 3.2: IMR32 cell numbers when seeded at $1x10^6$ at specific time intervals. Results were obtained from 3 independent experiments ±S.D. Statistically significant differences of differentiated cells compared to undifferentiated cells were calculated using the unpaired T-test ($p<0.05$*, $p<0.01$**, $p<0.001$***)

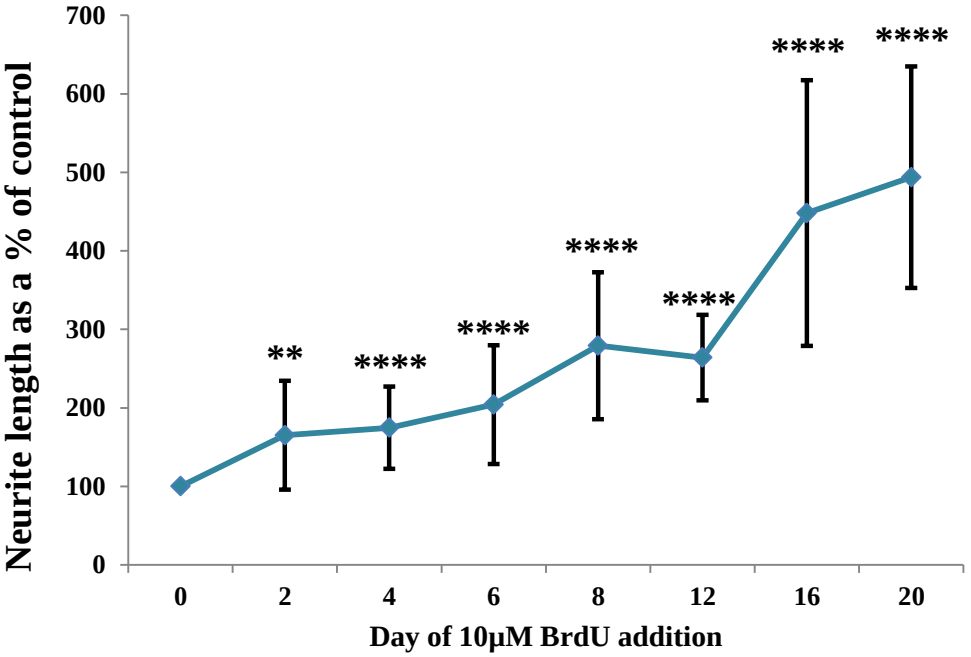

Figure 3.3: Average neurite length calculated as a percentage change compared to undifferentiated cells of the longest neurite extension of 19 IMR32 cells over 20 days of 10µM BrdU differentiation measured by ImageJ ±S.D. Statistically significant differences of differentiated cells compared to undifferentiated cells were calculated using the paired students T-test ($p<0.01$**, $p<0.0001$****).

IMR32 cells have a fibroblast like morphology with short cytoplasmic processes called neurites. Morphological changes instigated by differentiation included cells becoming less rounded, increased neurite extension and the cessation of proliferation. This was supported not only by morphological changes (Figure 3.1) but cell counts (Figure 3.2) and measurement of neurite length (Figure 3.3). Neurite length was measured using the NeuriteJ plug-in for ImageJ. The longest neurite of 19 different cells was measured and an average for each day was taken. This was then normalised to the undifferentiated control to calculate the percentage increase at each measurement compared to a control. This indicated an overall increase in neurite length of nearly 500% over the differentiation process. Both cell growth and neurite extension plateaued from day 16 suggesting that maximal differentiation had been reached.

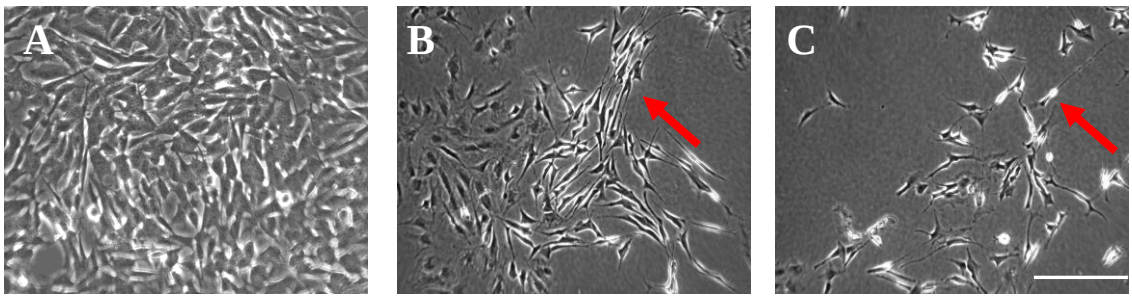

Figure 3.4: Representative images of SH-SY5Y differentiation achieved through treatment with 10µM retinoic acid, which induces a more neuronal phenotype with neurite extensions and reduced confluency. x10 maginifcation. Bars = 200µm.

A) undifferentiated cells. B) 2 days 10µM RA. C) 6 days 10µM RA.

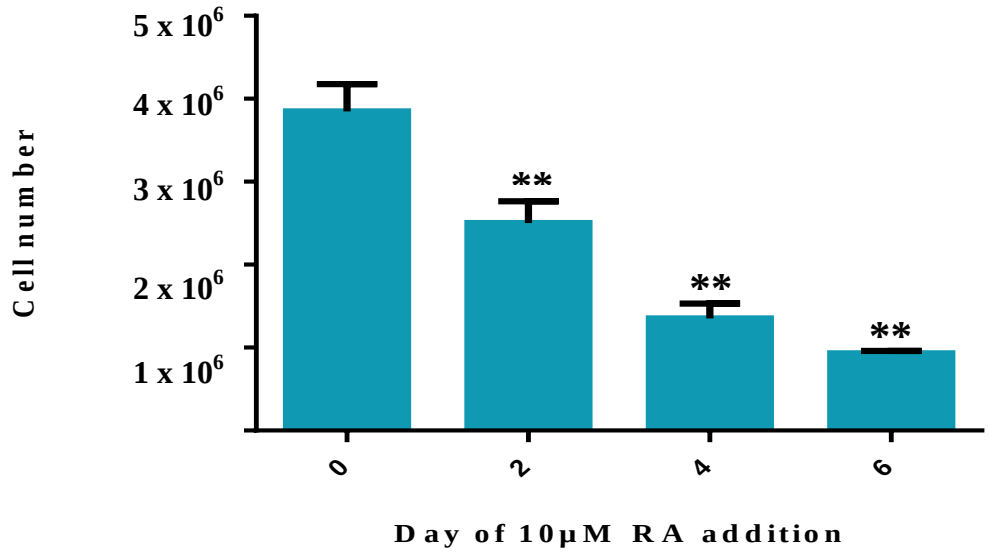

Figure 3.5: SH-SY5Y cell numbers when seeded at $1x10^6$ at specific time intervals. Results were obtained from 3 independent experiments ±S.D. Statistically significant differences of differentiated cells compared to undifferentiated cells were calculated using the unpaired T-test ($p<0.01$**).

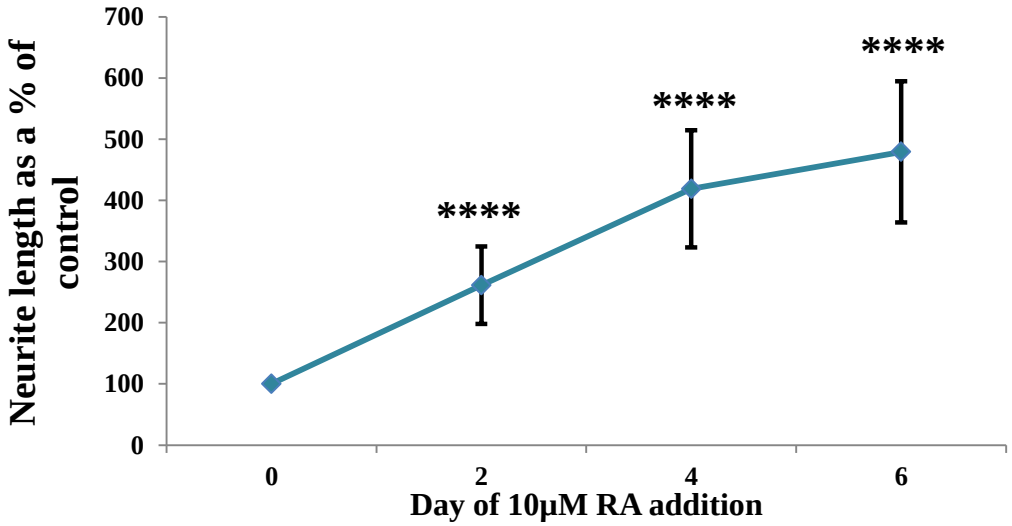

Figure 3.6: Average neurite length calculated as a percentage change compared to undifferentiated cells of the longest neurite extension of 24 SH-SY5Y cells over 6 days of 10µM RA differentiation, measured by ImageJ ±S.D. Statistically significant differences of differentiated cells compared to undifferentiated cells were calculated using the paired students T-test ($p<0.0001$****).

SH-SY5Y cells were seeded at $1x10^6$ at days 0, 2 and 4. Cell counts were performed as 3 independent experiments. Undifferentiated SH-SY5Y cells were fast growing and without extensions. After differentiation cells did not reach confluence and neurite extensions were prominent. Changes are evident from as early as day 2, where cells are fewer in number and significantly lower compared to the control as well as the formation of neurite extensions. By day 6 neurite extensions are obvious and cells remain sparse compared to day 0 (Figure 3.4) Cell numbers decreased significantly during differentiation and remained fairly constant between day 4 and day 6 (Figure 3.5).

Neurite length was also measured using the NeuriteJ plug-in for ImageJ. The longest neurite of 24 individual cells was measured and an average for each day was taken. This was then normalised to the undifferentiated control to calculate the percentage increase at each measurement compared to a control. Neurite extension in SH-SY5Y saw a steady and gradual significant increase until day 4 after which it began to plateau and by day 6 cells demonstrate nearly 500% increased neurite length compared to the control, indicative of widespread cellular differentiation (Figure 3.6).

3.3.2 Immunofluorescence of differentiated and undifferentiated cells using a Pan Neuronal marker antibody

A Pan Neuronal marker was used in differentiated and undifferentiated cells in order to study changes in fundamental somatic, nuclear, dendritic and axonal proteins. Many of these proteins are expressed throughout the cells including in the neurites. Figures 3.7 and 3.8 demonstrate that in undifferentiated cells, there are very low amounts of key neuronal proteins, however after differentiation both cell lines show an increase in antibody signal with increased intensity of staining and also increased neurite length. This change is observed in both IMR32 and SH-SY5Y.

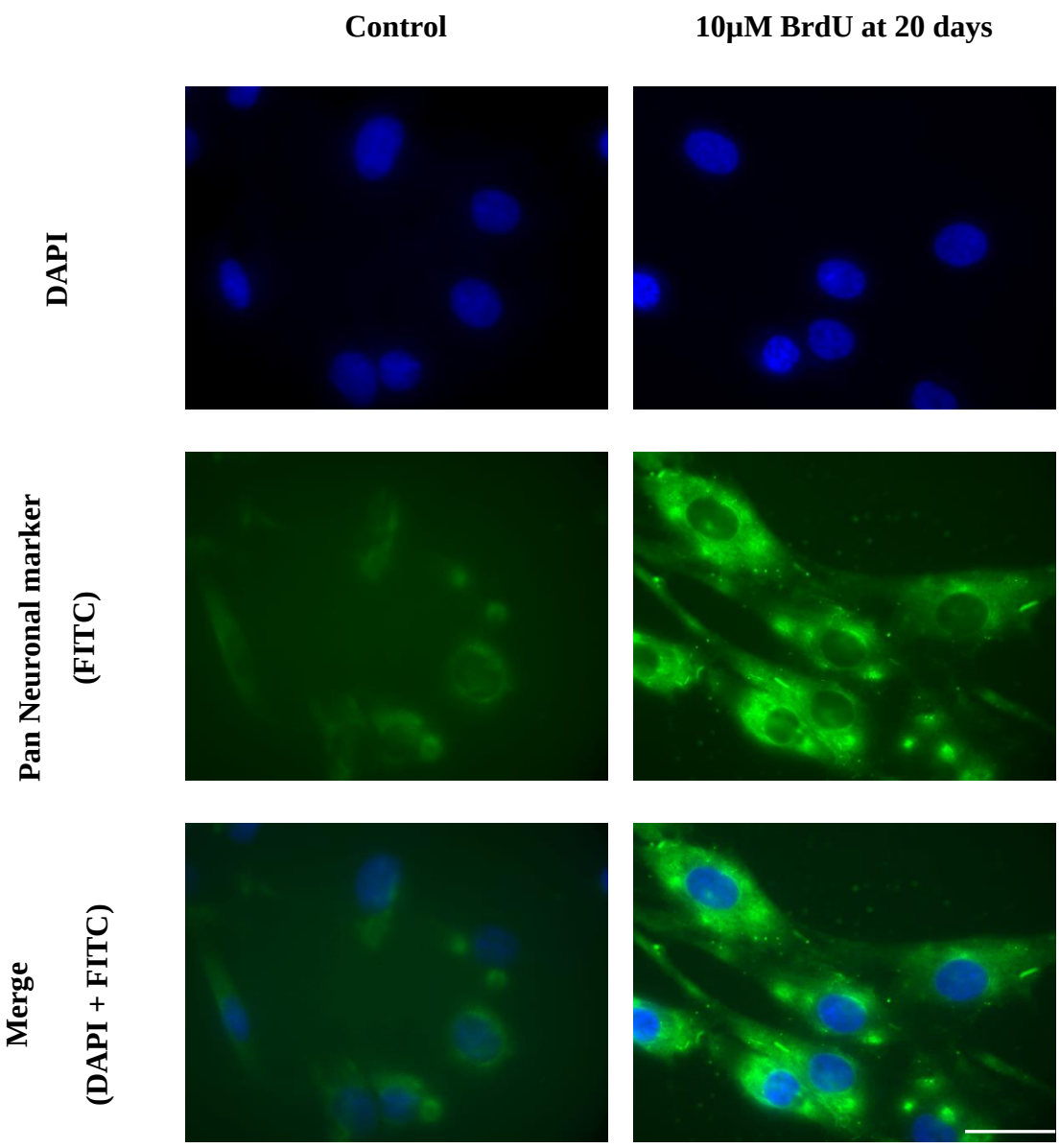

Figure 3.7: Immunostaining using a Pan Neuronal marker in undifferentiated IMR32 cells and after 20 days of 10µM BrdU differentiation. x40 magnification. Bars = 50 µm.

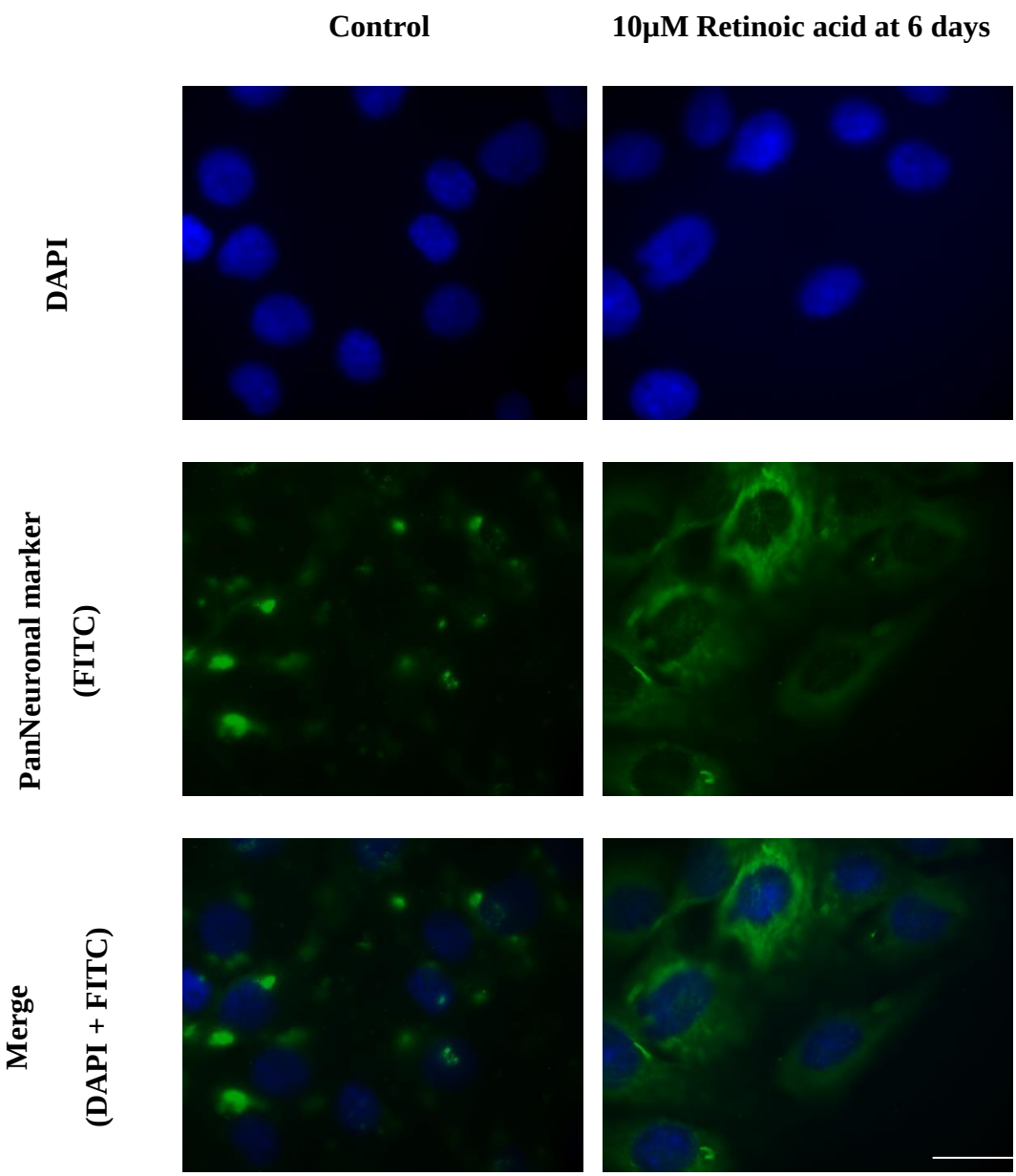

Figure 3.8: Immunostaining using a Pan Neuronal marker in undifferentiated SH-SY5Y cells and after 6 days of 10µM RA differentiation. x40 magnification. Bars = 50 µm.

3.3.3 GeNorm analysis of differentiated and undifferentiated cell lines

It is imperative that analysis of gene expression data be normalised to a fixed reference gene which exhibits consistent expression under experimental conditions as well as this being compliant with the Minimum Information for Publication of Quantitative Real-Time PCR Experiments (MIQE) guidelines (Bustin et al. 2009). The GeNorm array from PrimerDesign provides 12 human housekeeping genes to discern their expression under different experimental procedures. Data is then analysed using the qBASE software to identify which genes are the most stable and the optimum number of housekeeping genes to be used for the experimental model. This analysis issues an M value for each gene. The M value signifies the variance between given samples, and the lower a value the more stable the gene. It is recommended that anything below 1.5 is a stable gene. This is also used in accordance with a generated V value, which takes into account the M values and recommends the optimal number of genes to be used. IMR32 and SH-SY5Y GeNorm data was concurrently analysed so that the same housekeeping genes could be used for all qPCR to provide more consistency.

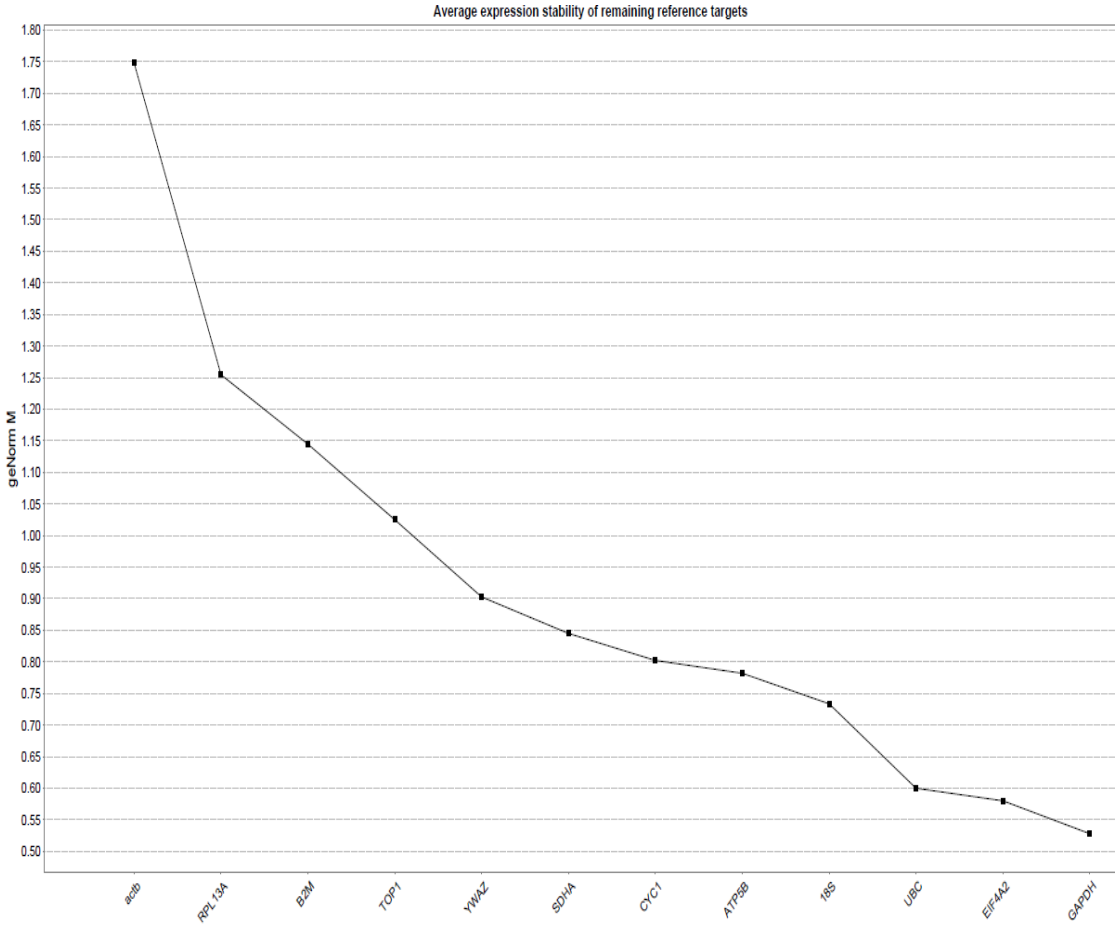

Figure 3.9: Representation of the most stable housekeeping genes through GeNorm analysis in undifferentiated and differentiated IMR32 and SH-SY5Y using GeNorm M values. GeNorm M values indicate gene instability between samples; therefore higher values indicate more variation. Using the qBase software we were able to identify *GAPDH*, *EIF4A2*, *UBC* and *18s* as being the most stable genes.

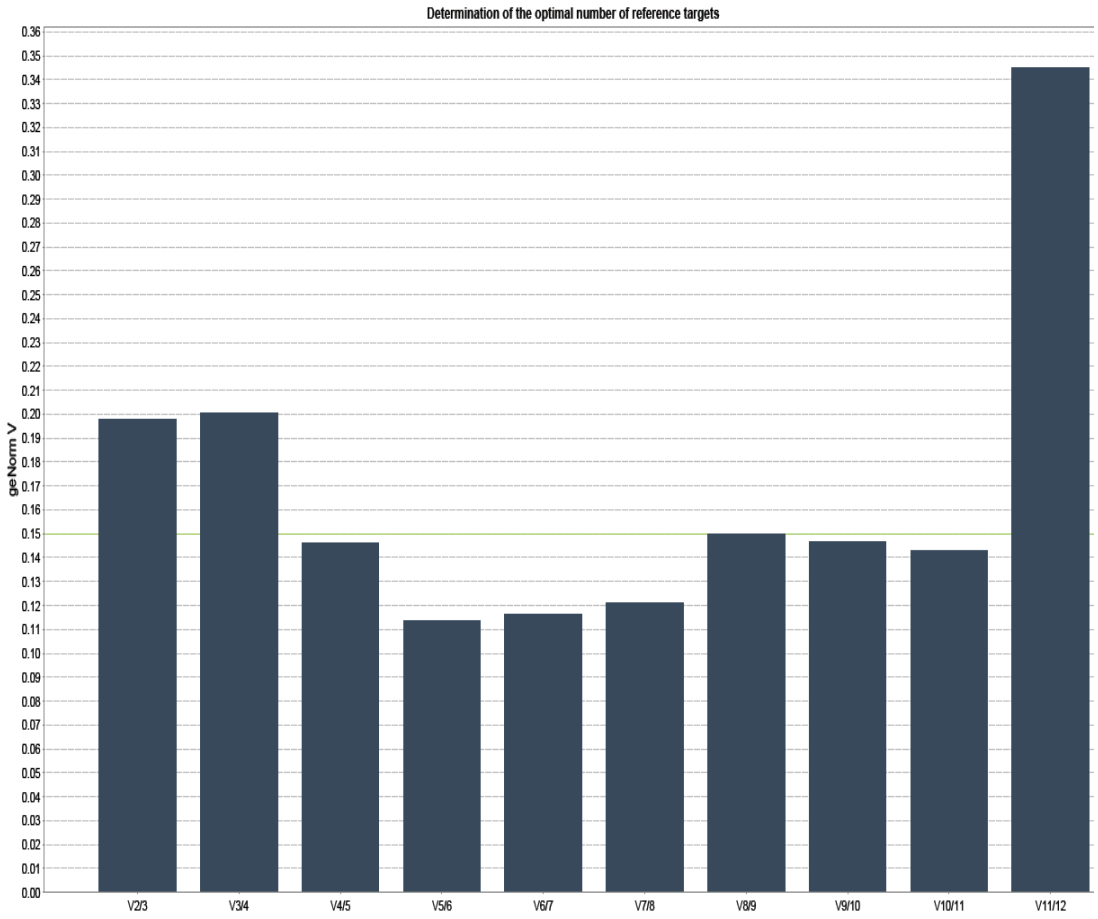

Figure 3.10: Recommended number of housekeeping genes using GeNorm for IMR32 and SH-SY5Y. Higher GeNorm V values indicate optimum number of housekeeping genes. The qBase software recommended the use of 2-4 reference genes when using these samples for qPCR.

Analysis of GeNorm performed on these samples suggested that 2/3 housekeeping genes should be used with glyceraldehyde 3-phosphate dehydrogenase (*GAPDH*) (M value = 0.52) and eukaryotic initiation factor 4A-II (*EIF4A2*) (M value = 0.62) being the most stable genes (Figure 3.9 and 3.10). However *18S* was also indicated as being stable with an M value of 0.75 which was very similar to the recommended *EIF4A2* and as we had already successfully used and validated *18S* in our lab this was decided to be an acceptable gene to use. Using 3 housekeeping genes is excessive so the lower end of the suggestion of 2 was used.

3.3.4 qPCR of undifferentiated and differentiated cDNA to display changes in neuronal marker gene expression

Nestin (*NES*), neuron specific enolase (*NSE*), microtubule-associated protein tau (*MAPT*) and neurogenin 1 (*NG1*) were used as neuronal markers. They have previously been used to confirm changes in neuron specific markers during neuroblastoma differentiation (Cheung et al. 2009; Constantinescu et al. 2007).

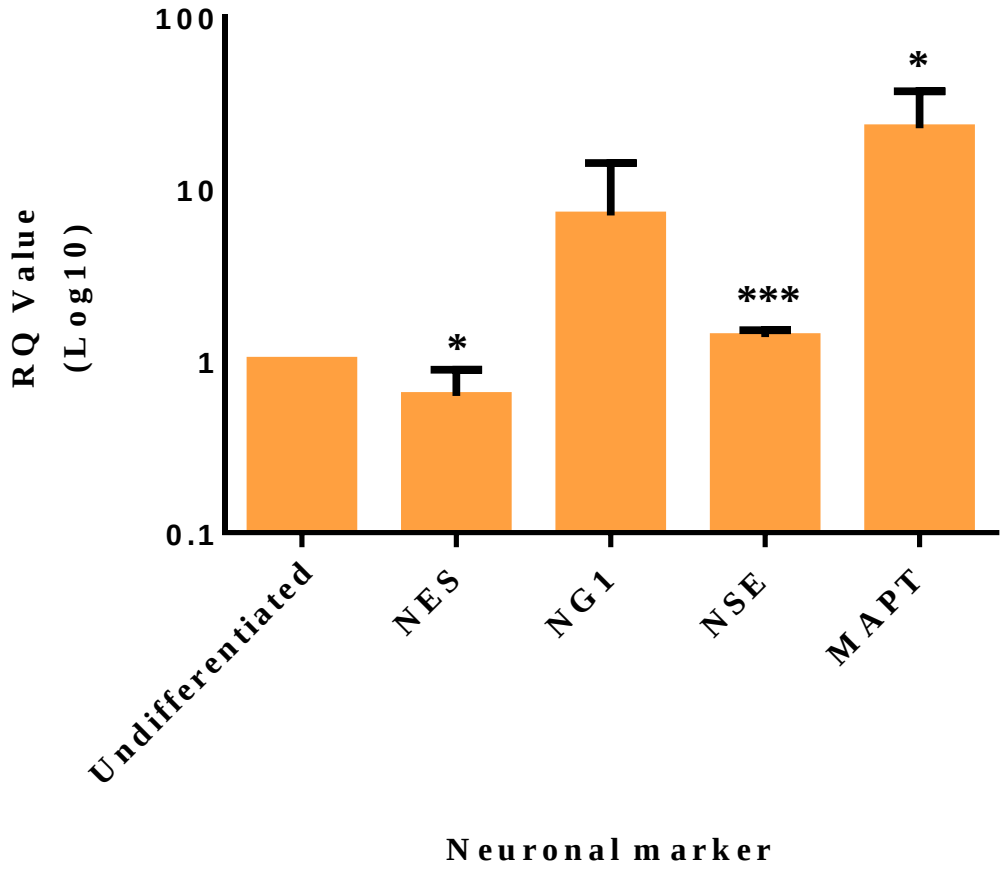

Figure 3.11: Graph representing gene expression changes of neuronal markers after 20 days of IMR32 differentiation compared to undifferentiated samples. Results were obtained from 2 independent experiments ±S.D. Statistically significant differences of differentiated cells compared to undifferentiated cells were calculated using the paired students T-test ($p<0.05$*, $p<0.001$***).

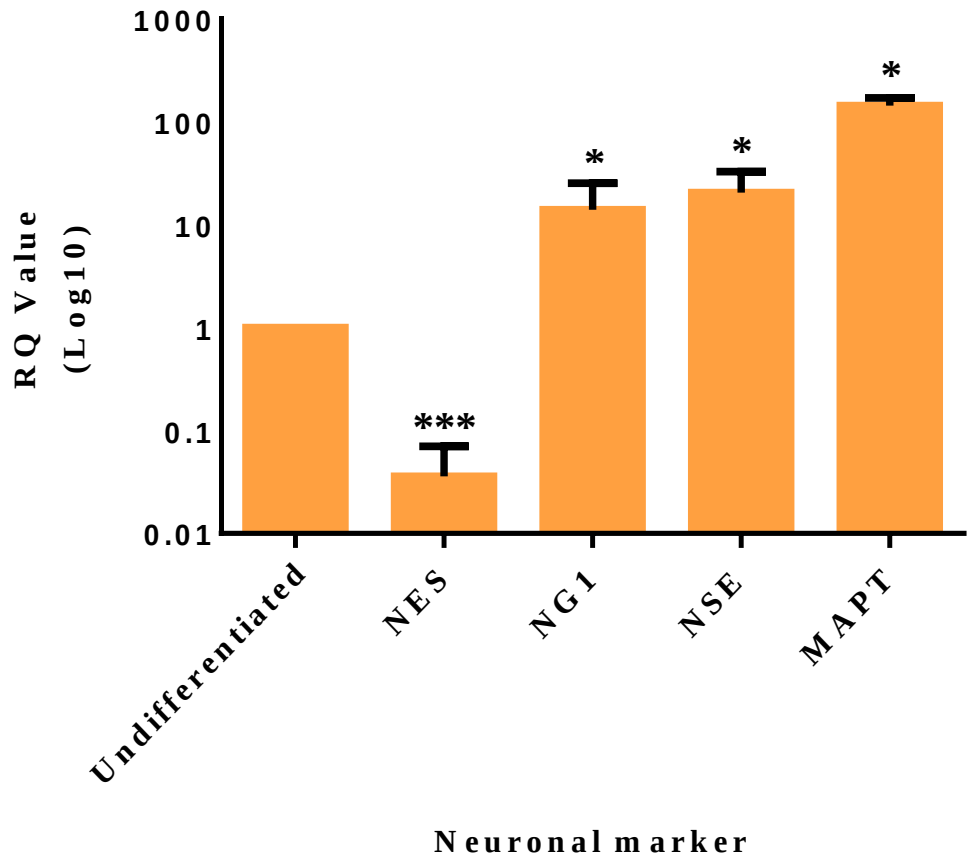

Figure 3.12: Graph representing gene expression changes of neuronal markers after 6 days of SH-SY5Y differentiation compared to undifferentiated sample. Results were obtained from 2 independent experiments ±S.D. Statistically significant differences of differentiated cells compared to undifferentiated cells were calculated using the paired students T-test ($p<0.05$*, $p<0.001$***).

qPCR analysis showed a significant decrease in *NES* gene expression in both cell lines, suggestive of a reduction in dividing neuronal cells. *NSE*, *MAPT* and *NG1* were all increased, with all being significantly increased in SH-SY5Y and *NSE* and *MAPT* being significantly increased in IMR32. Combined with reduced *NES* this expression profile suggests neuronal differentiation.

3.4 Results and Discussion

Many disease mechanisms involved in AD affect the structure as well as signalling pathways in neurons, thus it is essential to achieve a model that best represents the *in*

vivo environment in order to acquire meaningful data from a human cell line. Immortalised cell lines are an appropriate solution to study this, but they do however lack some of the key characteristics of human neurons such as morphology, cessation of mitosis and expression of neuronal markers. The transition to a more neuronal phenotype is vital for mimicking disease or a signalling milieu *in vitro*.

IMR32 cells grow as a predominantly N type cell, which is a small neuroblast like cell. It displays neuronal characteristics and exhibits adrenergic and cholinergic phenotypes and over expresses N-myc proto-oncogene protein (MYCN) (Koutsilieri et al. 1996). It has been shown to secrete APP including $A\beta^{1-42}$, but expresses $A\beta^{1-40}$ as its predominantly secreted Aβ peptide as would be expected in a non-disease situation. It secretes Aβ in large quantities compared to other Aβ secreting cell lines such as the human neuroblastoma cell line: SK-N-SH (Asami-Odaka et al. 1995). SH-SY5Y cells display some neuronal characteristics in their native form and are small and triangular shaped with short neurite extensions. They express a cholinergic and adrenergic phenotype, monoamine transporters and express tyrosine hydroxylase (Korecka et al. 2013; Biedler et al. 1978; Dwane, Durack & Kiely 2013; Agholme et al. 2010). These hallmarks make both cell lines a realistic model to be used in our *in vitro* studies.

Differentiation of both cell lines resulted in termination of mitosis which is reflected in the cell counts performed. IMR32 experienced a steady decline in cell number over time and a plateau at day 16 until day 20 which suggests terminal differentiation. SH-SY5Y also experienced the same trend but over a much shorter time span with a plateau of cells at day 4. Another indicator of differentiation is neurite extension. For both cell lines there was a significant increase in length over time when normalised to the undifferentiated control. IMR32 neurite length increased by 493% when compared to the control with SH-SY5Y experiencing much the same increase in neurite length with a 479% increase in extension by day 6. Although the starting neurite lengths were different between cell lines they both achieved a nearly 5 fold increase in length compared to undifferentiated cells. This neurite extension is particularly important when observing tau hyperphosphorylation as it resides in these extensions.

A Pan Neuronal marker targeted against key somatic, nuclear, dendritic and axonal proteins present in a mature neuron was also used to confirm differentiation. Some of these proteins would be present in an undifferentiated cell as they are of neuronal origin. However assuming differentiation confers a more neuronal phenotype, expression of these proteins will become increased upon differentiation. Undifferentiated cells displayed low levels of the Pan Neuronal maker which was localised to the nucleus and cytoplasm. After differentiation was completed, expression was markedly higher and expressed in vaster quantities in the nucleus, cytoplasm and newly formed neurites, confirming that differentiation using this protocol causes upregulation of key neuronal proteins.

qPCR was then performed to observe the expression of 4 genes implicated in neuronal differentiation. These were; *NES, NSE*, *MAPT* and *NG1*. NES is a class VI intermediate filament protein which is important in cellular migration, cell cycle regulation and is a neural stem cell marker. NES has been shown to be down regulated when neuroepithelial stem cells differentiate into neurons and is expressed transiently in nerve cells as they undergo mitosis (Thomas et al. 2004). As cells differentiate NES expression decreases as it is replaced with tissue specific intermediate filaments such as glial fibrillary acidic protein (Thomas et al. 2004). In neuroblastoma elevated NES levels correlate with tumour aggressiveness and in antisense NES transfected cells; population doubling time is increased by 60% (Dahlstrand, Collins & Lendahl 1992; Thomas et al. 2004). NES is known to be expressed in undifferentiated IMR32 and SH-SY5Y cell lines (Thomas et al. 2004; Mahller et al. 2009). Both cell lines experienced a reduction in *NES* expression that was significant compared to undifferentiated cells suggesting these intermediate filaments were replaced with other neurofilaments indicative of a termination of proliferation. *NG1* encodes the protein Neurogenin1 which is a transcription factor which contributes to the initiation of neuronal differentiation and neurogenesis and as a consequence is highly expressed in the mature neuron and upon cellular differentiation (Constantinescu et al. 2007; McCormick et al. 1996). In both cell lines *NG1* expression was increased compared to undifferentiated cells and was significantly increased in SH-SY5Y, further suggesting these cells had progressed to

mature neurons. *NSE* was also used as a marker of differentiation, which encodes the neuron specific enolase protein, an enzyme involved in glycolysis and it is the predominant enolase found in neural tissue and is only expressed in differentiated neurons (Constantinescu et al. 2007). It has previously been shown to be upregulated in IMR32 and SH-SY5Y which have undergone differentiation (Cheung et al. 2009; Thomas, Hartley & Mason 1991). This was significantly increased in both cell lines after differentiation treatment suggesting differentiation had indeed occurred. The fourth marker of differentiation used was *MAPT*, which encodes the protein tau which is expressed in the distal portion of axons. Tau is a microtubule associated protein which acts to stabilise microtubules within axons, aid in axonal development and in transportation (Munoz-Montano et al. 1999). Due to the limited length of neurites in undifferentiated cells and the neurite growth that occurs with differentiation, tau expression has been shown to increase after differentiation in both cell lines (Munoz-Montano et al. 1999; Jamsa et al. 2004). It has also been reported that neuroblastoma cell lines lack mature isoforms of tau, however when they are differentiated tau expression increases significantly compared to undifferentiated cells reaching levels comparable to the human brain (Agholme et al. 2010). Both cell lines displayed a significant increase in MAPT expression, with over a 20 fold increase for IMR32 and 145 fold increase for SH-SY5Y. This amplification is explained by the observed increase in neurite length for both cell lines and tau being expressed in the distal portion of neurite extensions.

Differentiation was accomplished to ensure accurate representation of an *in vivo* phenotype for future experimental procedures. To ensure validation cell morphology was observed and neurite extension was measured, which displayed a significant increase in differentiated cells. Using a Pan Neuronal marker and performing qPCR of 4 neuronal markers we confirmed that differentiation of these cells had occurred and that they were exhibiting a more neuronal phenotype whilst expressing increased neuronal proteins and could therefore be used as a more realistic neuronal model.

4

Chapter 4

Expression and signalling characteristics of OXR and GPR103 in differentiated and undifferentiated IMR32 and SH-SY5Y cell lines

4.1 Introduction

Mitogen activated protein kinases (MAPK) are a superfamily consisting of three major groups, notably: extracellular-receptor kinases (ERK), p38 and stress-activated protein kinase/c-Jun kinase (SAPK/JNK). ERK is composed of two proteins: ERK1 and ERK2, which share 83% sequence homology and are expressed in all tissues (Cruz, Cruz 2007). Activation of the ERK or ERK1/2 pathway is involved in proliferation, survival and metabolism (Roux, Blenis 2004). Ligand binding causes the small GTPase Ras to exchange a GDP for a GTP which leads to binding to Raf kinase resulting in its activation which can now phosphorylate proteins. Raf kinase phosphorylates MAP kinase kinases (MEK) 1 and 2. Upon ligand binding MEK 1 and 2 become phosphorylated which then results in phosphorylation of ERK at two tyrosine and threonine residues and both must be phosphorylated for full activation of MEK and ERK (Cruz, Cruz 2007). ERK1/2 can then initiate its downstream effects. ERK is associated with cellular survival through activation of the cAMP response element binding protein (CREB) and the mammalian target of rapamycin (mTOR). CREB is important in activation of cell survival genes and also mTOR through translational control (Guo, Feng 2012). In a suprachiasmatic nucleus rat cell line which is resistant to the toxic effects of glutamate, treatment with an ERK inhibitor rendered them susceptible to toxicity of glutamate and thus shows that ERK

activation can negate neurotoxic effects (Karmarkar et al. 2011). This is of particular relevance as glutamate toxicity is an important hallmark of AD (Butterfield, Pocernich 2003; Greenamyre et al. 1988). ERK is also implicated in AD, as activation of CREB regulates genes involved in memory and synaptic plasticity (Liu et al. 2013). Deregulation of MAPK can be a contributing factor to brain degeneration as evidenced in mice with Aβ induced amnesia that experienced a reduction in ERK1/2 activation (Liu et al. 2013).

ERK1/2 activation through OXRs has been most extensively studied in CHO cell lines over expressing OXR. However signalling mechanisms for OXR can vary by cell type and as OXs function mainly within the brain these systems may not be the best representation (Ammoun et al. 2006a; Hilairet et al. 2003). To our knowledge ERK1/2 signalling through OXRs and GPR103 has not been mapped in these human neuroblastoma cell lines.

4.2 Objectives

As previously shown, treating IMR32 and SH-SY5Y with differentiating agents induced changes in gene expression. It was therefore necessary to confirm that the receptors of interest were still being expressed after differentiation had occurred using immunofluorescence and qPCR. Differentiated cells were then treated with 100nM of OXA, OXB or QRFP to determine whether they activated ERK1/2 to assess the functionality of these receptors and thus potential roles in neuroprotection. Cells were also treated with these peptides in the presence of their receptor inhibitors to establish that any possible changes in ERK1/2 activation were indeed caused as a direct result of addition of the peptides and their specificity to the receptors. Changes in ERK1/2 were determined using western blot analysis.

4.3 Results

4.3.1 Immunofluorescence of differentiated and undifferentiated cells with OX1R, OX2R and GPR103 antibodies observe changes in their expression

Differentiated and undifferentiated cells were seeded at $1x10^5$ on glass coverslips and were allowed to proliferate for 1 day. Immunofluorescence was then performed as

previously described. DAPI is a fluorescent dye which strongly binds to areas of DNA rich in adenine-thymine (A-T) regions allowing identification of the nucleus (Zink, Sadoni & Stelzer 2003). Tetramethylrhodamine (TRITC) and fluorescein isothiocyanate (FITC) are dyes capable of binding to a primary antibody and producing a fluorescent signal for detection using fluorescent microscopy (Johnson, Cushman & Malekzadeh 1990).

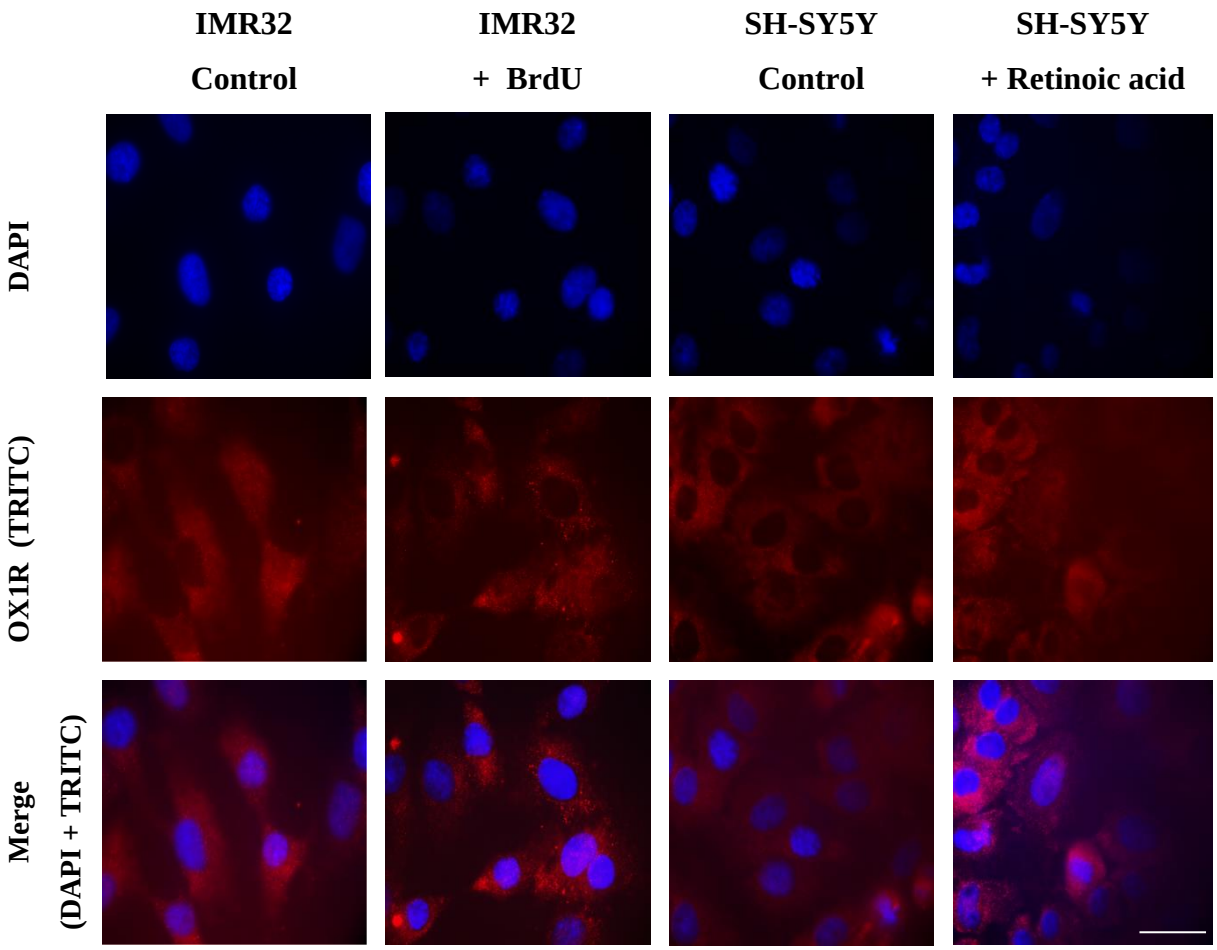

Figure 4.1: Immunostaining using an OX1R antibody in undifferentiated IMR32 and SH-SY5Y cells before and after differentiation. x40 magnification. Scale bar = 50μm.

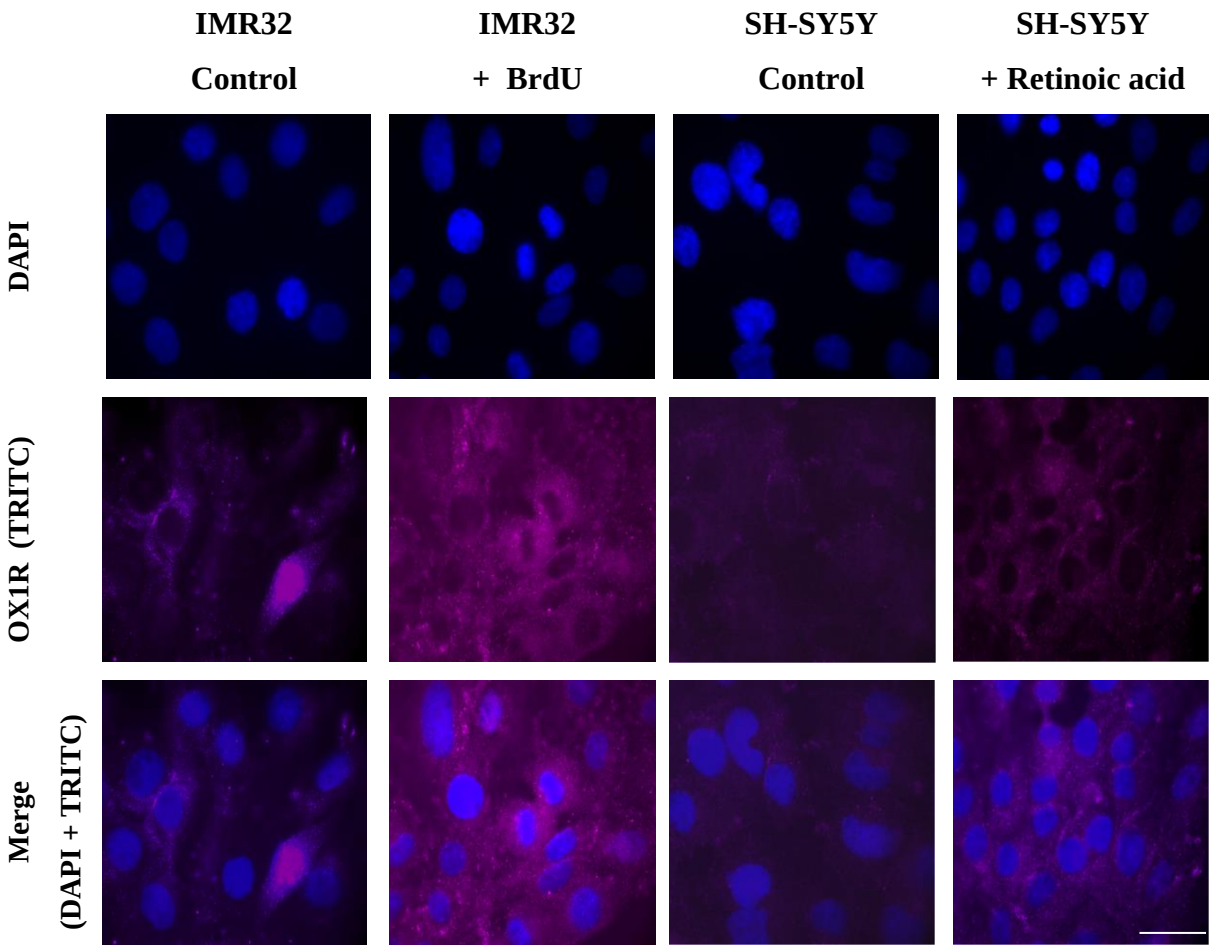

Figure 4.2: Immunostaining using an OX2R antibody in undifferentiated IMR32 and SH-SY5Y cells before and after differentiation. x40 magnification. Scale bar = 50μm.

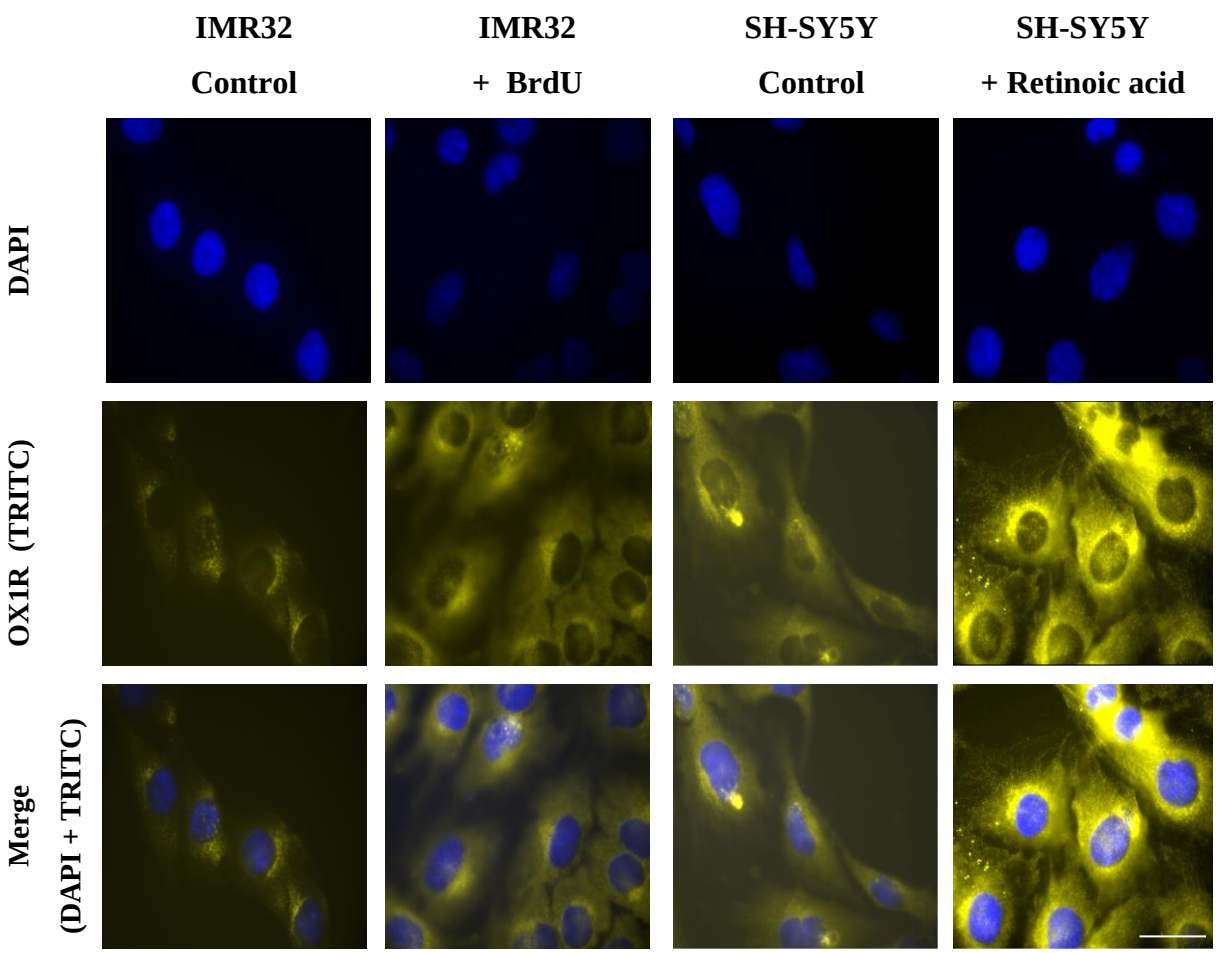

Figure 4.3: Immunostaining using a GPR103 antibody in undifferentiated IMR32 and SH-SY5Y cells before and after differentiation. x40 magnification. Scale bar = 50μm.

Immunoflourescent analysis of IMR32 and SH-SY5Y revealed that before differentiation OX1R, OX2R and GPR103 were expressed throughout the cells. Following differentiation, immunostaining for OX1R and OX2R remained similar without any obvious changes in cellular distribution or intesnity. GPR103 however appeared to show an increase in immunoflourescent staining and appeared more widely distirbuted after differentiation. ImageJ was then used to quantify the flourescence intensity in a given area. 50 cells were quantified for each cell line and each antibody, before and after differentiation. The background flourescence was compensated for and the fold change between undifferentiated and diferentiated cells was calculated (Figure 4.4). This revealed an increase in all of the receptors in both

cell lines. Although IMR32 experienced an increase in receptors, it was not as pronounced as in SH-SY5Y but was significantly increased for OX2R and GPR103. SH-SY5Y cells revealed a significant increase in expression of all of the receptors compared to the undifferentiated control.

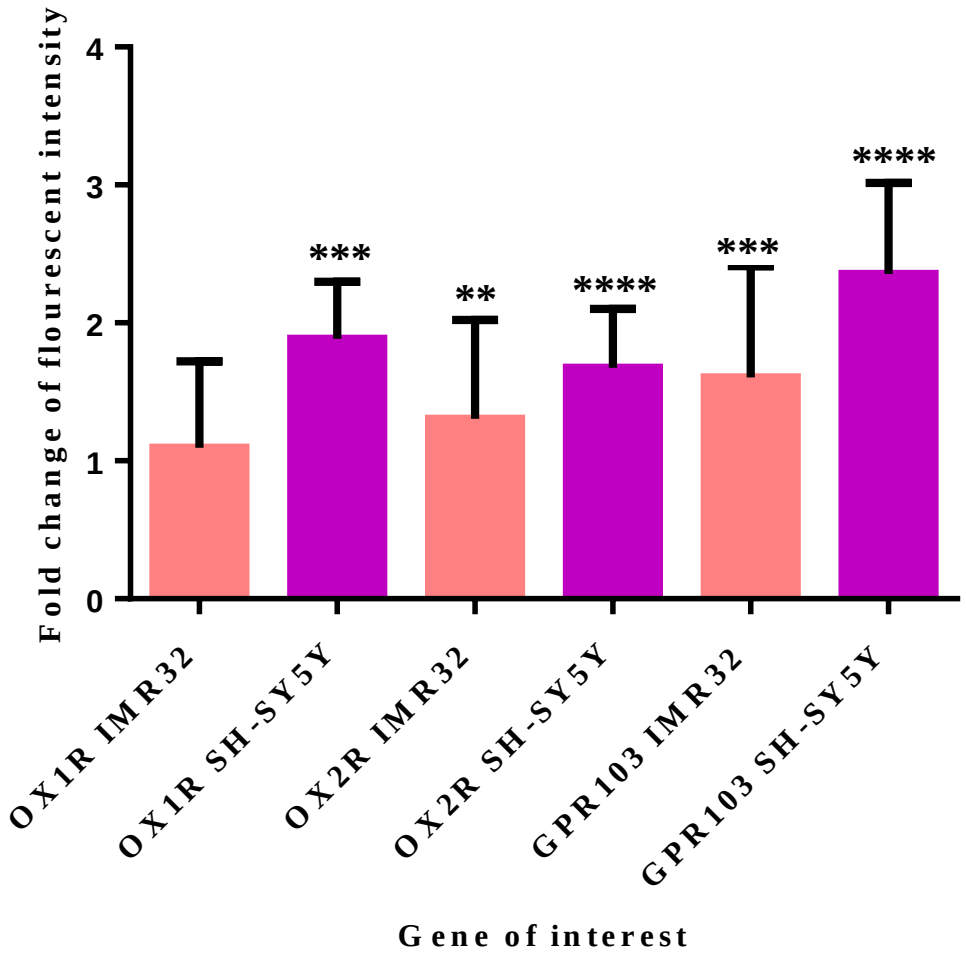

Figure 4.4: Immunoflourescent intensity was measured using ImageJ before and after differentiation and the fold change was calculated compared to the undifferentiated cells ±S.D. N=50 cells. Statistically significant differences of differentiated cells compared to undifferentiated cells were calculated by performing the paired students T- Test ($p<0.01$**, $p<0.001$***, $p<0.0001$****).

4.3.2 qPCR of differentiated and undifferentiated cell lines to observe gene expression changes in OX1R, OX2R and GPR103.

qPCR was performed on the receptors of interest to confirm the previous immunofluorescence results and obtain a better quantitative representation at mRNA level. Primers as previously described were used for *OX1R*, *OX2R* and *GPR103*.

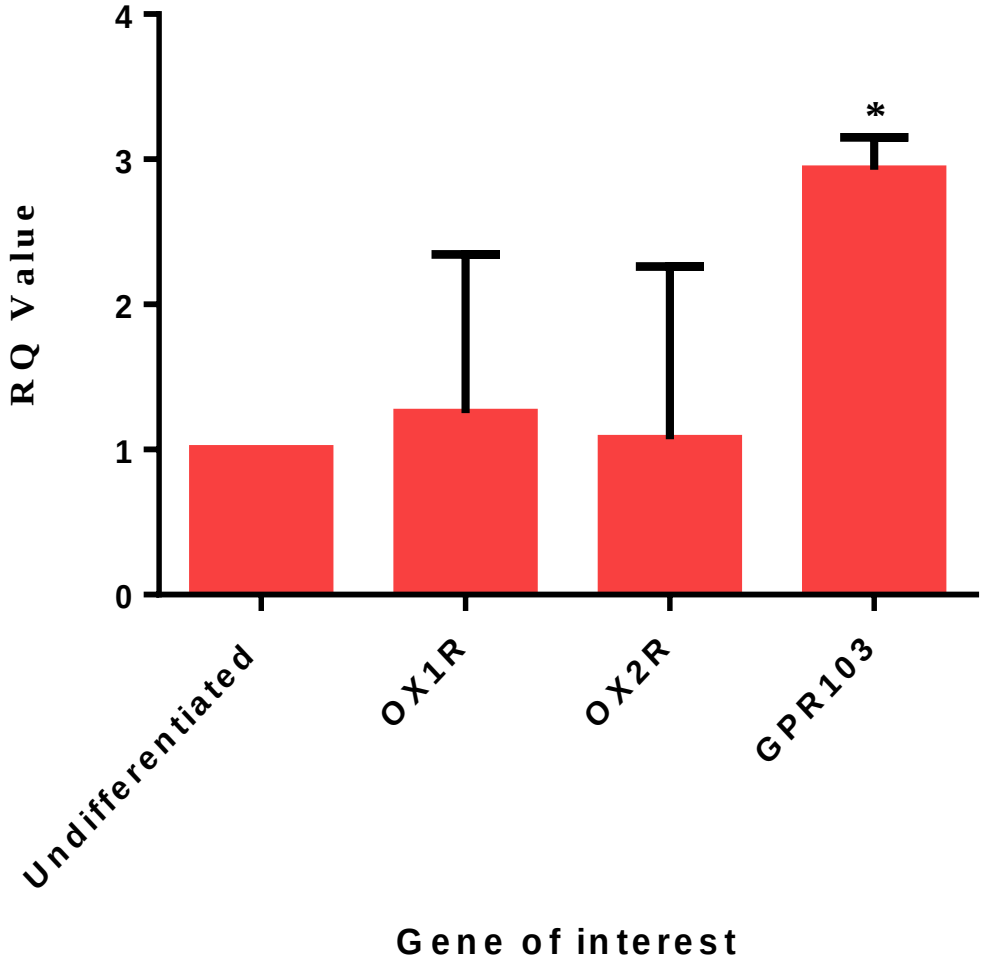

Figure 4.5: Graph representing gene expression changes of *OX1R*, *OX2R* and *GPR103* after 20 days of IMR32 differentiation compared to undifferentiated samples. Results were obtained from 3 independent experiments ±S.D. Statistically significant differences of differentiated cells compared to undifferentiated cells were calculated using the paired students T test ($p<0.05$*).

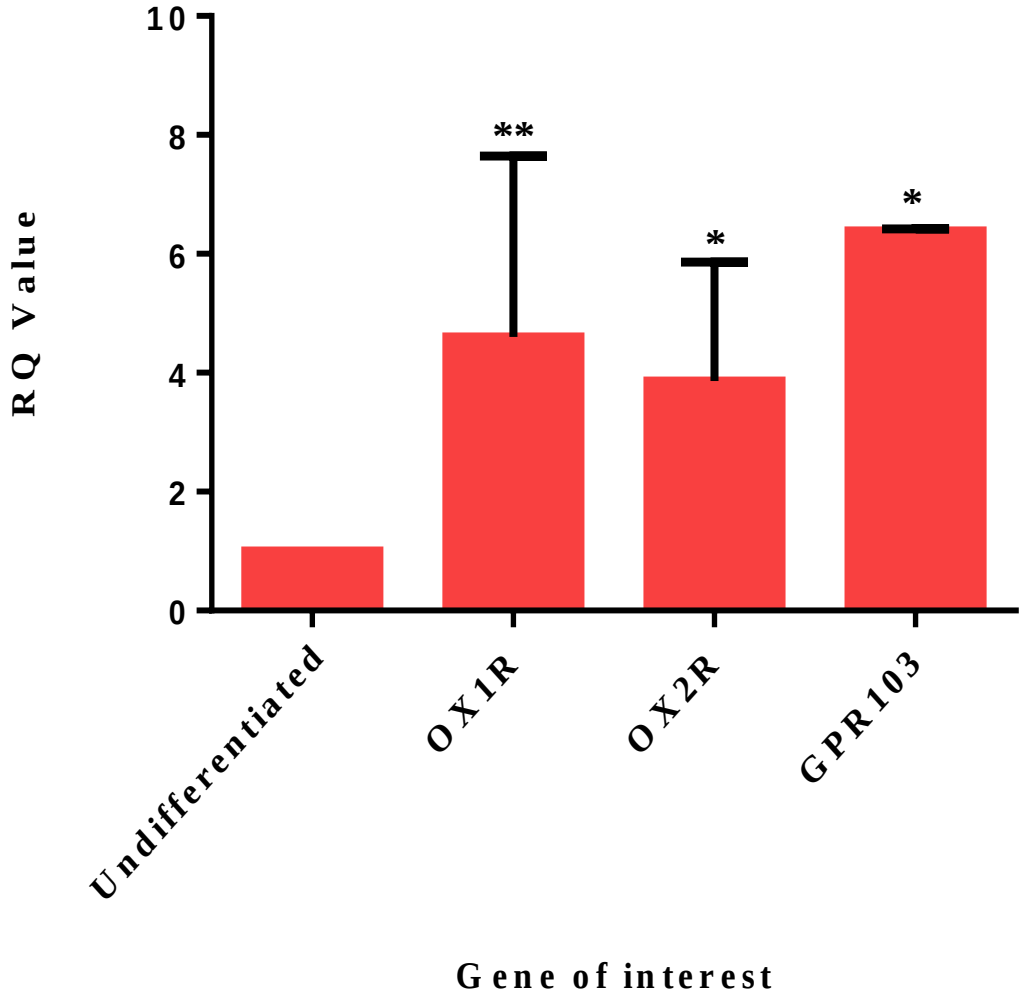

Figure 4.6: Graph representing gene expression changes of *OX1R*, *OX2R* and *GPR103* after 6 days of SH-SY5Y differentiation compared to undifferentiated samples. Results were obtained from 3 independent experiments ±S.D. Statistically significant differences of differentiated cells compared to undifferentiated cells were calculated using the paired students T test ($p<0.05$*, $p<0.01$**).

The data revealed that in both cell lines expression of *OX1R*, *OX2R* and *GPR103* increased compared to undifferentiated cells (Figure 4.5 and 4.6). However in IMR32 for OX1R and OX2R, the changes were not significant indicating steady expression of receptors before and after differentiation. This is somewhat consistent with the immunofluorescence data which revealed minimal changes in OX1R, however showed a significant increase for OX2R. GPR103 was significantly

increased upon differentiation when measured by immunofluorescence at nearly a 2 fold increase and qPCR with a 3 fold increase. Conversely SH-SY5Y cells experienced a significant increase in all receptors compared to undifferentiated cells in agreement with the immunofluorescence data.

4.3.3 ERK1/2 activation in IMR32 and SH-SY5Y cells after OXA, OXB and QRFP treatment.

To verify receptor functionality and confirm the activation of ERK1/2 in OXR and GPR103 signalling in mature neurons fully differentiated cell lines were treated with 100nM OXA, OXB or QRFP for time points of up to an hour. Cells were also treated with antagonists to ensure that any changes in ERK1/2 were specific to the receptor. The antagonists used were: SB-334867 (SB) and TCS OX229 (TCS). SB is a selective OX1R antagonist and binds with 50x higher affinity compared to OX2R. The antagonist TCS has a selectivity for OX2R 250x that of OX1R. In CHO cells OXA has an IC50 of 20nM for OX1R and 38nM for OX2R. It is therefore necessary to inhibit the activity of both of these receptors to prevent the action of OXA though binding to OX2R when it is unable to bind to OX1R. OXB has an IC50 of 420nM for OX1R and 36nM for OX2R. So although it has a low affinity for OX1R, in the absence of OXA and presence of an OX2R antagonist it may bind in small quantities to OX1R which could exert an effect (Sakurai et al. 1998). Given that both receptors are highly expressed in these cell lines and because OXs can potentially activate both receptors it was decided to use a combination of both OXR inhibitors in an attempt to block the action of both GPCRs and thus demonstrate receptor specificity. These concentrations were deemed appropriate as they have already been demonstrated to inhibit OXRs at this concentration (Huang et al. 2010). Given that GPR103 exerts orexigenic activities and shows 48 and 47% amino acid homology with OX1R and OX2R respectively, cells were treated with QRFP and each of the antagonists individually (Jiang et al. 2003).

For each treatment western blot analysis was performed using a phosphorylated ERK1/2 (p-ERK1/2) antibody and normalised to a total-ERK1/2 (t-ERK1/2) antibody. Blots were then analysed using ImageJ to quantify the optical densitometry (OD) of each band. Representative images of the blots are shown in figure 4.7.

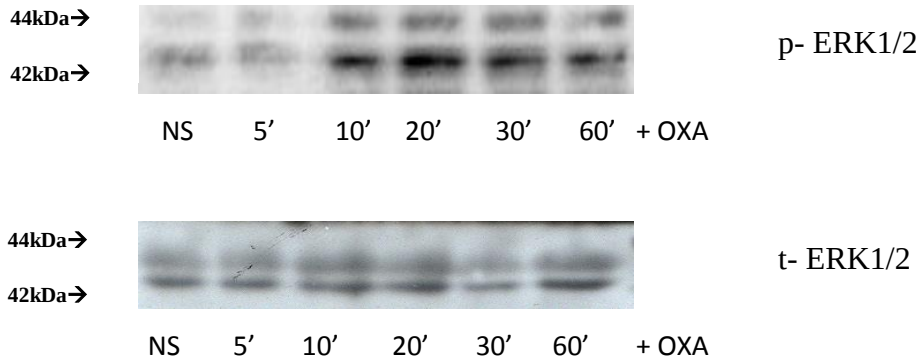

Figure 4.7: Representation of western blots probed with p-ERK1/2 and t-ERK1/2 antibodies.

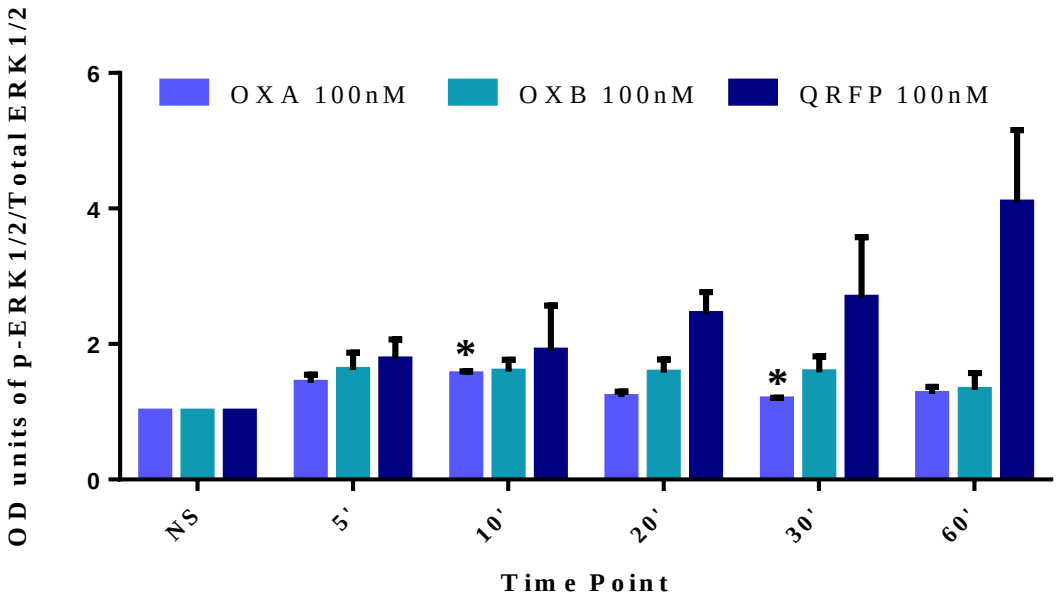

Figure 4.8: Densitometric analysis of differentiated IMR32 cells using ImageJ, of p-ERK1/2 protein normalised to t-ERK1/2 protein and displayed as OD units. Cells were treated with 100nM of OXA, OXB or QRFP for time points of up to an hour. Results were obtained from 3 independent experiments ±S.E.M. Statistically significant differences of treated cells compared to untreated cells were calculated using the paired student T test ($p<0.05$*).

IMR32 treatment of cells with OXA and OXB separately, revealed an increase in p-ERK1/2 from 5 to 10 minutes (Figure 4.8) and from 20 minutes there was an increase compared to control but it was less substantial than at 10 minutes. QRFP revealed a steady increase in p-ERK1/2 over the hour. OXA and OXB induced a similar degree of p-ERK1/2 activation; however QRFP induced much higher and sustained levels of activation than OX.

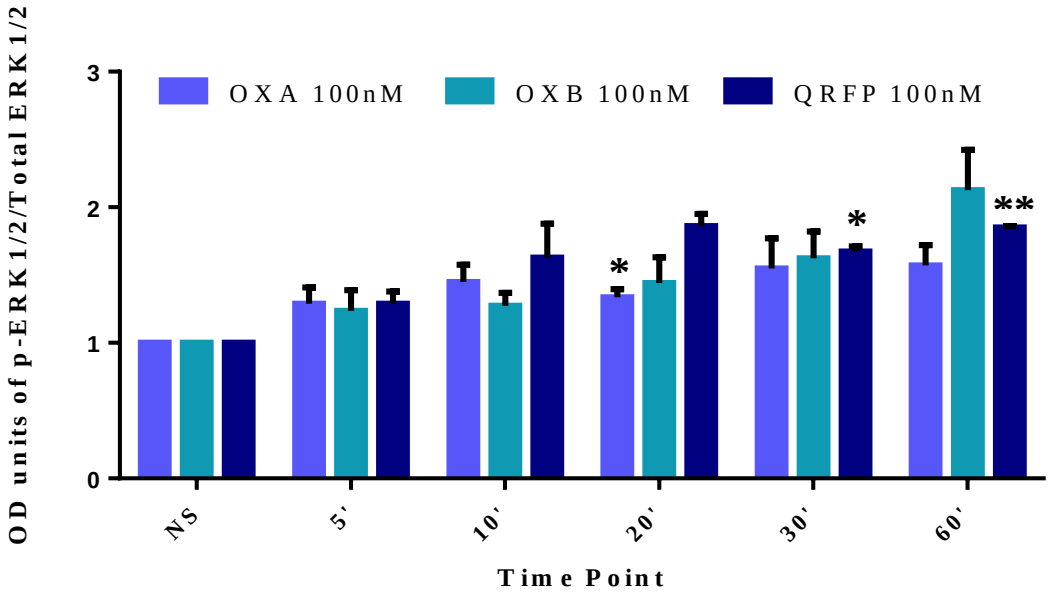

Figure 4.9: Densitometric analysis of differentiated SH-SY5Y cells using ImageJ, of p-ERK1/2 protein normalised to t-ERK1/2 protein and displayed as OD units. Cells were treated with 100nM of OXA, OXB or QRFP for time points of up to an hour. Results were obtained from 3 independent experiments ±S.E.M. Statistically significant differences of treated cells compared to untreated cells were calculated using the paired student T test ($p<0.05$*, $p<0.01$**).

For SH-SY5Y the pattern was slightly different compared to IMR32, as all three agonists induced a steady increase in p-ERK1/2 over the 60 minutes. However after 20 minutes, OXB induced more activation than OXA and this continued until 60 minutes (Figure 4.9). QRFP exhibited a steady increase in p-ERK1/2 over 60

minutes, however after 20 minutes the activation plateaued and remained steady until 60 minutes. The increase in activation was significant compared to the basal levels at 30 and 60 minutes.

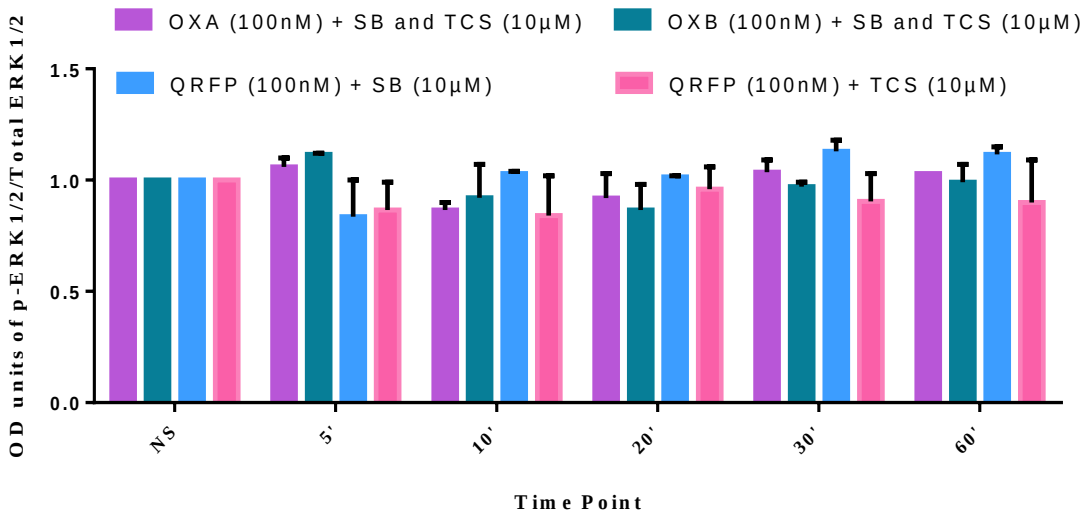

Figure 4.10: Densitometric analysis of differentiated IMR32 cells using ImageJ, of p-ERK1/2 protein normalised to t-ERK1/2 protein and displayed as OD units. Cells were treated with 100nM of OXA, OXB or QRFP in the presence of the OXR antagonists SB and TCS, for time points of up to an hour. Results were obtained from 2 independent experiments ±S.E.M.

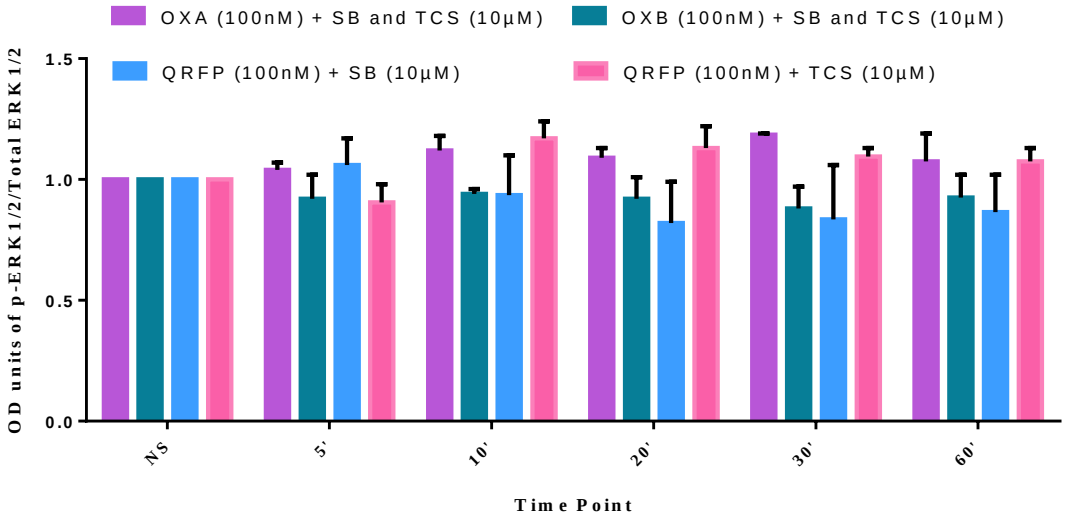

Figure 4.11: Densitometric analysis of differentiated SH-SY5Y cells using ImageJ, of p-ERK1/2 protein normalised to t-ERK1/2 protein and displayed as OD units. Cells were treated with 100nM of OXA, OXB or QRFP in the presence of the OXR antagonists SB and TCS, for time points of up to an hour. Results were obtained from 2 independent experiments ±S.E.M.

The use of OXR antagonists in these experiments revealed specificity for the receptors and that OXA and OXB induced p-ERK1/2 increases were blocked by the use of both of the antagonists together. This inhibition of the receptors was maintained across all of the time points. QRFP treatment of the cells with the antagonists individually revealed an inhibition of QRFP signaling across all of the time points. The same was true in both cell lines, although slight deviation from the basal control, the changes were negligible for all treatments (Figure 4.10 and 4.11).

4.5 Results and discussion

As previously described the differentiation process used in both IMR32 and SH-SY5Y results in genotype changes and OXR and GPR103 signalling has not yet been mapped in these cell lines at this stage. It was therefore necessary to confirm that OXR and GPR103 were still being expressed and thus the effects of these receptors could be monitored. Confirmation was achieved by examining expression at gene and protein level through immunofluorescence and qPCR. IMR32 OX1R

immunofluorescent expression appeared to remain consistent after differentiation and this was confirmed with ImageJ analysis of cells revealing that fluorescence in differentiated cells was 1.09 fold higher than in undifferentiated cells. qPCR analysis revealed a 1.5 fold increase in expression corroborating a slight increase. OX1R expression in SH-SY5Y cells appeared more intense upon differentiation and fluorescent analysis revealed a 1.89 fold significant increase after differentiation, although qPCR revealed a 5 fold significant increase compared to undifferentiated cells. Importantly, both analyses where in agreement with an increase in expression at gene and protein level. OX2R expression by immunofluorescence increased significantly after differentiation and fluorescence analysis revealed a 1.3 fold increase in differentiated cells, which corroborates with the qPCR data which revealed no change in expression. However for SH-SY5Y fluorescence intensity of OX2R showed a significant increase of 1.8 fold compared to undifferentiated cells and qPCR suggested there was a 3 fold significant increase. GPR103 fluorescence for both cell lines was noticeably upregulated from their undifferentiated counterparts. IMR32 revealed a 1.7 fold increase and SH-SY5Y a 2.5 fold increase in fluorescence intensity which correlates with the increase in expression as evidenced by qPCR of significant increases of 3 fold in IMR32 and 6 fold in SH-SY5Y. This discrepancy in data may be explained by qPCR examining a larger body of cells and being far less subjective than measuring fluorescent intensity. It must also be noted that changes at gene level do not necessarily manifest themselves as an exact representation at protein level and gene changes may take longer to become apparent at protein level as mRNA is translated into protein. GPCRs are synthesised at the endoplasmic reticulum (ER). Assembled receptors are then transported in ER-derived vesicles to the ER-golgi intermediate complex, the golgi apparatus and then the trans-golgi network (Duvernay, Filipeanu & Wu 2005). It is during this process where post-translation modification occurs. Receptors finally migrate to the plasma membrane where they can become fully functional. GPCRs can be internalised and recycled back to the membrane or degraded by lysosomes. This balance of export, endocytosis and degradation dictates the amount of receptor expressed at the membrane and the effect ligand binding will elicit (Duvernay, Filipeanu & Wu 2005). This GPCR trafficking may explain the vast distribution seen in the

fluorescence intensities of the OXRs and GPR103. As some of the expression will be on the plasma membrane as receptors are functional, but some may be cytoplasmic as receptors are being transported to the membrane or being recycled. It was previously shown that differentiation treatment of these cells caused changes in a plethora of genes it stands to reason that the genes of interest may also be subject to the same variations. Immunofluorescence and qPCR indicated stable expression of OXRs and GPR103 in both cell lines after differentiation and thus suitability for *in vitro* experiments examining the effects of OX and GPR103.

The majority of OXR G protein studies have been performed in CHO cells, which may be limited in its elucidation as the mechanisms do not necessarily translate to neuronal OX signalling. OXR activation causes activation of PLC through its coupling to the G protein Gq. This leads to catalysis of the breakdown of PIP2 to IP_3 and DAG. IP_3 causes calcium release from intracellular stores which activates PKC (Willie et al. 2001; Smart et al. 1999). Calcium and PKC allow the opening of voltage gated calcium channels which stimulates a calcium influx and results in membrane depolarisation (Yan et al. 2008, Ozcan et al. 2010) . Studies have shown that OX1R in BIM cells (a nerve like cell line) did not couple to pertussis toxin sensitive G proteins, however OX2R did couple to them and thus means that it can also couple to the inhibitory G proteins Gi/o. This Gi/o coupling will result in a potassium efflux and cell membrane hyperpolarisation, contradictory to the depolarisation incurred by coupling to Gq (Zhu et al. 2003; Beuckmann, Yanagisawa 2002; Spinazzi et al. 2006). Although OXR signalling has been studied extensively in some cell lines there is much less data regarding the brain. In a rat brain stem OXRs couple to Gi/o and in the rat hypothalamus to Gs and Gq. However it has been shown that OXRs are very promiscuous and differentially couple to G proteins in different tissues (Karteris et al. 2005). It has also been shown in CHO overexpressing OXR that the ERK pathway is activated upon agonist stimulation (Ammoun et al. 2006a; Guo, Feng 2012). In H295R (a human adrenocortical cell line) the ERK pathway was partially activated through AC when treated with OXA and OXB possibly through coupling to Gs and also through Gq coupling to hydrolyse PIP2 into DAG and IP_3 leading to PKC activation and thus ERK activation (Ramanjaneya et al.

2009). PKC inhibition in the cell line prevents any OXA mediated ERK phosphorylation (Wenzel et al. 2009). In cultured rat astrocytes PKC inhibitors prevented ERK1/2 phosphorylation suggesting that in a neuronal model ERK1/2 phosphorylation is achieved through the PLC-PKC pathway (Shu et al. 2014). Here we reveal that activation of OXRs through agonists induce ERK phosphorylation.

For all 3 peptides in both cell lines, p-ERK1/2 increased compared to the control over the 60 minutes. In IMR32 OXA and OXB elicited an increase in ERK activation with a peak at 10 minutes and a decrease until 60 minutes, whilst still remaining above basal levels. In H295R cells OXA and OXB activation of the ERK pathway displayed a significant increase at 10 minutes with a continual reduction until 60 minutes; this is in line with what has been observed in CHO stably overexpressing OXR and with what we observed in IMR32 (Ammoun et al. 2006a; Ramanjaneya et al. 2009). SH-SY5Y cells demonstrated the same increase in p-ERK1/2 as IMR32; however for all 3 peptides the effect was prolonged and did not peak and fall as in IMR32. After 20 minutes OXB elicited a stronger response than OXA which is concurrent with what was seen in IMR32. The continual increase in ERK activation in SH-SY5Y cells compared to the decrease after 10 minutes in IMR32 may be as a result of cell line differences. One possible mechanism for reduced ERK activation after 10 minutes in IMR32 is β-arrestin association and subsequent internalisation, in SH-SY5Y cells there may not be the same mechanism. At a concentration of 100nM OXA would bind to both OX1R (IC50 20nM) and OX2R (IC50 38nM) (Sakurai et al. 1998). It has been shown that in COS-7 or HEK293 cells stably transfected with OXRs, following OXA treatment after 20 minutes there was only 80% surface expression of OX1R and 40% expression of OX2R compared to no treatment (Dalrymple et al. 2011). β-arrestins are proteins which interact with most GPCRs and result in the desensitisation of the GPCRs, as this association causes internalisation of the receptor complex. After internalisation the receptor may become re-sensitised through dephosphorylation of the receptor complex so that it is recycled back to the membrane or alternatively it is targeted by late endosomes for degradation (Dalrymple et al. 2011; Evans et al. 2001). OXRs have been shown through GFP-tagging and bioluminescence resonance energy transfer (BRET)

analysis to strongly associate with β-arrestins; which facilitate its internalisation (Dalrymple et al. 2011; Evans et al. 2001). Due to ligand binding and subsequent internalisation by β-arrestins, there may be lower cell surface expression of receptors and this may result in reduced ERK activation due to lack of functional receptors. This could account for the effects of both OXA and OXB eliciting a strong response up to 10 minutes and after this prompting a lesser response in IMR32. β-arrestin and OXR associations have not been determined in these neuronal models and thus association of it between the 2 different cell lines is not known. It may also be as a result of differences in receptor expression between the 2 cell lines. If receptor expression is high enough as a result of increased starting expression or differences in β-arrestin mediated internalisation there will be an abundance of other receptors for the peptide to bind to and initiate an effect and hence increased p-ERK1/2 over 60 minutes. Another explanation for the differences observed in the cell lines could be sex related. IMR32 is a male cell line and SH-SY5Y a female cell line. It has been reported that OX elicits stronger effects in female mice as opposed to male mice because female mice experience increased obesity in transgenic models of narcolepsy as well as increased immunoreactivity of OX neurons during fasting (Fujiki et al. 2006; Funabashi et al. 2009). Female rats express higher quantities of OXA and OX1R in the hypothalamus than male rats, but in the adrenal gland OXR expression is higher in male rats (Johren et al. 2001; Taheri et al. 1999). Although some data in female cell lines suggests a trend of rapid ERK1/2 activation followed by a prolonged decrease upon OXA and OXB addition, like we demonstrate in IMR32 but these studies have not been performed in human cell lines or even neuronal cell lines (Guo, Feng 2012; Ramanjaneya et al. 2009). Thus receptor and peptide expression may have different signalling characteristics and may not be subject to the same sex differences that have been shown to occur in the brain.

QRFP treatment however showed a large increase in ERK activation, higher than that induced by OXA and OXB and it was sustained over the 60 minute time period in both cell lines. This may be as a result of increased availability of receptors which allows for increased ERK activation. The sustained activation induced by QRFP is difficult to dissect as there is no data on β-arrestin association. It is possible that if

there is any internalisation it occurs later than 60 minutes, is less pronounced than for the OXRs or GPR103 does not associate with β-arrestins. High receptor expression may also explain the prolonged increase in ERK activation allowing a continual increase in p-ERK1/2 over 60 minutes in both cell lines regardless of any β-arrestin association. If the receptor expression is high enough when receptors become internalised, QRFP may bind to the other receptors which have not yet been internalised resulting in the gradual increase in p-ERK1/2.

Treatment with OXR and GPR103 peptides with their respective antagonists was performed to determine that it was the agonists which caused increased p-ERK1/2. Indeed IMR32 and SH-SY5Y p-ERK1/2 showed insignificant fluctuations across all time points. This shows that previous increases of p-ERK1/2 due to treatment of OXA and OXB is negated by addition of selective OX1R and OX2R antagonists and thus p-ERK1/2 increases can be attributed to an activation of the receptors by OXA and OXB binding. QRFP interestingly, was inhibited in both cell lines by both antagonists individually. There is no data published on the use of OXR antagonists and its action on GPR103, however GPR103 is 47 and 48% similar to OX1R and OX2R respectively and we show here that both antagonists are capable of blocking ERK1/2 activation (Jiang et al. 2003). OXRs can function as homo or hetero-dimers (Xu et al. 2011; Wang et al. 2013). Although the dimerisation status of GPR103 is not known, GPCRs are known to form dimers and due to its involvement in the orexigenic system it is possible that it forms a cross-talk with the OXRs, hence antagonistic activity on the OXRs could lead to a halting of any activity incurred through its potential to cross-talk with GPR103 (Milligan et al. 2003).

We demonstrate here that neuronal differentiation of IMR32 and SH-SY5Y results in increased expression of OX1R, OX2R and GPR103 as evidenced through immunofluorescence and qPCR and that they are functional receptors which increase p-ERK1/2 levels within each cell line. Antagonists for the receptors prevented activation of OX1R and OX2R by the OXA and OXB peptides but also GPR103 through the QRFP peptide suggesting potential cross-talk mechanisms between GPR103 and OXRs.

5

Chapter 5

Microarray analysis of differentiated SH-SY5Y cells treated with 100nM OXA, OXB and QRFP

5.1 Introduction

A gene microarray is capable of observing transcript expression in a sample on a mass scale. It involves RNA extraction and cDNA production, which is then labelled with a fluorescent dye and hybridised to an array containing primer sequences for potentially thousands of genes. The intensity of the fluorescent dye is then measured to determine relative abundance when compared to a control sample (Kogenaru et al. 2012). We used a 12x 135k Nimblegen array which consists of 60mer oligonucleotide probes, 135,000 features on each array and includes multiple probes per target and is capable of running 12 independent samples on each slide. This array targets 44,049 genes and uses 3 probes for each target gene.

To date the effect of OX/QRFP on the entire human genome is not known. It is for this reason we performed a non-biased screen to examine the effects of OXA, OXB and QRFP on the human genome. This will allow identification of genes and pathways important in OXA, OXB and QRFP signalling.

5.2 Objectives

To the best of our knowledge, a microarray has not been performed on neuroblastoma cell lines treated with the OX or QRFP peptides. Little is known about the effects on gene expression incurred by these peptides, especially for QRFP. Using a fully differentiated neuronal cell line: SH-SY5Y, we determined the effects

at gene level of the neuronal peptides: OXA, OXB and QRFP and identified the most important pathways involved.

5.3 Results

SH-SY5Y cells were used for this microarray as it has been extensively studied with regards to both AD and OX. SH-SY5Y cells that were neuronally differentiated and treated with 10µM of RA for 6 days followed by 24 hour treatments with 100nM of OXA, OXB or QRFP. Experiments were performed as 3 independent experiments and RNA was extracted using a Qiagen RNeasy miniprep kit. The extracted RNA was quality verified on a 2100 expert Agilent bioanalyzer to confirm that all samples had an RNA yield greater than 30µg and RIN values above 9. This RNA was then hybridised to a 12x 135k Nimblegen array. The array slide was scanned at 3µM on an InnoScan 700 microarray scanner and converted into TIFF images using MAPIX version 5.1 software. The TIFF images were then aligned to their Nimblegen design files and converted into probe intensity values using the Nimblegen DEVA software. This data was then Loess normalised using R statistical program and then quintile normalised for array variation using DNAstar with the assistance of Dr. Ryan Pink (Oxford Brookes University). Values which had a p-value derived from the unpaired student T test of less than 0.05 compared to the control and with a fold change compared to the control more than 1.5 or less than 0.5 were included, all others were discounted as displaying no significance. qPCR was performed to validate the data obtained by microarray using 8 genes , the primer sequences of which are in table 2.4.

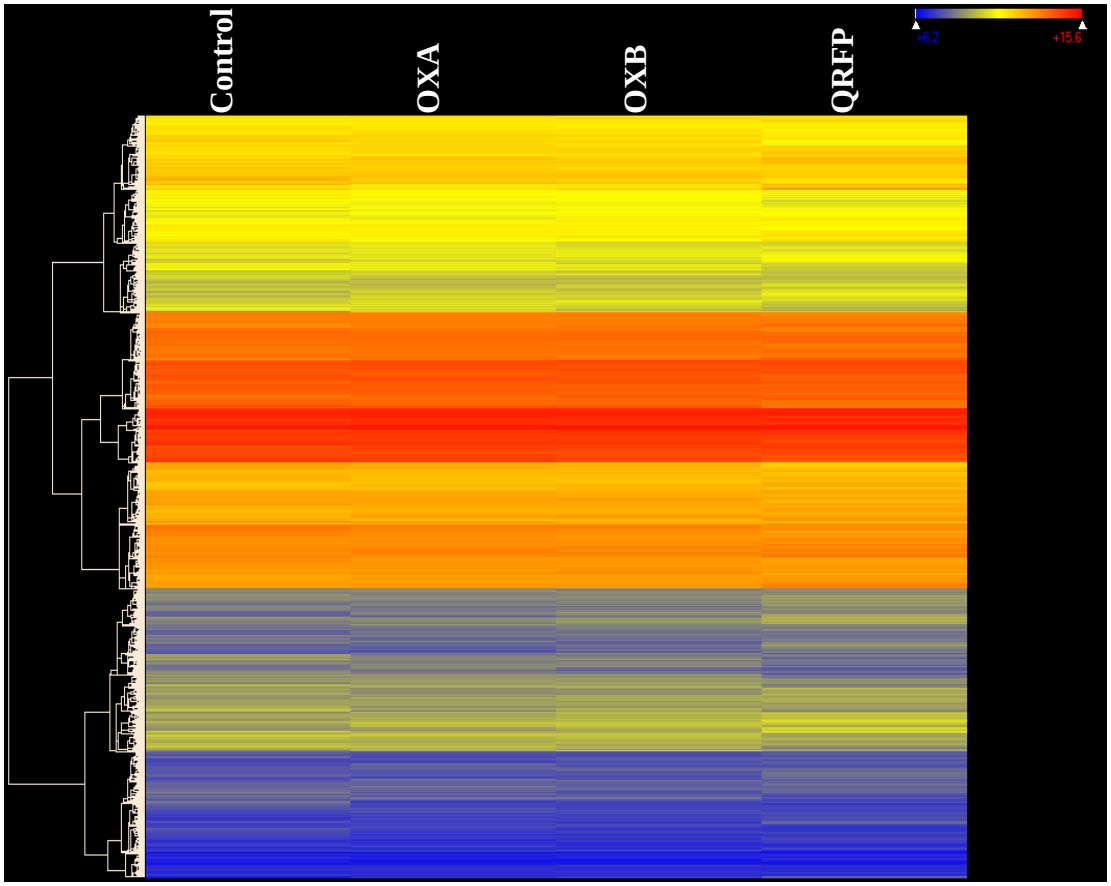

Figure 5.1: Heat map of neuronally differentiated SH-SY5Y cells treated with 100nM OXA, OXB or QRFP for 24 hours. Intensities of expression are shown in this heat map with red indicating more intense expression than blue. A dendrogram is displayed to the left of the map which shows hierarchical clustering based upon the similarity of genes.

Figure 5.1 demonstrates the heat map generated by this microarray experiment. Each spot represents a gene and the colour represents the expression within that sample. The intensity of each spot is measured and assigned a value and compared to the control value. This allows a relative expression compared to the control.

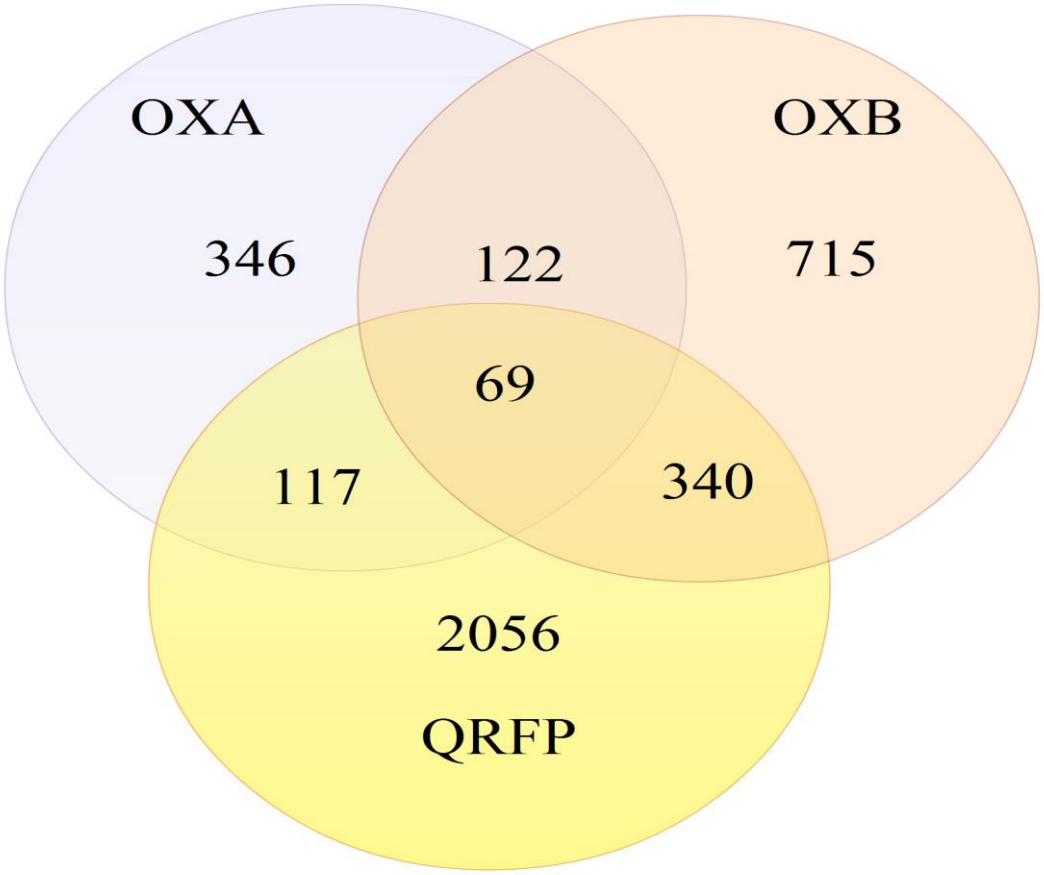

Figure 5.2: Venn diagram demonstrating the number of genes with over 1.5 or below 0.5 fold expression compared to a control. RNA was obtained from 3 independent experiments and only genes with a p value less than 0.05 when compared to the control were included.

Figure 5.2 represents the number of gene changes for each peptide individually and the commonalities of the different treatments in a Venn diagram. OXA had the smallest number of gene changes at only 346, OXB had more at 715 and QRFP had over 2000. Between all three treatments there were 69 genes that were regulated in a similar fashion.

Microarray data was analysed though Kyoto Encyclopaedia of Genes and Genomes (KEGG) pathways and Gene Ontology (GO) terms. The KEGG database allows amalgamation of genes to assign pathways involving multiple gene associations. This allows identification of the most likely pathways involved with a given gene list.

Based on the gene list GO terms were assigned to each peptide treatment using the ToppGene software. GO terms provide an ontology of distinct terms representative of a collection of gene properties. GO terms are assigned according to three domains: cellular component, molecular function or biological process. Cellular component ontology involves the location of subcellular structures and macromolecule complexes. The molecular function GO terms designates functions like catalytic or binding sites at molecular level. Molecular function GO terms can include more specific genes and functions that may involve only a few genes or larger more complex functions encompassing several genes. The biological process GO terms are the series of events achieved by ordered assemblies of molecular functions. These can include specific functions or broader processes including signal transduction (Gene Ontology Consortium 2008, Anonymous).

OXA treatment resulted in the change of 346 genes using the KEGG pathway. Table 5.1 highlights the pathways involved including more than 3 genes affected.

KEGG pathway	Number of genes involved	Genes involved
Metabolic pathways	8	PTGES, NAGLU, LALBA, GCDH, FTCD, DLST, ALOX12B
Neuroactive ligand-receptor interaction	7	GALR3, GRIN1, HRH4, HTR4, PTGER1, SSTR3, VIPR1
MAPK signalling pathway	5	FGFR4, IL1B, MAP3K14, MAPT, RASGRP1
NF-KB signalling pathway	5	BTK, IL1B, MAP3K14, SYK, TNFAIP3
TNF signalling pathway	4	EDN1, IL1B, MAP3K14, TNFAIP3
Osteoclast differentiation	4	BTK, IL1B, MAP3K14, SYK
PI3K-Akt signalling pathway	4	FGFR4, GNG13, SYK, TSC1
Cytokine-cytokine receptor interaction	4	CCR8, IL1B, IL8RA, TNFRSF19
Ras signalling pathway	4	FGFR4, GNG13, GRIN1, RASGRP1
Glutamatergic synapse	3	DLGAP1, GNG13, GRIN1
Chemokine signalling pathway	3	CCR8, GNG13, IL8RA
Calcium signalling pathway	3	GRIN1, HTR4, PTGER1
Alzheimer's disease	3	GRIN1, IL1B, MAPT
Serotonergic synapse	3	ALOX12B, GNG13, HTR4

Table 5.1: KEGG pathways associated with OXA treatment in SH-SY5Y

OXA only involved molecular function GO terms, represented in figure 5.3.

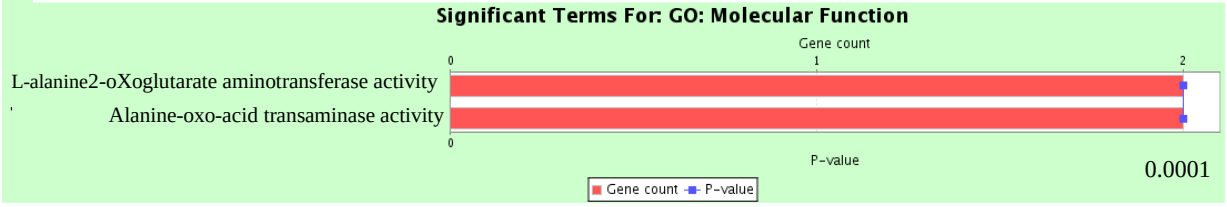

Figure 5.3: GO terms for OXA treatment in SH-SY5Y

715 genes changed regulation upon OXB addition. Only KEGG pathways involving 4 or more genes are illustrated in table 5.2

KEGG pathway	Number of genes involved	Genes involved
Metabolic pathways	16	THTPA, SDS, PTGES2, PPOX, PLCG2, PIGO, IVD, GPT, FUK, CSAD, B3GAT3, AUH, ALG10, AKR1A1, AGXT, ACAA1
PI3K-Akt signalling pathway	10	CCND3, CSF3R, DDIT4, EPO, FGFR4, GNG13, ITGA3, JAK2, LAMB2, SYK
Neuroactive ligand-receptor interaction	10	AVPR1B, CHRND, CRHR1, DRD3, GRM4, HTR4, NMUR1, P2RY6, PTGER1, SSTR3
Pathways in cancer	8	CSF3R, HHIP, ITGA3, KLK3, LAMB2, PLCG2, STAT5A, WNT11
Jak-STAT signalling pathway	7	CCND3, CSF2RB, CSF3R, EPO, IL22RA1, JAK2, STAT5A
Biosynthesis of secondary metabolites	6	ACAA1, AGXT, AKR1A1, DHDDS, PPOX, SDS
Cytokine-cytokine receptor interaction	6	CCR10, CSF2RB, CSF3R, EPO, IL22RA1, TNFSF14
Calcium signalling pathway	5	AVPR1B, CACNA1C, HTR4, PLCG2, PTGER1
Vascular smooth muscle contraction	5	ADCY6, AVPR1B, CACNA1C, PPP1R12C, PRKCD
Glutamatergic synapse	5	ADCY6, CACNA1C, GNG13, GRM4, SLC1A6
Peroxisome	5	ABCD4, ACAA1, AGXT, PECR, SLC27A2
Cholinergic synapse	5	ADCY6, CACNA1C, GNG13, JAK2, KCNQ2
Ras signaling pathway	4	FGFR4, GNG13, PLCG2, RASA4
Chemokine signalling pathway	4	ADCY6, CCR10, GNG13, JAK2
Focal adhesion	4	CCND3, ITGA3, LAMB2, PPP1R12C
Cell adhesion molecules	4	CD2, CD8B, LRRC4, PTPRF
HIF-1 signalling pathway	3	EPO, PLCG2,TF
Alzheimer's disease	1	CACNA1C

Table 5.2: KEGG pathways associated with OXB treatment in SH-SY5Y

OXB involved molecular function and biological process GO terms. Figure 5.4 illustrates the molecular function and biological process GO terms assigned to OXB addition.

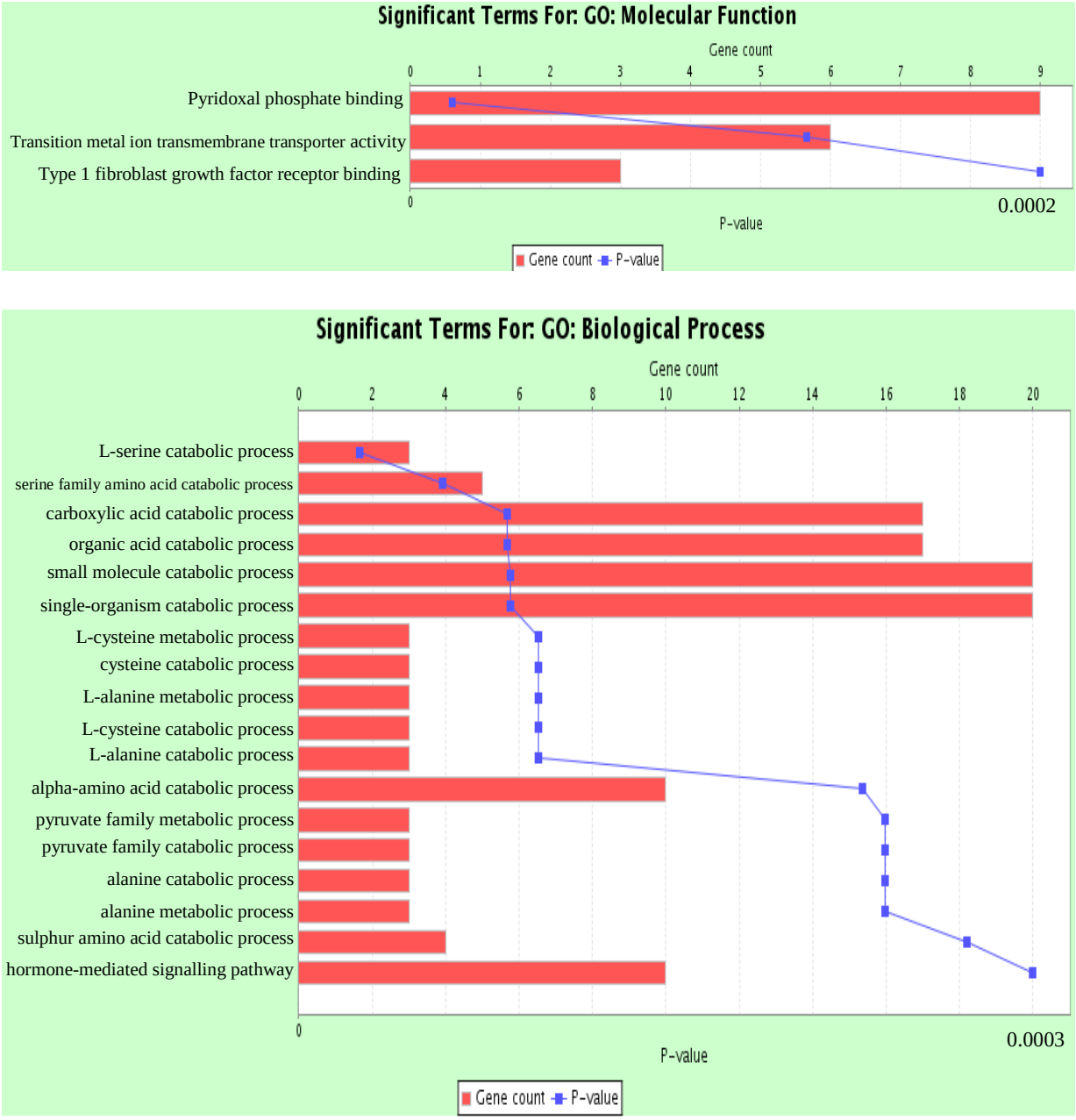

Figure 5.4: GO terms for OXB treatment in SH-SY5Y

Treatment of SH-SY5Y cells incurred changes in 2056 genes upon QRFP treatment. Table 5.3 demonstrate KEGG pathways involving 6 or more genes.

KEGG pathway	Number of genes involved	Genes involved
Neuroactive ligand-receptor interaction	26	ADRA1A, ADRA1B, AVPR2, CHRM5, CHRND, DRD3, GALR3, GCGR, GHRHR, GHSR, GLRA1, GRM4, GZMA, HCRTR1, HRH1, HRH3, MC3R, OPRM1, P2RX1, P2RX3, P2RX7, P2RY11, SSTR3, SSTR4, TBXA2R, TSHR
Metabolic pathways	24	ABO, ACAA1, ALG10, ALOX12, ALOX12B, ALOX15, ALOX15B, CYP4A11, CYP4F8, DPYS, EHHADH, FAHD1, FLAD1, FUK, IDUA, LTC4S, MVD, NDUFS7, NNMT, PCYT2, PKLR, PLCG2, PRODH, SDS
Cytokine-cytokine receptor interaction	21	CCL20, CCL3, CCL4, CCL5, CCR4, CSF2, CSF2RB, CSF3, CSF3R, EPO, IL11, IL17E, IL21, IL22, IL3RA, IL6, PDGFB, TNFSF14, TNFSF15, TNFSF18, XCR1
Calcium signalling pathway	19	ADRA1A, ADRA1B, CACNA1A, CACNA1B, CACNA1I, CACNA1H, CHRM5, ERBB2, ERBB3, GNA14, HRH1, ITPR1, P2RX1, P2RX3, P2RX7, PLCG2, PLN, RYR3, TBXA2R
PI3K-Akt signalling pathway	16	BCL2L11, CCND3, CHAD, CSF3, CSF3R, EPO, FGFR4, IL3RA, IL6, INS, ITGA11, ITGB4, JAK3, LAMC3, MYB, PDGFB
Jak-STAT signalling pathway	14	CCND3, CSF2, CSF2RB CSF3, CSF3R, EPO, IL11, IL21, IL22, IL3RA, IL6, JAK3, SOCS5, STAT5A
Hematopoietic cell lineage	14	CD2, CD34, CD37, CD4, CD8A, CD8B, CSF2, CSF3, CSF3R, EPO, GP9, IL11, IL3RA, IL6

HTLV-I infection	14	ATF3, CCND3, CSF2, E2F1, FZD3, IL6, JAK3, MYB, NRP1, PCAF, PDGFB, STAT5A, TERT, XBP1
Pathways in cancer	13	ARNT, CSF3R, E2F1, ERBB2, FZD3, IL6, KLK3, LAMC3, PAX8, PDGFB, PLCG2,STAT5A, STK4
MAPK signalling pathway	13	CACNA1A, CACNA1B, CACNA1H, CACNA1I, CACNA2D3, CACNB2, CACNG5, FGFR4, MAP3K5, MEF2C, PDGFB, STK3, STK4
Regulation of actin cytoskeleton	11	CHRM5, FGD3, FGFR4, GRLF1, INS, ITGA11, ITGB4, MYL2, MYL5, MYL9, PDGFB
Proteoglycans in cancer	11	ERBB2, ERBB3, FZD3, GAB1, GPC3, HSPB2, HSPG2, ITPR1, NUDT16L1, PLCG2, TIMP3
Focal adhesion	11	CCND3, CHAD, ERBB2, GRLF1, ITGA11, ITGB4, LAMC3, MYL2, MYL5, MYL9, PDGFB
Ras signalling pathway	9	FGFR4, GAB1, INS, PDGFB, PLCG2, RASA4, RASAL2, REL, STK4
Chemokine signalling pathway	9	CCL20, CCL3, CCL4, CCL5, CCR4, FGR, HCK, JAK3, XCR1
Maturity onset diabetes of the young	8	FOXA2, INS, NKX2, NR5A2, PAX4, PAX6, PKLR, TCF1
MicroRNAs in cancer	8	BCL2L11,E2F1, ERBB2, ERBB3, FZD3, PDGFB, PLCG2, TIMP3
Serotonergic synapse	8	ALOX12, ALOX12B, ALOX15, LOX15B, CACNA1A, CACNA1B, ITPR1, KCNJ5
Transcriptional misregulation in cancer	8	CEBPE, CSF2, GZMB, IL6, MEF2C, MPO, PAX8, REL
ECM-receptor interaction	8	CD47, CHAD, GP6, GP9, HSPG2, ITGA11, ITGB4, LAMC3
Salivary secretion	7	ADRA1A, ADRA1B, AQP5, CAMP, FXYD2, ITPR1, RYR3

Non-alcoholic fatty liver disease	7	BCL2L11, IL6, INS, MAP3K5, NDUFS7, PKLR, XBP1
Biosynthesis of secondary metabolites	7	ACAA1, ACOT7, MVD, NAGK, PDSS2, PRODH, SDS
Arachidonic acid metabolism	7	ALOX12,ALOX12B, ALOX15, ALOX15B, CYP4A11, CYP4F8, LTC4S
Primary immunodeficiency	7	AIRE, BLNK, BTK, CD4, CD79A, CD8A, CD8B
Cell adhesion molecules	7	CD2, CD34, CD4, CD8A, CD8B, MAG, SDC3
Natural killer cell mediated cytotoxicity	6	CSF2, GZMB, NCR2, NCR3, PLCG2, SH3BP2
Arrhythmogenic right ventricular cardiomyopathy	6	CACNA2D3, CACNB2, CACNG5, ITGA11, ITGB4, LMNA
HIF-1 signalling pathway	6	ARNT, EPO, ERBB2, IL6, INS, PLCG2
Protein processing in endoplasmic reticulum	6	DNAJC1, MAP3K5, MBTPS2, PPP1R15A, SSR1, XBP1
Complement and coagulation cascades	6	C1QA, C2, F3, PROC, SERPINF2, THBD
Dopaminergic synapse	6	CACNA1A, CACNA1B, DRD3, ITPR1, KCNJ5, PPP1R1B
Inflammatory mediator regulation of TRP channels	6	ALOX12,HRH1, ITPR1, PLCG2, PRKCD, TRPV4
Glutamatergic synapse	6	CACNA1A, GRM4, ITPR1, SLC1A1, SLC1A6, SLC1A7
TNF signalling pathway	6	CCL20, CCL5, CSF2, IL6, MAP3K5, MMP14
Rheumatoid arthritis	6	CCL20, CCL3, CCL5, CSF2, IL11, IL6
ABC transporters	6	ABCA1, ABCA5, ABCB9, ABCD4, ABCG1, ABCG2
Cardiac muscle contraction	6	CACNA2D3, CACNB2, CACNG5, FXYD2, MYL2, MYL3
Cholinergic synapse	6	CACNA1A, CACNA1B, CHRM5, ITPR1, KCNQ4, KCNJ4
NF-kappa B signalling pathway	5	BLNK, BTK,CCL4,PLCG2, TNFSF14

Alzheimer's disease	3	ITPR1, NDUFS7, RYR3

Table 5.3: KEGG pathways associated with QRFP treatment in SH-SY5Y

QRFP treatment involved molecular function, biological process and cellular component GO terms. These are demonstrated in figure 5.5.

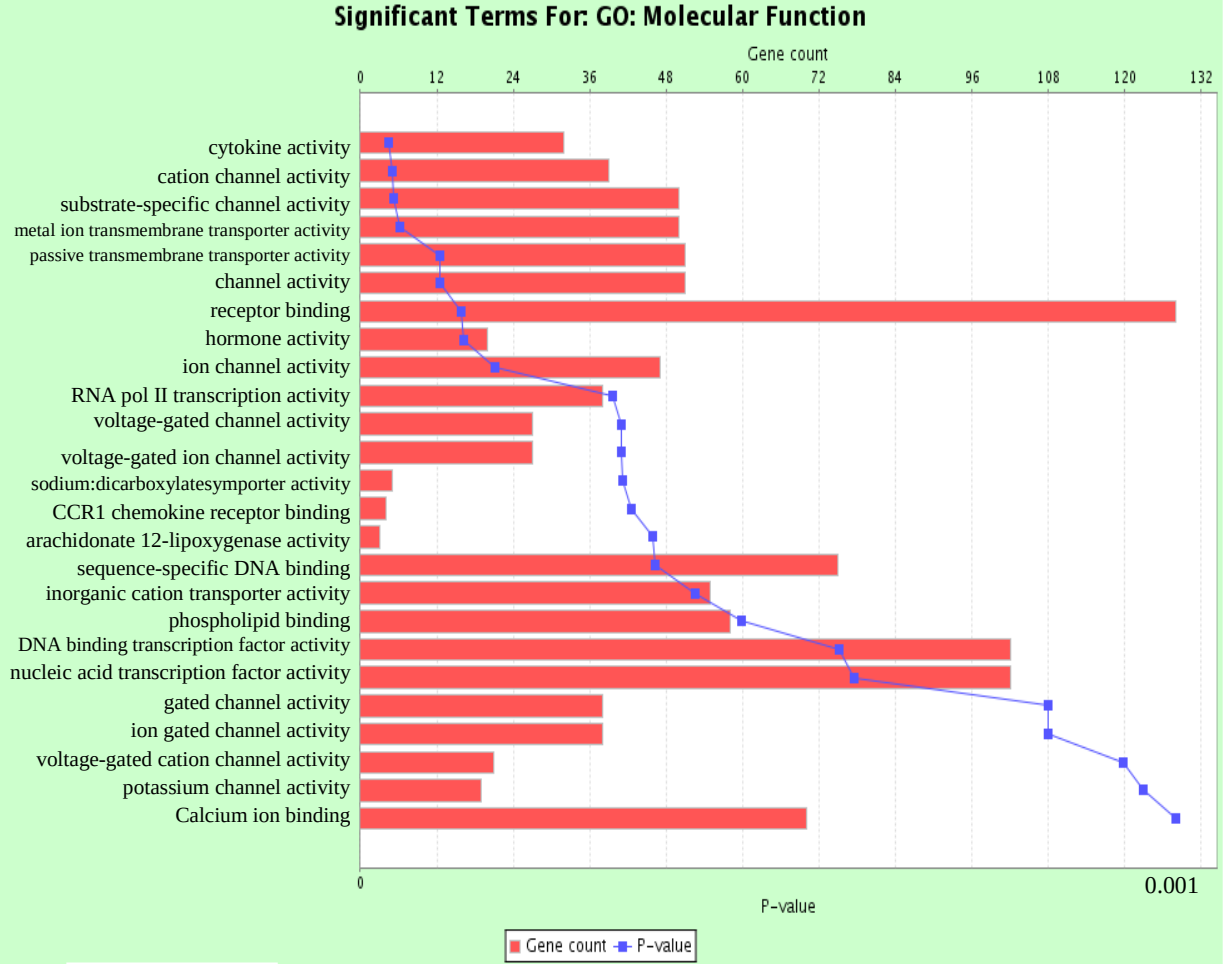

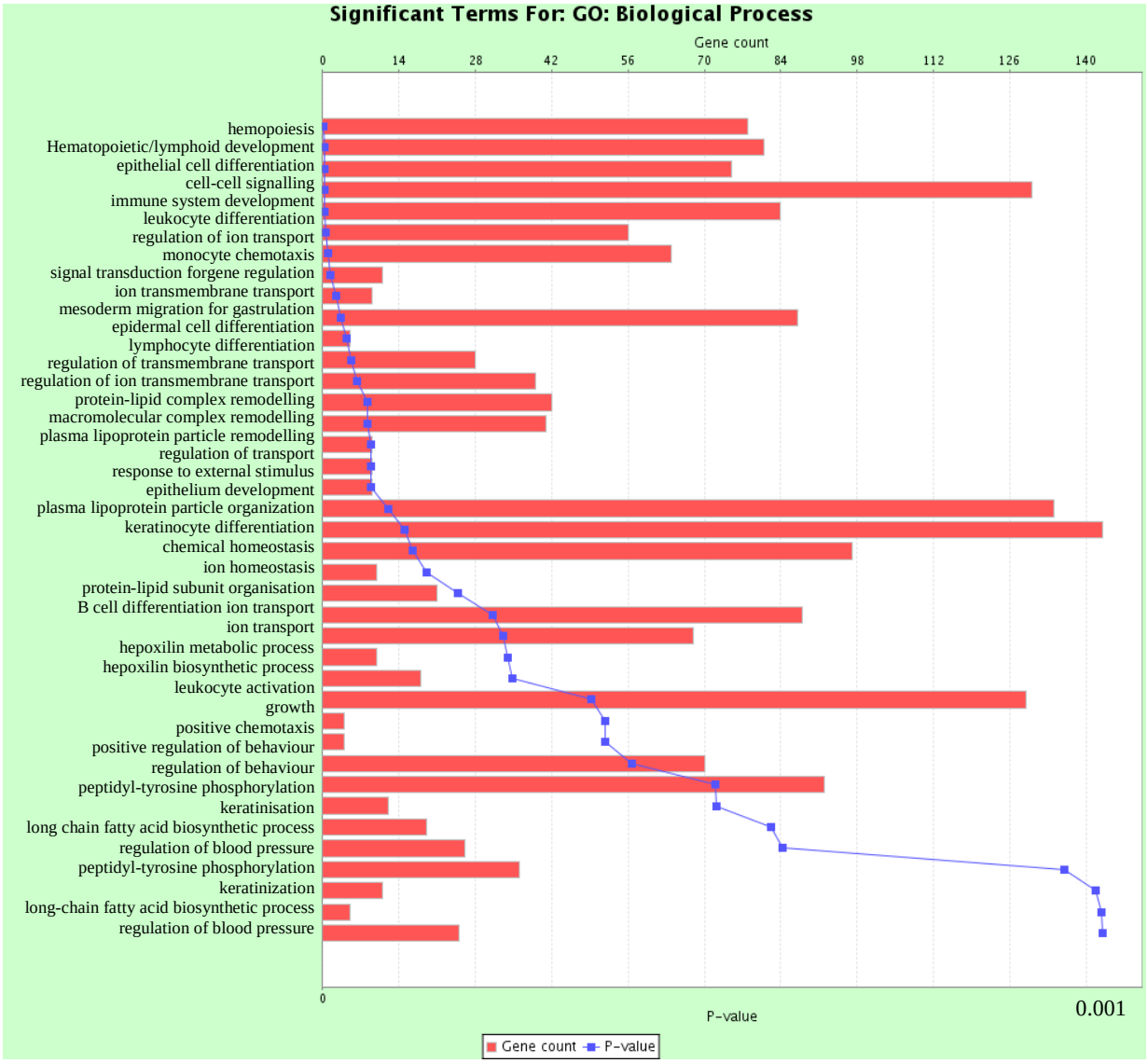

Figure 5.5: GO terms for QRFP treatment in SH-SY5Y

Representations of the genes involved upon OXA, OXB and QRFP addition in the specific KEGG pathways of: Alzheimer's disease, NF-KB and MAPK are illustrated in figures 5.9-11.

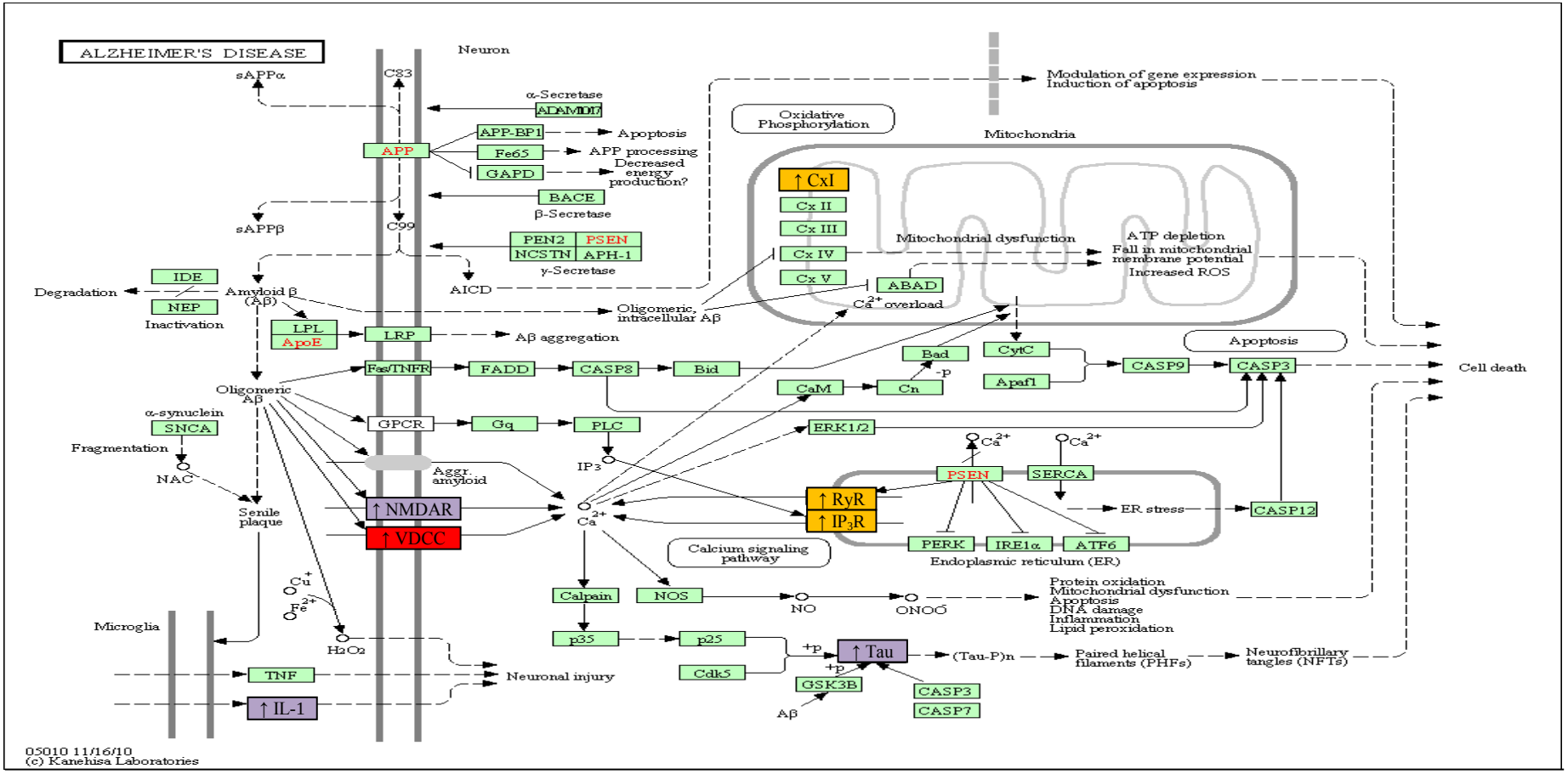

Figure 5.6: KEGG pathway illustration demonstrating genes involved in the Alzheimer's disease pathway as a result of OXA, OXB or QRFP treatment. Genes involved with OXA are shown in purple, OXB in red and QRFP in yellow.

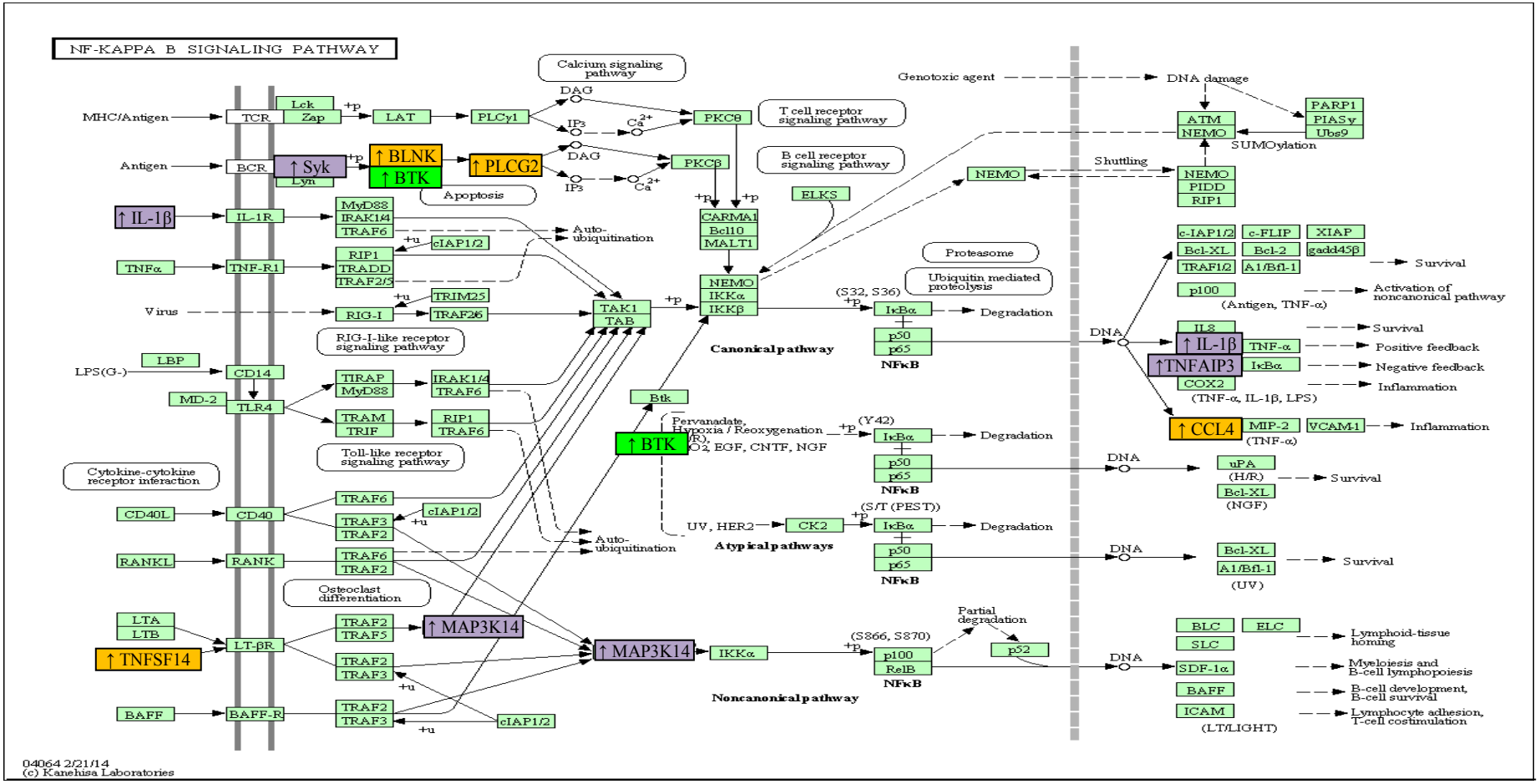

Figure 5.7: KEGG pathway illustration demonstrating genes involved in the NF-KB pathway as a result of OXA, OXB or QRFP treatment. Genes involved with OXA are shown in purple, QRFP in yellowand OXA & QRFP in green.

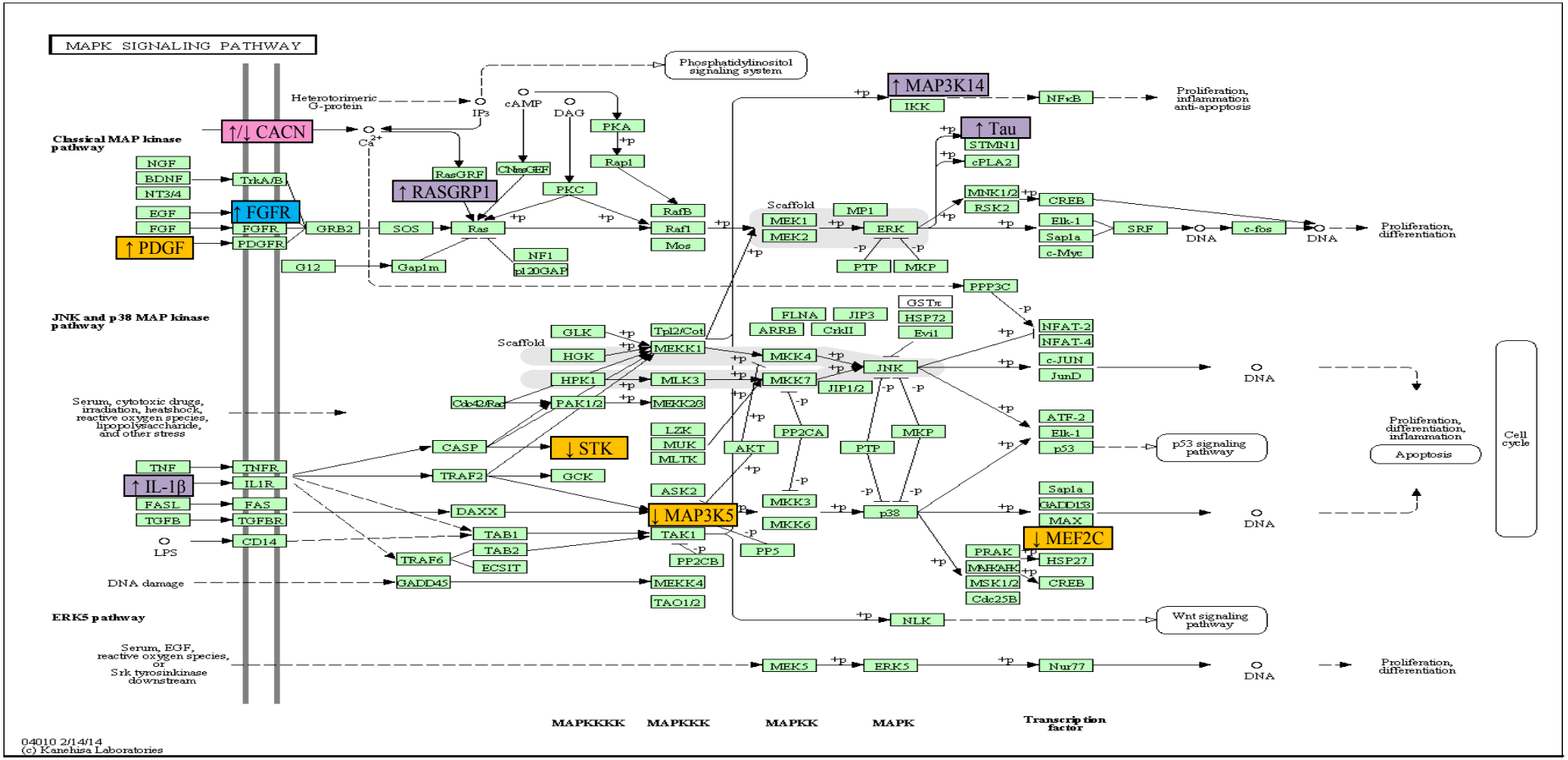

Figure 5.8: KEGG pathway illustration demonstrating genes involved in the MAPK signalling pathway as a result of OXA, OXB or QRFP treatment. Genes involved with OXA are shown in purple, QRFP in yellow, OXB and QRFP in pink and OXA, OXB & QRFP in blue.

The microarray was validated using qPCR to confirm changes in expression for 8 genes. These genes were picked at random from the list of genes that were common between all 3 peptide treatments. These included: *CSTF2T, DAB2IP, GPR148, KRT23, OSBPL7, PYCRL, ZFP4* and *ZP1*. *CSTF2T* is a cleavage stimulation factor and although its function is ambiguous it is thought to be involved in meiosis (Dass et al. 2002). *DAB2IP* is a GTPase-Activating Protein (GAP) that functions as a tumour suppressor gene and is methylated and subsequently inactivated in prostate and breast cancers (Yano et al. 2005). *GPR148* encodes a GPCR expressed in the brain and testes although its exact function is not yet known (Dharmadhikari et al. 2012). *KRT23* encodes a keratin protein which is highly expressed in colon adenocarcinomas and may be associated with reduced cell viability (Birkenkamp-Demtroder et al. 2013). *OSBPL7* is a cytosolic high affinity receptor for oxysterols which are oxygenated derivatives of cholesterol and thought to be involved in breast cancer metastasis but its functions remain unclear (Silva, Beckedorf & Bieberich 2003; Loilome et al. 2012). *PYCRL* is a pyrroline-5-carboxylate reductase which is involved in proline synthesis from the conversion of ornithine to proline (De Ingeniis et al. 2012). *ZFP42* encodes a zinc finger protein which functions as a DNA-binding transcription factor and is a marker for pluripotency and maintains a pluripotent state (Kim et al. 2011; Shi et al. 2006). *ZP1* encodes a glycoprotein which comprises the zona pellucid in the human egg and facilitates sperm binding (Ganguly et al. 2010). Table 5.4 illustrates the fold change compared to the control obtained in the microarray and the results obtained by qPCR for the same genes. The qPCR data correlated with the microarray data and all genes that observed a decrease or an increase compared to the control in the microarray showed the same change by qPCR.

Treatment	OXA		OXB		QRFP	
Gene	Microarray value	qPCR value	Microarray value	qPCR value	Microarray value	qPCR value
CSTF2T	2.41	1.42 ±0.25	2.07	1.64 ±0.05	2.58	1.48 ±0.17
DAB2IP	1.60	1.38 ±0.42	2.06	4.32 ±0.51	2.15	2.24 ±0.30
GPR148	0.48	0.97 ±0.52	0.43	0.39 ±0.11	0.47	0.66 ±0.12
KRT23	0.39	0.49 ±0.09	0.33	0.80 ±0.02	0.41	0.63 ±0.17
OSBPL7	1.50	1.81 ±0.15	1.58	2.02 ±1.01	1.75	2.01 ±0.73
PYCRL	2.02	1.39 ±0.16	1.86	1.59 ±0.48	2.30	3.03 ±0.30
ZFP42	0.46	0.82 ±0.04	0.48	0.77± 0.20	0.48	0.83 ±0.05
ZP1	2.20	1.47 ±0.19	1.76	3.24 ±0.33	3.43	3.36 ±0.69

Table 5.4: Values for 8 genes obtained by microarray and qPCR validation upon 24 hour treatment with 100nM OXA, OXB or QRFP ±S.D.

5.4 Results and discussion

We sought to perform a non-biased study to examine the effects exerted on the human genome by OXA, OXB and QRFP. The qPCR data corroborated the microarray, with the genes: *CSTF2T*, *DAB2IP*, *OSBPL7*, *PYCRL* and *ZP1* all increasing in both experiments. And the genes: *GPR148*, *KRT23* and *ZFP42* decreasing. Data sets treated with peptides were compared to the control and any results which had p-values less than 0.05 and above 1.5 or

less than 0.5 fold changes were considered significant. The genes generated from these stipulations were then analysed using KEGG pathway software and ToppGene software for GO terms.

OXA treatment of SH-SY5Y cells revealed changes in 346 genes. The most significant KEGG pathway was metabolic pathways involving 8 genes. Neuroactive ligand-receptor binding included 7 genes. Genes pinpointed in this pathway included ones involved in histamine, 5-hydroxytryptamine, galanin, prostaglandin E receptor type 1 (PTGER1), somatostatin, glutamate and vasoactive intestinal peptide (VIP) receptor binding. Previous studies have led to the assumption that OXs can exert their effects upon histaminergic neurons. Rats injected with a histamine receptor antagonist: pyrilamine, experienced shorter periods of wakefulness and in histamine receptor deficient mice, OXA administration did not have any effects on wakefulness (Yamanaka et al. 2002). However OXA resulted in a 0.5 fold reduction of the histamine receptor: HRH4. As OXs have already been shown to work synergistically with histamine, this reduction may be as a result of overstimulation of the receptor resulting in a negative feedback loop to reduce the impact of prolonged OX stimulation. 5-hyroxytryptamine or serotonin has been shown to reach a peak during periods of wakefulness with the highest firing rate of serotonin neurons occurring during alert wakeful periods and a reduction during sleep (Liu, van den Pol & Aghajanian 2002). OX neurons have been shown to input to serotonin neurons and exhibit a direct excitatory effect on them, however at high OX concentrations they can actually have an indirect inhibitory effect on serotonin by causing excitation of GABAergic interneurons (Liu, van den Pol & Aghajanian 2002). At a concentration of 100nM OXA the serotonin receptor: *HTR4* is reduced by 0.35 fold. This may be due to a high concentration of OXA over a prolonged period of 24 hours, leading to excitation of GABAergic neurons, which impose their inhibitory effect on serotonin neurons. Serotonin has also been shown to be decreased in AD (Bierer et al. 1995). The gene encoding the galanin receptor is increased upon OXA treatment and it is a neuropeptide which has been shown to be involved in modulation of feeding with OXs being capable of innervating galanin producing cells (Volkoff, Peter 2001). Interestingly galanin has been implicated in AD. Galanin and its receptors are overexpressed in AD and results in inhibition of cholinergic transmission in the hippocampus and impaired memory function in rats suggesting that overexpression in AD leads to increased deterioration

(Gabriel et al. 1994). However there is some conflict as to whether galanin overexpression is neurodegenerative or neuroprotective. Galanin can inhibit ACh release in the hippocampus and impair memory, but has also been shown to protect against Aβ induced toxicity through increasing survival signalling pathways such as Akt and reducing apoptotic signalling for example caspase 3 cleavage (Ding et al. 2006; Dutar, Lamour & Nicoll 1989). So OXA increasing this receptor could be to increase feeding behaviour in a non-disease situation, however in AD could lead to an increase or decrease in the severity of disease. Prostaglandins are important for mediating inflammatory responses and PTGER1 is a receptor for prostaglandins. We found that OXA increases the receptor expression which is intriguing as increased expression of this receptor and prostaglandins have been implicated in neurotoxicity of AD. In *PTGER1* KO mice with an *APP*/*PS1* mutation, neuronal cell death and neurobehavioral deficits were decreased compared to the mice with only APP/PS1 mutations (Zhen et al. 2012). This suggests a neurotoxic effect exerted by OXA through increase of PTGER1. OXA also increased glutamate receptor subunit zeta-1 (*GRIN1*). GRIN1 is a subunit, which combines with other glutamate receptor subunits to form N-methyl-D-aspartate receptor (NMDA). Increased glutamate in AD causes neurotoxicity by acting through NMDA receptors, in fact one treatment regime: memantine acts by blocking NMDA receptors to reduce glutamate toxicity (van Marum 2009). Somatostatin is a regulatory protein involved in modulation of neurotransmission and cellular proliferation. OXA increased somatostatin receptor expression and has also previously been shown to increase somatostatin in rat brains (Russell et al. 2000) However in AD there is a loss of somatostatin and its receptors and somatostatin increases neprilysin production Neprilysin is an enzyme capable of degrading Aβ plaques; hence in AD a reduction in somatostatin will lead to a reduction of neprilysin and consequently less degradation of plaques (Hama, Saido 2005). OXA may exert neuroprotective effects by increasing somatostatin, however a reduction in OXA signalling will hamper its ability to exert neuroprotective effects through this mechanism. The receptor for VIP is also increased upon OXA administration and has also been implicated in neuroprotection in AD. VIP inhibits Aβ induced microglia activation and the consequent release of toxic factors such as tumour necrosis factor-α (TNF-α) and nitric oxide (NO) and also inhibits nicotinamide adenine dinucleotide phosphate-oxidase (NADPH-oxidase) which produces ROS (Song et al. 2012; Fujimori et al. 2011). The

activation of neuroactive ligands by OXA causes the increase of VIP and somatostatin which have neuroprotective effects in AD.

OXA also regulates 5 genes involved in the MAPK signalling pathway. This includes the genes: fibroblast growth factor receptor 4 (*FGFR4*), interleukin-1 β (*IL-1β*), mitogen-activated protein kinase 14 (*MAP3K14*), *MAPT* and RAS guanyl-releasing protein 1 (*RASGRP1*). We have already demonstrated the OXA induces the MAPK pathway so this is not unexpected. However OXA also activates the P13K-Akt signalling pathways through: *FGFR4*, guanine nucleotide-binding protein subunit gamma-13 (*GNG13*), spleen tyrosine kinase (*SYK*) and tuberous sclerosis 1 (*TSC1*). All of the genes involved in these pathways are increased upon OXA treatment. Both MAPK and PI3K-Akt pathways have been implicated in neuroprotection (Karmarkar et al. 2011, Maher et al. 2011, Sokolowska et al. 2014).

5 genes regulated by OXA are implicated in the NF-KB signalling pathway including: bruton's tyrosine kinase (*BTK*), *IL-1β*, *MAP3K14*, *SYK* and TNF-α induced protein 3 (*TNFAIP3*). All of these genes are responsible for inducing NF-KB and OXA treatment caused their upregulation. This suggests that OXA treatment induces NF-KB, which can then regulate cell survival, growth, repair, neurogenesis, learning and memory (Crampton, O'Keeffe 2013). IL-1β is a proinflammatory cytokine involved in inflammatory responses through activation of T and B cells and other inflammatory related proteins. It is also thought to be involved in leptin regulation, which supresses' appetite (Mrak, Griffin 2001). The increased expression of IL-1β when cells are exposed to OXA may be a counteracting mechanism through leptin regulation for the increased feeding that OXA stimulates. IL-1β has also been found to be over expressed in AD and is associated with Aβ plaques and can cause a neuroinflammatory response which was reduced along with plaque deposition when AD transgenic mice were given ibuprofen to reduce IL-1 (Lim et al. 2000). So although OXA treatment may increase *IL-1β* to combat its pro-feeding response, it may exacerbate symptoms of AD. *MAP3K14* is also known as NF-KB-inducing kinase (NIK) and becomes increased during periods of oxidative stress and induces NF-KB (Sheng et al. 2012). The *SYK* gene encodes a tyrosine kinase protein which is involved in immune signalling pathways as well as being an activator of NF-KB (Mocsai, Ruland & Tybulewicz 2010). It has also been shown to phosphorylate tau at tyrosine 18 (Lebouvier et al. 2008). However this is not

thought to be a pathologically important phosphorylation site for tau in AD, as it does not affect tau microtubule binding and phosphorylation here does not increases susceptibility to multiple serine/threonine phosphorylations as it does for other sites (Lebouvier et al. 2008; Scales et al. 2011; Lee et al. 2004). Contrary to the other genes involved in NF-KB which result in positive regulation, TNFAIP3 is a negative regulator of NF-KB. Upon NF-KB activation, TNFAIP3 increases and inhibits NF-KB to control regulation (Kolodziej et al. 2011). It is increased upon OXA administration and although it is a negative regulator of NF-KB, it is the only gene involved with OXA which has a negative effect. It has been shown to be an important gene in regulation of the NF-KB pathway and acts as a negative feedback regulator of NF-KB in response to multiple stimuli (Vereecke, Beyaert & van Loo 2009).So in periods of OXA addition, it is possible that NF-KB becomes increased and concurrently *TNFAIP3* potentially increases to negatively regulate NF-KB signalling. Chronic sleep deprivation has also been shown to increase NF-KB, suggesting a possible involvement of OXA for increasing NF-KB during periods of wake (Brandt et al. 2004). In conclusion OXA appears to act as a switch: it exerts positive regulatory effects on NF-KB to potentially reduce oxidative stress, however it also results in upregulation of TNFAIP3 which functions as a negative feedback mechanism to reduce NF-KB activity.

The TNF pathway was found to be involved in OXA treatment. The genes implicated in this pathway were: *EDN1*, *IL-1β*, *MAP3K14* and *TNFAIP3*. *EDN1* encodes the endothelin-1 protein which is involved in vasoconstriction and has also been associated with AD. Endothelin-1 is increased in AD and decreased cerebral blood flow is a common symptom in AD which can contribute to pathology and it is thought that elevated endothelin-1 may contribute to this due to its vasoconstrictive effects (Palmer, Love 2011). Nevertheless it has also been shown to prevent cell death, when cells were treated with hydrogen peroxide to induce oxidative stress which is a common occurrence in AD (Luo, Grammas 2010). So although there may be involvement of endothelin-1 in AD, its exact role is not fully elucidated. *IL-1β*, *MAP3K14* and *TNFAIP3* have previously been mentioned as being involved in the NF-KB pathway, but can also be responsible for induction and regulation on the TNF pathway. TNF has previously been shown to be highly expressed during periods of wakefulness in mice and it has also been demonstrated that during sleep deprivation IL-1β and TNF accumulate in the CSF which help to induce sleep and IL-1β levels are highest at

the onset of sleep (Moldofsky et al. 1986; Kapas et al. 2008). So these genes may be increased during periods of chronic OX activation (for example 24 hours as in this study) to combat sleep deprivation and to try and induce sleep. Consequently TNF and IL-1β are extremely important in inducing sleep and preventing the sleep depriving actions of orexin (Krueger, Majde 1994). This may be of importance in AD where the sleep-wake cycle is disturbed.

AD was also highlighted as a KEGG pathway regulated by OXA. 3 genes were identified; *GRIN1*, *IL-1β* and *MAPT*. However there are other genes previously mentioned that are linked to AD, so the involvement of OXA in AD is not necessarily confined to these 3 genes. *GRIN1* encodes a subunit of the NMDA receptor, in AD excess glutamate binds to these receptors and allows calcium influx leading to excitotoxic cell death (Kotermanski, Johnson 2009). Therefore OXAs upregulation of *GRIN1* could lead to increased NMDA receptor expression, which in periods of glutamate toxicity could result in neurodegeneration. However the functional NMDA receptor is comprised of 4 subunits, only two of which are encoded by *GRIN1*, the other two by *GRIN2A-D* which did not change expression upon OXA treatment (Dingledine et al. 1999). So this is not entirely indicative of a negative involvement in AD since it requires 2 other subunits to be a fully functional receptor. IL-1β as previously discussed is involved in the TNF pathway, NF-KB and the MAPK pathway as well as encouraging the onset of sleep after chronic sleep deprivation. However it is also involved in AD as it leads to the induction of inflammatory cytokines and causes neuroinflammation; one of the hallmarks of AD (Shaftel, Griffin & O'Banion 2008). *MAPT* encodes the tau microtubule binding protein, one of the main proteins involved in the pathology of AD. OXA increases the expression of this protein, which in itself does not lend to either way as to whether it has a positive or negative influence regarding AD, as it is the post translational hyperphosphorylation of tau which causes pathology.

Treatment of SH-SY5Y with 100nM OXB for 24 hours resulted in the change of expression of 715 genes. Of the KEGG pathways identified within this gene list some of the more interesting ones included: PI3K-Akt signalling, neuroactive ligand receptor interaction, Jak-STAT signalling, cytokine-cytokine receptor interaction and 1 gene involved in AD.

OXB regulates neuroactive-ligand receptor interaction including the genes which regulate receptors for the following proteins: dopamine, serotonin, somatostatin, vasopressin, prostaglandin, corticotropin releasing hormone (CRH), metatropic glutamate and ACh. *HTR4*, *SSTR* and *PTGER1* are implicated, as they are with OXA treatment and as previously mentioned *PTGER1* can confer neurotoxicity and leads to increased neuronal cell death in transgenic AD mice (Zhen et al. 2012). *SSTR* which encodes the receptor for somatostatin, is decreased in AD which prevents its Aβ clearing ability and confers neurotoxicity and OXB increased its expression suggesting a beneficial role (Hama, Saido 2005; Thilakawardhana et al. 2005). *CRHR1* is also increased with OXB treatment, which encodes the CRH receptor. CRH has been implicated in neuroprotection in AD and CRHR1 is expressed in areas important in AD including the hippocampus (Elliott-Hunt et al. 2002). When Aβ was added to a primary neuronal culture, CRH protected against cell death instigated by lipid peroxidation and glutamate toxicity and an antagonist for the CRHR ablated this effect (Pedersen et al. 2001; Koutmani et al. 2013). OXBs increase of CRH receptors means more receptor availability for the CRH response towards neuroprotection mediated through the MAPK and cAMP pathways suggesting a protective function in AD (Elliott-Hunt et al. 2002). OXB also increases the neuroactive-ligand receptor interaction involving the dopamine receptor: *DRD3*. DRD3 has been implicated in drug addiction, which is interesting as OX is also involved in drug addiction and reward processes (Calipari, Espana 2012). Dopamine receptors have been shown to protect against free radical damage, a common occurrence in AD (Cassarino et al. 1998; Joyce, Millan 2007).

The P13K-Akt signalling pathway involved 10 genes including; *EPO*, *SYK*, *FGFR4*, *LAMB1*, *CSF3R*, *ITGA3* and *GNG13*. These genes were upregulated and are implicated in part of the P13K-Akt pathway responsible for cell cycle progression and cell survival. So activation by OXB of this pathway could indicate a neuroprotective function. OXB caused upregulation of *DDIT4* also known as *REDD1*, a gene involved in inhibition of mTOR and which is induced by hypoxia and ROS (Katiyar et al. 2009). mTOR coordinates cell growth in periods of growth factor and nutrient availability, however during times of stress REDD1 is increased which consequently inhibits mTOR to preserve the existing cell and limit growth with already potentially limited resources. mTOR has also been implicated in AD as it is increased in AD patients and there is an association of active mTOR and accumulation of

hyperphosphorylated tau and NFTs (Li et al. 2005). It is thought that mTOR can in fact not only mediate tau phosphorylation but also decrease autophagy and allow accumulation of tau and Aβ in AD, with the inhibitor of mTOR; rapamycin, having been shown to ameliorate symptoms in an AD model (Caccamo et al. 2010; Spilman et al. 2010). OXBs positive regulation of *REDD1* will result in inhibition of mTOR and could be implicated in reduction of NFT accumulation and increasing autophagy to allow toxic protein clearance in AD. The erythropoietin gene or *EPO* is also upregulated with OXB treatment. EPO is involved not only in erythropoiesis but also in cell survival and neuroprotection (Rabie, Marti 2008). EPO is expressed in the brain, particularly in the hippocampus which is an area sensitive to hypoxia where EPO may act as a protective agent as well as protecting against free radicals and glutamate toxicity (Rabie, Marti 2008; Zhong et al. 2007). EPO has been shown to not only protect against AD toxicity in a transgenic mouse model, but in SH-SY5Y to protect against tau phosphorylation, oxidative stress and apoptotic activation induced by Aβ (Lee et al. 2012). OXB induced upregulation of this gene indicates a neuroprotective effect particularly in the context of AD. *JAK2* and *STAT5* expression are also increased upon OXB treatment. This is of particular importance as not only are they involved in activation of genes important for survival but have also been implicated in AD through the promotion of cell survival after Aβ insult. EPO also promotes cell survival in these circumstances through activation of JAK2 (Digicaylioglu, Lipton 2001; Shaw, Bencherif & Marrero 2003; Ma et al. 2014).

The most significant molecular function GO term for OXB treatment was pyridoxal phosphate (PLP) binding. PLP is the catalytically active form of vitamin B6 and is a cofactor for an abundance of enzymes (Hashim et al. 2011). PLP reduces plasma homocysteine levels and administration of vitamin B6 has been shown to slow cortical shrinkage and atrophy in AD human patients and in AD transgenic mice with a B6 deficiency there was increased cognitive impairment and neurodegeneration (Hasegawa et al. 2010; Douaud et al. 2013). In AD, homocysteine levels are elevated and this can lead to neurodegeneration by oxidative stress and increased phosphorylated tau (Douaud et al. 2013). OXB could confer neuroprotection through increasing PLP binding and reduction of circulating homocysteine in AD.

6 genes altered by OXB are involved with the transition metal ion transmembrane transporter activity GO term. Transition metals include iron, zinc and copper; which have been shown to be involved in Aβ aggregation. All these metals play important roles in the functioning of the brain and are found in high concentrations in areas afflicted by AD. They have been found to propagate the aggregation of Aβ and are found at high concentrations in the plaques deposited in AD (Bush 2003). Of the genes involved in this GO term upon OXB treatment one is for the protein copper chaperone for superoxide dismutase (CCS). CCS not only binds to BACE1 to affect processing of APP but also to the neuronal adapter protein X11α, which when overexpressed inhibits Aβ production (McLoughlin et al. 2001; Angeletti et al. 2005). In a mouse model *CSS* KO neurons increased Aβ production and in SH-SY5Y *CCS* siRNA treated cells Aβ was also increased, possibly as a result of its inability to bind and activate X11α (Gray et al. 2010). OXB upregulates *CSS* and hence may be involved in reducing aggregation of Aβ.

QRFP treatment of SH-SY5Y cells affects 2056 genes, far more than for OXA or OXB treatment. The main KEGG pathways include; neuroactive-ligand receptor interaction, metabolic pathways, cytokine-cytokine receptor interaction, PI3K-Akt, Jak-STAT, MAPK, TNF, NF-KB and AD. The neuroactive-ligand receptor interaction pathway includes genes involved in the receptors for dopamine, serotonin, somatostatin and ACh. QRFP induces expression of the dopamine receptor *DRD3* and the somatostatin receptors: *SSTR3* and *SSTR4*, which as previously explained have been implicated in neuroprotection and the somatostatin receptors specifically in reduction of Aβ plaques (Hama, Saido 2005; Joyce, Millan 2007). QRFP also stimulates ghrelin receptor expression (*GHSR*). Ghrelin is a protein which stimulates feeding much like the OXs and has been shown to play a neuroprotective effect upon ischemic and AD assault. Ghrelin reduced neuronal cell death and apoptosis in the hippocampus of rats with cerebral ischemia and rescued memory deficits in transgenic AD mice as well as reducing neuronal loss and synaptic degeneration (Liu et al. 2006; Moon et al. 2011). An age related decline of ghrelin has been demonstrated, but levels do not seem to vary in AD patients compared to age matched controls. Although it may not have a direct effect in AD, if QRFP increases ghrelin signalling it may induce neuroprotection against the hallmarks of AD that have been shown in previous studies. QRFP also increases *OX1R*

expression, which is significant as it could indicate possible cross-talk of the two receptors, and QRFP causing upregulation of *OX1R* to manage with the increase in QRFP.

QRFP regulates 16 genes involved in the PI3K-Akt signalling pathway, many of which are involved in cell survival. *EPO* increases by 3.5 fold when treated with QRFP and as previously discussed is not only highly important in cell survival but is also neuroprotective in AD. The gene *BCL2L11* encodes the protein Bcl2-interacting mediator of cell death (BIM) and with QRFP treatment is down-regulated. BIM is induced by Aβ in AD brains and is highly expressed compared to controls and has also been shown to be essential for Aβ dependent neuronal death through activation of CDK4 and c-MYB (Biswas et al. 2007). Interestingly *c-MYB* is also down-regulated with QRFP addition. c-MYB binds to the promoter region of BIM and induces its expression, so the reduction seen in *c-MYB* will mean the protein cannot bind to the BIM promoter resulting in its observed reduction and thus increasing cell survival (Deng, Ishii & Sarai 1996; Biswas, Liu & Greene 2005). Therefore QRFP may evoke neuroprotective mechanisms by reducing *c-MYB* and *BCL2L11* and consequently promoting cellular survival. The gene *PDGFB* was upregulated upon QRFP treatment and is also involved in the PI3K-Akt pathway. It encodes the protein platelet-derived growth factor-β (PDGF-β) which binds to its receptor on pericytes and regulates proliferation, migration and recruitment of pericytes to the vascular wall (Bell et al. 2010a). Pericytes are cells embedded within the vessels of the brain and are situated between endothelial cells of capillaries, astrocytes and neurons (Armulik et al. 2010). They have been shown to regulate clearance of toxic products from the brain and pericyte loss in mice leads to brain vascular damage by breakdown of the BBB due to an inability to remove toxic products leading to hypoxia and degeneration (Sagare et al. 2013; Bell et al. 2010). Inability of PDGF-β to bind to pericytes leads to degeneration of these cells meaning that Aβ cannot be cleared and consequently accumulates. In mouse models with a PDGFR-β deficiency, Aβ is significantly higher than in *APP* mutation only mice as well as experiencing a significant increase in tau hyperphosphorylation (Sagare et al. 2013). Therefore PDGF-β is essential for functionality of pericytes which are then able to clear Aβ accumulation and loss of pericytes can worsen the burden of disease. QRFP treatment increases the expression of the gene encoding this protein, suggesting a neuroprotective role in increasing pericyte functionality to clear toxic protein accumulation.

QRFP treatment also regulated 14 genes involved in the JAK-STAT pathway. This pathway is important as it regulates cell survival, proliferation and differentiation as well as being involved in the brain and its neuroprotection (Nicolas et al. 2012). QRFP increased expression of *JAK2* and *STAT5* with the JAK2/STAT5 pathway being essential in EPO mediated neuroprotection and cell survival (Digicaylioglu, Lipton 2001; Ma et al. 2014).

We also show that QRFP regulates 13 genes involved in the MAPK pathway. This includes 7 voltage dependent calcium channel genes which are involved in MAPK signalling including: *$Ca_V2.1$, $Ca_V2.2$* and *$Ca_v3.2$*. Voltage-dependent calcium channels (VDCC) when activated allow an influx of calcium into the cells and mediates neurotransmitter release. *$Ca_V2.1$* KO mice result in a neurologically defective phenotype with deficits in learning, memory and circadian rhythm with survival being limited to 4 weeks (Mallmann et al. 2013). Loss of circadian rhythm in these KO mice, might suggest a possible OX/QRFP involvement and loss of $Ca_V2.1$ results in increased accumulation of Aβ plaques with Aβ suppressing the proper functioning of these channels (Mallmann et al. 2013). So QRFP mediated increase of VDCC could play an important role in AD. The gene *MAP3K5/ASK1* is also implicated in the MAPK pathway and upon QRFP treatment experiences a significant reduction in expression. This is of particular importance as activation of ASK1 through ROS is essential for the Aβ mediated death of neurons and hence a reduction in *ASK1*, as seen in QRFP treatment, will reduce Aβ mediated cell death through the JNK pathway which induces apoptosis (Kadowaki et al. 2005). Myocyte-specific enhancer factor 2C (*MEF2C*) was also implicated in MAPK and experienced a reduction. MEF2C functions to prevent excessive synapse formation and facilitates hippocampal-dependent learning and memory (Barbosa et al. 2008). Although its exact role in AD is not known, in a genome-wide association study (GWAS) mutations in this gene were found to be associated with AD (European Alzheimer's Disease Initiative (EADI) et al. 2013).

QRFP also regulated 3 genes involved in AD; *ITPR1*, *NDUFS7* and *RYR3*. *ITPR1* encodes the inositol 1,4,5trisphosphate receptor (IP_3R) and with QRFP treatment was found to be upregulated. The evidence of this genes involvement is contradictory as some studies suggest a protective effect and others suggest a degenerative effect. IP_3R can be upregulated upon excitotoxicity and can enhance calcium activated potassium channels. This can halt the

progression of excitotoxic damage and prevent increased cell death (Park, Yule & Bowers 2010). However IP_3R has also been shown to be linked to *PS* mutations in EOFAD and increased interaction of IP_3R-PS leads to a gain of function of the receptor and increased calcium signalling which may be detrimental to the cell (Cheung et al. 2010). So the increase in *ITPR1*caused by QRFP treatment could potentially be protective or damaging. *NDUFS7* encodes NADH dehydrogenase iron-sulphur protein 7 mitochondrial, which forms part of the mitochondrial respiratory chain and transfers electrons from nicotinamide adenine dinucleotide (NADH) to the respiratory chain. It is found to be increased in vulnerable neurons like pyramidal neurons in the hippocampus of AD brains and siRNA targeted to *NDUFS7* reduced Aβ levels in HEK cells overexpressing human *APP* (Frykman et al. 2012). *RYR3* encodes ryanodine receptor type 3, which is important in calcium regulation in the brain (Liu et al. 2014). In a transgenic mouse model of AD, deletion of *RYR3* resulted in accelerated AD pathology and using siRNA against *RYR3* in another transgenic AD mouse model there was enhanced neuronal cell death (Liu et al. 2014; Supnet et al. 2010). However other studies have suggested that increased *RYR3* is detrimental in AD and increases Aβ deposition and memory deficits (Oules et al. 2012). This study however was performed in SH-SY5Y as opposed to transgenic mouse models so may not be as accurate of a representation.

Microarray analysis revealed many genes important in AD to be regulated upon OXA, OXB and QRFP addition. And not all of the genes identified follow the same pattern of neuroprotection or neurodegeneration. For example genes implicated in neuroprotection in AD such as; *SSTR3*, *VIP*, *MAP3K14*, *CRH*, *DRD3*, *REDD1*, *EPO*, *BCL2L11*, c-*MYB* and *PDGF*-β are all regulated by OXA, OXB or QRFP suggesting that these peptides under AD circumstances can induce neuroprotection. However other genes such as *PTGER1* and *GRIN1* which exacerbated AD are also regulated upon peptide addition. Based on what we have described here more genes regulated by OXA, OXB and QRFP favour a neuroprotective role. Of note is that both OXA and QRFP regulate many genes involved in the increasing the NF-KB pathway, which could be of great importance due to the substantial effect of RNA oxidation implicated in AD and the cell surviving effects it exerts. Collectively, some data point towards a common regulation of certain genes by all 3 peptides. This microarray demonstrates that QRFP is capable of eliciting a response above and beyond what OXA and

OXB are capable of, suggesting that QRFP may be more integral than previously thought. Given that QRFP also increases the expression of OX1R and our previous data which shows OXR antagonists are capable of preventing QRFP signalling; it is attractive to speculate that there is a higher order of complexity in OXR/GPR103 signalling involving potential cross-talk mechanisms.

6

Chapter 6

Treatment of differentiated IMR32 and SH-SY5Y cell lines with $A\beta^{42}$ and zinc sulphate to mimic an Alzheimer's disease milieu

6.1 Introduction

Around 82% of AD sufferers experience dysregulated sleep patterns. This includes excessive sleepiness, REM dysregulation and circadian rhythm disturbances bearing a resemblance to narcolepsy (Fronczek et al. 2011). Increased nocturnal activity differentiates AD from other forms of dementia (Harper et al. 2001a). In a Tg2576 mouse model of AD with an APP mutation which were given an OXA infusion, Aβ levels were markedly increased compared to the control. This increase in Aβ was ablated by OX antagonist addition (Kang et al. 2009). These transgenic mice were also chronically sleep deprived and Aβ plaque formation increased compared to an age matched control, with OX antagonist treatment vastly reducing plaque formation (Kang et al. 2009). Another recent study showed that in AD patients there was a loss of up to 40% of orexigenic neurons and patients experienced stark reductions in circulating OX levels (Fronczek et al. 2011). However to date there have been no comprehensive studies observing or mapping of OXRs and GPR103 in human AD.

$A\beta^{42}$ in AD patients has been shown to reach concentrations lower than 100nM but can reach μM ranges (Kuo et al. 1996; Steinerman et al. 2008; Wang et al. 1999). 1 μM was deemed an appropriate representation of *in vivo* circumstances. Zinc sulphate has previously been shown to initiate tau hyperphosphorylation at a concentration of 100nM, resulting in NFTs and zinc has also been found to be associated with cells in AD which are NFT containing (An et al. 2005; Suh et al. 2000).

6.2 Objectives

Our aim was to treat fully differentiated IMR32 and SH-SY5Y cells with $A\beta^{42}$ and zinc sulphate to induce amyloid deposition and tau hyperphosphorylation respectively. This allows the mimicking of an AD milieu to examine their effects on the OXRs and GPR103 and the subsequent downstream effects on ERK1/2 signalling, which we have already shown is phosphorylated by OXA, OXB and QRFP.

6.3 Results

6.3.1 Conformation of tau hyperphosphorylation and $A\beta^{42}$ deposition

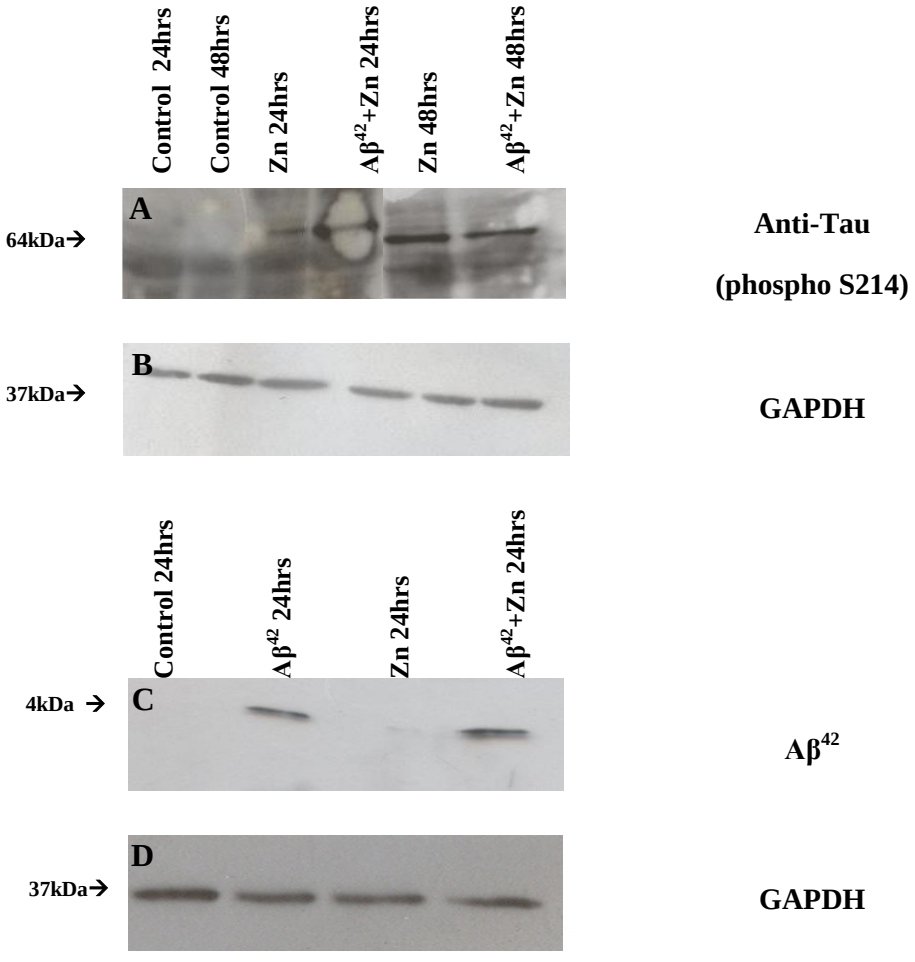

Figure 6.1: Western blot representations of A. phosphorylated tau after control and 100nM zinc sulphate treatments with or without 1μM $A\beta^{42}$ at 24 and 48 hours. B. GAPDH loading control of panel A. C. $A\beta^{42}$ deposition in control, 100nM zinc sulphate and 1μM $A\beta^{42}$ treatment and both together at 24 and 48 hours. D. GAPDH loading control of panel C.

Western blots were performed to ensure tau hyperphosphorylation after zinc treatment and $A\beta^{42}$ deposition after $A\beta^{42}$ treatment. Figure 6.1A shows there is more tau hyperphosphorylation after zinc sulphate treatment. Tau has 6 isoforms which are expressed in the brain, varying in range from 352 amino acids to 441(Avila et al. 2004; Deshpande, Win & Busciglio 2008). Phosphorylation of tau at its serine 214 site is particularly important as it causes powerful microtubule binding disruption (Illenberger et al. 1998). An antibody which detects the tau protein when phosphorylated at serine 214 was used. Phosphorylation at this site has also been found in AD as well as 79 other serine/threonine phosphorylation sites (Hanger et al. 2007). After zinc sulphate treatment in all samples, there was increased tau phosphorylation at ser214 and there were no detectable bands in the control samples at this molecular weight. Figure 6.1C shows that in samples treated with $A\beta^{42}$ there was protein deposition which was detected at 4kDa, but no discernable deposition in control samples.

6.3.2. qPCR of $A\beta^{42}$ and zinc sulphate treated cells after 24 and 48 hours to observe changes in OXRs and GPR103 expression.

Fully differentiated IMR32 and SH-SY5Y cell lines were seeded at $1x10^5$ in 6 well plates overnight. Cells were then serum starved for 6 hours to ensure all cells were at the same stage of the cell cycle and treatments of ; 1µM $A\beta^{42}$, 100nM zinc sulphate or both together were added to appropriate wells. 24 and 48 hour post treatment, RNA was extracted, cDNA synthesis performed and qPCR was completed on these samples as previously described.

In IMR32 cells, $A\beta^{42}$ treatment resulted in an increase in expression for all 3 genes (Figure 6.2-6.4). For *OX1R*, all treatments resulted in an increase in expression however these changes were all below a 2 fold increase and were not significant. For *OX2R* there were very small increases in expression, which were also not significant. *GPR103* displayed an increase in expression for both time points; however the change was only significant for 48 hour zinc sulphate treatment.

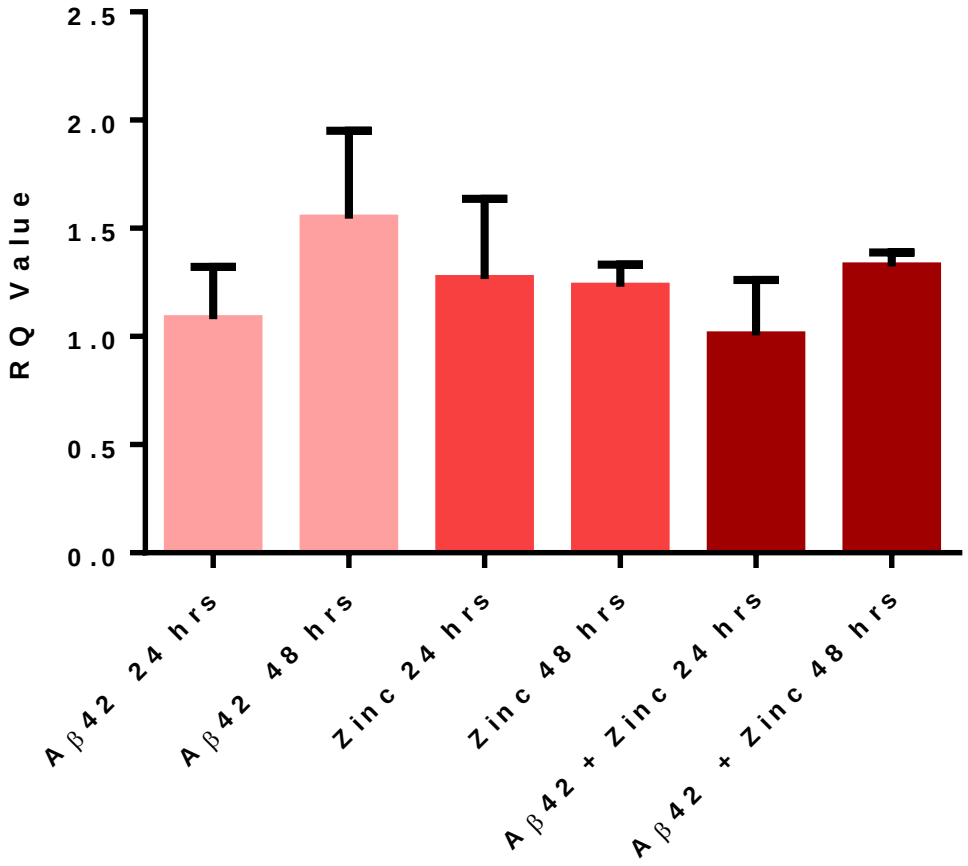

Figure 6.2: IMR32 gene expression changes of *OX1R* after 24 and 48 hours of 1µM $A\beta^{42}$, 100nM zinc sulphate or both together compared to the equivalent time points with no treatment ±S.D. Results were obtained from 3 independent experiments.

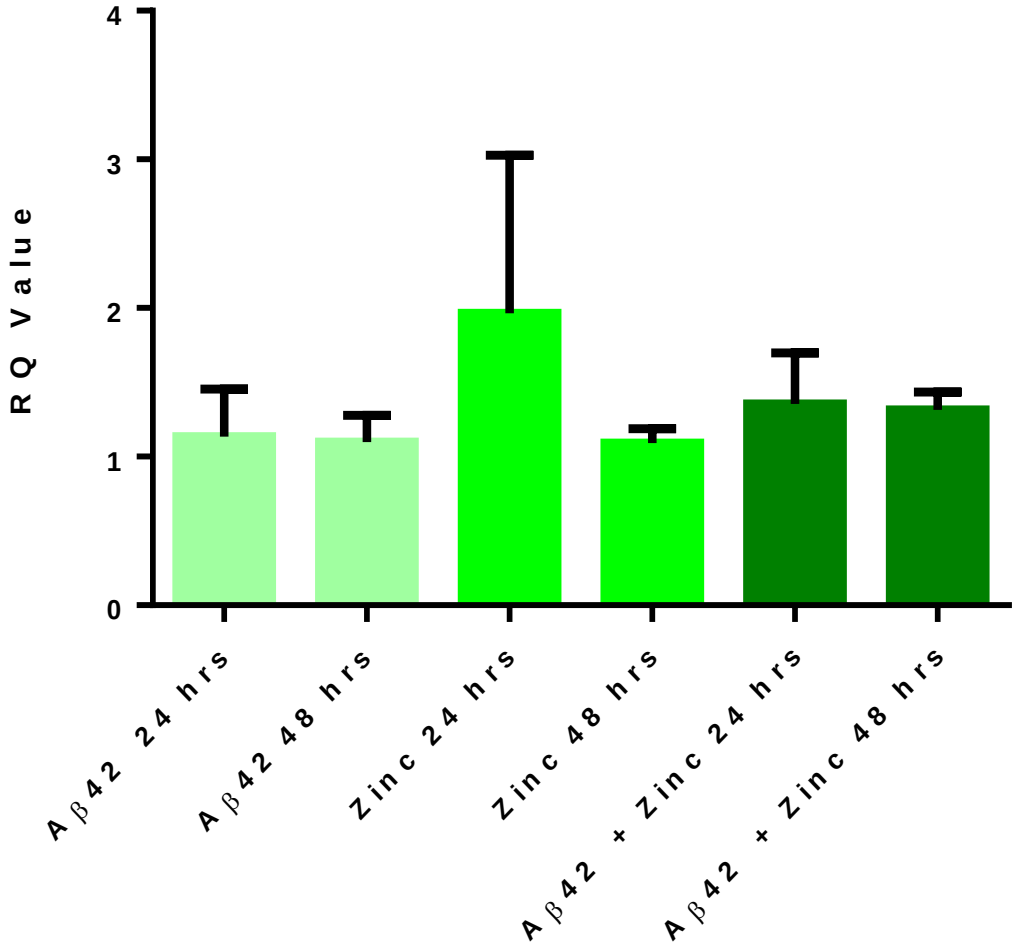

Figure 6.3: IMR32 gene expression changes of *OX2R* after 24 and 48 hours of 1µM $A\beta^{42}$, 100nM zinc sulphate or both together compared to the equivalent time points with no treatment. Results were obtained from 3 independent experiments ±S.D.

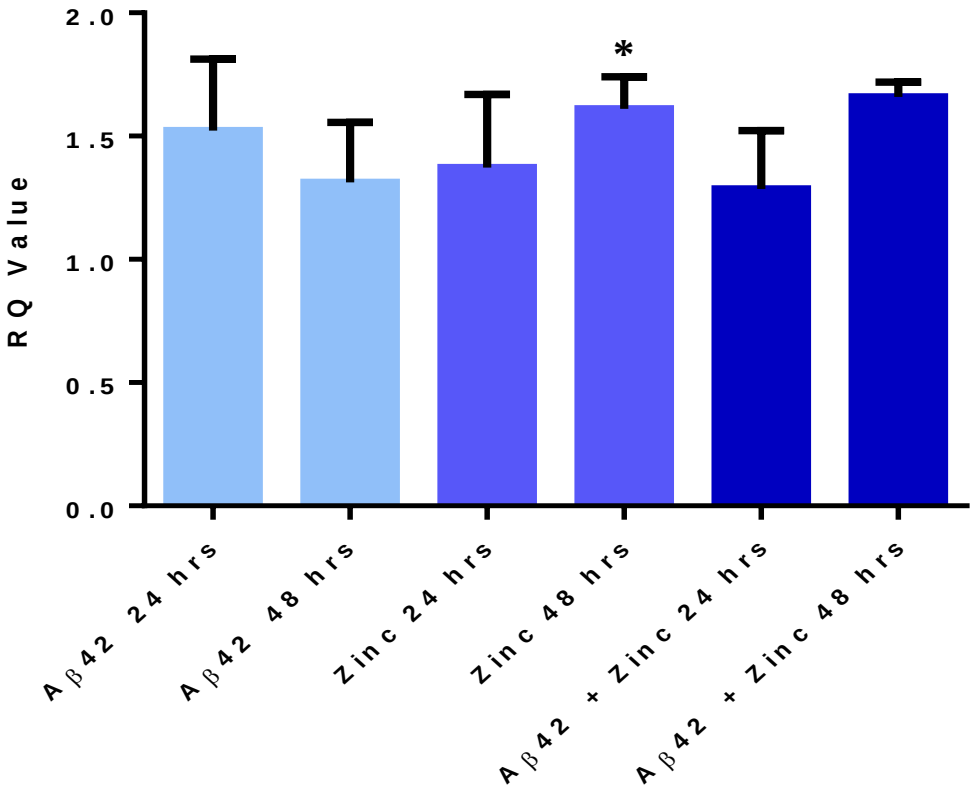

Figure 6.4: IMR32 gene expression changes of *GPR103* after 24 and 48 hours of 1µM $A\beta^{42}$, 100nM zinc sulphate or both together compared to the equivalent time point with no treatment. Results were obtained from 3 independent experiments ±S.D. Statistically significant differences of treated cells to corresponding control time points were calculated using the paired students T-test ($p<0.05$*).

$A\beta^{42}$ and zinc sulphate treatment in SH-SY5Y cells yielded very different results from IMR32. *OX1R* revealed a significant decrease in expression upon 24 hours of $A\beta^{42}$ treatment which increased slightly after 48 hours but was still lower than the control. After 24 hours $A\beta^{42}$, *OX2R* remained stable but after 48 hours was decreased. *GPR103* decreased significantly after 24 and 48 hours, but was slightly increased at 48 hours compared to 24 hours. Zinc sulphate induced significant decreases in *OX1R* expression after 24 and 48 hours treatment, but for *OX2R* there was an increase in the receptor expression after 48 hours, however this was only marginally higher than the control expression. *GPR103* was significantly decreased after 24 hours zinc treatment and was

decreased after 48 hours but not as pronounced as was seen at 24 hours. Aβ^{42} and zinc sulphate treatment yielded decreases in *OX1R* expression after 24 hours which was significantly reduced after 48 hours. For *OX2R* there was a slight increase after 24 hours followed by a significant reduction after 48 hours. *GPR103* was significantly reduced at 24 and 48 hours after Aβ^{42} and zinc sulphate treatment.

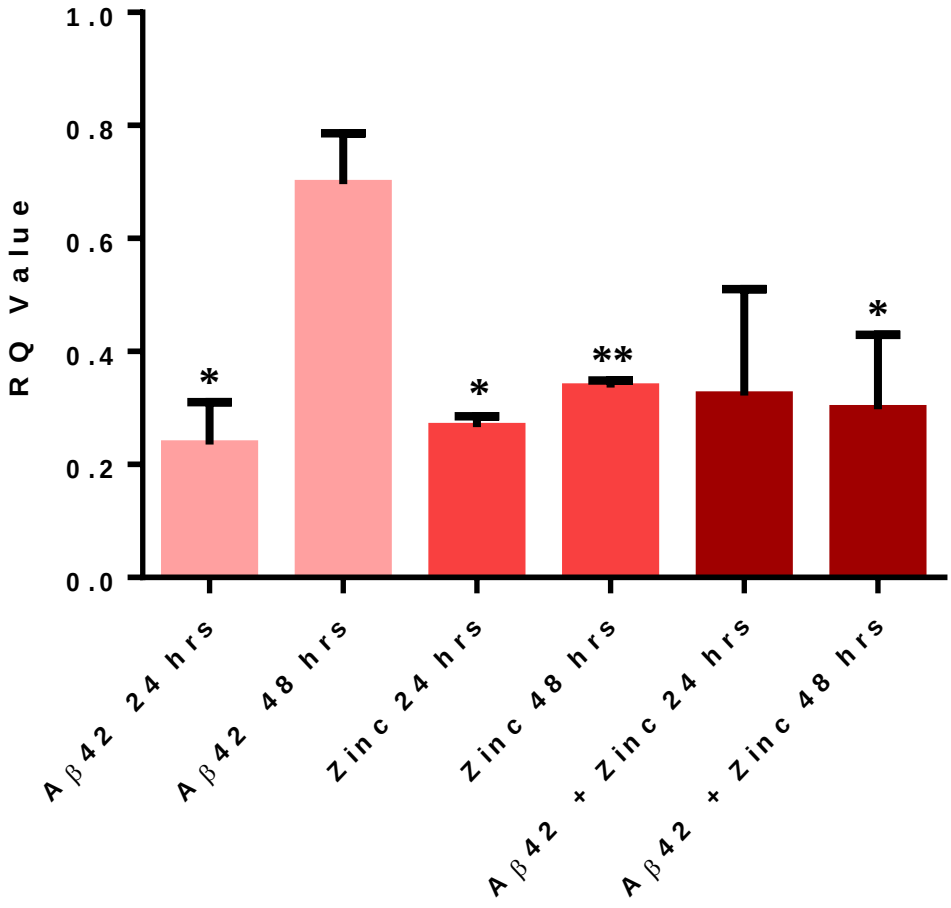

Figure 6.5: SH-SY5Y gene expression changes of *OX1R* after 24 and 48 hours of 1µM Aβ^{42}, 100nM zinc sulphate or both together compared to the equivalent time point with no treatment. Results were obtained from 3 independent experiments ±S.D. Statistically significant differences of treated cells to corresponding control time points were calculated using the paired students T-test ($p<0.05$*, $p<0.01$**).

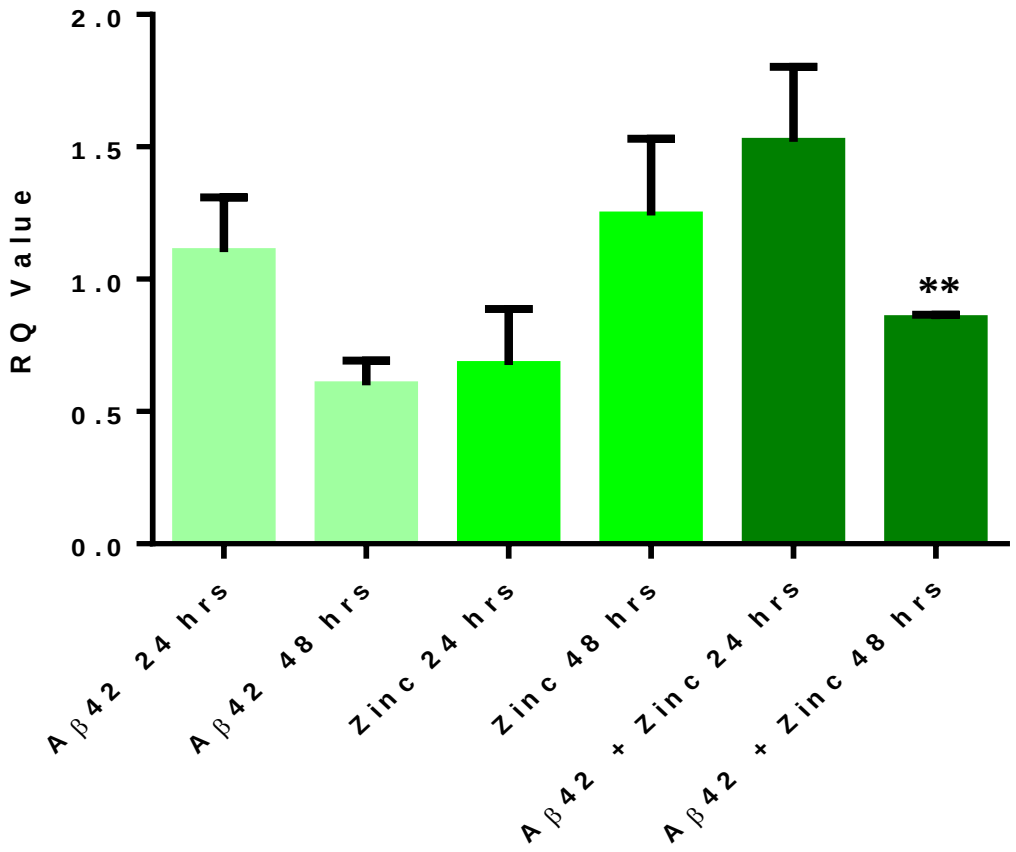

Figure 6.6: SH-SY5Y gene expression changes of *OX2R* after 24 and 48 hours of 1µM $A\beta^{42}$, 100nM zinc sulphate or both together compared to the equivalent time point with no treatment. Results were obtained from 3 independent experiments ±S.D. Statistically significant differences of treated cells to corresponding control time points were calculated using the paired students T-test ($p<0.01$**).

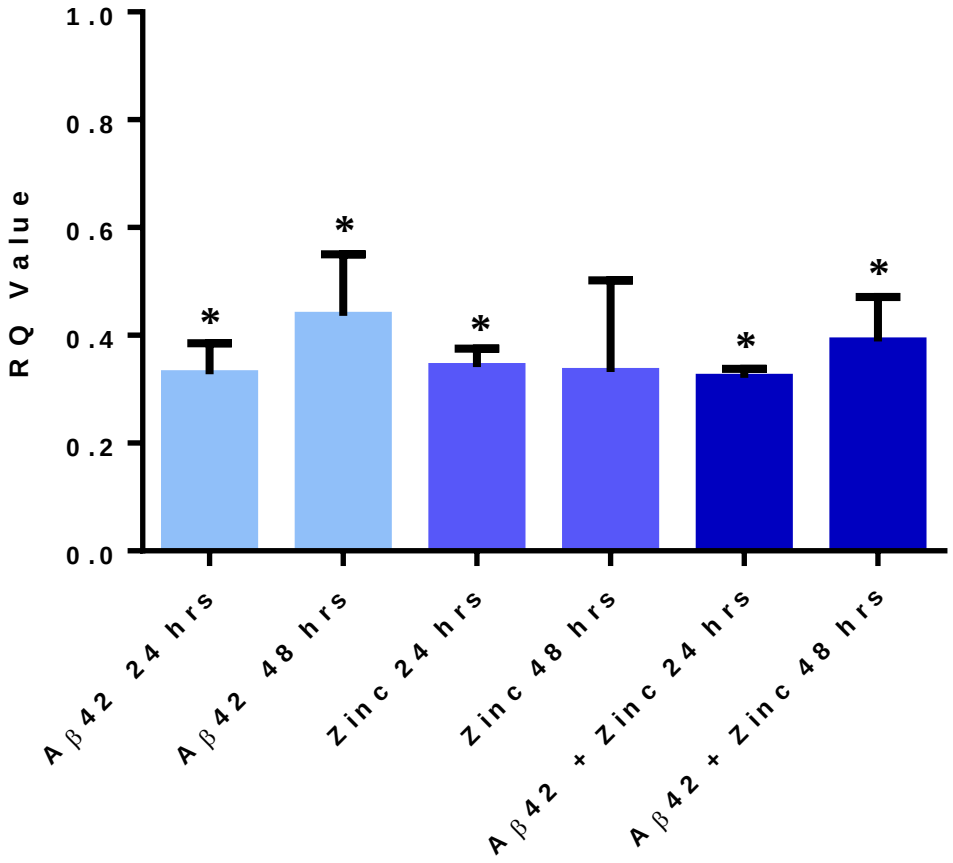

Figure 6.7: SH-SY5Y gene expression changes of *GPR103* after 24 and 48 hours of 1µM Aβ^{42}, 100nM zinc sulphate or both together compared to the equivalent time point with no treatment. Results were obtained from 3 independent experiments ±S.D. Statistically significant differences of treated cells to corresponding control time point were calculated using the paired students T-test ($p<0.05$*).

6.3.3. p-ERK1/2 activation in cells treated with Aβ^{42}, zinc sulphate or both upon treatment with 100nM OXA, OXB or QRFP.

We examined p-ERK1/2 in treated cells to investigate whether OX or QRFP differentially affect ERK1/2 phosphorylation in the presence of Aβ^{42} or tau hyperphosphorylation. Before doing so, we studied basal p-ERK1/2 levels to use as a reference point to observe any changes caused by peptide addition. After 24 and 48 hours of treatments with 1µM Aβ^{42}, 100nM zinc sulphate or both together; 100nM

OXA, OXB or QRFP was added for 20 minutes. This duration was used, as previous studies demonstrated a good activation of ERK1/2 at this time point when we treated cells with OXA, OXB or QRFP. Protein was then harvested and samples were analysed by western blot, using t-ERK1/2 to normalise the amount of p-ERK1/2. All samples treated with the peptides, were normalised to the basal levels of p-ERK1/2 when there was no peptide present at the same time points to account for any increases in p-ERK1/2 induced by $A\beta^{42}$ or zinc sulphate treatment. Figure 6.8 shows a representative view of ERK1/2 western blots performed on these samples.

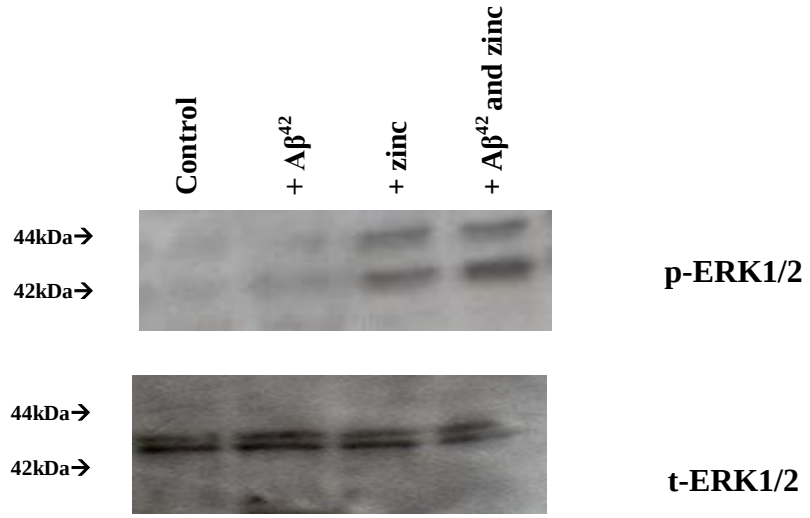

Figure 6.8: Representations of western blots probed with p-ERK1/2 and total-ERK 1/2 antibody in SH-SY5Y upon addition of $A\beta^{42}$ or zinc sulphate or $A\beta^{42}$ +zinc sulphate at 48 hours.

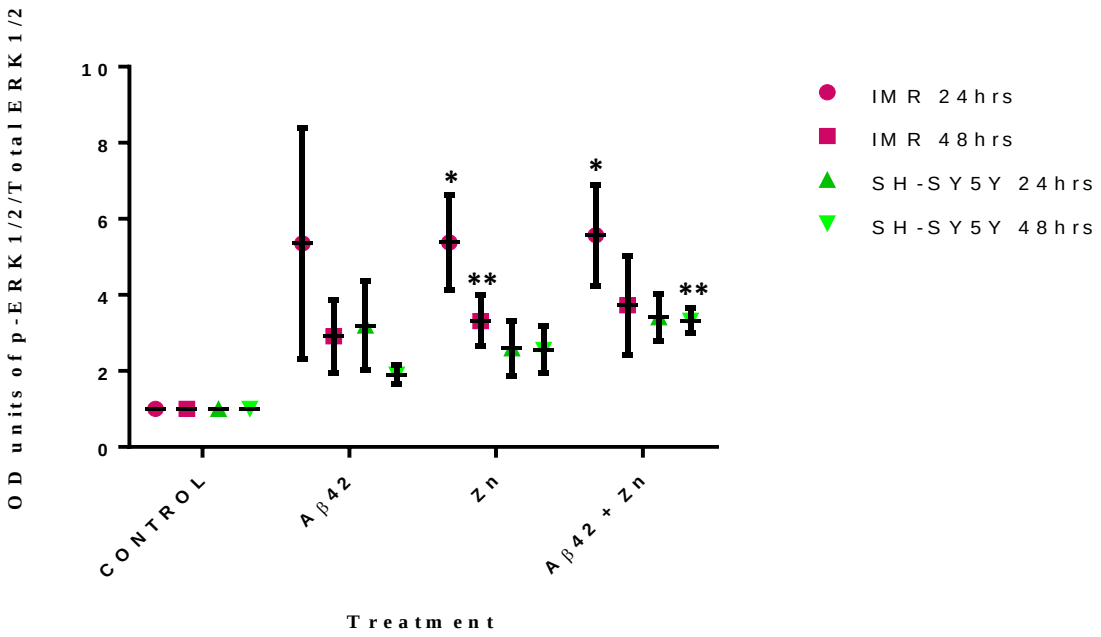

Figure 6.9: Densitometric analysis of basal p-ERK1/2 in IMR32 and SH-SY5Y cells using ImageJ. p-ERK1/2 protein was normalised to t-ERK1/2 protein and displayed as OD units. Results were obtained from 3 independent experiments ±S.D. Statistically significant differences of treated cells to corresponding control time points were calculated using the paired students T-test ($p<0.05$*,$p<0.01$**).

Figure 6.9 shows that at basal levels p-ERK1/2 expressed by both cell lines in all treatments was increased compared to the control. $A\beta^{42}$ induced an increase in p-ERK1/2 expression which was more apparent in both cell lines at 24 hours compared to 48 . However, p-ERK1/2 was consistently higher in IMR32 than in SH-SY5Y. Zinc treatment caused large increases in p-ERK1/2 in IMR32 which were even more elevated at 24 hours but at 48 hours still showed a large increase compared to the control. In SH-SY5Y although the increases in p-ERK1/2 were higher at 24 hours, the difference between the two time points was less than what was observed in IMR32 and they were not as increased as seen in IMR32. $A\beta^{42}$ + zinc treatment resulted in an increase in p-ERK1/2 in both cell lines, which is again higher at 24 hours than 48 and consistently higher in IMR32.

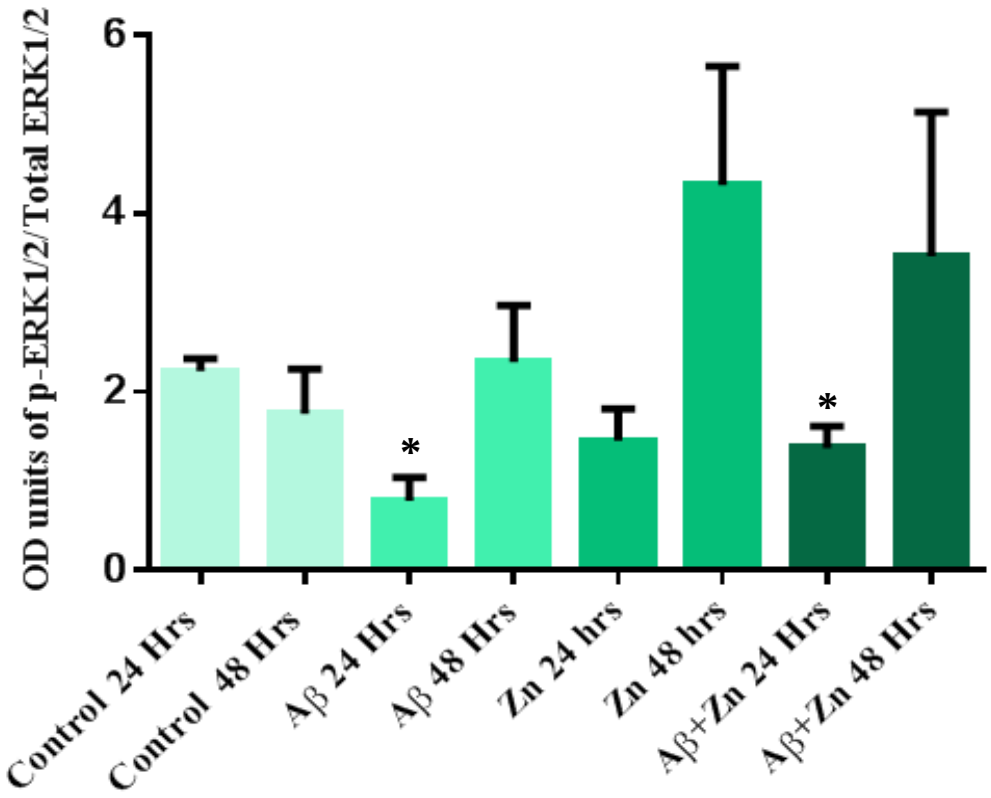

Figure 6.10: Densitometric analysis of IMR32 cells using ImageJ. Cell treatments of control, 1μM $A\beta^{42}$, 100nM zinc sulphate or 1μM $A\beta^{42}$+100nM zinc sulphate were treated with 100nM of OXA for 20 minutes. p-ERK1/2 protein was normalised to t-ERK1/2 protein and displayed as OD units when treated with OXA, and for each treatment this was normalised to corresponding basal ERK1/2 values. Results were obtained from 3 independent experiments ±S.D. Statistically significant differences of treated cells to corresponding control time point were calculated using the Wilcoxon signed-rank test ($p<0.05$*).

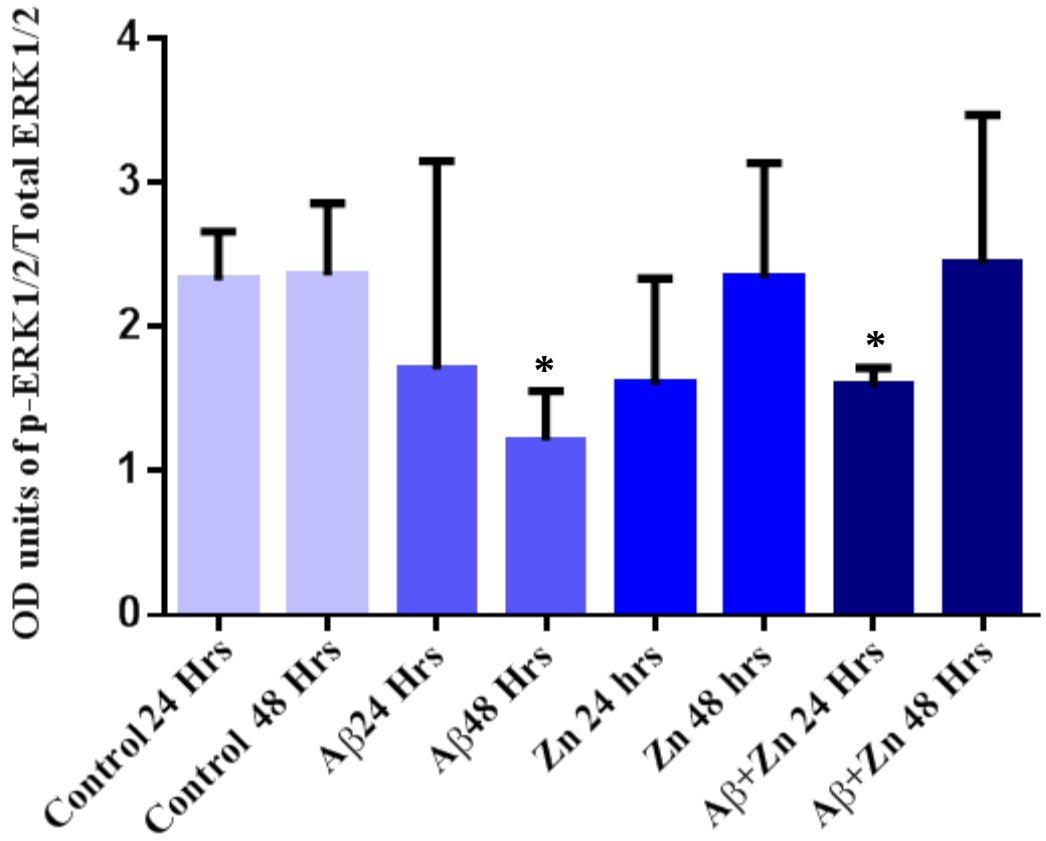

Figure 6.11: Densitometric analysis of IMR32 cells using ImageJ. Cell treatments of control, 1µM $A\beta^{42}$, 100nM zinc sulphate or 1µM $A\beta^{42}$+100nM zinc sulphate were treated with 100nM of OXB for 20 minutes. p-ERK1/2 protein was normalised to t-ERK1/2 protein and displayed as OD units when treated with OXB, and for each treatment this was normalized to corresponding basal ERK1/2 values. Results were obtained from 3 independent experiments ±S.D. Statistically significant differences of treated cells to corresponding control time point were calculated using the Wilcoxon signed-rank test ($p<0.05$*).

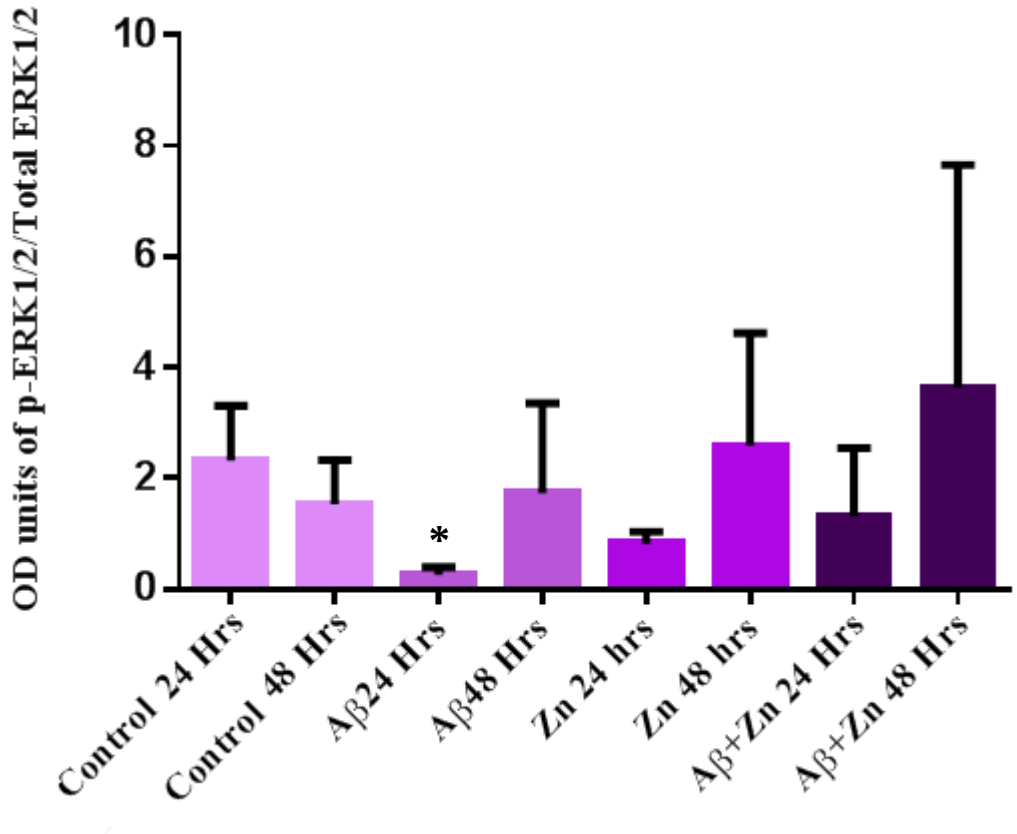

Figure 6.12: Densitometric analysis of IMR32 cells using ImageJ. Cell treatments of control, 1µM $A\beta^{42}$, 100nM zinc sulphate or 1µM $A\beta^{42}$+100nM zinc sulphate were treated with 100nM of QRFP for 20 minutes. p-ERK1/2 protein was normalised to t-ERK1/2 protein and displayed as OD units when treated with QRFP, and for each treatment this was normalised to corresponding basal ERK1/2 values. Results were obtained from 3 independent experiments ±S.D. Statistically significant differences of treated cells to corresponding control time point were calculated using the Wilcoxon signed-rank test ($p<0.05$*).

Western blot analysis of p-ERK1/2 in IMR32 upon treatment with OXA, OXB and QRFP revealed that after 24 hours of treatment with $A\beta^{42}$, zinc and $A\beta^{42}$ + zinc; p-ERK1/2 was reduced compared to the control treated with all peptides. After 48 hours of treatment with OXA and QRFP however the p-ERK1/2 levels for each treatment had increased compared not only to the same treatment at 24 hours but also to the control at 48 hours. For OXB, p-ERK increased in zinc and $A\beta^{42}$ + zinc treated cells after 48 hours, but was still lower than corresponding control values. However for the $A\beta^{42}$

treatment, p-ERK1/2 levels were significantly reduced after 48 hours compared to the control and were lower than the 24 hour $A\beta^{42}$ time point.

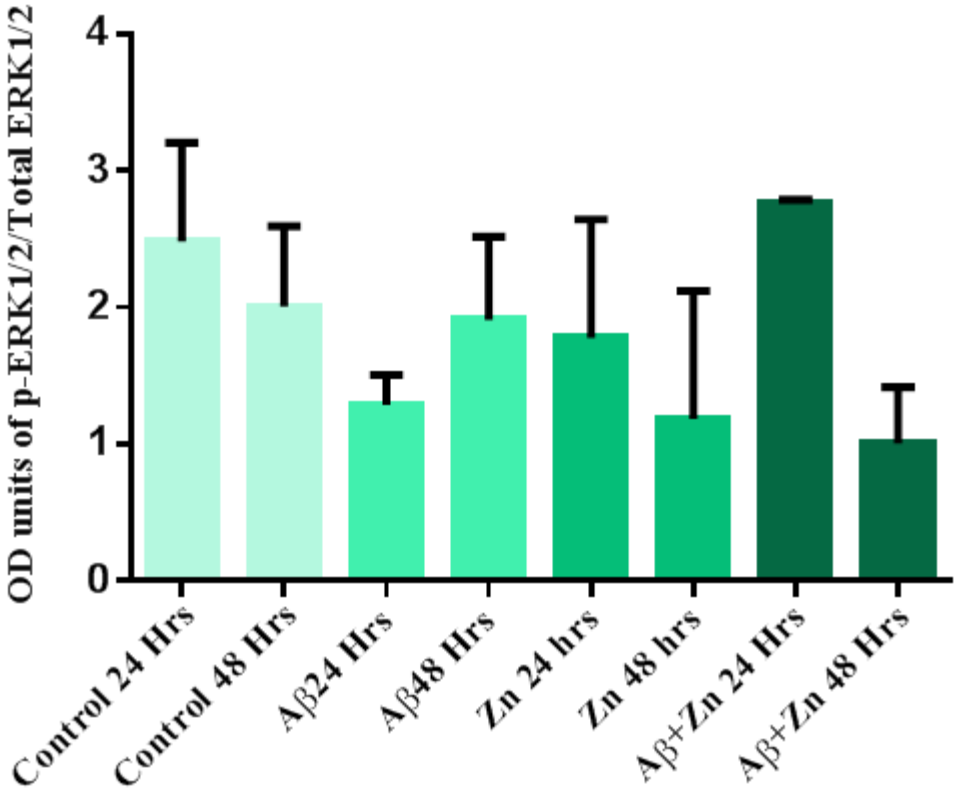

Figure 6.13: Densitometric analysis of SH-SY5Y cells using ImageJ. Cell treatments of control, 1µM $A\beta^{42}$, 100nM zinc sulphate or 1µM $A\beta^{42}$+100nM zinc sulphate were treated with 100nM of OXA for 20 minutes. p-ERK1/2 protein was normalised to t-ERK1/2 protein and displayed as OD units when treated with OXA, and for each treatment, this was normalised to corresponding basal ERK1/2 values. Results were obtained from 3 independent experiments ±S.D.

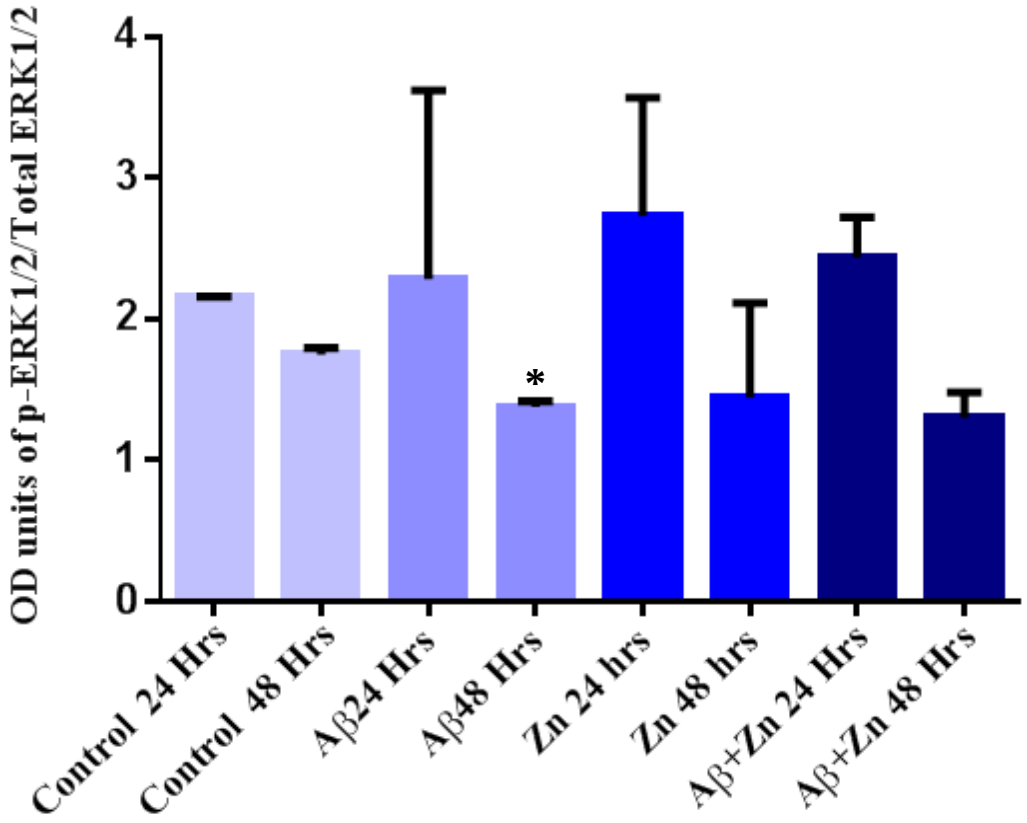

Figure 6.14: Densitometric analysis of SH-SY5Y cells using ImageJ. Cell treatments of control, 1µM $A\beta^{42}$, 100nM zinc sulphate or 1µM $A\beta^{42}$+100nM zinc sulphatewere treated with 100nM of OXB for 20 minutes.p-ERK1/2 protein was normalised to t-ERK1/2 protein and displayed as OD units when treated with OXB, and for each treatment, this was normalised to corresponding basal ERK1/2 values. Results were obtained from 3 independent experiments ±S.D. Statistically significant differences of treated cells to corresponding control time point were calculated using the Wilcoxon signed-rank test ($p<0.05$*).

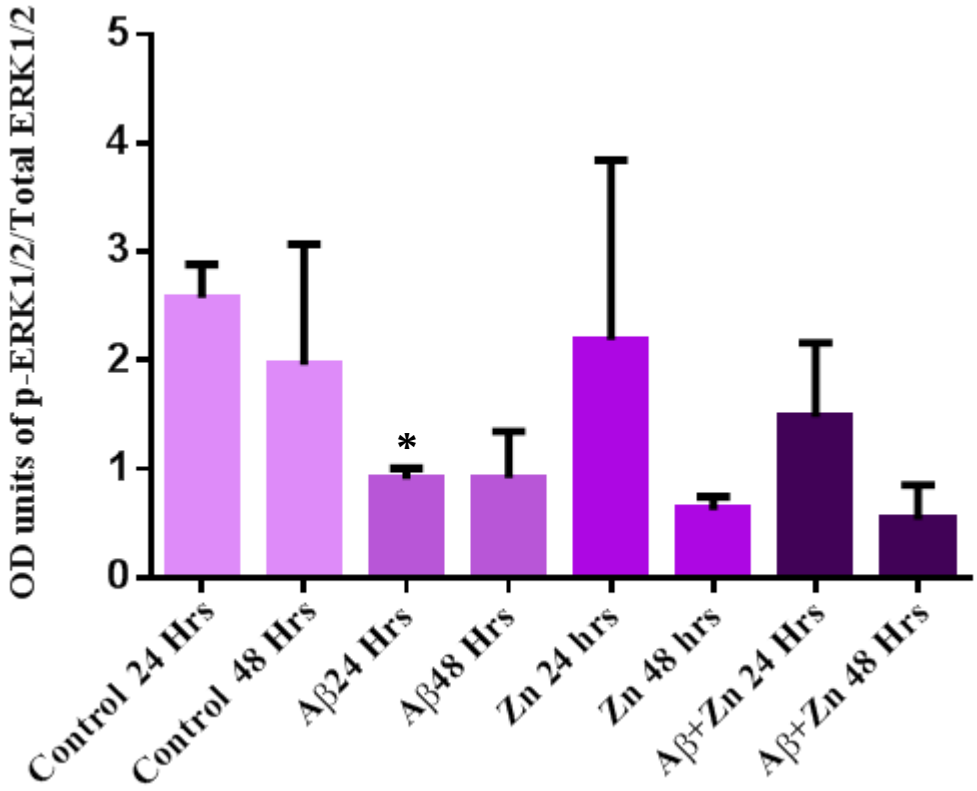

Figure 6.15: Densitometric analysis of SH-SY5Y cells using ImageJ. Cell treatments of control, 1µM $A\beta^{42}$, 100nM zinc sulphate or 1µM $A\beta^{42}$+100nM zinc sulphate were treated with 100nM of QRFP for 20 minutes.p-ERK1/2 protein was normalised to t-ERK1/2 protein and displayed as OD units when treated with QRFP, and for each treatment, this was normalized to corresponding basal ERK1/2 values. Results were obtained from 2 independent experiments S.D. Statistically significant differences of treated cells to corresponding control time point were calculated using the Wilcoxon signed-rank test ($p<0.05$*).

In SH-SY5Y, OXA treatment exhibited a reduction in p-ERK1/2 levels compared to the control for all treatments bar $A\beta^{42}$ + zinc at 24 hours. Expression remained fairly consistent between 24 and 48 hours for $A\beta^{42}$ and zinc, with a slight increase after 48 hours of $A\beta^{42}$ and a slight decrease at 48 hours with zinc treatment. $A\beta^{42}$ + zinc however expressed higher p-ERK1/2 after 24 hours, which reduced after 48 hours to levels lower than seen in the control. For OXB and QRFP however, p-ERK1/2 was higher at 24 hours than at 48 hours and for OXB the 24 hour treatments expressed more

p-ERK1/2 than in the control and by 48 hours they were relatively similar to the control levels. For QRFP $A\beta^{42}$ treatment resulted in much less p-ERK1/2 at both time points compared to the control, but zinc and $A\beta^{42}$ + zinc were higher at 24 hours, but then experienced a reduction at 48 hours.

6.4 Results and discussion

The two most important hallmarks of AD are the accumulation of $A\beta^{42}$ causing formation of Aβ plaques and hyperphosphorylation of tau resulting in NFTs and $A\beta^{42}$ and zinc sulphate can be used to mimic each of these effects respectively *in vitro* (An et al. 2005; He et al. 2013). Previous data suggests that in AD there is a ~40% loss of orexigenic neurons and a 14% reduction in circulating OXA in CSF (Fronczek et al. 2011). This implies that a mimicking of AD through Aβ and zinc could potentially lead to a loss of orexigenic neurons as seen in these previously mentioned clinical samples; however IMR32 did not experience a reduction in receptor expression. On the other hand, Aβ and zinc treatment led to a significant reduction in OX1R and GPR103 in SH-SY5Y. OX and Aβ have been shown to be linked, as an OXA infusion was shown to increase the burden of Aβ in a transgenic mouse model of AD and a dual OX receptor antagonist was shown to reduce the deposition of Aβ (Kang et al. 2009). This suggests that the orexigenic system can be manipulated to control the burden of disease.

IMR32 revealed minimal changes for all receptors apart from GPR103 at 48 hours of zinc treatment, which showed a significant increase compared to the control. SH-SY5Y produced much the opposite effect seen in IMR32, with OX1R and GPR103 experiencing a significant reduction in most of the treatments and some reduction in OX2R. At least 51 genes have been identified which are differentially expressed between female and male mice (Dewing et al. 2003). Sexual dimorphism is also particularly apparent in the brain with dopamine neurons having a different morphology depending on the sex of the rat and female diencephalic neurons have increased tyrosine hydroxylase compared to males (Carruth, Reisert & Arnold 2002; Beyer, Pilgrim & Reisert 1991). It has also been found that the male colon carcinoma cell line T-84 has lost the Y chromosome and when compared to the female equivalent: Ht-29 there are very few differences in biological properties. This could be because they are

functionally equivalent or because of loss of the Y chromosome. The X chromosome encodes up to 900 genes, but the Y chromosome still encodes 78 and thus determines more than just the sex which is evidenced by X-linked diseases such as haemophilia and red-green colour blindness (Fuller, Insel 2014). Severity and incidence of disease in AD has been shown to exhibit sexual dimorphism. More women are affected by AD than men; in the UK 222,000 men are thought to be affected compared with 445,000 women (Source: Dementia UK: The full report). In Tg2576 mice with an APP mutation comparisons of the area of the brain occupied by plaque formation at 15 months of age, revealed that female mice had nearly 3 times more plaque deposition than in males as well as females experiencing increased circulating $A\beta^{40}$ and $A\beta^{42}$ levels (Callahan et al. 2001; Wang et al. 2003). It is thought this could be a result of the loss of estrogen protection in post-menopausal women. Estrogen has been shown to protect against toxicity induced by Aβ as well as inhibiting lipid peroxidation in AD (Fitzpatrick et al. 2002; Perez et al. 2005). Female mice were also found to have increased β-secretase activity and reduced neprilysin which could result in increased Aβ production and decreased degradation contributing to an overall increase in the burden of disease (Hirata-Fukae et al. 2008). Differences in tau hyperphosphorylation have also been described. In TgP301L mice which are a strain noted for development of NFTs, there was increased NFT formation in female mice compared to male mice (Asuni et al. 2007). In human patients women have been shown to have more NFTs and more Aβ plaques than in men (Barnes et al. 2005). This reduction seen in the female cell line: SH-SY5Y compared to the male cell line: IMR32, of OXR/GPR103 may contribute to selective neurodegeneration and increased burden of disease in females. This evidence suggests that there could be a sexual dimorphic factor accounting for the differences we observed in these cell lines and any potential beneficial effect exerted by the orexigenic system could be negated in females who are potentially more susceptible to a loss of OXR/GPR103 than males.

At basal levels treatment with $A\beta^{42}$ and zinc increased p-ERK1/2 levels. These data corroborate other similar findings, as it has been previously demonstrated that $A\beta^{42}$ and zinc addition in rat hippocampal or renal cortical cultures respectively cause increases in p-ERK1/2 (Kohda et al. 2006; Dineley et al. 2001). $A\beta^{42}$ and zinc may cause this

increase through the alpha 7 nicotinic acetylcholine receptor (α7nAChR) which has been shown to increase p-ERK1/2 through PI3K (Dineley et al. 2001). It is possible that increases in the basal p-ERK1/2 are as a direct result of $A\beta^{42}$ or zinc stimulation. Although transient increases in p-ERK1/2 are linked to cell survival and neuroprotection, prolonged phosphorylation has been associated with neuronal death through glutamate induced oxidative toxicity (Stanciu et al. 2000). Glutamate causes toxicity by inhibiting cystine uptake through a glutamate /cystine antiporter and as cystine is a glutathione precursor (an anti-oxidant), it cannot be produced and ROS and NO accumulate (Inutsuka, Yamanaka 2013). NO has previously been demonstrated to cause selective degeneration of OX neurons (Togo, Katsuse & Iseki 2004). SH-SY5Y experiences a generally significant decrease in *OX1R*, *OX2R* and *GPR103* throughout the Aβ and zinc treatments and time points. It is possible that $A\beta^{42}$ and zinc lead to a chronic increase in p-ERK1/2 phosphorylation which leads to an increase in glutamate toxicity resulting in a reduction in OXR/GPR103. The net result could be compromised OXR/GPR103 signalling leading to loss of neuroprotection. There is a reduction of basal p-ERK1/2 in all samples after 48 hours and this may be due to adjustment of the cells to the toxic insult and an attempt to restore cellular normality.

Data was analysed taking into account the basal levels of p-ERK1/2 expression, so changes upon peptide treatment are entirely as a result of that specific treatment. In IMR32 upon addition of OXA and QRFP, most Aβ or zinc treatments follow the same trend: a reduction at 24 hours of p-ERK1/2 compared to the control and an increase after 48 hours. OXB however displays less drastic changes between 24 and 48 hours. OXA binds to both OX1R and OX2R with similar affinities, and OX1R expression is increased upon Aβ or zinc treatment. OX2R however remains relatively constant and does not experience the same changes as seen with OX1R. So OXA will be able to induce a response by binding to OX1R and OX2R and exhibit a response above and beyond that which OXB is capable off, which will bind selectively to OX2R and not OX1R. In SH-SY5Y p-ERK1/2 levels upon OXA treatment followed a general decrease in all treatments compared to the control. The reductions however are not significant and with the significant reduction of OX1R the difference in p-ERK1/2 between treated samples and the control aren't reflected in p-ERK1/2 levels; for example with a 0.2 fold

reduction in OX1R, upon addition of its peptide you might expect a significantly reduced amount of p-ERK activation. When SH-SY5Y cells were treated with OXB, the p-ERK1/2 levels were very similar to what was experienced in the control also treated with OXB, even though there was some reduction in OX2R expression. GPR103 expression was decreased in SH-SY5Y for all treatments and this is reflected in the QRFP treatments, where p-ERK1/2 expression was much lower compared to the control. This is presumably as a result of decreased receptor expression and hence less availability for with which the peptide to bind to. However as we have already implicated the possibility of a cross-talk of GPR103 and OXR, the combined reduction of OX1R and OX2R may seriously impair GPR103 functioning if they are required for its signalling; which is suggested with the previous antagonist study.

ERK is heavily implicated in neuroprotection. In a model of Huntington's disease inhibition of ERK increased cell death and increases in p-ERK1/2 lead to protection against cell death (Maher et al. 2011). It has also been shown to protect rat cortical neurons through BDNF induced ERK1/2 activation against apoptosis induced by DNA damage (Hetman et al. 1999). BDNF also protects through ERK1/2 activation in a rat exposed to hypoxic brain injury (Han, Holtzman 2000). Nicotine induces ERK in hippocampal slice cultures exposed to an excitotoxic insult, leading to neuroprotection (Ferchmin et al. 2003). ERK also leads to neuroprotection through estrogen receptor signalling when exposed to glutamate toxicity (Singer et al. 1999). Therefore ERK demonstrates a neuroprotective effect following a plethora of neuronally toxic insults. OXA has been shown to induce a neuroprotective effect via ERK1/2 in CHO stably expressing OX1R (Ammoun et al. 2006b). OX has also been implicated in neuroprotection through mechanisms other than p-ERK1/2 including protection against hydrogen peroxide induced hypoxia through decreasing lipid peroxidative stress and caspase dependent apoptosis (Butterick et al. 2012). It is thought that the main mechanisms through which OX mediates neuroprotection are through anti-apoptotic pathways. This may include the involvement of Akt, as OX induced neuroprotection of cultured cortical cells treated with cobalt chloride was completely ablated when treated with an Akt inhibitor (Sokolowska et al. 2014). Activation of Akt phosphorylates a number of transcription factors including the forkhead box transcription factor and

inhibits their ability to induce apoptotic gene expression. Akt also inhibits p53 and induces the CREB protein and NF-KB, which promote cellular survival (Sokolowska et al. 2014).

Our microarray data has shown that OXs and QRFP regulate HIF-1α as well as OXs having already been shown to regulate this pathway (Yuan et al. 2011; Sikder, Kodadek 2007). This is important in neuroprotection as it targets genes involved in fighting oxidative stress, improving blood oxygen and glucose supply, promoting glucose metabolism and blocking cell death signal pathways (Zhang et al. 2011). The HIF-1α inducer M30, attenuated tau hyperphosphorylation and protected against Aβ mediated toxicity in cortical neurons (Zhang et al. 2011; Avramovich-Tirosh et al. 2010). Over expression of HIF-1α in a rat nerve like cell line and cortical neurons also protected against Aβ induced toxicity (Soucek et al. 2003). In human patients with AD, treatment with the HIF-1α inducer; deferoxamine, experienced slowed cognitive decline (Zhang et al. 2011; Crapper McLachlan et al. 1991). This body of evidence suggest that HIF-1α can protect against AD, which could be important in OX mediated neuroprotection. So OX may act through a combination of pathways including ERK1/2, HIF-1α and Akt to promote cell survival.

Patients with AD have been shown to exhibit disrupted sleep-wake patterns, reduced circulating OX and a loss of orexigenic neurons (Kang et al. 2009; Fronczek et al. 2011). In SH-SY5Y cells we show that treatment with Aβ and zinc sulphate causes a reduction in OXRs and GPR103 through as yet unelucidated mechanisms. This mimicking of AD *in vitro* also shows that there is an increase in p-ERK1/2 which may be to induce neuroprotective effects. However $A\beta^{42}$ and zinc treatment of cells has been shown to cause increases in p-ERK1/2 activation, and chronic activation can lead to cell death. So although the toxic effects exerted by Aβ and zinc may cause chronic activation of p-ERK1/2 potentially leading to cell death, OX/GPR103 also increase p-ERK1/2, but may function in a neuroprotective fashion. OXs have also been shown to mediate an abundance of other signalling pathways including Akt and HIF-1α which protect against toxic insult and may be important regulators of cell survival in AD. This study raises the question of whether if in early AD when Aβ and tau deposition are low, could OXR/GPR103 mediate neuroprotection through its plethora of beneficial

pathways. And whether during late disease an accumulation of Aβ and tau can cause sustained p-ERK1/2 insult and degradation of OXR/GPR103 expression leading to a loss of neuroprotection and additional neurodegeneration.

We demonstrate here that addition of $A\beta^{42}$ and zinc sulfate specifically target OX1R and OX2R in SH-SY5Y and mediate their down-regulation and although OXA can compensate through activation of OX2R, QRFP is unable to do so and as such experiences a reduction in p-ERK1/2 activation upon peptide addition.

7

Chapter 7

Detailed analysis of RNA and protein levels of OXR and GPR103 in the hippocampal formation of patients with Alzheimer's disease

7.1 Introduction

The hippocampal formation is located in the medial temporal lobe beneath the cerebral cortex. Its main function is the formation of new memories and spatial awareness (Squire 2009). It comprises the dentate gyrus (DG), CA3, CA2, CA1 and subiculum (SUB) (Figure 7.1). The entorhinal cortex (EC) provides the main input to the hippocampus through projections to the DG. These inputs then travel to the CA3 and CA1 with the CA1 subsequently projecting to the SUB and sending the output back to the EC (Schuff et al. 2009). The DG contains a subgranular zone, one of the few areas of the brain to be capable of adult neurogenesis and is involved in formation of memories and spatial awareness (Saab et al. 2009; Xavier, Costa 2009). The earliest symptoms of AD are short term memory loss and this is due to hippocampal destruction. In AD the hippocampal formation is one of the earliest areas of the brain to be affected with significant damage when the first clinical symptoms become apparent and significant volume loss of the hippocampus compared to age matched healthy controls (Schuff et al. 2009; Frisoni et al. 2008). GPR103 has been shown to be expressed in the human and rat hippocampus (Baribault et al. 2006; Bruzzone et al. 2007). OXRs are expressed throughout the hippocampal formation in rat brains but to

date detailed expression profiles have not been explored in the human brain particularly with regards to neurodegenerative disease (Trivedi et al. 1998; Hervieu et al. 2001).

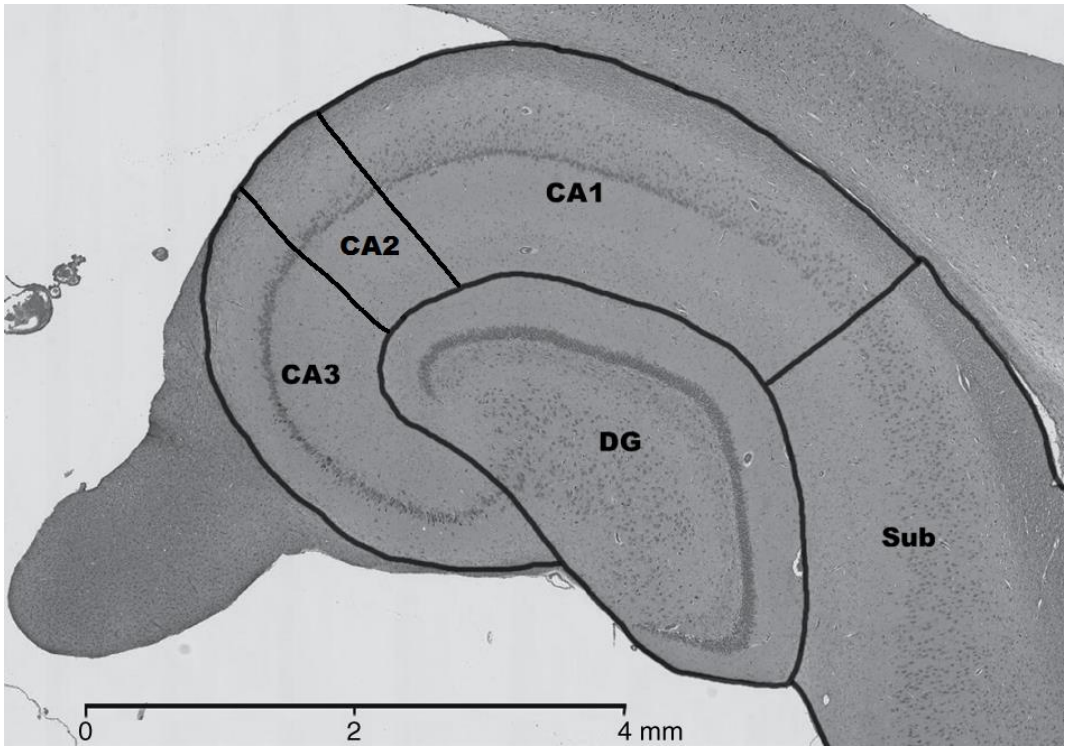

Figure 7.1: Anatomy of the hippocampal formation [adapted from (Conrad et al. 2012)]

7.2 Objectives

Using clinical patient samples from EOFAD, LOAD and a control group of both young and old patients, we studied the expression of *OX1R*, *OX2R* and *GPR103* at mRNA and protein level. GeNorm was used to validate the patient samples and find the most stable housekeeping genes across all samples. qPCR was then performed to monitor any differences in receptor expression for all samples. These receptors were then mapped at protein level, using antibodies specific for each receptor and using an immunohistochemical DAB staining method to identify receptor expression in each sample. Correlation between receptors within each patient at RNA and protein level was ascertained as well as the correlation between Aβ/tau deposition and protein expression within specific areas of the hippocampal formation.

7.3 Results

7.3.1 GeNorm of clinical samples to identify the most stable housekeeping genes to be used for qPCR normalisation

Clinical samples were provided by the Brains for Dementia Research bank (Table 7.1).

	Hippocampal patient samples			
	EOFAD	LOAD	Control (young)	Control (old)
RNA samples	7	6	3	3

Table 7.1: Sample distribution of RNA human hippocampal samples.

GeNorm analysis was performed on the clinical samples to identify the most stable housekeeping genes out of a panel of 6 genes. EIF4A2 and succinate dehydrogenase complex, subunit A (SDHA) were identified as the most stable across the different clinical samples, so both genes were used (Figure 7.2).

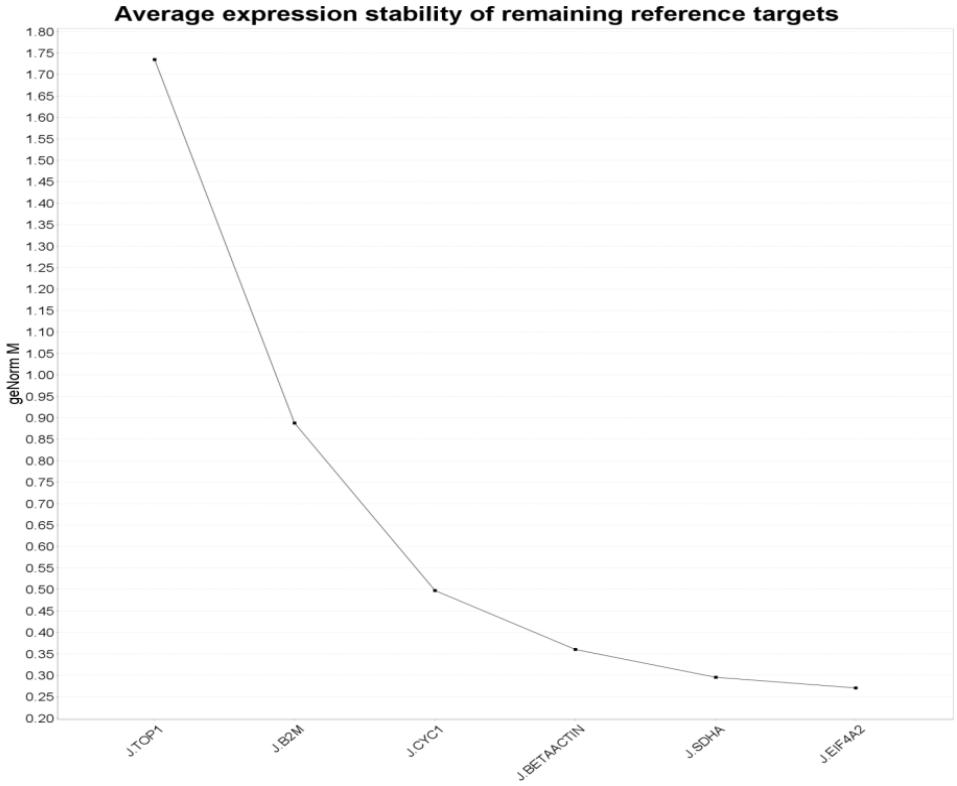

Figure 7.2: GeNorm analysis of clinical samples. The 2 most stable genes were *EIF4A2* and *SDHA* due to their low GeNorm M values indicating more stability between different samples.

7.3.2 qPCR analysis of clinical samples observing changes in *OX1R, OX2R* and *GPR103* expression

qPCR was performed on the clinical samples observing changes in *OX1R*, *OX2R* and *GPR103* expression. Values for each sample were normalised to a housekeeping gene to calculate the ΔCT and the equation $2^{-\Delta CT}$ was calculated to expresses the values as an RQ value or fold change compared to the housekeeping gene.

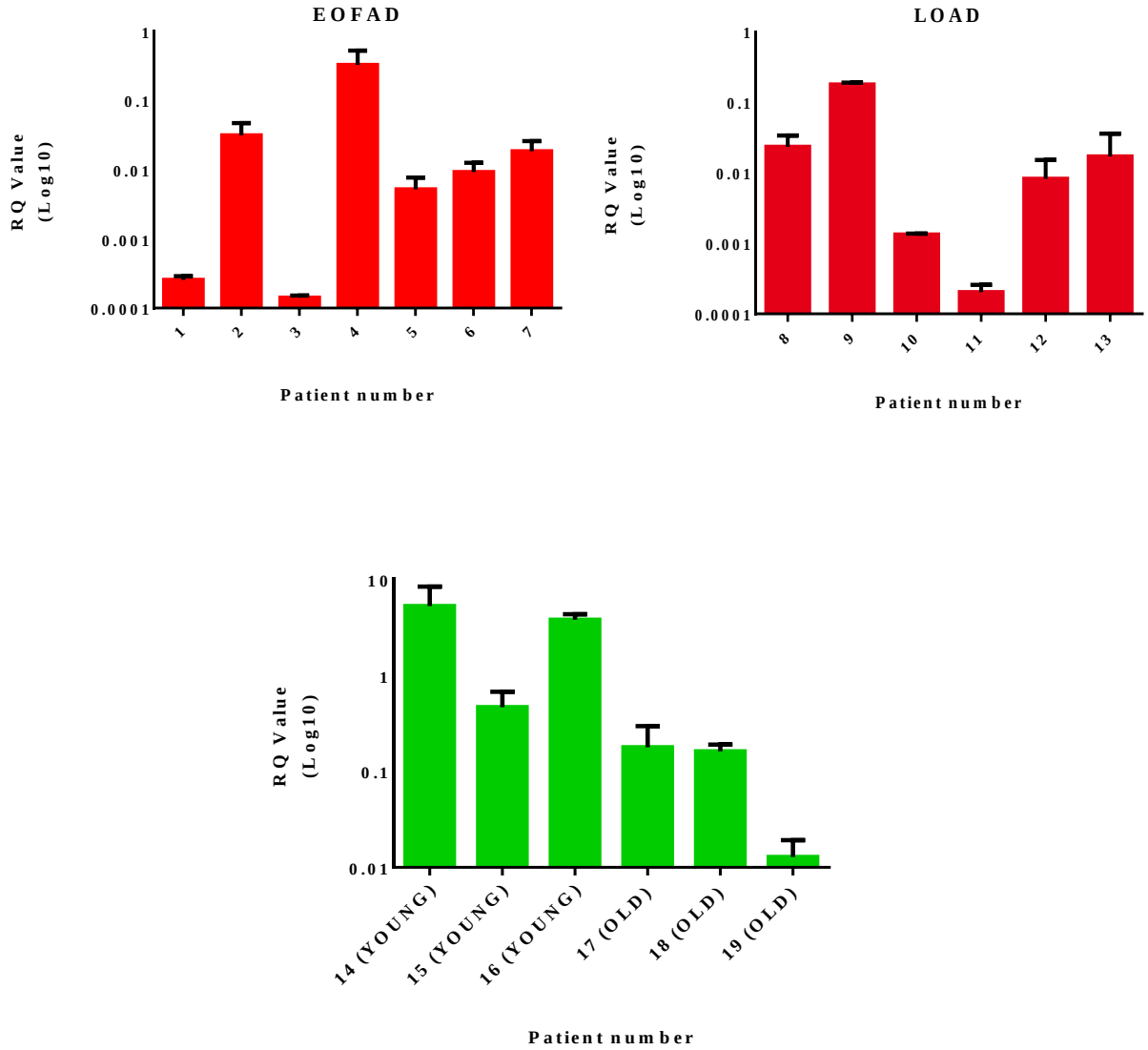

Figure 7.3: qPCR analysis of *OX1R* expression of patient samples from EOFAD, LOAD and young and old controls. Data is represented as an RQ value ($2^{-\Delta CT}$) ± S.D.

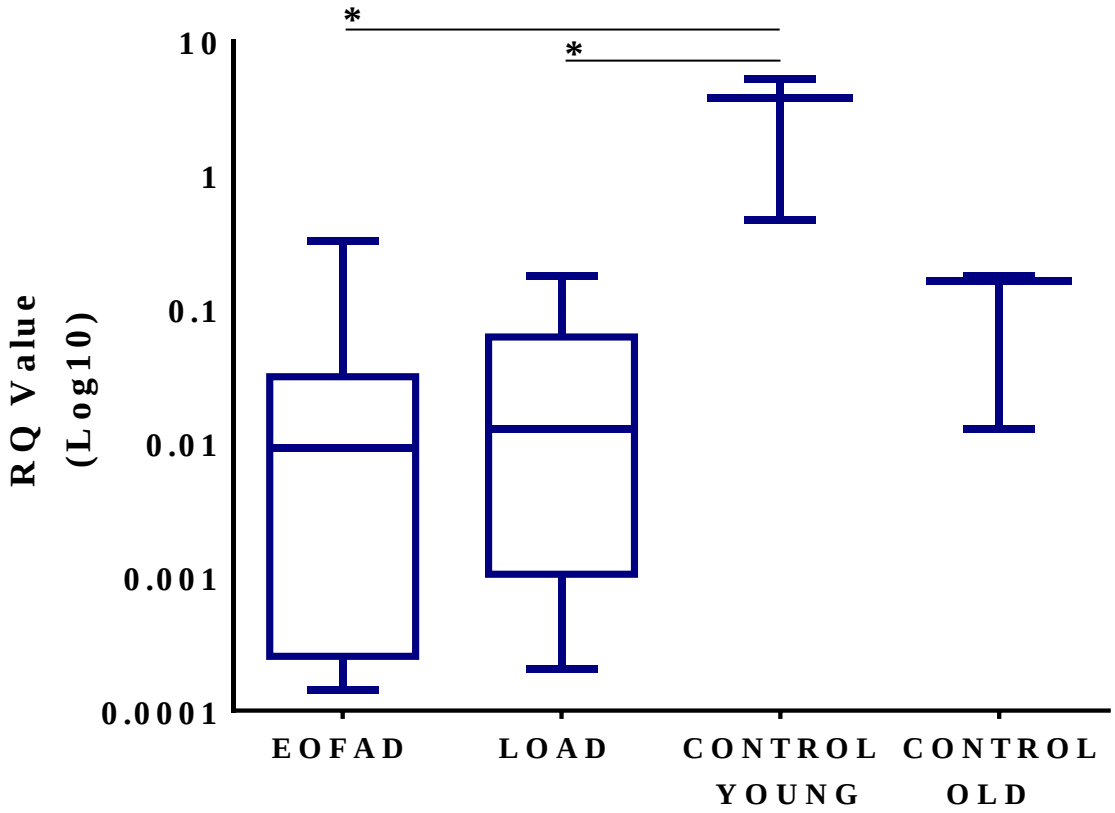

Figure 7.4: qPCR analysis of 7 EOFAD, 6 LOAD and 3 young controls and 3 old controls of *OX1R* represented in a box plot. Q1: 1st quartile/25th percentile, Min: minimum value, Median: 2nd quartile/50th percentile, Max: maximum value, Q3: 3rd quartile/75th percentile. Statistical significance was performed using the Mann-Whitney U test ($p<0.05$*).

	EOFAD	LOAD	CONTROL YOUNG	CONTROL OLD
Q1	0.000255	0.001048	0.4668	0.01282
Min	0.000142	0.000203	0.4668	0.01282
Median	0.009192	0.01268	3.799	0.1616
Max	0.3247	0.1782	5.269	0.1783
Q3	0.03132	0.06208	5.269	0.1783

Table 7.2: Q1: 1st quartile/25th percentile, Min: minimum value, Median: 2nd quartile/50th percentile, Max: maximum value, Q3: 3rd quartile/75th percentile values for EOFAD, LOAD and control samples upon qPCR analysis of *OX1R*.

Changes in *OX1R* gene expression between individual samples are displayed on a log10 graph for each sub-set of patients (Figure 7.3). Results showed an interpatient variation between each sub-set of patients; however EOFAD and LOAD display markedly lower expression than the control samples; with old control samples exhibiting lower expression than the young control samples. Figure 7.4 and table 7.2 indicate the variation for *OX1R* between patient samples, with EOFAD and LOAD having much lower median values than the control, but also exhibiting more variation. *OX1R* expression was significantly lower in EOFAD and LOAD compared to the young control.

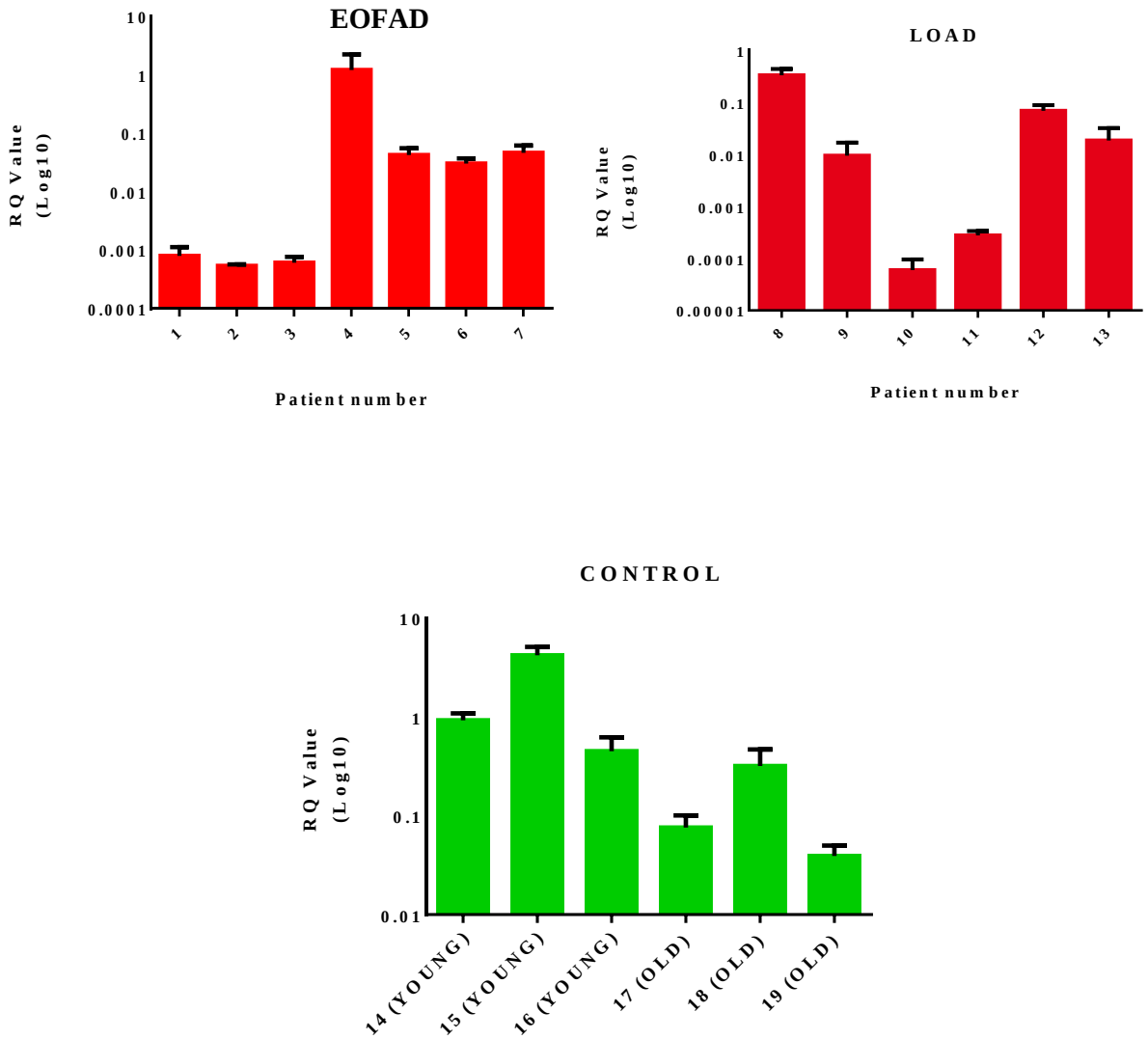

Figure 7.5: qPCR analysis of *OX2R* expression of patient samples from EOFAD, LOAD and young and old controls. Data is represented as an RQ value ($2^{-\Delta CT}$) ± S.D.

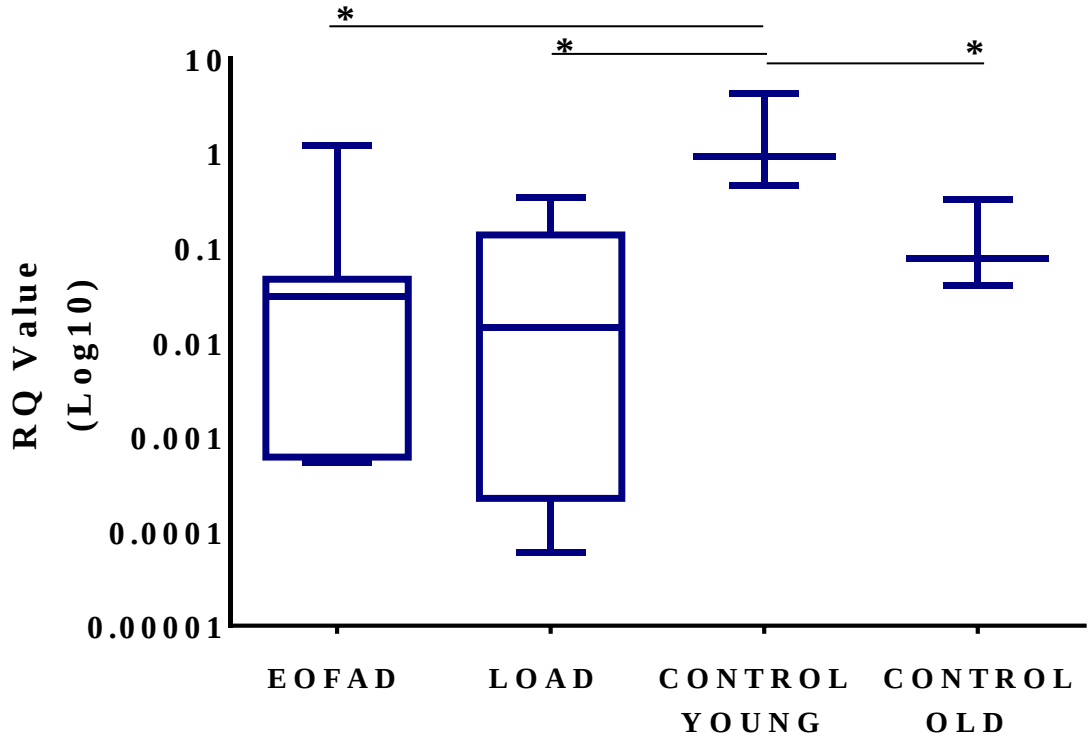

Figure 7.6: qPCR analysis of 7 EOFAD, 6 LOAD and 3 young controls and 3 old controls of *OX2R* represented in a box plot. Q1: 1st quartile/25th percentile, Min: minimum value, Median: 2nd quartile/50th percentile, Max: maximum value, Q3: 3rd quartile/75th percentile. Statistical significance was performed using the Mann-Whitney U test ($p<0.05$*).

	EOFAD	LOAD	CONTROL YOUNG	CONTROL OLD
Q1	0.000607	0.000223	0.4509	0.03928
Min	0.000532	0.00006	0.4509	0.03928
Median	0.03013	0.01405	0.9233	0.07624
Max	1.196	0.3342	4.199	0.3197
Q3	0.04592	0.1356	4.199	0.3197

Table 7.3: Q1: 1st quartile/25th percentile, Min: minimum value, Median: 2nd quartile/50th percentile, Max: maximum value, Q3: 3rd quartile/75th percentile values for EOFAD, LOAD and control samples upon qPCR analysis of OX2R.

For *OX2R*, individual data for each patient displayed fluctuations between each subset of patients, however the EOFAD and LOAD patients demonstrated lower expression than the control groups (Figure 7.5) Figure 7.6 and table 7.3 show the variation in each sub-set of patient samples for *OX2R* gene expression. The medians for the AD groups were lower than in the control samples; however there was much variation between the AD patients which was not seen in the control samples. EOFAD and LOAD were significantly lower than the young control. Interestingly the old control was also significantly lower than the young control.

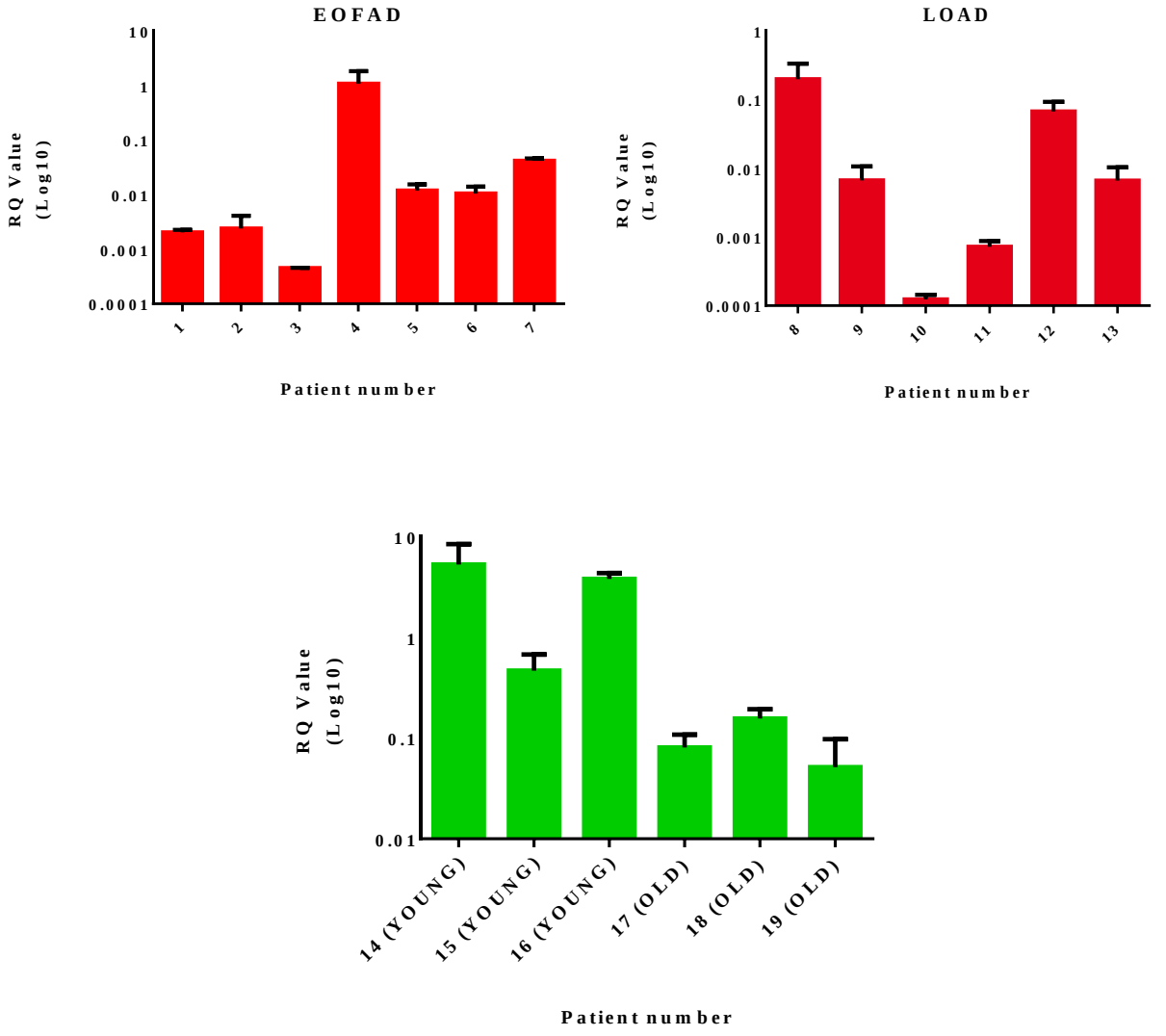

Figure 7.7: qPCR analysis of *GPR103* expression of patient samples from EOFAD, LOAD and young and old controls. Data is represented as an RQ value ($2^{-\Delta CT}$) ± S.D.

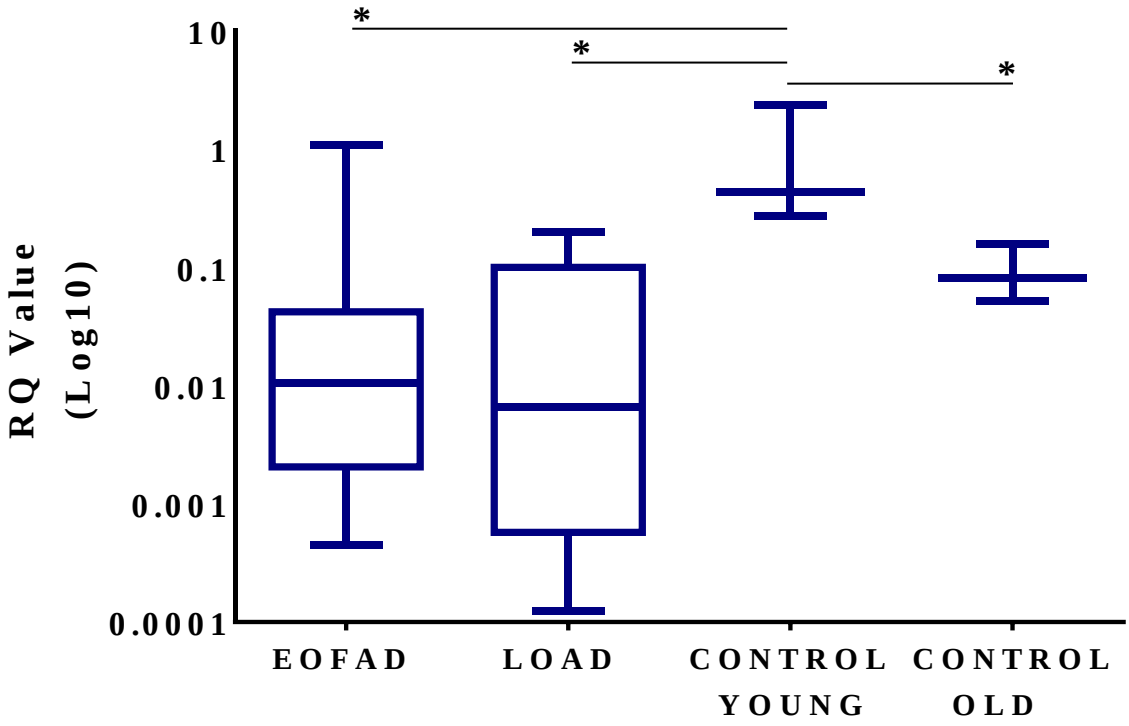

Figure 7.8: qPCR analysis of 7 EOFAD, 6 LOAD and 3 young controls and 3 old controls of *GPR103* represented in a box plot. Q1: 1st quartile/25th percentile, Min: minimum value, Median: 2nd quartile/50th percentile, Max: maximum value, Q3: 3rd quartile/75th percentile. Statistical significance was performed using the Mann-Whitney U test ($p<0.05$*).

	EOFAD	LOAD	CONTROL YOUNG	CONTROL OLD
Q1	0.002051	0.000573	0.2702	0.05136
Min	0.000452	0.000123	0.2702	0.05136
Median	0.0105	0.006658	0.4351	0.08051
Max	1.836	0.198	2.359	0.156
Q3	0.04198	0.1	2.359	0.156

Table 7.4: Q1: 1st quartile/25th percentile, Min: minimum value, Median: 2nd quartile/50th percentile, Max: maximum value, Q3: 3rd quartile/75th percentile values for EOFAD, LOAD and control samples upon qPCR analysis of GPR103.

Figure 7.8 and table 7.4 demonstrate the variation between sub-sets of patients for *GPR103* gene expression. EOFAD and LOAD exhibited lower expression than both the young and old control. However there was vastly more variation observed between the AD patients. *GPR103* gene expression in EOFAD and LOAD followed the same pattern as *OX1R* and *OX2R* and exhibited reduced expression compared to the control samples and when compared to the young control was significantly lower (Figure 7.7). The young control demonstrated significantly higher *GPR103* expression than the old control as is seen with *OX2R*.

Pearson correlation was used to determine whether gene expression was correlated amongst the receptors to determine if expression of genes occurred in tandem and followed the same pattern. It is thought that in basal conditions OX1R exists as a homodimer and for OX2R the data is unclear (Xu et al. 2011). Correlation may give an indication as to whether receptors are co-expressed to enable hetero-dimerisation. The dimerisation status of GPR103 is unknown, but as we have already demonstrated a potential cross-talk with OXRs, correlation with OXR could reveal potential co-expression to facilitate dimerisation.

		OX1R EOFAD	*OX2R* EOFAD	*GPR103* EOFAD
OX1R EOFAD	Pearson correlation		0.9949	0.9959
	Significance		< 0.0001 ****	< 0.0001 ****
OX2R EOFAD	Pearson correlation	0.9949		0.9996
	Significance	< 0.0001 ****		< 0.0001 ****
GPR103 EOFAD	Pearson correlation	0.9959	0.9996	
	Significance	< 0.0001 ****	< 0.0001 ****	

Table 7.5: Correlation between different genes for each EOFAD patient sample using Pearson correlation between each of the genes in EOFAD. ($p<0.0001$****). (N=7)

		OX1R LOAD	*OX2R* LOAD	*GPR103* LOAD
OX1R LOAD	Pearson correlation		-0.1336	-0.1528
	Significance		0.8008	0.7727
OX2R LOAD	Pearson correlation	-0.1336		0.9899
	Significance	0.8008		0.0002 ***
GPR103 LOAD	Pearson correlation	-0.1528	0.9899	
	Significance	0.7727	0.0002 ***	

Table 7.6: Correlation between different genes for each LOAD patient sample using Pearson correlation between each of the genes in LOAD. ($p<0.001$***). (N=6)

		OX1R CONTROL	*OX2R* CONTROL	*GPR103* CONTROL
OX1R CONTROL	Pearson correlation		-0.07094	-0.1041
	Significance		0.8938	0.8444
OX2R CONTROL	Pearson correlation	-0.07094		0.9988
	Significance	0.8938		< 0.0001 ****
GPR103 CONTROL	Pearson correlation	-0.1041	0.9988	
	Significance	0.8444	< 0.0001 ****	

Table 7.7: Correlation between different genes for each control patient sample using Pearson correlation between each of the genes in control. ($p<0.0001$****). (N=6)

In EOFAD there was significant positive correlation between *OX1R, OX2R* and *GPR103* (Table 7.5). So all of the genes followed the same pattern of reduced expression and they all experienced correlation between the reductions of the genes within this group. However for LOAD and the control samples (Table 7.6 and 7.7) there was only positive correlation between OX2R and GPR103. This shows a distinct pattern of regulation depending on the onset of the disease.

7.3.3 Immunohistochemistry performed on clinical samples observing changes in OX1R, OX2R and GPR103 protein expression in different areas of the hippocampus

	Hippocampal patient samples			
	EOFAD	LOAD	Control (young)	Control (old)
Paraffin embedded samples	6	6	3	3

Table 7.8 Sample distribution paraffin embedded human hippocampal samples.

Immunohistochemistry was performed on paraffin embedded slides for each patient using the DAB method with OX1R, OX2R and GPR103 antibodies. The paraffin embedded samples used are displayed in table 7.8. Within the hippocampus 5 different areas: DG, CA3, CA2, CA1 and the SUB were observed. Scoring was performed by observing each specific area of the hippocampus and counting the number of nuclei and the amount of positively DAB stained cells within 5 areas of each part of the hippocampus. This was used to calculate the percentage of positive cells. Figure 7.9 shows a representation of staining with different antibodies.

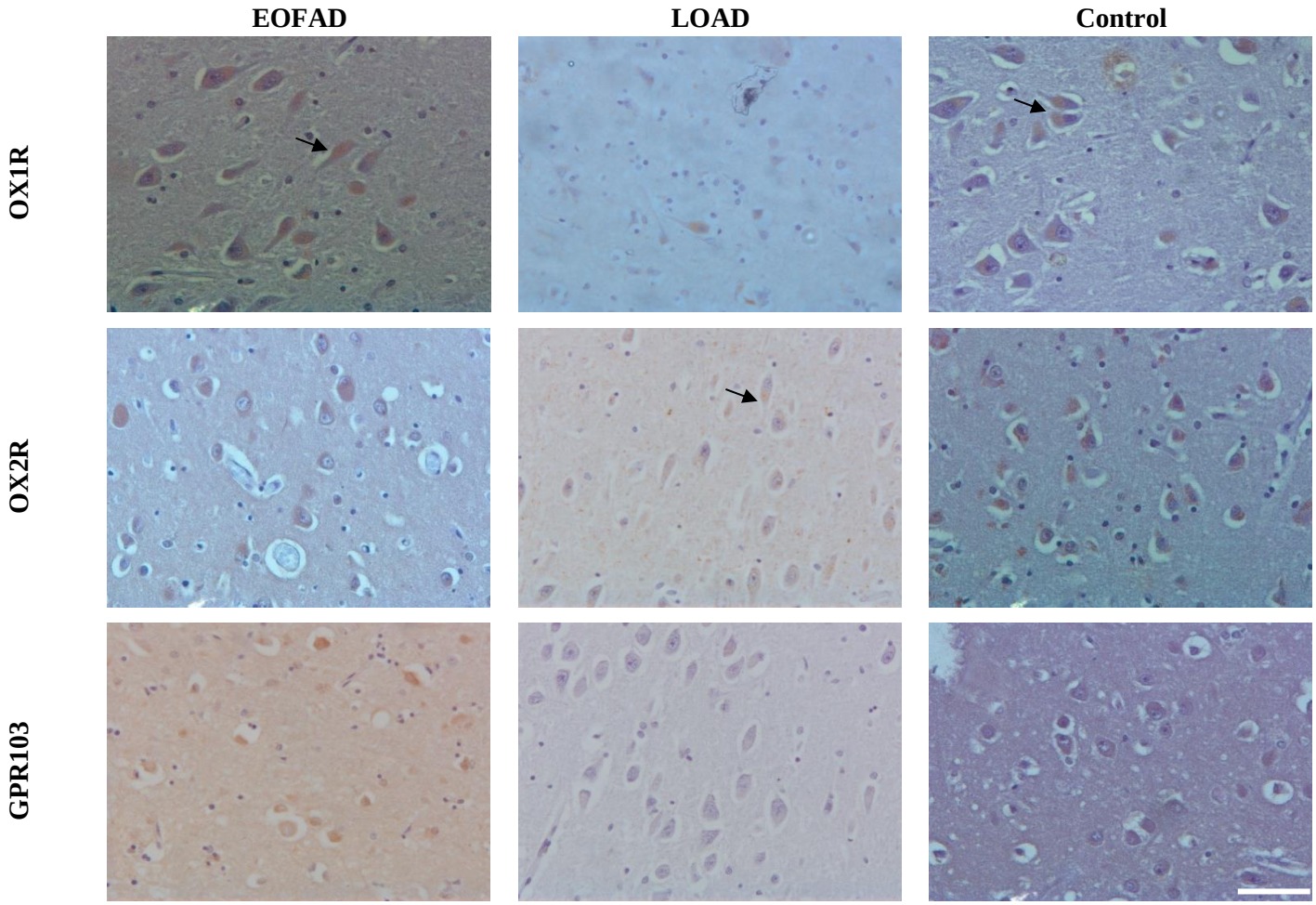

Figure 7.9: Representative images of IHC using DAB staining in EOFAD, LOAD and control patients with OX1R, OX2R or a GPR103 antibody. X40 magnification, bar = 50µm.

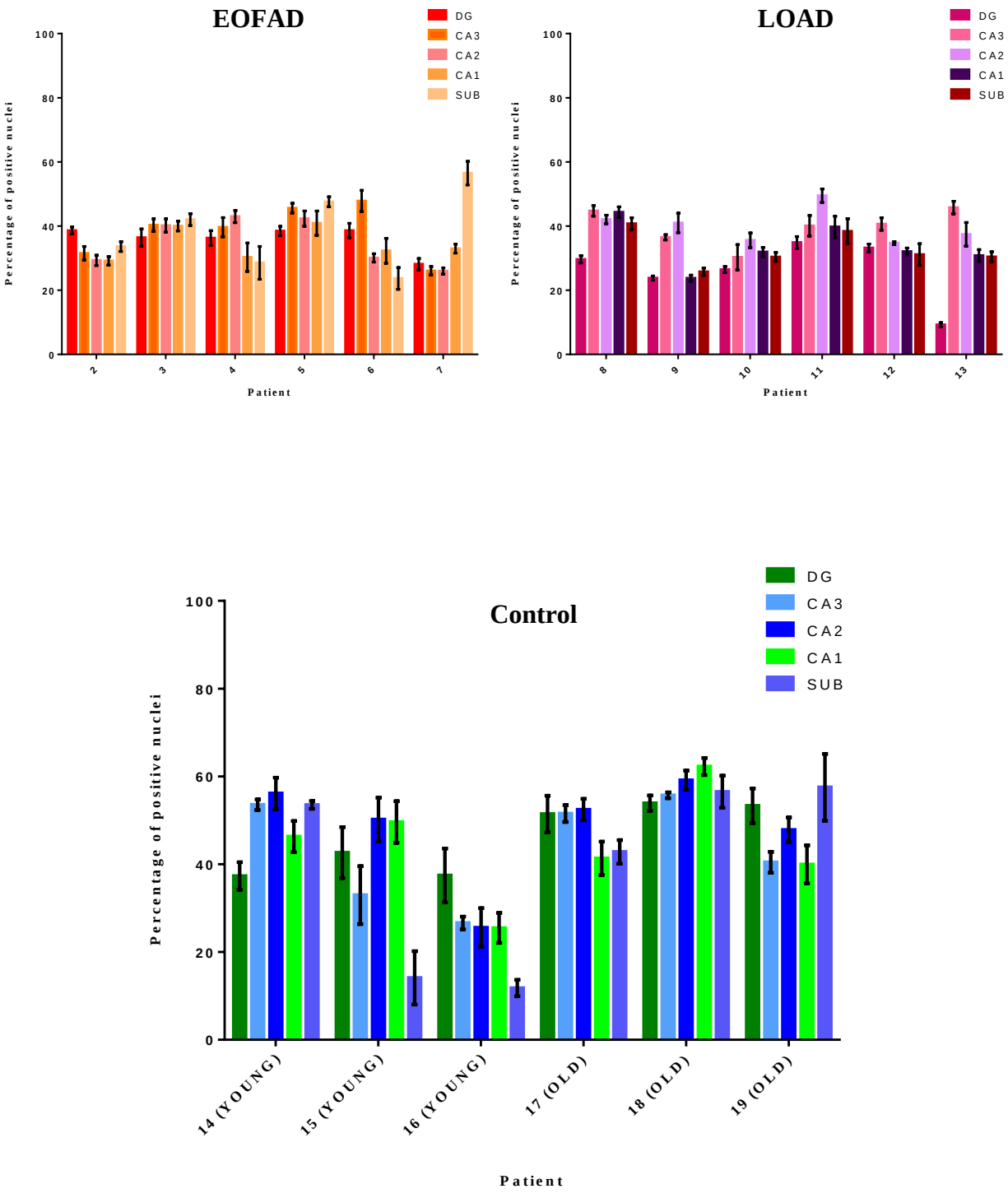

Figure 7.10: Immunohistochemical analysis of paraffin embedded hippocampal slides of patients stained with an OX1R antibody. Scoring was performed by counting the amount of nuclei and the amount of positive cells within an area and a percentage of positive cells was calculated. 5 areas of the dentate gyrus, CA3, CA2, CA1 and subiculum were counted for each patient and an average was calculated ± S.D.

Figure 7.10 demonstrates the spread of OX1R expression within 5 different areas of the hippocampus in EOFAD, LOAD and control samples. There is some fluctuation between different areas for each patient however EOFAD and LOAD stay generally below 40% of cells positively stained with the antibody whereas most of the control samples stay above 40%.

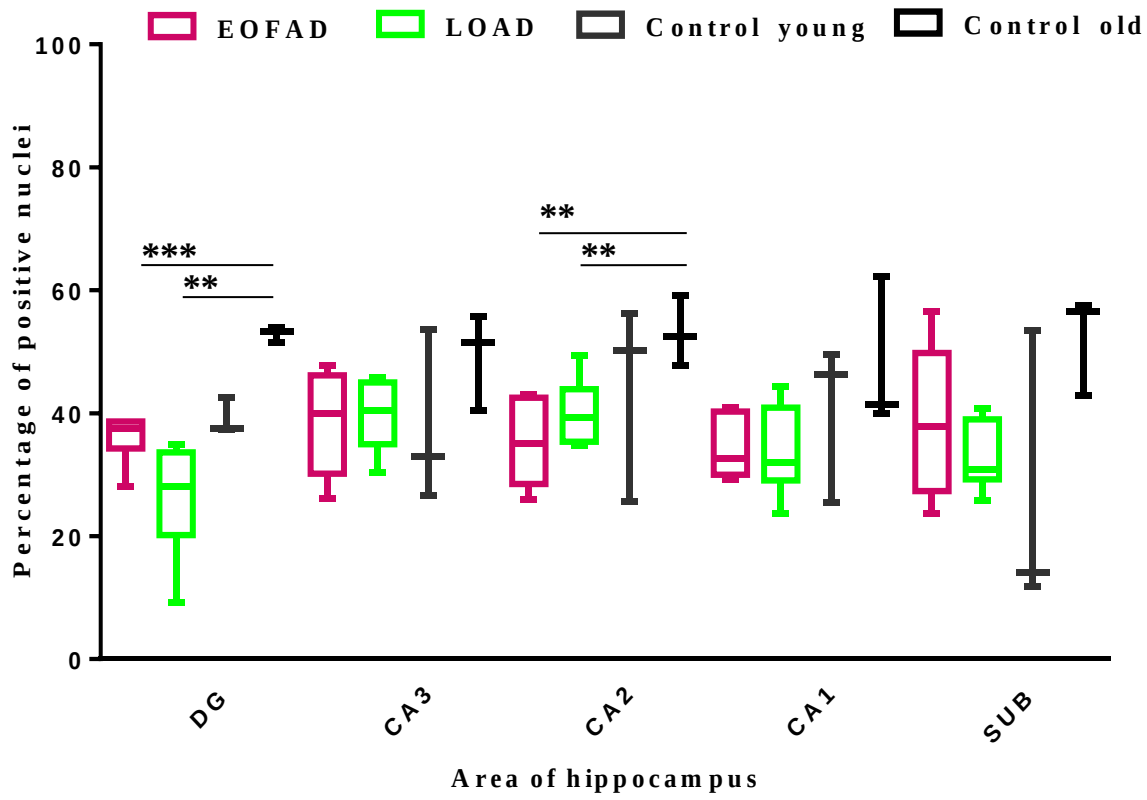

Figure 7.11: Immunohistochemical analysis of paraffin embedded hippocampal slides of patients stained with an OX1R antibody. Scoring was performed by counting the amount of nuclei and the amount of positive cells within an area and a percentage of positive cells was calculated. 5 areas of the dentate gyrus, CA3, CA2, CA1 and subiculum were counted for each patient and an average was calculated ± S.D. Statistical significance was calculated using the Mann-Whitney U test ($p<0.01$**, $p<0.001$***).

	EOFAD					LOAD				
	DG	**CA3**	**CA2**	**CA1**	**SUB**	**DG**	**CA3**	**CA2**	**CA1**	**SUB**
Q1	34.24	30.16	28.49	30	27.34	20.16	34.94	35.36	29.08	29.23
Min	28.14	26.07	26.02	29.16	23.68	9.253	30.3	34.72	23.76	25.77
Median	37.45	39.98	35.12	32.64	37.81	28.04	40.37	39.21	32.02	30.78
Max	38.64	47.84	42.99	40.92	56.5	34.92	45.78	49.48	44.33	40.76
Q3	38.63	46.16	42.5	40.25	49.81	33.64	45	43.92	40.9	38.99
	Control young					**Control old**				
	DG	**CA3**	**CA2**	**CA1**	**SUB**	**DG**	**CA3**	**CA2**	**CA1**	**SUB**
Q1	37.31	26.62	25.58	25.48	11.79	51.45	40.43	47.81	39.98	42.82
Min	37.31	26.62	25.58	25.48	11.79	51.45	40.43	47.81	39.98	42.82
Median	37.44	32.96	50.18	46.3	14.12	53.32	51.56	52.45	41.36	56.5
Max	42.64	53.56	56.13	49.61	53.51	53.93	55.72	59.14	62.27	57.52
Q3	42.64	53.56	56.13	49.61	53.51	53.93	55.72	59.14	62.27	57.52

Table 7.9: Q1: 1st quartile/25th percentile, Min: minimum value, Median: 2nd quartile/50th percentile, Max: maximum value, Q3: 3rd quartile/75th percentile values for EOFAD, LOAD and control samples upon immunohistochemical staining with OX1R.

The distribution within each sub-set of patients is presented in figure 7.11 and table 7.9, which show that EOFAD and LOAD have median values lower than the control. In the CA3 and SUB the young control have less expression than seen in the AD patients; however there is substantial interpatient variation between the controls, with the old control staying consistently higher than the AD patient and displays less variation.

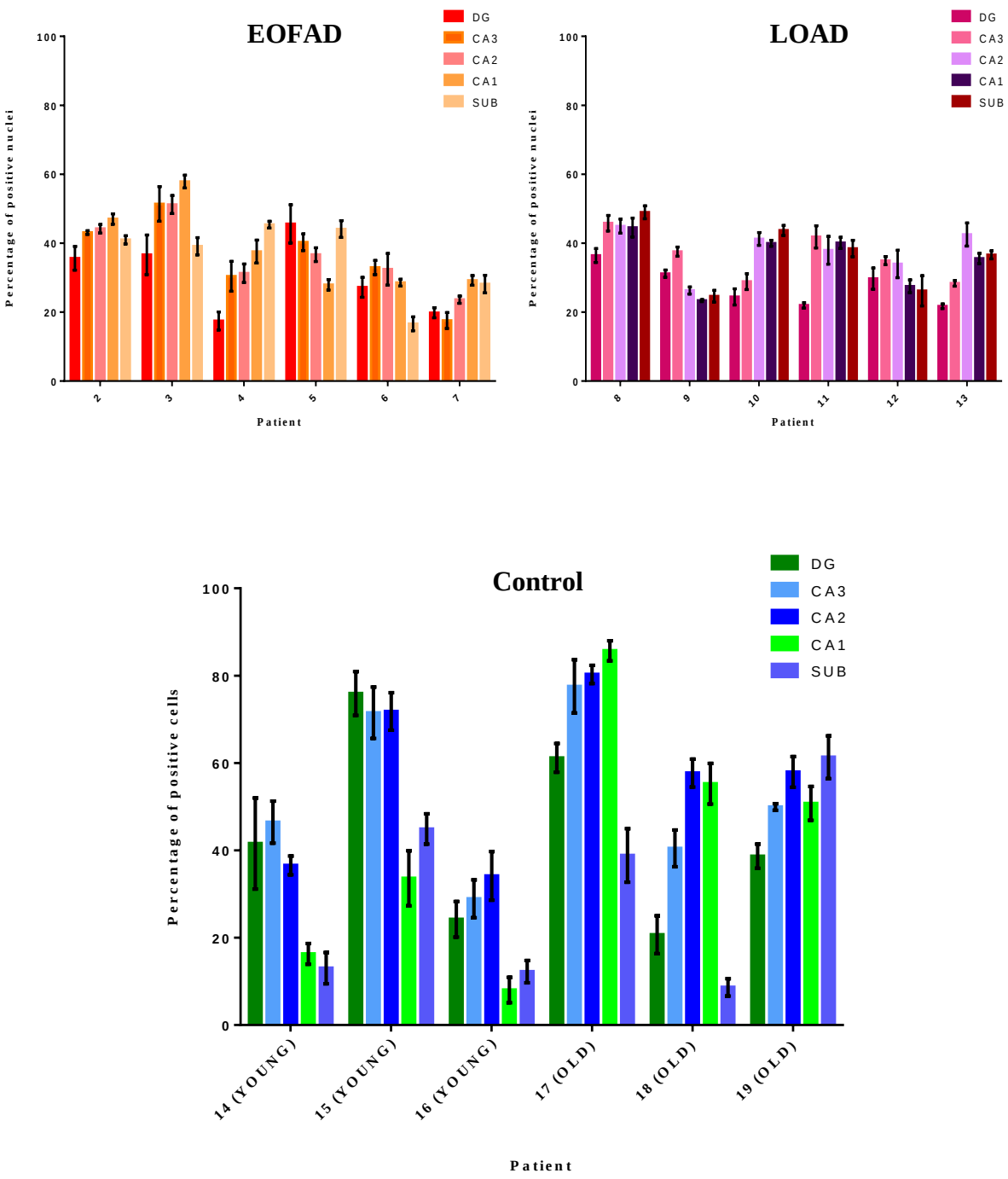

Figure 7.12: Immunohistochemical analysis of paraffin embedded hippocampal slides of patients stained with an OX2R antibody. Scoring was performed by counting the amount of nuclei and the amount of positive cells within an area and a percentage of positive cells was calculated. 5 areas of the dentate gyrus, CA3, CA2, CA1 and subiculum were counted for each patient and an average was calculated ± S.D.

Expression of OX2R in EOFAD and LOAD showed a general trend of expression less than 40% of positively stained cells (Figure 7.12). Although there was variation between different areas of the brain within each patient, expression remained fairly consistent with a decrease in expression in the DG compared to other areas for most of the AD patients. The control samples showed more variation. The young control had slightly lower expression of OX2R compared to the old control, but was markedly reduced in the CA1 and SUB.

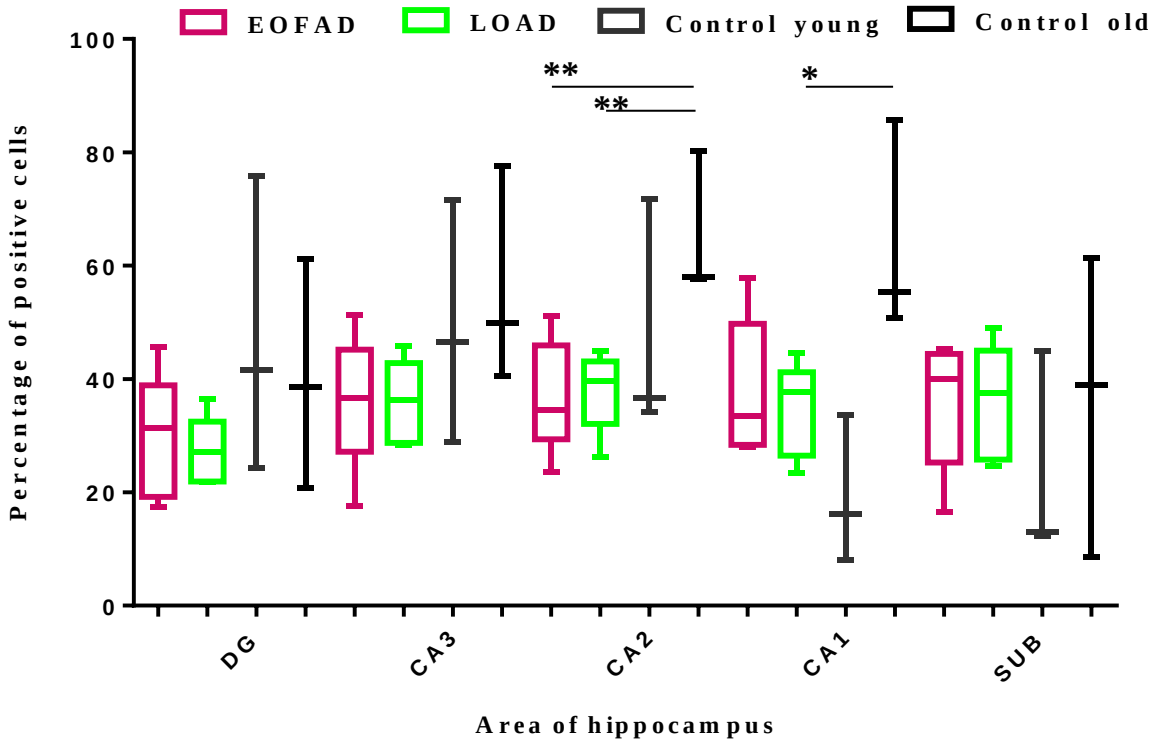

Figure 7.13: Immunohistochemical analysis of 7 EOFAD, 6 LOAD and 6 age matched controls stained with OX2R represented in a box plot. Scoring was performed by counting the amount of nuclei and the amount of positive cells within an area and a percentage of positive cells was calculated. 5 areas of the dentate gyrus, CA3, CA2, CA1 and subiculum were counted for each patient and an average calculated. Q1: 1st quartile/25th percentile, Min: minimum value, Median: 2nd quartile/50th percentile, Max: maximum value, Q3: 3rd quartile/75th percentile. Statistical significance was calculated using the Mann-Whitney U test ($p<0.05$*, $p<0.01$**).

	EOFAD					LOAD				
	DG	**CA3**	**CA2**	**CA1**	**SUB**	**DG**	**CA3**	**CA2**	**CA1**	**SUB**
Q1	19.22	27.19	29.36	28.41	25.27	21.9	28.74	32.05	26.47	25.79
Min	17.44	17.57	23.63	27.93	16.6	21.72	28.36	26.26	23.36	24.62
Median	31.4	36.61	34.56	33.38	40.04	27.07	36.24	39.58	37.77	37.53
Max	45.58	51.38	51.21	57.86	45.37	36.44	45.8	44.94	44.54	48.96
Q3	38.88	45.16	45.94	49.73	44.42	32.48	42.83	43.13	41.21	45.02
	Control young					**Control old**				
	DG	**CA3**	**CA2**	**CA1**	**SUB**	**DG**	**CA3**	**CA2**	**CA1**	**SUB**
Q1	24.22	28.9	34.16	8.02	12.24	20.68	40.44	57.7	50.76	8.64
Min	24.22	28.9	34.16	8.02	12.24	20.68	40.44	57.7	50.76	8.64
Median	41.56	46.46	36.56	16.28	13.02	38.66	49.94	57.96	55.26	38.86
Max	75.92	71.5	71.8	33.62	44.9	61.18	77.54	80.28	85.7	61.32
Q3	75.92	71.5	71.8	33.62	44.9	61.18	77.54	80.28	85.7	61.32

Table 7.10: Q1: 1st quartile/25th percentile, Min: minimum value, Median: 2nd quartile/50th percentile, Max: maximum value, Q3: 3rd quartile/75th percentile values for EOFAD, LOAD and control samples upon immunohistochemical staining with OX2R.

Figure 7.13 and table 7.10 showss the distribution of OX2R between the different patients and different hippocampal regions. The controls showed more variation between different patients, although the old control was consistently higher than the median values for EOFAD and LOAD. The young control however showed more expression in the DG and CA3, but showed reduced expression compared to the AD samples in the CA2, CA2 and SUB.

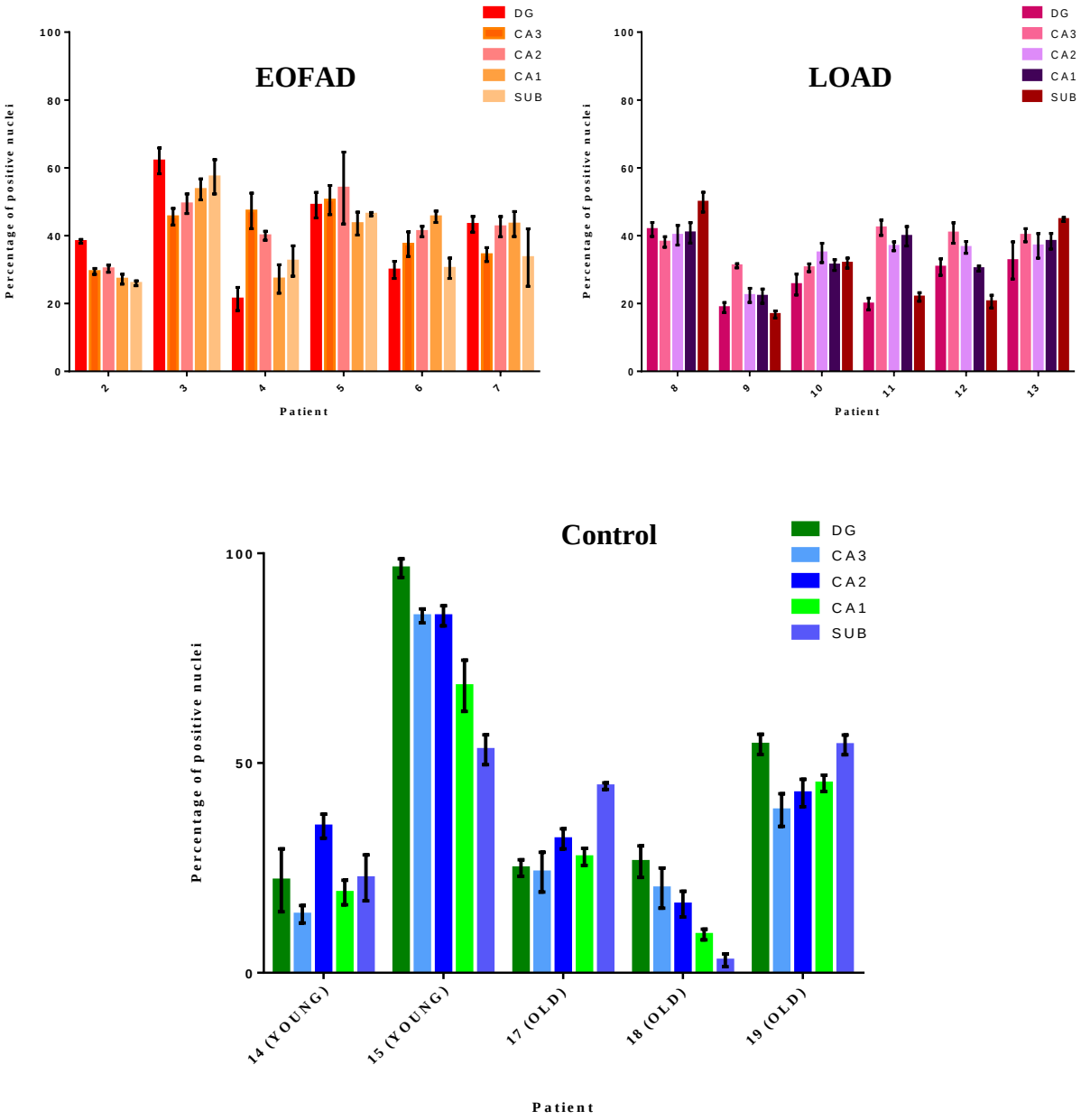

Figure 7.14: Immunohistochemical analysis of paraffin embedded hippocampal slides of patients stained with a GPR103 antibody. Scoring was performed by counting the amount of nuclei and the amount of positive cells within an area and a percentage of positive cells was calculated. 5 areas of the dentate gyrus, CA3, CA2, CA1 and subiculum were counted for each patient and an average was calculated ± S.D.

GPR103 staining generally remained below 50% in EOFAD and below 40% in LOAD for all of the patients and hippocampal regions as seen in figure 7.14. One young control, showed no GPR103 expression and there was large variation between the other two young controls. The old controls also display reduced expression in two patients but in patient 19 there is higher expression in all areas.

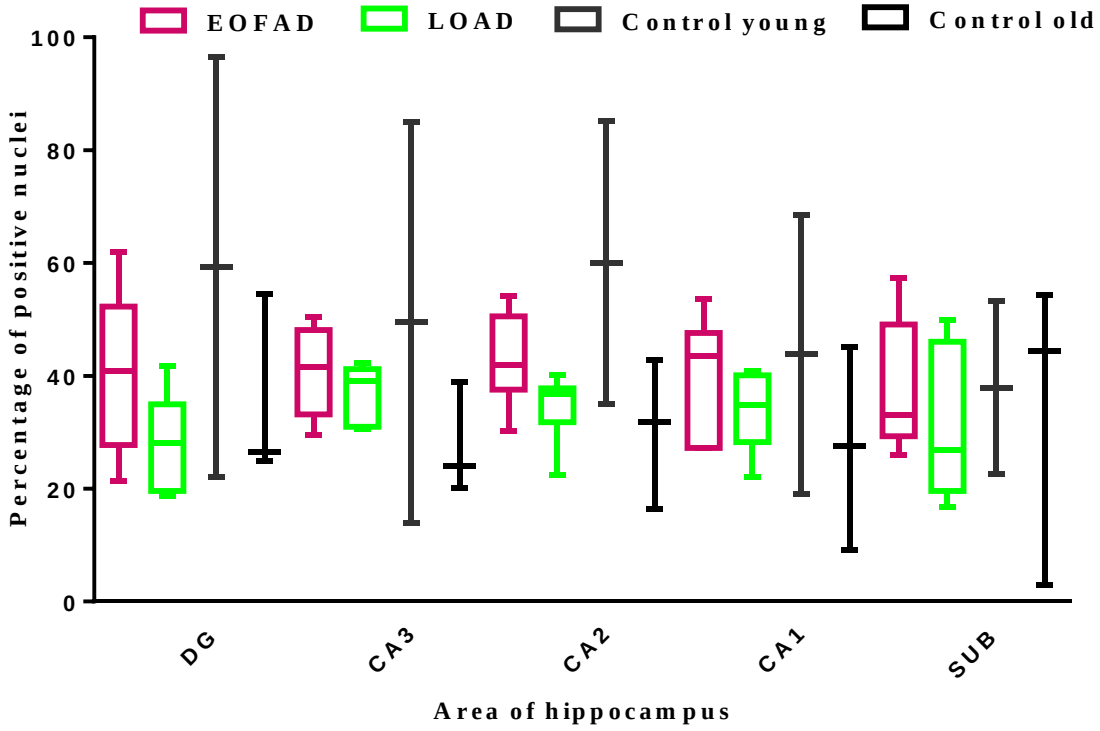

Figure 7.15: Immunohistochemical analysis of 7 EOFAD, 6 LOAD and 6 age matched controls stained with GPR103 represented in a box plot. Scoring was performed by counting the amount of nuclei and the amount of positive cells within an area and a percentage of positive cells was calculated. 5 areas of the dentate gyrus, CA3, CA2, CA1 and subiculum were counted for each patient and an average calculated. Q1: 1st quartile/25th percentile, Min: minimum value, Median: 2nd quartile/50th percentile, Max: maximum value, Q3: 3rd quartile/75th percentile.

	EOFAD					LOAD				
	DG	**CA3**	**CA2**	**CA1**	**SUB**	**DG**	**CA3**	**CA2**	**CA1**	**SUB**
Q1	27.77	33.19	37.56	27.23	29.28	19.6	31	31.81	28.25	19.62
Min	21.34	29.47	30.27	27.19	25.95	18.81	30.55	22.4	22.14	16.78
Median	40.84	41.54	41.95	43.49	33.04	28.18	39.14	36.72	34.86	26.93
Max	62.05	50.51	54.04	53.65	57.36	41.84	42.35	40.15	40.83	49.88
Q3	52.27	48.1	50.57	47.59	49.11	34.98	41.18	37.8	40.09	46.06
	Control young					**Control old**				
	DG	**CA3**	**CA2**	**CA1**	**SUB**	**DG**	**CA3**	**CA2**	**CA1**	**SUB**
Q1	22.06	13.95	34.96	19.14	22.63	24.99	20.19	16.36	9.108	2.967
Min	22.06	13.95	34.96	19.14	22.63	24.99	20.19	16.36	9.108	2.967
Median	59.26	49.52	60.03	43.78	37.9	26.5	24	31.91	27.63	44.5
Max	96.47	85.1	85.11	68.42	53.18	54.46	38.81	42.86	45.18	54.35
Q3	96.47	85.1	85.11	68.42	53.18	54.46	38.81	42.86	45.18	54.35

Table: 7.11: Q1: 1st quartile/25th percentile, Min: minimum value, Median: 2nd quartile/50th percentile, Max: maximum value, Q3: 3rd quartile/75th percentile values for EOFAD, LOAD and control samples upon immunohistochemical staining with GPR103.

Figure 7.15 and table 7.11 show the spread of staining across all samples for GPR103. The controls reveal much variation and the EOFAD remains higher that what is seen in LOAD. Both EOFAD and LOAD stay consistently lower than the old controls and apart from in the SUB also remain lower than the young control.

7.4: Correlation between OX1R, OX2R, GPR103 and Aβ^{42} or tau staining within 5 different regions of the hippocampal formation

In AD one of the first symptoms are memory deficits which are correlated with disease progression. This can be as a result of Aβ deposition in areas of the hippocampal formation with denser depositions with progressing disease (Biron et al. 2013; Reilly et al. 2003). NFTs are also shown to be deposited within areas of the hippocampus in AD which has been shown to increase with disease advancement (Lace et al. 2009; Lund et

al. 2014). An Aβ^{42} and tau antibody was used to stain paraffin embedded hippocampal slides of the patients to observe protein deposition and distribution and identify any correlation with toxic protein accumulation and receptors (Figure 7.16). Scoring was performed by assessing each of 5 areas of the hippocampus: DG, CA3, CA2, CA1 and SUB and assigning values between 1-10; with 10 being the most dense protein expression.

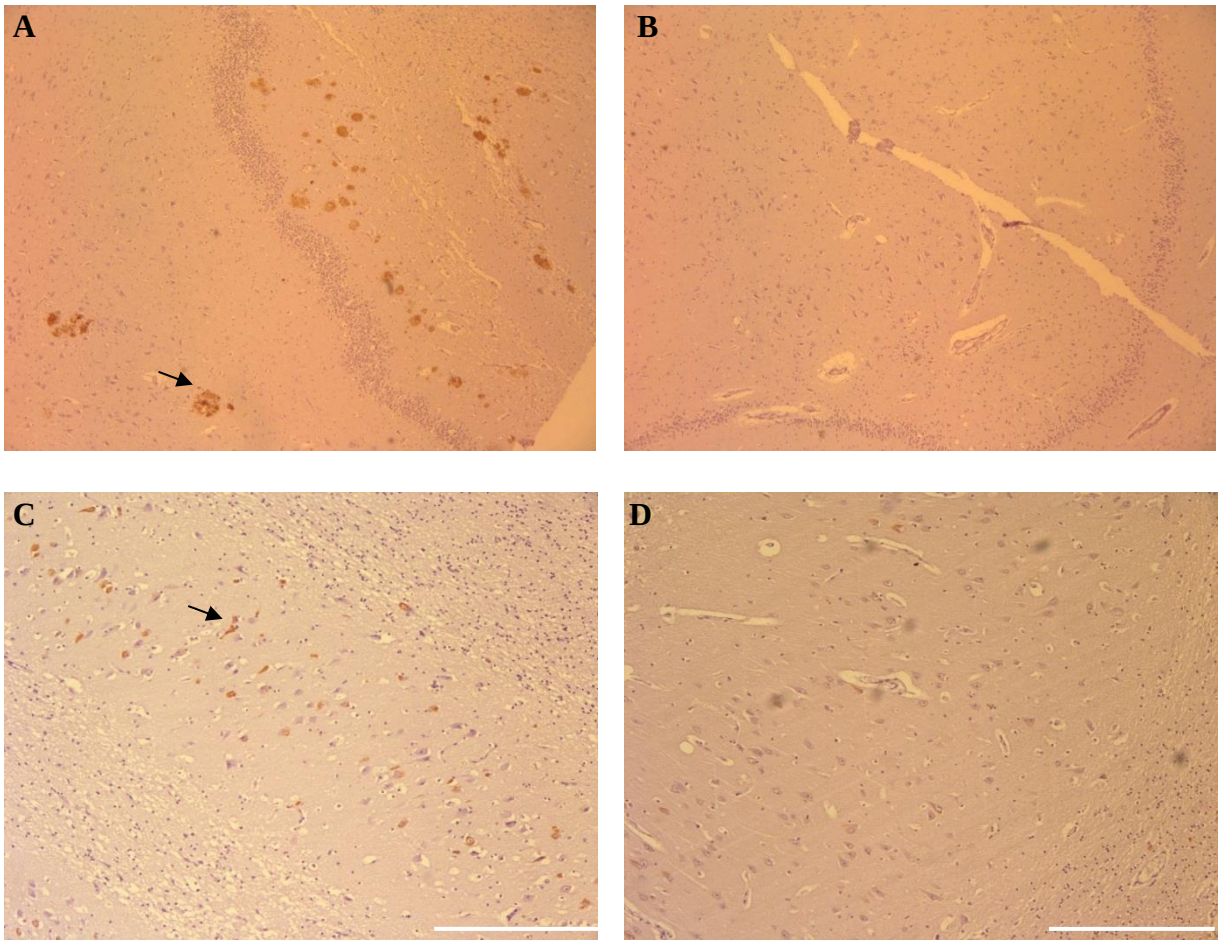

Figure 7.16: Representative images of immunohistochemistry using DAB staining in patient hippocampal slides with A. Aβ^{42} in an EOFAD patient. B. Aβ^{42} in a control patient. C. Tau in an EOFAD patient. D. Tau in a control patient. A and B x10 magnification, Bar = 200µm. C and D x20 magnification, Bar = 100µm.

Pearson correlation was used to correlate deposition of Aβ^{42} or tau with receptor expression in EOFAD and LOAD within specific areas of the hippocampus. Most patient samples did not display any significant correlation between receptor expression and protein deposition. Patient 7 however had a significant positive correlation between

OX2R and deposition of $A\beta^{42}$ and tau (Table 7.12). Patient 6 also exhibited significant positive correlation between OX2R and tau deposition. LOAD samples only showed correlation for patient 11 between OX1R and $A\beta^{42}$ (Table 7.13).

EOFAD		Patient 2	Patient 3	Patient 4	Patient 5	Patient 6	Patient 7
		OX1R	**OX1R**	**OX1R**	**OX1R**	**OX1R**	**OX1R**
$A\beta^{42}$	Pearson correlation	-0.6329	-0.6047	-0.3618	0.7091	-0.59	0.7634
	Significance	0.2517	0.28	0.5496	0.1799	0.295	0.1332
		OX2R	**OX2R**	**OX2R**	**OX2R**	**OX2R**	**OX2R**
$A\beta^{42}$	Pearson correlation	0.7156	0.504	0.7534	0.4098	-0.5469	0.9034
	Significance	0.1741	0.3866	0.1414	0.4932	0.3401	0.0355 *
		GPR103	**GPR103**	**GPR103**	**GPR103**	**GPR103**	**GPR103**
$A\beta^{42}$	Pearson correlation	-0.9538	-0.3291	-0.05687	-0.3247	0.1368	-0.1856
	Significance	0.0118	0.5886	0.9276	0.5940	0.8263	0.7651
		OX1R	**OX1R**	**OX1R**	**OX1R**	**OX1R**	**OX1R**
Tau	Pearson correlation	-0.2509	0.6061	-0.5923	0.3183	-0.8324	0.6827
	Significance	0.684	0.2785	0.2926	0.1013	0.0803	0.2041
		OX2R	**OX2R**	**OX2R**	**OX2R**	**OX2R**	**OX2R**
Tau	Pearson correlation	0.3036	0.3927	0.8342	-0.3772	-0.8937	0.9857
	Significance	0.6195	0.5131	0.079	0.5313	0.041 *	0.0021 **
		GPR103	**GPR103**	**GPR103**	**GPR103**	**GPR103**	**GPR103**
Tau	Pearson correlation	-0.822	-0.02661	-0.1634	-0.8530	-0.1706	-0.04441
	Significance	0.0877	0.9661	0.7929	0.0662	0.7839	0.9435

Table 7.12: Correlation between Aβ or tau deposition and OX1R, OX2R and GPR103 expression in paraffin embedded slides of EOFAD patients using Pearson correlation ($p<0.05$*,$p<0.01$**), (N=6).

LOAD		Patient 8	Patient 9	Patient 10	Patient 11	Patient 12	Patient 13
		OX1R	**OX1R**	**OX1R**	**OX1R**	**OX1R**	**OX1R**
Aβ^{42}	Pearson correlation	0.6396	0.04563	0.7623	0.5819	0.546	0.1712
	Significance	0.2452	0.9419	0.134	0.3033	0.3411	0.7831
		OX2R	**OX2R**	**OX2R**	**OX2R**	**OX2R**	**OX2R**
Aβ^{42}	Pearson correlation	0.9553	-0.8522	0.7422	0.9821	0.6755	0.1099
	Significance	0.0113	0.0667	0.1509	0.0029**	0.2107	0.8603
		GPR103	**GPR103**	**GPR103**	**GPR103**	**GPR103**	**GPR103**
Aβ^{42}	Pearson correlation	0.6302	-0.3634	0.8758	0.654	0.9523	0.07475
	Significance	0.2545	0.5477	0.0515	0.2312	0.0124	0.9049
		OX1R	**OX1R**	**OX1R**	**OX1R**	**OX1R**	**OX1R**
Tau	Pearson correlation	0.5783	-0.1683	0.6346	-0.2426	-0.1498	0.1712
	Significance	0.3071	0.7867	0.2501	0.6941	0.81	0.7831
		OX2R	**OX2R**	**OX2R**	**OX2R**	**OX2R**	**OX2R**
Tau	Pearson correlation	0.5528	-0.7787	0.2899	0.1712	0.3792	0.1099
	Significance	0.3339	0.1207	0.6361	0.7831	0.5291	0.8603
		GPR103	**GPR103**	**GPR103**	**GPR103**	**GPR103**	**GPR103**
Tau	Pearson correlation	0.1841	-0.4938	0.7012	-0.1141	0.6478	0.07475
	Significance	0.7669	0.3978	0.187	0.8550	0.2372	0.9049

Table 7.13: Correlation between Aβ or tau deposition and OX1R, OX2R and GPR103 expression in paraffin embedded slides of LOAD patients using Pearson correlation, ($p<0.01$**), (N=6).

Pearson correlation was then used to identify correlation between immunohistochemistry scoring of each receptor to one another. EOFAD revealed a significant negative correlation between OX1R and OX2R in patient 2 whilst LOAD showed significant positive correlation in patient 10 between OX1R and GPR103. Patient 13 also displayed significant positive correlation between OX2R and GPR103. There was no correlation between any receptors for the control samples (summarised in Table 7.14)

	Patient 2 (EOFAD)	**Patient 10 (LOAD)**	**Patient 13 (LOAD)**
	OX1R vs OX2R	OX1R vs GPR103	OX2R vs GPR103
Pearson correlation	-0.9747	0.9586	0.9318
Significance	0.0048 **	0.01 *	0.0212 *

Table 7.14: Significant correlation between OX1R, OX2R and GPR103 expression in paraffin embedded slides of EOFAD, LOAD and control patients using Pearson correlation ($p<0.05$*, $p<0.01$**).

7.5 Results and discussion

It has long been thought that there may be some involvement of the orexigenic system in AD. This is due to symptoms of AD encompassing sleep-wake cycle dysregulation and decreased feeding; both of which could be attributable to OX signalling as well as a loss of 40% of immunoreactive OX neurons in AD and lower circulating OXA (Fronczek et al. 2011). We sought to investigate OXR and GPR103 expression profiles in AD and control patients at RNA and protein level. This is the first time such a study has been performed to the best of our knowledge.

qPCR analysis revealed that there was much lower expression of *OX1R*, *OX2R* and *GPR103* in EOFAD and LOAD when compared to the control. With age matching it may be more appropriate to compare the EOFAD (median age 64) to the young controls (median age 58) and the LOAD (median age 88) to the old controls (median age 85), to account for any age related changes in receptor expression. Between EOFAD and

LOAD the medians and variation were fairly similar, with there being much more variation than seen in the control. The old controls had consistently lower expression than seen in the young controls; however it still remained higher than the AD samples. OXR levels have been shown to decrease with age in rats with a reduction ranging from 33-44%, so the reduction observed in old controls compared to the young controls is anticipated (Terao et al. 2002). EOFAD revealed a significant positive correlation between all of the genes, suggesting that receptor reduction is occurring in tandem between all the genes. In LOAD however, there is only a significant positive correlation between *OX2R* and *GPR103*. So *OX1R* only correlates with *OX2R* and *GPR103* when there is genetic involvement in AD. The same correlation is seen in the control samples, with positive correlation between *OX2R* and *GPR103*. OXRs have been shown to form homo or hetero–dimers. For example OX1R is capable of forming a dimer with the cannabinoid receptor (CB1) (Hilairet et al. 2003). Although it is known OXRs can form dimers, the dimerisation capabilities of GPR103 are not known. In the human brain OXRs can be co-expressed or differentially expressed, for example only OX1R is expressed in the VTA and LC and only OX2R is expressed in the amygdala and LHA (Tsujino, Sakurai 2009). Therefore it is possible the correlation observed is as a result of dimerisation of the receptors and co-expression to allow full functioning of the receptors, or that both receptors play an important role in the hippocampus and expression of both is required.

RNA oxidation has been shown to occur in up to 70% of mRNA isolated from the frontal cortex of an AD patient through immunoprecipitation and separation of oxidised and non-oxidised RNA (Shan, Lin 2006). 8-hydroxyguanosine (8-OHG) is an indicator of hydroxyl radical damage to RNA and accumulates upon reactive oxygen or nitrogen species assault. In the CSF of AD patients levels of 8-OHG were increased 5 fold compared to control samples (Abe et al. 2002). Although RNA oxidation has been well documented in AD the focus has been on identifying levels of oxidation and not the effect on specific genes. NO causes neurotoxicity through several mechanisms including: forming the destructive radical peroxynitrite, lipid peroxidation, DNA/RNA/protein damage as well as nitrosylation of proteins including protein kinase C (Law, Gauthier & Quirion 2001). This is of particular importance in AD where Aβ is

capable of exerting a synergistic action with glutamate causing the induction of the NO pathway and hence neuronal damage (Yang et al. 1998). NO has been demonstrated to selectively cause degeneration of OX neurons (Togo, Katsuse & Iseki 2004). Therefore OXR/GPR103 in AD may be selectively targeted through mechanisms of RNA oxidation or targeted NO degeneration leading to the observed reduction in RNA levels that are exhibited in EOFAD and LOAD patient samples. The microarray data that we previously performed revealed that upon OXA treatment 5 genes involved in the NF-KB signalling pathway changed regulation compared to the control leading to induction of the pathway and with QRFP treatment 6 genes involved with the HIF-1α signalling pathway changed expression causing induction of the pathway. The NF-KB signalling pathway is activated in response to many factors including oxidative stress (Li, Karin 1999). The HIF-1α pathway is activated in response to low oxygen and incurs protection against hypoxic conditions (Ziello, Jovin & Huang 2007). The NF-KB pathway has been shown to play a role in neuroprotection of oxidative stress caused by $A\beta^{42}$ in cultured rat hippocampal neurons (Mattson et al. 1997). Although it is not known whether OXR/GPR103 are directly affected by oxidation of RNA in AD, up to 70% of RNA is affected by oxidation and it is possible that they too are affected. It is attractive to speculate that the reduction of receptors observed in patient samples is as a result of oxidative stress, with damage possibly being exacerbated by inability of OXR/GPR103 signalling leading to a loss of oxidative protection.

Immunohistochemistry was then performed on paraffin embedded slides for each of the patients studying the protein expression for OX1R, OX2R and GPR103 in 5 hippocampal regions: DG, CA3, CA2, CA1 and SUB. Within each area, 5 areas were scored by counting the amount of nuclei and the amount of positively stained cells and thus calculating the percentage of cells expressing the protein. For OX1R the amount of protein was similar between EOFAD and LOAD and in all areas was lower than that seen in the old controls and lower than in the young controls in the DG, CA2 and SUB. There was a similar pattern for OX2R with comparable expression between EOFAD and LOAD which maintained lower levels than the old control across all hippocampal regions. The young controls however exhibited lower expression in the CA1 and SUB. GPR103 expression again remained accordant between EOFAD and LOAD, this time

however the expression in the old controls was consistently lower than the AD patients and the young controls were consistently higher. Although there was variation seen in the qPCR data, it was far less than seen with protein expression and illustrated a clear difference in expression between diseased and control samples. At protein level however there was more variation between each group of samples. It is very important to remember that DAB staining is not quantitative and can only be viewed as a percentage of cells expressing the protein and not the extent to which they express a protein. So a collection of cells may all be scored as positive, but in actual fact some cells may be expressing vast quantities of the proteins and others low amounts. This difference in protein expression may also be attributable to RNA being extracted from an area containing the hippocampus and hence encompassing a larger area, whereas protein staining was performed on a clearly defined area. It is possible that differences in receptor expression are noticeable over a large area of brain and not within specific areas. Small losses in receptors in definitive areas may not be noticeable through DAB staining, but over a larger area may present a physiologically relevant loss. The reduction seen in the qPCR data is in agreement with previous studies where a 40% loss of orexigenic neurons in AD was observed (Fronczek et al. 2011). It should also be noted that OXR mRNA in rat brains has been documented and OX1R immunoreactivity was found in all areas of the hippocampal formation, but mRNA was not found in the CA3. OX2R immunoreactivity was not studied, but its mRNA was not found to be expressed in the CA1 or CA2 of the rat hippocampus (Trivedi et al. 1998). We however found protein expressed in all areas of the human hippocampal formation for the patients. These discrepancies may arise from the fact that this study was performed on human samples, whereas OXR expression studies were previously performed in the rat. Although the OXR are generally highly conserved between species there are also differences in homology between species (Jiang et al. 2003). So the OX system between the two species may not be identical, therefore mRNA expression profiling in the rat is not necessarily an exact indicator of what transpires in the human brain. In the human adrenal OX1R and OX2R expression is found in the zona fasciculata (ZF), zona reticularis (ZR) and the medulla and OX1R is also found in the zona glomerulosa (ZG) (Mazzocchi et al. 2001; Nanmoku et al. 2000). In the rat adrenal however, there is very low expression of OX1R and OX2R is expressed only in the ZG and ZR and there is no

expression in the ZF. As OXR expression has not been as extensively mapped in the brain as it has in the rat (particularly the hippocampus) it is possible that differences in expression that occur in the adrenal also occur in the human brain.

The discrepancy in expression seen at protein level compared to RNA level may not directly reflect a state of functional receptor expression. Non-functional receptors include receptors with post-translational modifications and receptors undergoing trafficking. These receptors may still be detected even if they are not fully functional. OXRs have been shown to tightly associate with β-arrestin which can result in internalisation into recycling endosomes (Evans et al. 2001). This results in their eventual degradation or they can be recycled to the membrane, so they may be recognised by an antibody but in actual fact not be fully functional receptors. DAB staining is not specific and cannot localise expression to within certain areas of the cell, consequently the location and therefore possible functionality of the receptors cannot be ascertained through this technique. DAB also only stains cells as positive or negative it cannot be used to quantify the amount of receptor expression within each cell. A decrease in expression of all cells in AD could still produce the same amount of DAB staining as control samples. So this may explain discrepancies between receptor expression at RNA level and positive staining of protein.

Data is unclear on any post-translational modifications involved in OXR or GPR103 production, but this can affect the expression at protein level and may explain differences seen in RNA and protein level (Baribault et al. 2006). Post-translational modifications of GPCRs include the glycosylation of the amino terminus, extracellular loops and carboxy-terminal phosphorylation (Goddard, Watts 2012). So although there is a smaller decrease at protein level in AD samples compared to the controls than what is observed at RNA level, these receptors may not be functional and DAB protein expression is only semi-quantitative and observes only a small area.

Slides were then stained with $A\beta^{42}$ and a tau antibody to discern if any changes in OXR/GPR103 receptors were correlated with $A\beta^{42}$ deposition or tau hyperphosphorylation. These slides were scored from 1-10 with 10 being the most dense staining. EOFAD patient 7 exhibited positive correlation between OX2R and

$A\beta^{42}$ and also between OX2R and tau. Patient 6 revealed negative correlation between OX2R and tau. In LOAD there was no correlation with $A\beta^{42}$ or tau and protein expression. This suggests that within the hippocampal formation reduction observed at protein level does not correlate with damage caused by $A\beta^{42}$ or tau in AD.

In the control samples there was no observed correlation between receptors at protein level. For EOFAD only patient 2 had significant negative correlation between OX1R and OX2R. In LOAD samples, patient 10 had significant positive correlation between OX1R and GPR103 and in patient 13 for OX2R and GPR103. However this was not observed across multiple samples and neither the same gene correlations nor the same direction of correlation was seen, so this is an individual patient occurrence and not a trend. Therefore at the protein level there is no significant correlation between OX1R, OX2R or GPR103 expression. Although there is no correlation in the immunohistochemistry samples and differences are more variable than seen in the qPCR, immunohistochemistry is only semi-quantitative and observes very small, distinct regions. Expression and correlation seen in qPCR was statistically significant as well as focusing on a larger area of the hippocampus and surrounding tissue.

To summarise; there is a reduction in *OX1R*, *OX2R* and *GPR103* mRNA expression in EOFAD and LOAD when compared to control samples, and although there is a similar reduction at protein level it is not entirely reflective of what occurs at RNA level. We demonstrate in AD that there is a reduction at RNA and protein level of OX1R, OX2R and GPR103 which may lead to compromised OXR/GPR103 signalling in AD resulting in the symptoms observed in AD including sleep-wake dysregulation and weight loss.

8

Chapter 8

General discussion

8.1 Validation of neuronal model and ERK signalling with OX and QRFP

IMR32 and SH-SY5Y cell lines were differentiated and this was confirmed through increasing neurite length, increased expression of key neuronal proteins and increases in *MAPT*, *NG1* and *NSE* as well as a reduction in the neuronal marker of immaturity *NES*. OXR and GPR103 were found to be expressed in both cell lines once they had become differentiated and were shown to be fully functional and capable of phosphorylating ERK1/2. ERK1/2, when phosphorylated can directly regulate the expression of BDNF through the CREB protein, insulin-like growth factor 1 (IGF-I) and many anti-apoptotic genes as well as increasing ROS detoxification though antioxidants like heme oxygenase 1 and manganese superoxide dismutase; all of which contribute to neuronal survival (Tabuchi et al. 2002; Lambert, Weiss & Lauder 2001; Gong et al. 2002; Sakamoto, Karelina & Obrietan 2011). CREB also regulates genes involved in memory and synaptic plasticity and in mice with Aβ induced amnesia there was reduced ERK1/2 phosphorylation (Liu et al. 2013). ERK induced neuroprotection has also been demonstrated in the rat suprachiasmatic nucleus cell line: SCN2.2 which is resistant to glutamate toxicity; an important mediator of neurodegeneration in AD. ERK1/2 inhibition in this cell line prevented any glutamate resistance and resulted in neurotoxicity (Karmarkar et al. 2011). ERK inhibition in a Huntington's model resulted in increased cell death and ERK1/2 can also directly protect cells from DNA damage and hypoxia (Maher et al. 2011; Hetman et al. 1999; Han, Holtzman 2000).

We showed that in our hands we could create a differentiated human neuronal model and induce p-ERK1/2 through addition of OXA, OXB and QRFP. We demonstrate for

the first time signalling through ERK1/2 of OXA, OXB and QRFP in a neuronally differentiated model and thus indicative of potential neuroprotective effects.

8.2 Reduction in OXR/GPR103 in AD models; *in vitro* and in clinical samples

Our clinical sample studies using $A\beta^{42}$ and zinc sulphate to induce an AD phenotype by $A\beta^{42}$ deposition and tau hyperphosphorylation respectively resulted in significant down regulation of *OX1R* and *GPR103* at mRNA level in SH-SY5Y with minimal changes in *OX2R*, however this was not reflected in IMR32. This suggests a preferential targeting and thus down regulation of *OX1R* and *GPR103* over *OX2R* in SH-SY5Y. The significant reduction observed in *OX1R* is not reflected in its activation of p-ERK1/2 and this may be due to OXAs ability to signal through *OX2R* which is minimally affected by the treatment. The fact that *GPR103* experiences significant down regulation in all treatments and yet has vastly reduced levels of p-ERK1/2 compared to OXA and OXB treatment supports this. Although this might suggest that OX signalling can be compensated for through *OX2R*, addition of the peptide was exogenous and circulating levels of OXs cannot be accounted for in an *in vivo* system and how they may be affected in AD.

In EOFAD and LOAD all the 3 receptors mRNA were also significantly reduced compared to healthy controls. There were significant differences compared to the young control but not to the old control; although the average for AD samples was consistently lower than the old control for all receptors. The mean age for EOFAD samples was 61 years old and for the young controls 57; this makes it an appropriate control and signifies that there is significant down regulation of *OXR* and *GPR103* in EOFAD when compared to an age matched control. The mean age in LOAD samples is 84 years old and for old controls 85. This seems a more appropriate control for these samples and although there was no significant reduction there was certainly a trend for reduced expression of all receptors in LOAD samples. One of the main mechanisms though which AD can exert a damaging effect on cells is through oxidation of the RNA (Shan, Lin 2006; Nunomura et al. 1999). Increased ageing has also been demonstrated to lead to increased oxidative damage which can result in defects in memory (Liu et al. 2002; Marchal et al. 2013). So although RNA oxidation is amplified in AD due to toxic insult

it also occurs as a consequence of ageing and OXRs have been shown to be decreased with normal ageing (Terao et al. 2002a; Porkka-Heiskanen et al. 2004). This may explain why there is reduced expression in the old control compared to the young control. However it must be noted that in LOAD there is still a trend of reduced receptor expression compared to the old control.

We have demonstrate that $A\beta^{42}$ and zinc sulphate *in vitro* to mimic AD results in a significant reduction of *OX1R* and *GPR103* in SH-SY5Y and in AD patients there is a loss of *OX1R*, *OX2R* and *GPR103* at mRNA and protein level compared to a healthy control.

8.3 The loss of OXR/QRFP and potential loss of neuroprotection

Acute p-ERK increases have been shown to confer neuroprotection and OX and QRFP signalling through this pathway may provide protection (Karmarkar et al. 2011; Maher et al. 2011; Xia et al. 1995). Indeed OXs have already been shown to exert a neuroprotective role through activation of Akt, NF-KB, HIF-1α and ERK1/2 (Sokolowska et al. 2014; Yuan et al. 2011; Yuan et al. 2011; Harada, Yamazaki & Tokuyama 2013; Yamada et al. 2009). Our microarray data highlighted key genes involved in neurodegeneration for example; GRIN1 and PTGER1. However there are an overwhelming number of KEGG pathways and individual genes regulated by OXA, OXB and QRFP which confer neuroprotection. Of note with OXA treatment is the induced upregulation of somatostatin receptors, *VIP*, *EDN1* and the NF-KB KEGG pathway, all of which contribute to neuroprotection (Hama, Saido 2005; Song et al. 2012; Palmer, Love 2011; Mattson et al. 1997). OXB increases *CRHR1*, *REDD1* and *EPO* which have all been heavily implicated in AD and protection (Pedersen et al. 2001; Li et al. 2005; Rabie, Marti 2008; Lee et al. 2012). QRFP treatment led to a decrease of *c-myb* and *BIM* and up regulation of many neuroprotective genes including *PDGF-β* and *EPO*, all of which are suggestive of a neuroprotective function (Deng, Ishii & Sarai 1996; Sagare et al. 2013).

Neurodegeneration is also a normal process of ageing. For example the widely accepted free radical theory of ageing proposed by Harman in 1956, postulated that free radicals from oxygen accumulate over time and cause the damage associated with ageing and

the antioxidant systems are incapable of counteracting this damage over a lifespan (Harman 1956; Vina, Borras & Miquel 2007; Edrey, Salmon 2014). In normal ageing there is thought to be a reduction of approximately 5% of brain mass for each decade after the age of 40, with rate of decline increasing after 70 (Svennerholm, Bostrom & Jungbjer 1997; Scahill et al. 2003) . This appears to particularly affect the hippocampus and the frontal lobes, and between the ages of 30-90 there is a 14% cerebral cortex loss, 35% in the hippocampus and 26% in cerebral white matter (Jernigan et al. 2001). And as such there are many cognitive related declines associated with normal ageing, which becomes more apparent with increasing age but are not pathological (Zamzow et al. 2013; Verhaeghen, Cerella 2002). Loss of the orexigenic system associated with normal ageing is also associated with poor sleep quality and increased sleep fragmentation (Porkka-Heiskanen, Zitting & Wigren 2013). This raises the importance of two factors associated with ageing: loss of the OX system and increased oxidative damage. This could imply that that loss of the OX system causes a loss of neuroprotection particularly with regards to protection against oxidative damage and could contribute to age related cognitive decline.

It has been suggested that in transgenic AD mouse models that OX infusion can exacerbate the burden of disease (Kang et al. 2009). Based on this assumption it could be expected that in narcoleptic patients which experience a loss of orexigenic signalling systems that they would have a lower incidence of disease due to the predicted neurotoxic effects of AD in these mouse models. However a recent study which examined rates of AD in human narcoleptics found that 1 in 3 narcoleptic patients had AD (Scammell, Matheson et al. 2012). This suggests that OX does not exacerbate the chances of AD and in fact these narcoleptic patients have a higher incidence of disease than would be expected in a group of this age range further suggesting protective effects of OX in AD.

Calorie restriction has been shown to extend life span through its antioxidant effects, anti-inflammatory effects and enhanced neurogenesis (Maalouf, Rho & Mattson 2009).This can occur through regulation of sirtuin1 (SIRT1) (Satoh et al. 2010). Calorie restriction has been shown to cause up regulation of SIRT1 which then results in an increase in OX2R (Satoh et al. 2010). However the data on calorie restriction effects on

OXR and PPO expression are conflicting, but there seems to be more data suggesting an upregulation during restricted feeding, with increased OX mediating an anti-depressant like effect upon calorie restriction (Lutter et al. 2008; Cai et al. 1999; Lopez et al. 2000; Mondal et al. 1999). It is thought that SIRT1 is one of the primary mechanisms which results in increased life span, through regulation of metabolic pathways and promotion of cell survival (Satoh et al. 2010). It has also been implicated in AD and shown to reduce Aβ deposition in a transgenic mouse model of AD through upregulation of ADAM10 and subsequent APP processing by α-secretase in a non-amyloidegenic fashion (Satoh et al. 2010; Qin et al. 2006). Circulating SIRT1 is significantly reduced in human AD patients and is directly correlated with AD progression (Julien et al. 2009). And it is calorie restriction which is an incredibly important regulator of SIRT1. Calorie restriction has been shown to have specific effects on neuroprotection and can limit neuronal damage in response to neuronal injury and in transgenic mouse models of AD calorie restriction significantly reduced neuronal damage (Bruce-Keller et al. 1999; Anson et al. 2003). This indicates the potential for up regulation of OX or OXR which has been previously shown to occur during calorie restriction, to confer neuroprotection.

Collectively, based on our *in vitro* findings and clinical data; there is a loss of OXR and GPR103 which could worsen not only symptoms of weight loss and dysregulation of the sleep wake cycle but also confer a loss of neuroprotection through these signalling pathways including ERK1/2; exacerbating the symptoms of the disease. This raises the question of potential therapeutic targets to improve the symptoms of dysregulated sleep-wake and weight loss which are major contributors to institutionalisation and malnutrition, but also improve neuroprotection which could slow progression of the disease (Bird 2008; Bianchetti et al. 1995).

8.4 Function of GPR103 and its potential cross-talk with OXR

This study has also highlighted the novel roles of the peptide QRFP and its receptor GPR103. A multitude of studies provide evidence that there is an interaction and subsequent cross-talk of GPCRs and for the existence of homodimeric and heterodimeric structures upon agonist stimulation, which can form new receptor complexes or provide distinctive characteristics which exhibit functional properties

separate from the monomeric GPCR form (Angers, Salahpour & Bouvier 2002; Szafran et al. 2013). There is limited data on GPR103/QRFP and we demonstrate for the first time the genes which it regulates in a neuronal cell line. In our model it regulates many more genes that OXA or OXB and as it has previously been demonstrated to have orexigenic activity it may be more pivotal in regulation of the systems attributed to OXs than previously thought (Takayasu et al. 2006). It regulates many genes involved in neuroactive ligand-receptor interaction, metabolic pathways, calcium signalling, HIF-1α, PI3K-Akt, Jak-STAT, MAPK, regulation of the actin cytoskeleton and the TNF pathway as well as cardiac muscle contraction and cytokine interactions. This suggests it has many physiological functions which are far reaching and extend beyond the brain and a merely orexigenic like activity.

We show that that QRFP can induce phosphorylation of ERK1/2 to initiate its downstream effects. Both IMR32 and SH-SY5Y showed increasing activation over 60 minutes, which may suggest a lack of receptor internalisation or desensitisation that is seen with OXA and OXB. Antagonists for OX1R and OX2R can individually block QRFP induced phosphorylation of ERK1/2. This suggests a possible cross-talk between GPR103 and the OXRs. Because each antagonist used has a higher selectivity for one of the receptors this suggests possible coupling to both of the OXR and indicates that to activate ERK1/2 GPR103 must couple to at least one of these receptors. OXRs are not always co-expressed in the brain so GPR103 may have a proclivity for promiscuously coupling to whichever OXR is available to initiate its action when only one of the receptors is available (Trivedi et al. 1998; Bruzzone et al. 2007). Indeed, in the clinical samples there was a positive correlation between expression of GPR103 and OX2R for all of the patient samples at mRNA level. In the microarray QRFP also resulted in increased expression of OX1R, suggesting that QRFP stimulation of neuronal cells could selectively increase OX1R to enable a cross-talk and further signalling. It is attractive to speculate that co-expression of GPR103/OXRs in the hippocampus is needed to allow GPR103 to become fully functional.

8.5 Limitations of study

We would like to acknowledge that our study has a number of limitations. With regards to the clinical samples one of the problems was inability to sufficiently quantify protein levels. Although DAB staining was performed this does not give an accurate enough representation at protein level. This could be studied in the future, by performing a western blot on extracted protein, which unfortunately in this study was not possible due to ethical restrictions. The PM delay for the patients was incredibly variable and this may have had an effect on degradation of RNA/protein, in the future collection of samples with early PM delays or from roughly the same time would make for more representative data. However this may not be feasible as there are so many constraints to this, which are out of our control. As there are not many cases of EOFAD it would indeed be highly unlikely to obtain further samples from Brains for Dementia Research bank. Although we observed receptor expression in patient samples at mRNA level, we did not correlate this with circulating ISF levels of the peptides within each patient, which could have provided interesting insights. Due to the limitations in obtaining samples, we were only able to study one area of the brain. Many other areas of the brain are affected by the orexigenic system and are targeted in AD which could elucidate the mechanisms behind this interaction further.

In addition we only measure one end point of receptor activation: p-ERK1/2 and so other signalling pathways in a neuronal model which were affected through OXR/GPR103 signalling were not identified. Furthermore the microarray we performed was only on one of the two cell lines we successfully differentiated and we did not perform a proteomic screen on the treated samples. We also treated cells for 24 hours and *in vivo* exposure to OX/QRFP for this extended period of time may have effects which are physiologically abnormal.

8.6 Future work

Due to certain constraints regarding feasibility the microarray was only performed on one cell line which we perceived as being more valuable to the study. However to get a wider view of peptide effects on neuronal cells, multiple cell lines could be used to get a more consistent view on OX and QRFP signalling as well as observing different

exposure times to the peptides. Measurement of receptor expression in AD patients through western blot would provide more quantitative results at protein level and measuring circulating OX and QRFP in the same patients could further dissect any correlations between circulating peptide levels and receptors. This could identify if it is not only a loss of the receptors but also of the ligands which lead to the characteristic symptoms associated with the orexigenic system. If possible, to obtain the clinical history of the patients would allow us to correlate the extent of the loss of OXR/GPR103 with the severity of sleep related disorder or weight loss to examine if there is indeed a direct correlation between symptoms and loss of receptors. We observed more variation in receptor expression in AD samples than in control samples, and if we could correlate symptoms with reductions in receptor expression it may explain the variations. That is, patients which experience more of a reduction in receptors may have worse symptoms. Because there can be sexual dimorphism in AD a larger cohort from each female and male groups could identify any sexual dimorphisms in OXR and GPR103. A larger cross section of the brain and surrounding neuronal structures would provide an interesting insight as to whether OXR/GPR103 loss is confined to hippocampal areas or is more widespread. It would also be very interesting to investigate how addition of $A\beta^{42}$ and zinc sulphate affects HIF-1α and Akt; already identified as being important in OX signalling and neuroprotection, and whether treatment with OXA, OXB and QRFP could confer neuroprotection using these pathways. Also observing cell viability upon peptide addition could reveal any cell pro-survival effects of the peptides. Moreover it would be interesting to examine OX and QRFP neuroprotective effects in a non-AD situation for example by addition of hydrogen peroxide to see if the peptides are capable of protecting against oxidative insult and whether there is any HIF-1α involvement.

Performing the studies we have demonstrated in human primary neurons would remove the necessity of differentiating the immortalised cell lines and could provide data which is more representative of an *in vivo* system than what we have already observed. It would also be of great interest to further dissect the possible dimerisation of GPR103 with the OXRs, by performing co-localisation studies to determine upon peptide addition whether they co-localise and this could be performed using BRET analysis.

Due to the failure of IMR32 to produce any significant data when treated with $A\beta^{42}$ or zinc sulphate it would be ideal to use another neuronal cell line to observe the effects across a wider spectrum of cell lines and dissect whether there is a sexual dimorphism in neuronal cell lines. Although SH-SY5Y confirmed what was seen in the patient samples a broader spectrum would allow clearer identification of possible gene changes.

9

Chapter 9

Bibliography

Abe T., Tohgi H., Isobe C., Murata T. and Sato C. (2002) Remarkable increase in the concentration of 8-hydroxyguanosine in cerebrospinal fluid from patients with alzheimer's disease. *J. Neurosci. Res.*, **70**, 447-450.

Agholme L., Lindstrom T., Kagedal K., Marcusson J. and Hallbeck M. (2010) An in vitro model for neuroscience: Differentiation of SH-SY5Y cells into cells with morphological and biochemical characteristics of mature neurons. *J. Alzheimers Dis.*, **20**, 1069-1082.

Aittaleb M., Boguth C.A. and Tesmer J.J. (2010) Structure and function of heterotrimeric G protein-regulated rho guanine nucleotide exchange factors. *Mol. Pharmacol.*, **77**, 111-125.

Akbari E., Motamedi F., Naghdi N. and Noorbakhshnia M. (2008) The effect of antagonization of orexin 1 receptors in CA1 and dentate gyrus regions on memory processing in passive avoidance task. *Behav. Brain Res.*, **187**, 172-177.

Akbari E., Naghdi N. and Motamedi F. (2006) Functional inactivation of orexin 1 receptors in CA1 region impairs acquisition, consolidation and retrieval in morris water maze task. *Behav. Brain Res.*, **173**, 47-52.

Allinson T.M., Parkin E.T., Turner A.J. and Hooper N.M. (2003) ADAMs family members as amyloid precursor protein alpha-secretases. *J. Neurosci. Res.*, **74**, 342-352.

Alonso A.D., Zaidi T., Novak M., Barra H.S., Grundke-Iqbal I. and Iqbal K. (2001) Interaction of tau isoforms with alzheimer's disease abnormally hyperphosphorylated tau and in vitro phosphorylation into the disease-like protein. *J. Biol. Chem.*, **276**, 37967-37973.

Alzheimer's Disease International . Available: http://www.alz.co.uk/research/statistics [2014, 04/04].

Ammoun S., Johansson L., Ekholm M.E., Holmqvist T., Danis A.S., Korhonen L., Sergeeva O.A., Haas H.L., Akerman K.E. and Kukkonen J.P. (2006) OX1 orexin receptors activate extracellular signal-regulated kinase in chinese hamster ovary cells via multiple mechanisms: The role of Ca2+ influx in OX1 receptor signaling. *Mol. Endocrinol.*, **20**, 80-99.

Ammoun S., Lindholm D., Wootz H., Akerman K.E. and Kukkonen J.P. (2006) G-protein-coupled OX1 orexin/hcrtr-1 hypocretin receptors induce caspase-dependent and -independent cell death through p38 mitogen-/stress-activated protein kinase. *J. Biol. Chem.*, **281**, 834-842.

An W.L., Bjorkdahl C., Liu R., Cowburn R.F., Winblad B. and Pei J.J. (2005) Mechanism of zinc-induced phosphorylation of p70 S6 kinase and glycogen synthase kinase 3beta in SH-SY5Y neuroblastoma cells. *J. Neurochem.*, **92**, 1104-1115.

Anderson R.I., Becker H.C., Adams B.L., Jesudason C.D. and Rorick-Kehn L.M. (2014) Orexin-1 and orexin-2 receptor antagonists reduce ethanol self-administration in high-drinking rodent models. *Front. Neurosci.*, **8**, 33.

Angeletti B., Waldron K.J., Freeman K.B., Bawagan H., Hussain I., Miller C.C., Lau K.F., Tennant M.E., Dennison C., Robinson N.J. *et al.* (2005) BACE1 cytoplasmic domain interacts with the copper chaperone for superoxide dismutase-1 and binds copper. *J. Biol. Chem.*, **280**, 17930-17937.

Angers S., Salahpour A. and Bouvier M. (2002) Dimerization: An emerging concept for G protein-coupled receptor ontogeny and function. *Annu. Rev. Pharmacol. Toxicol.*, **42**, 409-435.

Anson R.M., Guo Z., de Cabo R., Iyun T., Rios M., Hagepanos A., Ingram D.K., Lane M.A. and Mattson M.P. (2003) Intermittent fasting dissociates beneficial effects of dietary restriction on glucose metabolism and neuronal resistance to injury from calorie intake. *Proc. Natl. Acad. Sci. U. S. A.*, **100**, 6216-6220.

Armstrong R.A. (2009) The molecular biology of senile plaques and neurofibrillary tangles in alzheimer's disease. *Folia Neuropathol.*, **47**, 289-299.

Armulik A., Genove G., Mae M., Nisancioglu M.H., Wallgard E., Niaudet C., He L., Norlin J., Lindblom P., Strittmatter K. *et al.* (2010) Pericytes regulate the blood-brain barrier. *Nature*, **468**, 557-561.

Asami-Odaka A., Ishibashi Y., Kikuchi T., Kitada C. and Suzuki N. (1995) Long amyloid beta-protein secreted from wild-type human neuroblastoma IMR-32 cells. *Biochemistry*, **34**, 10272-10278.

Asuni A.A., Boutajangout A., Quartermain D. and Sigurdsson E.M. (2007) Immunotherapy targeting pathological tau conformers in a tangle mouse model reduces brain pathology with associated functional improvements. *J. Neurosci.*, **27**, 9115-9129.

Avila J., Lucas J.J., Perez M. and Hernandez F. (2004) Role of tau protein in both physiological and pathological conditions. *Physiol. Rev.*, **84**, 361-384.

Avramovich-Tirosh Y., Bar-Am O., Amit T., Youdim M.B. and Weinreb O. (2010) Up-regulation of hypoxia-inducible factor (HIF)-1alpha and HIF-target genes in cortical

neurons by the novel multifunctional iron chelator anti-alzheimer drug, M30. *Curr. Alzheimer Res.,* **7**, 300-306.

Bagyinszky E., Youn Y.C., An S.S. and Kim S. (2014) The genetics of alzheimer's disease. *Clin. Interv. Aging,* **9**, 535-551.

Ballatore C., Lee V.M. and Trojanowski J.Q. (2007) Tau-mediated neurodegeneration in alzheimer's disease and related disorders. *Nat. Rev. Neurosci.,* **8**, 663-672.

Barbosa A.C., Kim M.S., Ertunc M., Adachi M., Nelson E.D., McAnally J., Richardson J.A., Kavalali E.T., Monteggia L.M., Bassel-Duby R. *et al.* (2008) MEF2C, a transcription factor that facilitates learning and memory by negative regulation of synapse numbers and function. *Proc. Natl. Acad. Sci. U. S. A.,* **105**, 9391-9396.

Baribault H., Danao J., Gupte J., Yang L., Sun B., Richards W. and Tian H. (2006) The G-protein-coupled receptor GPR103 regulates bone formation. *Mol. Cell. Biol.,* **26**, 709-717.

Barnes L.L., Wilson R.S., Bienias J.L., Schneider J.A., Evans D.A. and Bennett D.A. (2005) Sex differences in the clinical manifestations of alzheimer disease pathology. *Arch. Gen. Psychiatry,* **62**, 685-691.

Bell R.D., Winkler E.A., Sagare A.P., Singh I., LaRue B., Deane R. and Zlokovic B.V. (2010) Pericytes control key neurovascular functions and neuronal phenotype in the adult brain and during brain aging. *Neuron,* **68**, 409-427.

Bergsdorf C., Paliga K., Kreger S., Masters C.L. and Beyreuther K. (2000) Identification of cis-elements regulating exon 15 splicing of the amyloid precursor protein pre-mRNA. *J. Biol. Chem.,* **275**, 2046-2056.

Bernard R., Lydic R. and Baghdoyan H.A. (2003) Hypocretin-1 causes G protein activation and increases ACh release in rat pons. *Eur. J. Neurosci.,* **18**, 1775-1785.

Bernard R., Lydic R. and Baghdoyan H.A. (2002) Hypocretin-1 activates G proteins in arousal-related brainstem nuclei of rat. *Neuroreport,* **13**, 447-450.

Bernardis L.L. and Bellinger L.L. (1996) The lateral hypothalamic area revisited: Ingestive behavior. *Neurosci. Biobehav. Rev.,* **20**, 189-287.

Beuckmann C.T. and Yanagisawa M. (2002) Orexins: From neuropeptides to energy homeostasis and sleep/wake regulation. *J. Mol. Med. (Berl),* **80**, 329-342.

Beyer C., Pilgrim C. and Reisert I. (1991) Dopamine content and metabolism in mesencephalic and diencephalic cell cultures: Sex differences and effects of sex steroids. *J. Neurosci.,* **11**, 1325-1333.

Bianchetti A., Scuratti A., Zanetti O., Binetti G., Frisoni G.B., Magni E. and Trabucchi M. (1995) Predictors of mortality and institutionalization in alzheimer disease patients 1 year after discharge from an alzheimer dementia unit. *Dementia,* **6**, 108-112.

Biedler J.L., Helson L. and Spengler B.A. (1973) Morphology and growth, tumorigenicity, and cytogenetics of human neuroblastoma cells in continuous culture. *Cancer Res.,* **33**, 2643-2652.

Biedler J.L., Roffler-Tarlov S., Schachner M. and Freedman L.S. (1978) Multiple neurotransmitter synthesis by human neuroblastoma cell lines and clones. *Cancer Res.,* **38**, 3751-3757.

Bierer L.M., Haroutunian V., Gabriel S., Knott P.J., Carlin L.S., Purohit D.P., Perl D.P., Schmeidler J., Kanof P. and Davis K.L. (1995) Neurochemical correlates of dementia severity in alzheimer's disease: Relative importance of the cholinergic deficits. *J. Neurochem.,* **64**, 749-760.

Bird T.D. (2008) Genetic aspects of alzheimer disease. *Genet. Med.,* **10**, 231-239.

Bird T.D. (1993) Early-Onset Familial Alzheimer Disease. In Pagon R.A., Bird T.D., Dolan C.R. and Stephens K. (eds.), *Genereviews.* University of Washington, Seattle. (WA).

Birkenkamp-Demtroder K., Hahn S.A., Mansilla F., Thorsen K., Maghnouj A., Christensen R., Oster B. and Orntoft T.F. (2013) Keratin23 (KRT23) knockdown decreases proliferation and affects the DNA damage response of colon cancer cells. *PLoS One,* **8**, e73593.

Biron K.E., Dickstein D.L., Gopaul R., Fenninger F. and Jefferies W.A. (2013) Cessation of neoangiogenesis in alzheimer's disease follows amyloid-beta immunization. *Sci. Rep.,* **3**, 1354.

Biswas S.C., Liu D.X. and Greene L.A. (2005) Bim is a direct target of a neuronal E2F-dependent apoptotic pathway. *J. Neurosci.,* **25**, 8349-8358.

Biswas S.C., Shi Y., Vonsattel J.P., Leung C.L., Troy C.M. and Greene L.A. (2007) Bim is elevated in alzheimer's disease neurons and is required for beta-amyloid-induced neuronal apoptosis. *J. Neurosci.,* **27**, 893-900.

Blacker D., Haines J.L., Rodes L., Terwedow H., Go R.C., Harrell L.E., Perry R.T., Bassett S.S., Chase G., Meyers D. *et al.* (1997) ApoE-4 and age at onset of alzheimer's disease: The NIMH genetics initiative. *Neurology,* **48**, 139-147.

Blanco M., Garcia-Caballero T., Fraga M., Gallego R., Cuevas J., Forteza J., Beiras A. and Dieguez C. (2002) Cellular localization of orexin receptors in human adrenal gland, adrenocortical adenomas and pheochromocytomas. *Regul. Pept.,* **104**, 161-165.

Blennow K., de Leon M.J. and Zetterberg H. (2006) Alzheimer's disease. *Lancet*, **368**, 387-403.

Borovecki F., Klepac N., Muck-Seler D., Hajnsek S., Mubrin Z. and Pivac N. (2010) Unraveling the biological mechanisms in alzheimer's disease - lessons from genomics. *Prog. Neuropsychopharmacol. Biol. Psychiatry*, .

Boschen K.E., Fadel J.R. and Burk J.A. (2009) Systemic and intrabasalis administration of the orexin-1 receptor antagonist, SB-334867, disrupts attentional performance in rats. *Psychopharmacology (Berl)*, **206**, 205-213.

Bowen D.M., Smith C.B., White P. and Davison A.N. (1976) Neurotransmitter-related enzymes and indices of hypoxia in senile dementia and other abiotrophies. *Brain*, **99**, 459-496.

Brandt J.A., Churchill L., Rehman A., Ellis G., Memet S., Israel A. and Krueger J.M. (2004) Sleep deprivation increases the activation of nuclear factor kappa B in lateral hypothalamic cells. *Brain Res.*, **1004**, 91-97.

Brickell K.L., Steinbart E.J., Rumbaugh M., Payami H., Schellenberg G.D., Van Deerlin V., Yuan W. and Bird T.D. (2006) Early-onset alzheimer disease in families with late-onset alzheimer disease: A potential important subtype of familial alzheimer disease. *Arch. Neurol.*, **63**, 1307-1311.

Brown R.E., Sergeeva O., Eriksson K.S. and Haas H.L. (2001) Orexin A excites serotonergic neurons in the dorsal raphe nucleus of the rat. *Neuropharmacology*, **40**, 457-459.

Bruce-Keller A.J., Umberger G., McFall R. and Mattson M.P. (1999) Food restriction reduces brain damage and improves behavioral outcome following excitotoxic and metabolic insults. *Ann. Neurol.*, **45**, 8-15.

Brunden K.R., Trojanowski J.Q. and Lee V.M. (2009) Advances in tau-focused drug discovery for alzheimer's disease and related tauopathies. *Nat. Rev. Drug Discov.*, **8**, 783-793.

Bruzzone F., Lectez B., Alexandre D., Jegou S., Mounien L., Tollemer H., Chatenet D., Leprince J., Vallarino M., Vaudry H. *et al.* (2007) Distribution of 26RFa binding sites and GPR103 mRNA in the central nervous system of the rat. *J. Comp. Neurol.*, **503**, 573-591.

Bruzzone F., Lectez B., Tollemer H., Leprince J., Dujardin C., Rachidi W., Chatenet D., Baroncini M., Beauvillain J.C., Vallarino M. *et al.* (2006) Anatomical distribution and biochemical characterization of the novel RFamide peptide 26RFa in the human hypothalamus and spinal cord. *J. Neurochem.*, **99**, 616-627.

Burdakov D., Liss B. and Ashcroft F.M. (2003) Orexin excites GABAergic neurons of the arcuate nucleus by activating the sodium--calcium exchanger. *J. Neurosci.,* **23**, 4951-4957.

Bush A.I. (2003) The metallobiology of alzheimer's disease. *Trends Neurosci.,* **26**, 207-214.

Bustin S.A., Benes V., Garson J.A., Hellemans J., Huggett J., Kubista M., Mueller R., Nolan T., Pfaffl M.W., Shipley G.L. *et al.* (2009) The MIQE guidelines: Minimum information for publication of quantitative real-time PCR experiments. *Clin. Chem.,* **55**, 611-622.

Butterfield D.A. and Pocernich C.B. (2003) The glutamatergic system and alzheimer's disease: Therapeutic implications. *CNS Drugs,* **17**, 641-652.

Butterick T.A., Nixon J.P., Billington C.J. and Kotz C.M. (2012) Orexin A decreases lipid peroxidation and apoptosis in a novel hypothalamic cell model. *Neurosci. Lett.,* **524**, 30-34.

Caccamo A., Majumder S., Richardson A., Strong R. and Oddo S. (2010) Molecular interplay between mammalian target of rapamycin (mTOR), amyloid-beta, and tau: Effects on cognitive impairments. *J. Biol. Chem.,* **285**, 13107-13120.

Caccamo A., Oddo S., Sugarman M.C., Akbari Y. and LaFerla F.M. (2005) Age- and region-dependent alterations in abeta-degrading enzymes: Implications for abeta-induced disorders. *Neurobiol. Aging,* **26**, 645-654.

Caescu C.I., Jeschke G.R. and Turk B.E. (2009) Active-site determinants of substrate recognition by the metalloproteinases TACE and ADAM10. *Biochem. J.,* **424**, 79-88.

Cai X.J., Widdowson P.S., Harrold J., Wilson S., Buckingham R.E., Arch J.R., Tadayyon M., Clapham J.C., Wilding J. and Williams G. (1999) Hypothalamic orexin expression: Modulation by blood glucose and feeding. *Diabetes,* **48**, 2132-2137.

Calipari E.S. and Espana R.A. (2012) Hypocretin/orexin regulation of dopamine signaling: Implications for reward and reinforcement mechanisms. *Front. Behav. Neurosci.,* **6**, 54.

Callahan M.J., Lipinski W.J., Bian F., Durham R.A., Pack A. and Walker L.C. (2001) Augmented senile plaque load in aged female beta-amyloid precursor protein-transgenic mice. *Am. J. Pathol.,* **158**, 1173-1177.

Cannon B. and Nedergaard J. (2004) Brown adipose tissue: Function and physiological significance. *Physiol. Rev.,* **84**, 277-359.

Carpentier M., Robitaille Y., DesGroseillers L., Boileau G. and Marcinkiewicz M. (2002) Declining expression of neprilysin in alzheimer disease vasculature: Possible involvement in cerebral amyloid angiopathy. *J. Neuropathol. Exp. Neurol.,* **61**, 849-856.

Carrillo-Mora P., Luna R. and Colin-Barenque L. (2014) Amyloid beta: Multiple mechanisms of toxicity and only some protective effects? *Oxid Med. Cell. Longev,* **2014**, 795375.

Carruth L.L., Reisert I. and Arnold A.P. (2002) Sex chromosome genes directly affect brain sexual differentiation. *Nat. Neurosci.,* **5**, 933-934.

Caspersen C., Wang N., Yao J., Sosunov A., Chen X., Lustbader J.W., Xu H.W., Stern D., McKhann G. and Yan S.D. (2005) Mitochondrial abeta: A potential focal point for neuronal metabolic dysfunction in alzheimer's disease. *FASEB J.,* **19**, 2040-2041.

Cassarino D.S., Fall C.P., Smith T.S. and Bennett J.P.,Jr (1998) Pramipexole reduces reactive oxygen species production in vivo and in vitro and inhibits the mitochondrial permeability transition produced by the parkinsonian neurotoxin methylpyridinium ion. *J. Neurochem.,* **71**, 295-301.

Chan J.S., Lee J.W., Ho M.K. and Wong Y.H. (2000) Preactivation permits subsequent stimulation of phospholipase C by G(i)-coupled receptors. *Mol. Pharmacol.,* **57**, 700-708.

Chartrel N., Alonzeau J., Alexandre D., Jeandel L., Alvear-Perez R., Leprince J., Boutin J., Vaudry H., Anouar Y. and Llorens-Cortes C. (2011) The RFamide neuropeptide 26RFa and its role in the control of neuroendocrine functions. *Front. Neuroendocrinol.,* **32**, 387-397.

Chartrel N., Dujardin C., Anouar Y., Leprince J., Decker A., Clerens S., Do-Rego J.C., Vandesande F., Llorens-Cortes C., Costentin J. *et al.* (2003) Identification of 26RFa, a hypothalamic neuropeptide of the RFamide peptide family with orexigenic activity. *Proc. Natl. Acad. Sci. U. S. A.,* **100**, 15247-15252.

Chemelli R.M., Willie J.T., Sinton C.M., Elmquist J.K., Scammell T., Lee C., Richardson J.A., Williams S.C., Xiong Y., Kisanuki Y. *et al.* (1999) Narcolepsy in orexin knockout mice: Molecular genetics of sleep regulation. *Cell,* **98**, 437-451.

Chen J. and Randeva H.S. (2010) Genomic organization and regulation of the human orexin (hypocretin) receptor 2 gene: Identification of alternative promoters. *Biochem. J.,* **427**, 377-390.

Cheung K.H., Mei L., Mak D.O., Hayashi I., Iwatsubo T., Kang D.E. and Foskett J.K. (2010) Gain-of-function enhancement of IP3 receptor modal gating by familial alzheimer's disease-linked presenilin mutants in human cells and mouse neurons. *Sci. Signal.,* **3**, ra22.

Cheung Y.T., Lau W.K., Yu M.S., Lai C.S., Yeung S.C., So K.F. and Chang R.C. (2009) Effects of all-trans-retinoic acid on human SH-SY5Y neuroblastoma as in vitro model in neurotoxicity research. *Neurotoxicology,* **30**, 127-135.

Christen Y. (2000) Oxidative stress and alzheimer disease. *Am. J. Clin. Nutr.,* **71**, 621S-629S.

Cirrito J.R., Deane R., Fagan A.M., Spinner M.L., Parsadanian M., Finn M.B., Jiang H., Prior J.L., Sagare A., Bales K.R. *et al.* (2005) P-glycoprotein deficiency at the blood-brain barrier increases amyloid-beta deposition in an alzheimer disease mouse model. *J. Clin. Invest.,* **115**, 3285-3290.

Cirrito J.R., Kang J.E., Lee J., Stewart F.R., Verges D.K., Silverio L.M., Bu G., Mennerick S. and Holtzman D.M. (2008) Endocytosis is required for synaptic activity-dependent release of amyloid-beta in vivo. *Neuron,* **58**, 42-51.

Conde C. and Caceres A. (2009) Microtubule assembly, organization and dynamics in axons and dendrites. *Nat. Rev. Neurosci.,* **10**, 319-332.

Conrad M.S., Dilger R.N., Nickolls A. and Johnson R.W. (2012) Magnetic resonance imaging of the neonatal piglet brain. *Pediatr. Res.,* **71**, 179-184.

Constantinescu R., Constantinescu A.T., Reichmann H. and Janetzky B. (2007) Neuronal differentiation and long-term culture of the human neuroblastoma line SH-SY5Y. *J. Neural Transm. Suppl.,* **(72)**, 17-28.

Craig L.A., Hong N.S. and McDonald R.J. (2011) Revisiting the cholinergic hypothesis in the development of alzheimer's disease. *Neurosci. Biobehav. Rev.,* **35**, 1397-1409.

Crampton S.J. and O'Keeffe G.W. (2013) NF-kappaB: Emerging roles in hippocampal development and function. *Int. J. Biochem. Cell Biol.,* **45**, 1821-1824.

Crapper McLachlan D.R., Dalton A.J., Kruck T.P., Bell M.Y., Smith W.L., Kalow W. and Andrews D.F. (1991) Intramuscular desferrioxamine in patients with alzheimer's disease. *Lancet,* **337**, 1304-1308.

Crowther R.A. (1991) Straight and paired helical filaments in alzheimer disease have a common structural unit. *Proc. Natl. Acad. Sci. U. S. A.,* **88**, 2288-2292.

Cruts M., Theuns J. and Van Broeckhoven C. (2012) Locus-specific mutation databases for neurodegenerative brain diseases. *Hum. Mutat.,* **33**, 1340-1344.

Cruz C.D. and Cruz F. (2007) The ERK 1 and 2 pathway in the nervous system: From basic aspects to possible clinical applications in pain and visceral dysfunction. *Curr. Neuropharmacol.,* **5**, 244-252.

Daffu G., del Pozo C.H., O'Shea K.M., Ananthakrishnan R., Ramasamy R. and Schmidt A.M. (2013) Radical roles for RAGE in the pathogenesis of oxidative stress in cardiovascular diseases and beyond. *Int. J. Mol. Sci.*, **14**, 19891-19910.

Dahlstrand J., Collins V.P. and Lendahl U. (1992) Expression of the class VI intermediate filament nestin in human central nervous system tumors. *Cancer Res.*, **52**, 5334-5341.

Dalrymple M.B., Jaeger W.C., Eidne K.A. and Pfleger K.D. (2011) Temporal profiling of orexin receptor-arrestin-ubiquitin complexes reveals differences between receptor subtypes. *J. Biol. Chem.*, **286**, 16726-16733.

Dass B., McDaniel L., Schultz R.A., Attaya E. and MacDonald C.C. (2002) The gene CSTF2T, encoding the human variant CstF-64 polyadenylation protein tauCstF-64, lacks introns and may be associated with male sterility. *Genomics*, **80**, 509-514.

De Ingeniis J., Ratnikov B., Richardson A.D., Scott D.A., Aza-Blanc P., De S.K., Kazanov M., Pellecchia M., Ronai Z., Osterman A.L. *et al.* (2012) Functional specialization in proline biosynthesis of melanoma. *PLoS One*, **7**, e45190.

De la Herran-Arita A.K., Guerra-Crespo M. and Drucker-Colin R. (2011) Narcolepsy and orexins: An example of progress in sleep research. *Front. Neurol.*, **2**, 26.

de Lecea L., Kilduff T.S., Peyron C., Gao X., Foye P.E., Danielson P.E., Fukuhara C., Battenberg E.L., Gautvik V.T., Bartlett F.S.,2nd *et al.* (1998) The hypocretins: Hypothalamus-specific peptides with neuroexcitatory activity. *Proc. Natl. Acad. Sci. U. S. A.*, **95**, 322-327.

De Strooper B. and Annaert W. (2000) Proteolytic processing and cell biological functions of the amyloid precursor protein. *J. Cell. Sci.*, **113 (Pt 11)**, 1857-1870.

De Strooper B., Saftig P., Craessaerts K., Vanderstichele H., Guhde G., Annaert W., Von Figura K. and Van Leuven F. (1998) Deficiency of presenilin-1 inhibits the normal cleavage of amyloid precursor protein. *Nature*, **391**, 387-390.

Deadwyler S.A., Porrino L., Siegel J.M. and Hampson R.E. (2007) Systemic and nasal delivery of orexin-A (hypocretin-1) reduces the effects of sleep deprivation on cognitive performance in nonhuman primates. *J. Neurosci.*, **27**, 14239-14247.

Deane R. and Zlokovic B.V. (2007) Role of the blood-brain barrier in the pathogenesis of alzheimer's disease. *Curr. Alzheimer Res.*, **4**, 191-197.

Deng Q.L., Ishii S. and Sarai A. (1996) Binding site analysis of c-myb: Screening of potential binding sites by using the mutation matrix derived from systematic binding affinity measurements. *Nucleic Acids Res.*, **24**, 766-774.

Desai A. and Mitchison T.J. (1997) Microtubule polymerization dynamics. *Annu. Rev. Cell Dev. Biol.,* **13**, 83-117.

Deshpande A., Win K.M. and Busciglio J. (2008) Tau isoform expression and regulation in human cortical neurons. *FASEB J.,* **22**, 2357-2367.

Dewing P., Shi T., Horvath S. and Vilain E. (2003) Sexually dimorphic gene expression in mouse brain precedes gonadal differentiation. *Brain Res. Mol. Brain Res.,* **118**, 82-90.

Dhaher R., Hauser S.R., Getachew B., Bell R.L., McBride W.J., McKinzie D.L. and Rodd Z.A. (2010) The orexin-1 receptor antagonist SB-334867 reduces alcohol relapse drinking, but not alcohol-seeking, in alcohol-preferring (P) rats. *J. Addict. Med.,* **4**, 153-159.

Dharmadhikari A.V., Kang S.H., Szafranski P., Person R.E., Sampath S., Prakash S.K., Bader P.I., Phillips J.A.,3rd, Hannig V., Williams M. *et al.* (2012) Small rare recurrent deletions and reciprocal duplications in 2q21.1, including brain-specific ARHGEF4 and GPR148. *Hum. Mol. Genet.,* **21**, 3345-3355.

Digicaylioglu M. and Lipton S.A. (2001) Erythropoietin-mediated neuroprotection involves cross-talk between Jak2 and NF-kappaB signalling cascades. *Nature,* **412**, 641-647.

Dineley K.T., Westerman M., Bui D., Bell K., Ashe K.H. and Sweatt J.D. (2001) Beta-amyloid activates the mitogen-activated protein kinase cascade via hippocampal alpha7 nicotinic acetylcholine receptors: In vitro and in vivo mechanisms related to alzheimer's disease. *J. Neurosci.,* **21**, 4125-4133.

Ding X., MacTavish D., Kar S. and Jhamandas J.H. (2006) Galanin attenuates beta-amyloid (abeta) toxicity in rat cholinergic basal forebrain neurons. *Neurobiol. Dis.,* **21**, 413-420.

Dingledine R., Borges K., Bowie D. and Traynelis S.F. (1999) The glutamate receptor ion channels. *Pharmacol. Rev.,* **51**, 7-61.

do Rego J.C., Leprince J., Chartrel N., Vaudry H. and Costentin J. (2006) Behavioral effects of 26RFamide and related peptides. *Peptides,* **27**, 2715-2721.

Doody R.S., Dunn J.K., Clark C.M., Farlow M., Foster N.L., Liao T., Gonzales N., Lai E. and Massman P. (2001) Chronic donepezil treatment is associated with slowed cognitive decline in alzheimer's disease. *Dement. Geriatr. Cogn. Disord.,* **12**, 295-300.

Douaud G., Refsum H., de Jager C.A., Jacoby R., Nichols T.E., Smith S.M. and Smith A.D. (2013) Preventing alzheimer's disease-related gray matter atrophy by B-vitamin treatment. *Proc. Natl. Acad. Sci. U. S. A.,* **110**, 9523-9528.

Doyle E., Bruce M.T., Breen K.C., Smith D.C., Anderton B. and Regan C.M. (1990) Intraventricular infusions of antibodies to amyloid-beta-protein precursor impair the acquisition of a passive avoidance response in the rat. *Neurosci. Lett.,* **115**, 97-102.

Ducy P., Amling M., Takeda S., Priemel M., Schilling A.F., Beil F.T., Shen J., Vinson C., Rueger J.M. and Karsenty G. (2000) Leptin inhibits bone formation through a hypothalamic relay: A central control of bone mass. *Cell,* **100**, 197-207.

Dutar P., Lamour Y. and Nicoll R.A. (1989) Galanin blocks the slow cholinergic EPSP in CA1 pyramidal neurons from ventral hippocampus. *Eur. J. Pharmacol.,* **164**, 355-360.

Duvernay M.T., Filipeanu C.M. and Wu G. (2005) The regulatory mechanisms of export trafficking of G protein-coupled receptors. *Cell. Signal.,* **17**, 1457-1465.

Dwane S., Durack E. and Kiely P.A. (2013) Optimising parameters for the differentiation of SH-SY5Y cells to study cell adhesion and cell migration. *BMC Res. Notes,* **6**, 366-0500-6-366.

Ebrahim I.O., Howard R.S., Kopelman M.D., Sharief M.K. and Williams A.J. (2002) The hypocretin/orexin system. *J. R. Soc. Med.,* **95**, 227-230.

Ebrahim I.O., Sharief M.K., de Lacy S., Semra Y.K., Howard R.S., Kopelman M.D. and Williams A.J. (2003) Hypocretin (orexin) deficiency in narcolepsy and primary hypersomnia. *J. Neurol. Neurosurg. Psychiatry.,* **74**, 127-130.

Edbauer D., Winkler E., Regula J.T., Pesold B., Steiner H. and Haass C. (2003) Reconstitution of gamma-secretase activity. *Nat. Cell Biol.,* **5**, 486-488.

Edrey Y.H. and Salmon A.B. (2014) Revisiting an age-old question regarding oxidative stress. *Free Radic. Biol. Med.,* **71C**, 368-378.

Elliott-Hunt C.R., Kazlauskaite J., Wilde G.J., Grammatopoulos D.K. and Hillhouse E.W. (2002) Potential signalling pathways underlying corticotrophin-releasing hormone-mediated neuroprotection from excitotoxicity in rat hippocampus. *J. Neurochem.,* **80**, 416-425.

Encinas M., Iglesias M., Liu Y., Wang H., Muhaisen A., Cena V., Gallego C. and Comella J.X. (2000) Sequential treatment of SH-SY5Y cells with retinoic acid and brain-derived neurotrophic factor gives rise to fully differentiated, neurotrophic factor-dependent, human neuron-like cells. *J. Neurochem.,* **75**, 991-1003.

Engler H., Santillo A.F., Wang S.X., Lindau M., Savitcheva I., Nordberg A., Lannfelt L., Langstrom B. and Kilander L. (2008) In vivo amyloid imaging with PET in frontotemporal dementia. *Eur. J. Nucl. Med. Mol. Imaging,* **35**, 100-106.

Eriksson K.S., Sergeeva O., Brown R.E. and Haas H.L. (2001) Orexin/hypocretin excites the histaminergic neurons of the tuberomammillary nucleus. *J. Neurosci.,* **21**, 9273-9279.

Esmaeili-Mahani S., Vazifekhah S., Pasban-Aliabadi H., Abbasnejad M. and Sheibani V. (2013) Protective effect of orexin-A on 6-hydroxydopamine-induced neurotoxicity in SH-SY5Y human dopaminergic neuroblastoma cells. *Neurochem. Int.,* **63**, 719-725.

Estabrooke I.V., McCarthy M.T., Ko E., Chou T.C., Chemelli R.M., Yanagisawa M., Saper C.B. and Scammell T.E. (2001) Fos expression in orexin neurons varies with behavioral state. *J. Neurosci.,* **21**, 1656-1662.

European Alzheimer's Disease Initiative (EADI), Genetic and Environmental Risk in Alzheimer's Disease, Alzheimer's Disease Genetic Consortium and Cohorts for Heart and Aging Research in Genomic Epidemiology (2013) Meta-analysis of 74,046 individuals identifies 11 new susceptibility loci for Alzheimer's disease. *Nat. Genet.,* **45**, 1452-1458.

Evans N.A., Groarke D.A., Warrack J., Greenwood C.J., Dodgson K., Milligan G. and Wilson S. (2001) Visualizing differences in ligand-induced beta-arrestin-GFP interactions and trafficking between three recently characterized G protein-coupled receptors. *J. Neurochem.,* **77**, 476-485.

Felgner H., Frank R., Biernat J., Mandelkow E.M., Mandelkow E., Ludin B., Matus A. and Schliwa M. (1997) Domains of neuronal microtubule-associated proteins and flexural rigidity of microtubules. *J. Cell Biol.,* **138**, 1067-1075.

Ferchmin P.A., Perez D., Eterovic V.A. and de Vellis J. (2003) Nicotinic receptors differentially regulate N-methyl-D-aspartate damage in acute hippocampal slices. *J. Pharmacol. Exp. Ther.,* **305**, 1071-1078.

Fernandez M., Gobartt A.L., Balana M. and COOPERA Study Group (2010) Behavioural symptoms in patients with alzheimer's disease and their association with cognitive impairment. *BMC Neurol.,* **10**, 87-2377-10-87.

Fitzpatrick J.L., Mize A.L., Wade C.B., Harris J.A., Shapiro R.A. and Dorsa D.M. (2002) Estrogen-mediated neuroprotection against beta-amyloid toxicity requires expression of estrogen receptor alpha or beta and activation of the MAPK pathway. *J. Neurochem.,* **82**, 674-682.

Francis P.T., Palmer A.M., Snape M. and Wilcock G.K. (1999) The cholinergic hypothesis of Alzheimer's disease: A review of progress. *J. Neurol. Neurosurg. Psychiatry.,* **66**, 137-147.

Francis R., McGrath G., Zhang J., Ruddy D.A., Sym M., Apfeld J., Nicoll M., Maxwell M., Hai B., Ellis M.C. *et al.* (2002) Aph-1 and pen-2 are required for notch pathway

signaling, gamma-secretase cleavage of betaAPP, and presenilin protein accumulation. *Dev. Cell.,* **3**, 85-97.

Fredriksson R., Lagerstrom M.C., Lundin L.G. and Schioth H.B. (2003) The G-protein-coupled receptors in the human genome form five main families. phylogenetic analysis, paralogon groups, and fingerprints. *Mol. Pharmacol.,* **63**, 1256-1272.

Friedhoff P., von Bergen M., Mandelkow E.M. and Mandelkow E. (2000) Structure of tau protein and assembly into paired helical filaments. *Biochim. Biophys. Acta,* **1502**, 122-132.

Friedman L.F., Zeitzer J.M., Lin L., Hoff D., Mignot E., Peskind E.R. and Yesavage J.A. (2007) In alzheimer disease, increased wake fragmentation found in those with lower hypocretin-1. *Neurology,* **68**, 793-794.

Frisoni G.B., Ganzola R., Canu E., Rub U., Pizzini F.B., Alessandrini F., Zoccatelli G., Beltramello A., Caltagirone C. and Thompson P.M. (2008) Mapping local hippocampal changes in alzheimer's disease and normal ageing with MRI at 3 tesla. *Brain,* **131**, 3266-3276.

Fronczek R., van Geest S., Frolich M., Overeem S., Roelandse F.W., Lammers G.J. and Swaab D.F. (2011) Hypocretin (orexin) loss in alzheimer's disease. *Neurobiol. Aging,* .

Frykman S., Teranishi Y., Hur J.Y., Sandebring A., Yamamoto N.G., Ancarcrona M., Nishimura T., Winblad B., Bogdanovic N., Schedin-Weiss S. *et al.* (2012) Identification of two novel synaptic gamma-secretase associated proteins that affect amyloid beta-peptide levels without altering notch processing. *Neurochem. Int.,* **61**, 108-118.

Fujiki N., Yoshida Y., Zhang S., Sakurai T., Yanagisawa M. and Nishino S. (2006) Sex difference in body weight gain and leptin signaling in hypocretin/orexin deficient mouse models. *Peptides,* **27**, 2326-2331.

Fujimori N., Oono T., Igarashi H., Ito T., Nakamura T., Uchida M., Coy D.H., Jensen R.T. and Takayanagi R. (2011) Vasoactive intestinal peptide reduces oxidative stress in pancreatic acinar cells through the inhibition of NADPH oxidase. *Peptides,* **32**, 2067-2076.

Fukusumi S., Yoshida H., Fujii R., Maruyama M., Komatsu H., Habata Y., Shintani Y., Hinuma S. and Fujino M. (2003) A new peptidic ligand and its receptor regulating adrenal function in rats. *J. Biol. Chem.,* **278**, 46387-46395.

Fuller C.M. and Insel P.A. (2014) I don't know the question, but sex is definitely the answer! focus on "in pursuit of scientific excellence: Sex matters" and "do you know the sex of your cells?". *Am. J. Physiol. Cell. Physiol.,* **306**, C1-2.

Funabashi T., Hagiwara H., Mogi K., Mitsushima D., Shinohara K. and Kimura F. (2009) Sex differences in the responses of orexin neurons in the lateral hypothalamic area and feeding behavior to fasting. *Neurosci. Lett.*, **463**, 31-34.

Gabriel S.M., Bierer L.M., Davidson M., Purohit D.P., Perl D.P. and Harotunian V. (1994) Galanin-like immunoreactivity is increased in the postmortem cerebral cortex from patients with alzheimer's disease. *J. Neurochem.*, **62**, 1516-1523.

Ganguly A., Bansal P., Gupta T. and Gupta S.K. (2010) 'ZP domain' of human zona pellucida glycoprotein-1 binds to human spermatozoa and induces acrosomal exocytosis. *Reprod. Biol. Endocrinol.*, **8**, 110-7827-8-110.

Garcia-Osta A. and Alberini C.M. (2009) Amyloid beta mediates memory formation. *Learn. Mem.*, **16**, 267-272.

Gautvik K.M., de Lecea L., Gautvik V.T., Danielson P.E., Tranque P., Dopazo A., Bloom F.E. and Sutcliffe J.G. (1996) Overview of the most prevalent hypothalamus-specific mRNAs, as identified by directional tag PCR subtraction. *Proc. Natl. Acad. Sci. U. S. A.*, **93**, 8733-8738.

Geller L.N. and Potter H. (1999) Chromosome missegregation and trisomy 21 mosaicism in alzheimer's disease. *Neurobiol. Dis.*, **6**, 167-179.

Gendreau K.L. and Hall G.F. (2013) Tangles, toxicity, and tau secretion in AD - new approaches to a vexing problem. *Front. Neurol.*, **4**, 160.

Gene Ontology Consortium (2008) The gene ontology project in 2008. *Nucleic Acids Res.*, **36**, D440-4.

George A.J., Hannan R.D. and Thomas W.G. (2013) Unravelling the molecular complexity of GPCR-mediated EGFR transactivation using functional genomics approaches. *FEBS J.*, **280**, 5258-5268.

Geula C., Nagykery N., Nicholas A. and Wu C.K. (2008) Cholinergic neuronal and axonal abnormalities are present early in aging and in alzheimer disease. *J. Neuropathol. Exp. Neurol.*, **67**, 309-318.

Gilsanz V., Hu H.H. and Kajimura S. (2013) Relevance of brown adipose tissue in infancy and adolescence. *Pediatr. Res.*, **73**, 3-9.

Goddard A.D. and Watts A. (2012) Regulation of G protein-coupled receptors by palmitoylation and cholesterol. *BMC Biol.*, **10**, 27-7007-10-27.

Gong C.X. and Iqbal K. (2008) Hyperphosphorylation of microtubule-associated protein tau: A promising therapeutic target for alzheimer disease. *Curr. Med. Chem.*, **15**, 2321-2328.

Gong C.X., Shaikh S., Wang J.Z., Zaidi T., Grundke-Iqbal I. and Iqbal K. (1995) Phosphatase activity toward abnormally phosphorylated tau: Decrease in alzheimer disease brain. *J. Neurochem.,* **65**, 732-738.

Gong C.X., Singh T.J., Grundke-Iqbal I. and Iqbal K. (1993) Phosphoprotein phosphatase activities in alzheimer disease brain. *J. Neurochem.,* **61**, 921-927.

Gong P., Stewart D., Hu B., Vinson C. and Alam J. (2002) Multiple basic-leucine zipper proteins regulate induction of the mouse heme oxygenase-1 gene by arsenite. *Arch. Biochem. Biophys.,* **405**, 265-274.

Gotter A.L., Webber A.L., Coleman P.J., Renger J.J. and Winrow C.J. (2012) International union of basic and clinical pharmacology. LXXXVI. orexin receptor function, nomenclature and pharmacology. *Pharmacol. Rev.,* **64**, 389-420.

Gralle M. and Ferreira S.T. (2007) Structure and functions of the human amyloid precursor protein: The whole is more than the sum of its parts. *Prog. Neurobiol.,* **82**, 11-32.

Gray E.H., De Vos K.J., Dingwall C., Perkinton M.S. and Miller C.C. (2010) Deficiency of the copper chaperone for superoxide dismutase increases amyloid-beta production. *J. Alzheimers Dis.,* **21**, 1101-1105.

Greenamyre J.T., Maragos W.F., Albin R.L., Penney J.B. and Young A.B. (1988) Glutamate transmission and toxicity in alzheimer's disease. *Prog. Neuropsychopharmacol. Biol. Psychiatry,* **12**, 421-430.

Guo Y. and Feng P. (2012) OX2R activation induces PKC-mediated ERK and CREB phosphorylation. *Exp. Cell Res.,* **318**, 2004-2013.

Haapasalo A. and Kovacs D.M. (2011) The many substrates of presenilin/gamma-secretase. *J. Alzheimers Dis.,* **25**, 3-28.

Hama E. and Saido T.C. (2005) Etiology of sporadic alzheimer's disease: Somatostatin, neprilysin, and amyloid beta peptide. *Med. Hypotheses,* **65**, 498-500.

Han B.H. and Holtzman D.M. (2000) BDNF protects the neonatal brain from hypoxic-ischemic injury in vivo via the ERK pathway. *J. Neurosci.,* **20**, 5775-5781.

Hanger D.P., Byers H.L., Wray S., Leung K.Y., Saxton M.J., Seereeram A., Reynolds C.H., Ward M.A. and Anderton B.H. (2007) Novel phosphorylation sites in tau from alzheimer brain support a role for casein kinase 1 in disease pathogenesis. *J. Biol. Chem.,* **282**, 23645-23654.

Harada A., Oguchi K., Okabe S., Kuno J., Terada S., Ohshima T., Sato-Yoshitake R., Takei Y., Noda T. and Hirokawa N. (1994) Altered microtubule organization in small-calibre axons of mice lacking tau protein. *Nature,* **369**, 488-491.

Harada S., Yamazaki Y. and Tokuyama S. (2013) Orexin-A suppresses postischemic glucose intolerance and neuronal damage through hypothalamic brain-derived neurotrophic factor. *J. Pharmacol. Exp. Ther.*, **344**, 276-285.

Harman D., (1956) Aging: A theory based on free radical and radiation chemistry. *J. Gerontol.*, **11**, 298-300.

Harper D.G., Stopa E.G., McKee A.C., Satlin A., Harlan P.C., Goldstein R. and Volicer L. (2001) Differential circadian rhythm disturbances in men with alzheimer disease and frontotemporal degeneration. *Arch. Gen. Psychiatry*, **58**, 353-360.

Harris G.C., Wimmer M. and Aston-Jones G. (2005) A role for lateral hypothalamic orexin neurons in reward seeking. *Nature*, **437**, 556-559.

Hasegawa T., Mikoda N., Kitazawa M. and LaFerla F.M. (2010) Treatment of alzheimer's disease with anti-homocysteic acid antibody in 3xTg-AD male mice. *PLoS One*, **5**, e8593.

Hashim A., Wang L., Juneja K., Ye Y., Zhao Y. and Ming L.J. (2011) Vitamin B6s inhibit oxidative stress caused by alzheimer's disease-related cu(II)-beta-amyloid complexes-cooperative action of phospho-moiety. *Bioorg. Med. Chem. Lett.*, **21**, 6430-6432.

Haynes A.C., Chapman H., Taylor C., Moore G.B., Cawthorne M.A., Tadayyon M., Clapham J.C. and Arch J.R. (2002) Anorectic, thermogenic and anti-obesity activity of a selective orexin-1 receptor antagonist in ob/ob mice. *Regul. Pept.*, **104**, 153-159.

Hazel J.R. and Williams E.E. (1990) The role of alterations in membrane lipid composition in enabling physiological adaptation of organisms to their physical environment. *Prog. Lipid Res.*, **29**, 167-227.

He N., Jin W.L., Lok K.H., Wang Y., Yin M. and Wang Z.J. (2013) Amyloid-beta(1-42) oligomer accelerates senescence in adult hippocampal neural stem/progenitor cells via formylpeptide receptor 2. *Cell. Death Dis.*, **4**, e924.

Hervieu G.J., Cluderay J.E., Harrison D.C., Roberts J.C. and Leslie R.A. (2001) Gene expression and protein distribution of the orexin-1 receptor in the rat brain and spinal cord. *Neuroscience*, **103**, 777-797.

Hetman M., Kanning K., Cavanaugh J.E. and Xia Z. (1999) Neuroprotection by brain-derived neurotrophic factor is mediated by extracellular signal-regulated kinase and phosphatidylinositol 3-kinase. *J. Biol. Chem.*, **274**, 22569-22580.

Heutink P. (2000) Untangling tau-related dementia. *Hum. Mol. Genet.*, **9**, 979-986.

Hilairet S., Bouaboula M., Carriere D., Le Fur G. and Casellas P. (2003) Hypersensitization of the orexin 1 receptor by the CB1 receptor: Evidence for cross-talk blocked by the specific CB1 antagonist, SR141716. *J. Biol. Chem.,* **278**, 23731-23737.

Hirata-Fukae C., Li H.F., Hoe H.S., Gray A.J., Minami S.S., Hamada K., Niikura T., Hua F., Tsukagoshi-Nagai H., Horikoshi-Sakuraba Y. *et al.* (2008) Females exhibit more extensive amyloid, but not tau, pathology in an alzheimer transgenic model. *Brain Res.,* **1216**, 92-103.

Hirokawa N., Shiomura Y. and Okabe S. (1988) Tau proteins: The molecular structure and mode of binding on microtubules. *J. Cell Biol.,* **107**, 1449-1459.

Holmqvist T., Akerman K.E. and Kukkonen J.P. (2002) Orexin signaling in recombinant neuron-like cells. *FEBS Lett.,* **526**, 11-14.

Holmqvist T., Johansson L., Ostman M., Ammoun S., Akerman K.E. and Kukkonen J.P. (2005) OX1 orexin receptors couple to adenylyl cyclase regulation via multiple mechanisms. *J. Biol. Chem.,* **280**, 6570-6579.

Hu Y. and Fortini M.E. (2003) Different cofactor activities in gamma-secretase assembly: Evidence for a nicastrin-aph-1 subcomplex. *J. Cell Biol.,* **161**, 685-690.

Huang S.C., Dai Y.W., Lee Y.H., Chiou L.C. and Hwang L.L. (2010) Orexins depolarize rostral ventrolateral medulla neurons and increase arterial pressure and heart rate in rats mainly via orexin 2 receptors. *J. Pharmacol. Exp. Ther.,* **334**, 522-529.

Huber G., Martin J.R., Loffler J. and Moreau J.L. (1993) Involvement of amyloid precursor protein in memory formation in the rat: An indirect antibody approach. *Brain Res.,* **603**, 348-352.

Hungs M. and Mignot E. (2001) Hypocretin/orexin, sleep and narcolepsy. *Bioessays,* **23**, 397-408.

Hwang L.L., Chen C.T. and Dun N.J. (2001) Mechanisms of orexin-induced depolarizations in rat dorsal motor nucleus of vagus neurones in vitro. *J. Physiol.,* **537**, 511-520.

Illenberger S., Zheng-Fischhofer Q., Preuss U., Stamer K., Baumann K., Trinczek B., Biernat J., Godemann R., Mandelkow E.M. and Mandelkow E. (1998) The endogenous and cell cycle-dependent phosphorylation of tau protein in living cells: Implications for alzheimer's disease. *Mol. Biol. Cell,* **9**, 1495-1512.

Inutsuka A. and Yamanaka A. (2013) The physiological role of orexin/hypocretin neurons in the regulation of sleep/wakefulness and neuroendocrine functions. *Front. Endocrinol. (Lausanne),* **4**, 18.

Ishida A., Furukawa K., Keller J.N. and Mattson M.P. (1997) Secreted form of beta-amyloid precursor protein shifts the frequency dependency for induction of LTD, and enhances LTP in hippocampal slices. *Neuroreport*, **8**, 2133-2137.

Ivanov A. and Aston-Jones G. (2000) Hypocretin/orexin depolarizes and decreases potassium conductance in locus coeruleus neurons. *Neuroreport*, **11**, 1755-1758.

Iwata N., Tsubuki S., Takaki Y., Shirotani K., Lu B., Gerard N.P., Gerard C., Hama E., Lee H.J. and Saido T.C. (2001) Metabolic regulation of brain abeta by neprilysin. *Science*, **292**, 1550-1552.

Iwata N., Tsubuki S., Takaki Y., Watanabe K., Sekiguchi M., Hosoki E., Kawashima-Morishima M., Lee H.J., Hama E., Sekine-Aizawa Y. *et al.* (2000) Identification of the major Abeta1-42-degrading catabolic pathway in brain parenchyma: Suppression leads to biochemical and pathological deposition. *Nat. Med.*, **6**, 143-150.

Jalili T., Takeishi Y. and Walsh R.A. (1999) Signal transduction during cardiac hypertrophy: The role of G alpha q, PLC beta I, and PKC. *Cardiovasc. Res.*, **44**, 5-9.

Jamsa A., Hasslund K., Cowburn R.F., Backstrom A. and Vasange M. (2004) The retinoic acid and brain-derived neurotrophic factor differentiated SH-SY5Y cell line as a model for alzheimer's disease-like tau phosphorylation. *Biochem. Biophys. Res. Commun.*, **319**, 993-1000.

Jernigan T.L., Archibald S.L., Fennema-Notestine C., Gamst A.C., Stout J.C., Bonner J. and Hesselink J.R. (2001) Effects of age on tissues and regions of the cerebrum and cerebellum. *Neurobiol. Aging*, **22**, 581-594.

Jiang Y., Luo L., Gustafson E.L., Yadav D., Laverty M., Murgolo N., Vassileva G., Zeng M., Laz T.M., Behan J. *et al.* (2003) Identification and characterization of a novel RF-amide peptide ligand for orphan G-protein-coupled receptor SP9155. *J. Biol. Chem.*, **278**, 27652-27657.

Johnson D.A., Cushman R. and Malekzadeh R. (1990) Orientation of cobra alpha-toxin on the nicotinic acetylcholine receptor. fluorescence studies. *J. Biol. Chem.*, **265**, 7360-7368.

Johnson G.V. and Stoothoff W.H. (2004) Tau phosphorylation in neuronal cell function and dysfunction. *J. Cell. Sci.*, **117**, 5721-5729.

Johren O., Neidert S.J., Kummer M., Dendorfer A. and Dominiak P. (2001) Prepro-orexin and orexin receptor mRNAs are differentially expressed in peripheral tissues of male and female rats. *Endocrinology*, **142**, 3324-3331.

Joyce J.N. and Millan M.J. (2007) Dopamine D3 receptor agonists for protection and repair in parkinson's disease. *Curr. Opin. Pharmacol.*, **7**, 100-105.

Julien C., Tremblay C., Emond V., Lebbadi M., Salem N.,Jr, Bennett D.A. and Calon F. (2009) Sirtuin 1 reduction parallels the accumulation of tau in alzheimer disease. *J. Neuropathol. Exp. Neurol.,* **68**, 48-58.

Kadowaki H., Nishitoh H., Urano F., Sadamitsu C., Matsuzawa A., Takeda K., Masutani H., Yodoi J., Urano Y., Nagano T. *et al.* (2005) Amyloid beta induces neuronal cell death through ROS-mediated ASK1 activation. *Cell Death Differ.,* **12**, 19-24.

Kaether C. and Haass C. (2004) A lipid boundary separates APP and secretases and limits amyloid beta-peptide generation. *J. Cell Biol.,* **167**, 809-812.

Kamenetz F., Tomita T., Hsieh H., Seabrook G., Borchelt D., Iwatsubo T., Sisodia S. and Malinow R. (2003) APP processing and synaptic function. *Neuron,* **37**, 925-937.

Kanemitsu H., Tomiyama T. and Mori H. (2003) Human neprilysin is capable of degrading amyloid beta peptide not only in the monomeric form but also the pathological oligomeric form. *Neurosci. Lett.,* **350**, 113-116.

Kang J.E., Lim M.M., Bateman R.J., Lee J.J., Smyth L.P., Cirrito J.R., Fujiki N., Nishino S. and Holtzman D.M. (2009) Amyloid-beta dynamics are regulated by orexin and the sleep-wake cycle. *Science,* **326**, 1005-1007.

Kapas L., Bohnet S.G., Traynor T.R., Majde J.A., Szentirmai E., Magrath P., Taishi P. and Krueger J.M. (2008) Spontaneous and influenza virus-induced sleep are altered in TNF-alpha double-receptor deficient mice. *J. Appl. Physiol. (1985),* **105**, 1187-1198.

Kar S., Fan J., Smith M.J., Goedert M. and Amos L.A. (2003) Repeat motifs of tau bind to the insides of microtubules in the absence of taxol. *EMBO J.,* **22**, 70-77.

Karmarkar S.W., Bottum K.M., Krager S.L. and Tischkau S.A. (2011) ERK/MAPK is essential for endogenous neuroprotection in SCN2.2 cells. *PLoS One,* **6**, e23493.

Karteris E., Chen J. and Randeva H.S. (2004) Expression of human prepro-orexin and signaling characteristics of orexin receptors in the male reproductive system. *J. Clin. Endocrinol. Metab.,* **89**, 1957-1962.

Karteris E., Machado R.J., Chen J., Zervou S., Hillhouse E.W. and Randeva H.S. (2005) Food deprivation differentially modulates orexin receptor expression and signaling in rat hypothalamus and adrenal cortex. *Am. J. Physiol. Endocrinol. Metab.,* **288**, E1089-100.

Karteris E., Randeva H.S., Grammatopoulos D.K., Jaffe R.B. and Hillhouse E.W. (2001) Expression and coupling characteristics of the CRH and orexin type 2 receptors in human fetal adrenals. *J. Clin. Endocrinol. Metab.,* **86**, 4512-4519.

Kastin A.J. and Akerstrom V. (1999) Orexin A but not orexin B rapidly enters brain from blood by simple diffusion. *J. Pharmacol. Exp. Ther.*, **289**, 219-223.

Katiyar S., Liu E., Knutzen C.A., Lang E.S., Lombardo C.R., Sankar S., Toth J.I., Petroski M.D., Ronai Z. and Chiang G.G. (2009) REDD1, an inhibitor of mTOR signalling, is regulated by the CUL4A-DDB1 ubiquitin ligase. *EMBO Rep.*, **10**, 866-872.

Kawabe J., Iwami G., Ebina T., Ohno S., Katada T., Ueda Y., Homcy C.J. and Ishikawa Y. (1994) Differential activation of adenylyl cyclase by protein kinase C isoenzymes. *J. Biol. Chem.*, **269**, 16554-16558.

Kawasumi M., Chiba T., Yamada M., Miyamae-Kaneko M., Matsuoka M., Nakahara J., Tomita T., Iwatsubo T., Kato S., Aiso S. *et al.* (2004) Targeted introduction of V642I mutation in amyloid precursor protein gene causes functional abnormality resembling early stage of alzheimer's disease in aged mice. *Eur. J. Neurosci.*, **19**, 2826-2838.

Kessler B.A., Stanley E.M., Frederick-Duus D. and Fadel J. (2011) Age-related loss of orexin/hypocretin neurons. *Neuroscience*, **178**, 82-88.

Kim J.D., Kim H., Ekram M.B., Yu S., Faulk C. and Kim J. (2011) Rex1/Zfp42 as an epigenetic regulator for genomic imprinting. *Hum. Mol. Genet.*, **20**, 1353-1362.

Kim W. and Hecht M.H. (2006) Generic hydrophobic residues are sufficient to promote aggregation of the alzheimer's Abeta42 peptide. *Proc. Natl. Acad. Sci. U. S. A.*, **103**, 15824-15829.

Kobilka B.K. (2007) G protein coupled receptor structure and activation. *Biochim. Biophys. Acta*, **1768**, 794-807.

Kogenaru S., Qing Y., Guo Y. and Wang N. (2012) RNA-seq and microarray complement each other in transcriptome profiling. *BMC Genomics*, **13**, 629-2164-13-629.

Kohda Y., Matsunaga Y., Shiota R., Satoh T., Kishi Y., Kawai Y. and Gemba M. (2006) Involvement of raf-1/MEK/ERK1/2 signaling pathway in zinc-induced injury in rat renal cortical slices. *J. Toxicol. Sci.*, **31**, 207-217.

Kohlmeier K.A., Watanabe S., Tyler C.J., Burlet S. and Leonard C.S. (2008) Dual orexin actions on dorsal raphe and laterodorsal tegmentum neurons: Noisy cation current activation and selective enhancement of Ca2+ transients mediated by L-type calcium channels. *J. Neurophysiol.*, **100**, 2265-2281.

Kolarova M., Garcia-Sierra F., Bartos A., Ricny J. and Ripova D. (2012) Structure and pathology of tau protein in alzheimer disease. *Int. J. Alzheimers Dis.*, **2012**, 731526.

Kolodziej L.E., Lodolce J.P., Chang J.E., Schneider J.R., Grimm W.A., Bartulis S.J., Zhu X., Messer J.S., Murphy S.F., Reddy N. *et al.* (2011) TNFAIP3 maintains intestinal barrier function and supports epithelial cell tight junctions. *PLoS One,* **6**, e26352.

Konieczny V., Keebler M.V. and Taylor C.W. (2012) Spatial organization of intracellular Ca2+ signals. *Semin. Cell Dev. Biol.,* **23**, 172-180.

Kopan R. and Ilagan M.X. (2004) Gamma-secretase: Proteasome of the membrane? *Nat. Rev. Mol. Cell Biol.,* **5**, 499-504.

Kopke E., Tung Y.C., Shaikh S., Alonso A.C., Iqbal K. and Grundke-Iqbal I. (1993) Microtubule-associated protein tau. abnormal phosphorylation of a non-paired helical filament pool in alzheimer disease. *J. Biol. Chem.,* **268**, 24374-24384.

Korecka J.A., van Kesteren R.E., Blaas E., Spitzer S.O., Kamstra J.H., Smit A.B., Swaab D.F., Verhaagen J. and Bossers K. (2013) Phenotypic characterization of retinoic acid differentiated SH-SY5Y cells by transcriptional profiling. *PLoS One,* **8**, e63862.

Kotermanski S.E. and Johnson J.W. (2009) Mg2+ imparts NMDA receptor subtype selectivity to the alzheimer's drug memantine. *J. Neurosci.,* **29**, 2774-2779.

Koutmani Y., Politis P.K., Elkouris M., Agrogiannis G., Kemerli M., Patsouris E., Remboutsika E. and Karalis K.P. (2013) Corticotropin-releasing hormone exerts direct effects on neuronal progenitor cells: Implications for neuroprotection. *Mol. Psychiatry,* **18**, 300-307.

Koutsilieri E., Kornhuber J., Degen H.J., Lesch K.P., Sopper S., ter Meulen V. and Riederer P. (1996) U-373 MG glioblastoma and IMR-32 neuroblastoma cell lines express the dopamine and vesicular monoamine transporters. *J. Neurosci. Res.,* **45**, 269-275.

Kroeze W.K., Sheffler D.J. and Roth B.L. (2003) G-protein-coupled receptors at a glance. *J. Cell. Sci.,* **116**, 4867-4869.

Krueger J.M. and Majde J.A. (1994) Microbial products and cytokines in sleep and fever regulation. *Crit. Rev. Immunol.,* **14**, 355-379.

Kukkonen J.P. (2013) Physiology of the orexinergic/hypocretinergic system: A revisit in 2012. *Am. J. Physiol. Cell. Physiol.,* **304**, C2-32.

Kukkonen J.P. (2004) Regulation of receptor-coupling to (multiple) G proteins. A challenge for basic research and drug discovery. *Receptors Channels,* **10**, 167-183.

Kukkonen J.P. and Leonard C.S. (2014) Orexin/hypocretin receptor signalling cascades. *Br. J. Pharmacol.,* **171**, 314-331.

Kuo Y.M., Emmerling M.R., Vigo-Pelfrey C., Kasunic T.C., Kirkpatrick J.B., Murdoch G.H., Ball M.J. and Roher A.E. (1996) Water-soluble abeta (N-40, N-42) oligomers in normal and alzheimer disease brains. *J. Biol. Chem.,* **271**, 4077-4081.

Kurata S., Wakabayashi T., Ito Y., Miwa N., Ueno R., Marunouchi T. and Kurata N. (1993) Human neuroblastoma cells produce the NF-kappa B-like HIV-1 transcription activator during differentiation. *FEBS Lett.,* **321**, 201-204.

Lace G., Savva G.M., Forster G., de Silva R., Brayne C., Matthews F.E., Barclay J.J., Dakin L., Ince P.G., Wharton S.B. *et al.* (2009) Hippocampal tau pathology is related to neuroanatomical connections: An ageing population-based study. *Brain,* **132**, 1324-1334.

LaFerla F.M. (2002) Calcium dyshomeostasis and intracellular signalling in alzheimer's disease. *Nat. Rev. Neurosci.,* **3**, 862-872.

Lai M.T., Chen E., Crouthamel M.C., DiMuzio-Mower J., Xu M., Huang Q., Price E., Register R.B., Shi X.P., Donoviel D.B. *et al.* (2003) Presenilin-1 and presenilin-2 exhibit distinct yet overlapping gamma-secretase activities. *J. Biol. Chem.,* **278**, 22475-22481.

Lamb B.T., Sisodia S.S., Lawler A.M., Slunt H.H., Kitt C.A., Kearns W.G., Pearson P.L., Price D.L. and Gearhart J.D. (1993) Introduction and expression of the 400 kilobase amyloid precursor protein gene in transgenic mice [corrected]. *Nat. Genet.,* **5**, 22-30.

Lambe E.K., Olausson P., Horst N.K., Taylor J.R. and Aghajanian G.K. (2005) Hypocretin and nicotine excite the same thalamocortical synapses in prefrontal cortex: Correlation with improved attention in rat. *J. Neurosci.,* **25**, 5225-5229.

Lambert H.W., Weiss E.R. and Lauder J.M. (2001) Activation of 5-HT receptors that stimulate the adenylyl cyclase pathway positively regulates IGF-I in cultured craniofacial mesenchymal cells. *Dev. Neurosci.,* **23**, 70-77.

Law A., Gauthier S. and Quirion R. (2001) Say NO to alzheimer's disease: The putative links between nitric oxide and dementia of the alzheimer's type. *Brain Res. Brain Res. Rev.,* **35**, 73-96.

Lawrence A.J., Cowen M.S., Yang H.J., Chen F. and Oldfield B. (2006) The orexin system regulates alcohol-seeking in rats. *Br. J. Pharmacol.,* **148**, 752-759.

Lebouvier T., Scales T.M., Hanger D.P., Geahlen R.L., Lardeux B., Reynolds C.H., Anderton B.H. and Derkinderen P. (2008) The microtubule-associated protein tau is phosphorylated by syk. *Biochim. Biophys. Acta,* **1783**, 188-192.

Lectez B., Jeandel L., El-Yamani F.Z., Arthaud S., Alexandre D., Mardargent A., Jegou S., Mounien L., Bizet P., Magoul R. *et al.* (2009) The orexigenic activity of the

hypothalamic neuropeptide 26RFa is mediated by the neuropeptide Y and proopiomelanocortin neurons of the arcuate nucleus. *Endocrinology,* **150**, 2342-2350.

Lee D.K., Nguyen T., Lynch K.R., Cheng R., Vanti W.B., Arkhitko O., Lewis T., Evans J.F., George S.R. and O'Dowd B.F. (2001) Discovery and mapping of ten novel G protein-coupled receptor genes. *Gene,* **275**, 83-91.

Lee G., Thangavel R., Sharma V.M., Litersky J.M., Bhaskar K., Fang S.M., Do L.H., Andreadis A., Van Hoesen G. and Ksiezak-Reding H. (2004) Phosphorylation of tau by fyn: Implications for alzheimer's disease. *J. Neurosci.,* **24**, 2304-2312.

Lee J.H., Bang E., Chae K.J., Kim J.Y., Lee D.W. and Lee W. (1999) Solution structure of a new hypothalamic neuropeptide, human hypocretin-2/orexin-B. *Eur. J. Biochem.,* **266**, 831-839.

Lee M.G., Hassani O.K. and Jones B.E. (2005) Discharge of identified orexin/hypocretin neurons across the sleep-waking cycle. *J. Neurosci.,* **25**, 6716-6720.

Lee S.T., Chu K., Park J.E., Jung K.H., Jeon D., Lim J.Y., Lee S.K., Kim M. and Roh J.K. (2012) Erythropoietin improves memory function with reducing endothelial dysfunction and amyloid-beta burden in alzheimer's disease models. *J. Neurochem.,* **120**, 115-124.

Lesne S., Ali C., Gabriel C., Croci N., MacKenzie E.T., Glabe C.G., Plotkine M., Marchand-Verrecchia C., Vivien D. and Buisson A. (2005) NMDA receptor activation inhibits alpha-secretase and promotes neuronal amyloid-beta production. *J. Neurosci.,* **25**, 9367-9377.

Lessard C.B., Wagner S.L. and Koo E.H. (2010) And four equals one: Presenilin takes the gamma-secretase role by itself. *Proc. Natl. Acad. Sci. U. S. A.,* **107**, 21236-21237.

Li N. and Karin M. (1999) Is NF-kappaB the sensor of oxidative stress? *FASEB J.,* **13**, 1137-1143.

Li X., Alafuzoff I., Soininen H., Winblad B. and Pei J.J. (2005) Levels of mTOR and its downstream targets 4E-BP1, eEF2, and eEF2 kinase in relationships with tau in alzheimer's disease brain. *FEBS J.,* **272**, 4211-4220.

Lim G.P., Yang F., Chu T., Chen P., Beech W., Teter B., Tran T., Ubeda O., Ashe K.H., Frautschy S.A. *et al.* (2000) Ibuprofen suppresses plaque pathology and inflammation in a mouse model for alzheimer's disease. *J. Neurosci.,* **20**, 5709-5714.

Lin L., Faraco J., Li R., Kadotani H., Rogers W., Lin X., Qiu X., de Jong P.J., Nishino S. and Mignot E. (1999) The sleep disorder canine narcolepsy is caused by a mutation in the hypocretin (orexin) receptor 2 gene. *Cell,* **98**, 365-376.

Ling Y., Morgan K. and Kalsheker N. (2003) Amyloid precursor protein (APP) and the biology of proteolytic processing: Relevance to alzheimer's disease. *Int. J. Biochem. Cell Biol.*, **35**, 1505-1535.

Liu F., Grundke-Iqbal I., Iqbal K. and Gong C.X. (2005) Contributions of protein phosphatases PP1, PP2A, PP2B and PP5 to the regulation of tau phosphorylation. *Eur. J. Neurosci.*, **22**, 1942-1950.

Liu J., Head E., Gharib A.M., Yuan W., Ingersoll R.T., Hagen T.M., Cotman C.W. and Ames B.N. (2002) Memory loss in old rats is associated with brain mitochondrial decay and RNA/DNA oxidation: Partial reversal by feeding acetyl-L-carnitine and/or R-alpha -lipoic acid. *Proc. Natl. Acad. Sci. U. S. A.*, **99**, 2356-2361.

Liu J., Supnet C., Sun S., Zhang H., Good L., Popugaeva E. and Bezprozvanny I. (2014) The role of ryanodine receptor type 3 in a mouse model of alzheimer disease. *Channels (Austin)*, **8**.

Liu R., Zhang T.T., Zhou D., Bai X.Y., Zhou W.L., Huang C., Song J.K., Meng F.R., Wu C.X., Li L. *et al.* (2013) Quercetin protects against the abeta(25-35)-induced amnesic injury: Involvement of inactivation of rage-mediated pathway and conservation of the NVU. *Neuropharmacology*, **67**, 419-431.

Liu R.J., van den Pol A.N. and Aghajanian G.K. (2002) Hypocretins (orexins) regulate serotonin neurons in the dorsal raphe nucleus by excitatory direct and inhibitory indirect actions. *J. Neurosci.*, **22**, 9453-9464.

Liu Y., Wang P.S., Xie D., Liu K. and Chen L. (2006) Ghrelin reduces injury of hippocampal neurons in a rat model of cerebral ischemia/reperfusion. *Chin. J. Physiol.*, **49**, 244-250.

Loilome W., Wechagama P., Namwat N., Jusakul A., Sripa B., Miwa M., Kuver R. and Yongvanit P. (2012) Expression of oxysterol binding protein isoforms in opisthorchiasis-associated cholangiocarcinoma: A potential molecular marker for tumor metastasis. *Parasitol. Int.*, **61**, 136-139.

Lopez M., Seoane L., Garcia M.C., Lago F., Casanueva F.F., Senaris R. and Dieguez C. (2000) Leptin regulation of prepro-orexin and orexin receptor mRNA levels in the hypothalamus. *Biochem. Biophys. Res. Commun.*, **269**, 41-45.

Louhivuori L.M., Bart G., Larsson K.P., Louhivuori V., Nasman J., Nordstrom T., Koivisto A.P. and Akerman K.E. (2009) Differentiation dependent expression of TRPA1 and TRPM8 channels in IMR-32 human neuroblastoma cells. *J. Cell. Physiol.*, **221**, 67-74.

Lu X.Y., Bagnol D., Burke S., Akil H. and Watson S.J. (2000) Differential distribution and regulation of OX1 and OX2 orexin/hypocretin receptor messenger RNA in the brain upon fasting. *Horm. Behav.*, **37**, 335-344.

Lund H., Gustafsson E., Svensson A., Nilsson M., Berg M., Sunnemark D. and von Euler G. (2014) MARK4 and MARK3 associate with early tau phosphorylation in alzheimer's disease granulovacuolar degeneration bodies. *Acta Neuropathol. Commun.*, **2**, 22-5960-2-22.

Lund P.E., Shariatmadari R., Uustare A., Detheux M., Parmentier M., Kukkonen J.P. and Akerman K.E. (2000) The orexin OX1 receptor activates a novel Ca2+ influx pathway necessary for coupling to phospholipase C. *J. Biol. Chem.*, **275**, 30806-30812.

Lundstrom K. (2009) An overview on GPCRs and drug discovery: Structure-based drug design and structural biology on GPCRs. *Methods Mol. Biol.*, **552**, 51-66.

Luo J. and Grammas P. (2010) Endothelin-1 is elevated in alzheimer's disease brain microvessels and is neuroprotective. *J. Alzheimers Dis.*, **21**, 887-896.

Luo W.J., Wang H., Li H., Kim B.S., Shah S., Lee H.J., Thinakaran G., Kim T.W., Yu G. and Xu H. (2003) PEN-2 and APH-1 coordinately regulate proteolytic processing of presenilin 1. *J. Biol. Chem.*, **278**, 7850-7854.

Lustbader J.W., Cirilli M., Lin C., Xu H.W., Takuma K., Wang N., Caspersen C., Chen X., Pollak S., Chaney M. *et al.* (2004) ABAD directly links abeta to mitochondrial toxicity in alzheimer's disease. *Science*, **304**, 448-452.

Lutter M., Krishnan V., Russo S.J., Jung S., McClung C.A. and Nestler E.J. (2008) Orexin signaling mediates the antidepressant-like effect of calorie restriction. *J. Neurosci.*, **28**, 3071-3075.

Ma H., Lesne S., Kotilinek L., Steidl-Nichols J.V., Sherman M., Younkin L., Younkin S., Forster C., Sergeant N., Delacourte A. *et al.* (2007) Involvement of beta-site APP cleaving enzyme 1 (BACE1) in amyloid precursor protein-mediated enhancement of memory and activity-dependent synaptic plasticity. *Proc. Natl. Acad. Sci. U. S. A.*, **104**, 8167-8172.

Ma R., Huang C., Hu J., Wang M., Xiang J. and Li G. (2014) JAK2/STAT5/Bcl-xL signaling is essential for erythropoietin-mediated protection against PC12 cells apoptosis induced by abeta. *Br. J. Pharmacol.*, .

Maalouf M., Rho J.M. and Mattson M.P. (2009) The neuroprotective properties of calorie restriction, the ketogenic diet, and ketone bodies. *Brain Res. Rev.*, **59**, 293-315.

Magga J., Bart G., Oker-Blom C., Kukkonen J.P., Akerman K.E. and Nasman J. (2006) Agonist potency differentiates G protein activation and Ca2+ signalling by the orexin receptor type 1. *Biochem. Pharmacol.*, **71**, 827-836.

Maher P., Dargusch R., Bodai L., Gerard P.E., Purcell J.M. and Marsh J.L. (2011) ERK activation by the polyphenols fisetin and resveratrol provides neuroprotection in multiple models of huntington's disease. *Hum. Mol. Genet.*, **20**, 261-270.

Mahlios J., De la Herran-Arita A.K. and Mignot E. (2013) The autoimmune basis of narcolepsy. *Curr. Opin. Neurobiol.,* **23**, 767-773.

Mahller Y.Y., Williams J.P., Baird W.H., Mitton B., Grossheim J., Saeki Y., Cancelas J.A., Ratner N. and Cripe T.P. (2009) Neuroblastoma cell lines contain pluripotent tumor initiating cells that are susceptible to a targeted oncolytic virus. *PLoS One,* **4**, e4235.

Mallmann R.T., Elgueta C., Sleman F., Castonguay J., Wilmes T., van den Maagdenberg A. and Klugbauer N. (2013) Ablation of ca(V)2.1 voltage-gated ca(2)(+) channels in mouse forebrain generates multiple cognitive impairments. *PLoS One,* **8**, e78598.

Manczak M., Mao P., Calkins M.J., Cornea A., Reddy A.P., Murphy M.P., Szeto H.H., Park B. and Reddy P.H. (2010) Mitochondria-targeted antioxidants protect against amyloid-beta toxicity in alzheimer's disease neurons. *J. Alzheimers Dis.,* **20 Suppl 2**, S609-31.

Marchal J., Dal-Pan A., Epelbaum J., Blanc S., Mueller S., Wittig Kieffer M., Metzger F., Aujard F. and RESTRIKAL Consortium (2013) Calorie restriction and resveratrol supplementation prevent age-related DNA and RNA oxidative damage in a non-human primate. *Exp. Gerontol.,* **48**, 992-1000.

Mattson M.P., Goodman Y., Luo H., Fu W. and Furukawa K. (1997) Activation of NF-kappaB protects hippocampal neurons against oxidative stress-induced apoptosis: Evidence for induction of manganese superoxide dismutase and suppression of peroxynitrite production and protein tyrosine nitration. *J. Neurosci. Res.,* **49**, 681-697.

Mazzocchi G., Malendowicz L.K., Gottardo L., Aragona F. and Nussdorfer G.G. (2001) Orexin A stimulates cortisol secretion from human adrenocortical cells through activation of the adenylate cyclase-dependent signaling cascade. *J. Clin. Endocrinol. Metab.,* **86**, 778-782.

McCormick M.B., Tamimi R.M., Snider L., Asakura A., Bergstrom D. and Tapscott S.J. (1996) NeuroD2 and neuroD3: Distinct expression patterns and transcriptional activation potentials within the neuroD gene family. *Mol. Cell. Biol.,* **16**, 5792-5800.

McCurry S.M., Logsdon R.G., Teri L., Gibbons L.E., Kukull W.A., Bowen J.D., McCormick W.C. and Larson E.B. (1999) Characteristics of sleep disturbance in community-dwelling alzheimer's disease patients. *J. Geriatr. Psychiatry Neurol.,* **12**, 53-59.

McLoughlin D.M., Standen C.L., Lau K.F., Ackerley S., Bartnikas T.P., Gitlin J.D. and Miller C.C. (2001) The neuronal adaptor protein X11alpha interacts with the copper chaperone for SOD1 and regulates SOD1 activity. *J. Biol. Chem.,* **276**, 9303-9307.

Medeiros R., Baglietto-Vargas D. and Laferla F.M. (2010) The role of tau in alzheimer's disease and related disorders. *CNS Neurosci. Ther.*, .

Meyer M.R., Tschanz J.T., Norton M.C., Welsh-Bohmer K.A., Steffens D.C., Wyse B.W. and Breitner J.C. (1998) APOE genotype predicts when--not whether--one is predisposed to develop alzheimer disease. *Nat. Genet.*, **19**, 321-322.

Milligan G., Ramsay D., Pascal G. and Carrillo J.J. (2003) GPCR dimerisation. *Life Sci.*, **74**, 181-188.

Mocsai A., Ruland J. and Tybulewicz V.L. (2010) The SYK tyrosine kinase: A crucial player in diverse biological functions. *Nat. Rev. Immunol.*, **10**, 387-402.

Moe K.E., Vitiello M.V., Larsen L.H. and Prinz P.N. (1995) Symposium: Cognitive processes and sleep disturbances: Sleep/wake patterns in alzheimer's disease: Relationships with cognition and function. *J. Sleep Res.*, **4**, 15-20.

Mohandas E., Rajmohan V. and Raghunath B. (2009) Neurobiology of alzheimer's disease. *Indian. J. Psychiatry.*, **51**, 55-61.

Mohs R.C., Doody R.S., Morris J.C., Ieni J.R., Rogers S.L., Perdomo C.A., Pratt R.D. and "312" Study Group (2001) A 1-year, placebo-controlled preservation of function survival study of donepezil in AD patients. *Neurology*, **57**, 481-488.

Moldofsky H., Lue F.A., Eisen J., Keystone E. and Gorczynski R.M. (1986) The relationship of interleukin-1 and immune functions to sleep in humans. *Psychosom. Med.*, **48**, 309-318.

Mondal M.S., Nakazato M., Date Y., Murakami N., Yanagisawa M. and Matsukura S. (1999) Widespread distribution of orexin in rat brain and its regulation upon fasting. *Biochem. Biophys. Res. Commun.*, **256**, 495-499.

Moon M., Choi J.G., Nam D.W., Hong H.S., Choi Y.J., Oh M.S. and Mook-Jung I. (2011) Ghrelin ameliorates cognitive dysfunction and neurodegeneration in intrahippocampal amyloid-beta1-42 oligomer-injected mice. *J. Alzheimers Dis.*, **23**, 147-159.

Moreira I.S. (2014) Structural features of the G-protein/GPCR interactions. *Biochim. Biophys. Acta*, **1840**, 16-33.

Moriya R., Sano H., Umeda T., Ito M., Takahashi Y., Matsuda M., Ishihara A., Kanatani A. and Iwaasa H. (2006) RFamide peptide QRFP43 causes obesity with hyperphagia and reduced thermogenesis in mice. *Endocrinology*, **147**, 2916-2922.

Mrak R.E. and Griffin W.S. (2001) Interleukin-1, neuroinflammation, and alzheimer's disease. *Neurobiol. Aging*, **22**, 903-908.

Mudher A. and Lovestone S. (2002) Alzheimer's disease-do tauists and baptists finally shake hands? *Trends Neurosci.,* **25**, 22-26.

Munoz-Montano J.R., Moreno F.J., Avila J. and Diaz-Nido J. (1999) Downregulation of glycogen synthase kinase-3beta (GSK-3beta) protein expression during neuroblastoma IMR-32 cell differentiation. *J. Neurosci. Res.,* **55**, 278-285.

Muroya S., Funahashi H., Yamanaka A., Kohno D., Uramura K., Nambu T., Shibahara M., Kuramochi M., Takigawa M., Yanagisawa M. *et al.* (2004) Orexins (hypocretins) directly interact with neuropeptide Y, POMC and glucose-responsive neurons to regulate ca 2+ signaling in a reciprocal manner to leptin: Orexigenic neuronal pathways in the mediobasal hypothalamus. *Eur. J. Neurosci.,* **19**, 1524-1534.

Murphy M.P. (2009) How mitochondria produce reactive oxygen species. *Biochem. J.,* **417**, 1-13.

Nagy Z., Esiri M.M., Jobst K.A., Morris J.H., King E.M., McDonald B., Litchfield S., Smith A., Barnetson L. and Smith A.D. (1995) Relative roles of plaques and tangles in the dementia of alzheimer's disease: Correlations using three sets of neuropathological criteria. *Dementia,* **6**, 21-31.

Nalivaeva N.N., Belyaev N.D., Zhuravin I.A. and Turner A.J. (2012) The alzheimer's amyloid-degrading peptidase, neprilysin: Can we control it? *Int. J. Alzheimers Dis.,* **2012**, 383796.

Nalivaeva N.N. and Turner A.J. (2013) The amyloid precursor protein: A biochemical enigma in brain development, function and disease. *FEBS Lett.,* **587**, 2046-2054.

Nanmoku T., Isobe K., Sakurai T., Yamanaka A., Takekoshi K., Kawakami Y., Ishii K., Goto K. and Nakai T. (2000) Orexins suppress catecholamine synthesis and secretion in cultured PC12 cells. *Biochem. Biophys. Res. Commun.,* **274**, 310-315.

Naslund J., Haroutunian V., Mohs R., Davis K.L., Davies P., Greengard P. and Buxbaum J.D. (2000) Correlation between elevated levels of amyloid beta-peptide in the brain and cognitive decline. *JAMA,* **283**, 1571-1577.

Nasman J., Bart G., Larsson K., Louhivuori L., Peltonen H. and Akerman K.E. (2006) The orexin OX1 receptor regulates Ca2+ entry via diacylglycerol-activated channels in differentiated neuroblastoma cells. *J. Neurosci.,* **26**, 10658-10666.

Navarro V.M., Fernandez-Fernandez R., Nogueiras R., Vigo E., Tovar S., Chartrel N., Le Marec O., Leprince J., Aguilar E., Pinilla L. *et al.* (2006) Novel role of 26RFa, a hypothalamic RFamide orexigenic peptide, as putative regulator of the gonadotropic axis. *J. Physiol.,* **573**, 237-249.

Neves S.R., Ram P.T. and Iyengar R. (2002) G protein pathways. *Science,* **296**, 1636-1639.

Nicolas C.S., Peineau S., Amici M., Csaba Z., Fafouri A., Javalet C., Collett V.J., Hildebrandt L., Seaton G., Choi S.L. *et al.* (2012) The Jak/STAT pathway is involved in synaptic plasticity. *Neuron*, **73**, 374-390.

Nishino S., Ripley B., Overeem S., Lammers G.J. and Mignot E. (2000) Hypocretin (orexin) deficiency in human narcolepsy. *Lancet*, **355**, 39-40.

Nunomura A., Perry G., Pappolla M.A., Wade R., Hirai K., Chiba S. and Smith M.A. (1999) RNA oxidation is a prominent feature of vulnerable neurons in alzheimer's disease. *J. Neurosci.*, **19**, 1959-1964.

Obukuro K., Nobunaga M., Takigawa M., Morioka H., Hisatsune A., Isohama Y., Shimokawa H., Tsutsui M. and Katsuki H. (2013) Nitric oxide mediates selective degeneration of hypothalamic orexin neurons through dysfunction of protein disulfide isomerase. *J. Neurosci.*, **33**, 12557-12568.

Oules B., Del Prete D., Greco B., Zhang X., Lauritzen I., Sevalle J., Moreno S., Paterlini-Brechot P., Trebak M., Checler F. *et al.* (2012) Ryanodine receptor blockade reduces amyloid-beta load and memory impairments in Tg2576 mouse model of alzheimer disease. *J. Neurosci.*, **32**, 11820-11834.

Ozcan M., Ayar A., Serhatlioglu I., Alcin E., Sahin Z. and Kelestimur H. (2010) Orexins activates protein kinase C-mediated ca(2+) signaling in isolated rat primary sensory neurons. *Physiol. Res.*, **59**, 255-262.

Palmer J. and Love S. (2011) Endothelin receptor antagonists: Potential in alzheimer's disease. *Pharmacol. Res.*, **63**, 525-531.

Pardossi-Piquard R., Dunys J., Yu G., St George-Hyslop P., Alves da Costa C. and Checler F. (2006) Neprilysin activity and expression are controlled by nicastrin. *J. Neurochem.*, **97**, 1052-1056.

Parent M.B. and Baxter M.G. (2004) Septohippocampal acetylcholine: Involved in but not necessary for learning and memory? *Learn. Mem.*, **11**, 9-20.

Park K.M., Yule D.I. and Bowers W.J. (2010) Impaired TNF-alpha control of IP3R-mediated Ca2+ release in alzheimer's disease mouse neurons. *Cell. Signal.*, **22**, 519-526.

Parks A.L. and Curtis D. (2007) Presenilin diversifies its portfolio. *Trends Genet.*, **23**, 140-150.

Patel S.R., Murphy K.G., Thompson E.L., Patterson M., Curtis A.E., Ghatei M.A. and Bloom S.R. (2008) Pyroglutamylated RFamide peptide 43 stimulates the hypothalamic-pituitary-gonadal axis via gonadotropin-releasing hormone in rats. *Endocrinology*, **149**, 4747-4754.

Pearson H.A. and Peers C. (2006) Physiological roles for amyloid beta peptides. *J. Physiol.,* **575**, 5-10.

Pedersen W.A., McCullers D., Culmsee C., Haughey N.J., Herman J.P. and Mattson M.P. (2001) Corticotropin-releasing hormone protects neurons against insults relevant to the pathogenesis of alzheimer's disease. *Neurobiol. Dis.,* **8**, 492-503.

Perez E., Liu R., Yang S.H., Cai Z.Y., Covey D.F. and Simpkins J.W. (2005) Neuroprotective effects of an estratriene analog are estrogen receptor independent in vitro and in vivo. *Brain Res.,* **1038**, 216-222.

Perry E.K., Gibson P.H., Blessed G., Perry R.H. and Tomlinson B.E. (1977) Neurotransmitter enzyme abnormalities in senile dementia. choline acetyltransferase and glutamic acid decarboxylase activities in necropsy brain tissue. *J. Neurol. Sci.,* **34**, 247-265. .

Peyron C., Tighe D.K., van den Pol A.N., de Lecea L., Heller H.C., Sutcliffe J.G. and Kilduff T.S. (1998) Neurons containing hypocretin (orexin) project to multiple neuronal systems. *J. Neurosci.,* **18**, 9996-10015.

Pierce K.L., Premont R.T. and Lefkowitz R.J. (2002) Seven-transmembrane receptors. *Nat. Rev. Mol. Cell Biol.,* **3**, 639-650.

Plant L.D., Boyle J.P., Smith I.F., Peers C. and Pearson H.A. (2003) The production of amyloid beta peptide is a critical requirement for the viability of central neurons. *J. Neurosci.,* **23**, 5531-5535.

Pollak C.P. and Perlick D. (1991) Sleep problems and institutionalization of the elderly. *J. Geriatr. Psychiatry Neurol.,* **4**, 204-210.

Porkka-Heiskanen T., Alanko L., Kalinchuk A., Heiskanen S. and Stenberg D. (2004) The effect of age on prepro-orexin gene expression and contents of orexin A and B in the rat brain. *Neurobiol. Aging,* **25**, 231-238.

Porkka-Heiskanen T., Zitting K.M. and Wigren H.K. (2013) Sleep, its regulation and possible mechanisms of sleep disturbances. *Acta Physiol. (Oxf),* **208**, 311-328.

Putula J. and Kukkonen J.P. (2012) Mapping of the binding sites for the OX1 orexin receptor antagonist, SB-334867, using orexin/hypocretin receptor chimaeras. *Neurosci. Lett.,* **506**, 111-115.

Qin W., Yang T., Ho L., Zhao Z., Wang J., Chen L., Zhao W., Thiyagarajan M., MacGrogan D., Rodgers J.T. *et al.* (2006) Neuronal SIRT1 activation as a novel mechanism underlying the prevention of alzheimer disease amyloid neuropathology by calorie restriction. *J. Biol. Chem.,* **281**, 21745-21754.

Qosa H., Abuznait A.H., Hill R.A. and Kaddoumi A. (2012) Enhanced brain amyloid-beta clearance by rifampicin and caffeine as a possible protective mechanism against alzheimer's disease. *J. Alzheimers Dis.*, **31**, 151-165.

Rabie T. and Marti H.H. (2008) Brain protection by erythropoietin: A manifold task. *Physiology (Bethesda)*, **23**, 263-274.

Ramanjaneya M., Conner A.C., Chen J., Kumar P., Brown J.E., Johren O., Lehnert H., Stanfield P.R. and Randeva H.S. (2009) Orexin-stimulated MAP kinase cascades are activated through multiple G-protein signalling pathways in human H295R adrenocortical cells: Diverse roles for orexins A and B. *J. Endocrinol.*, **202**, 249-261.

Ramanjaneya M., Karteris E., Chen J., Rucinski M., Ziolkowska A., Ahmed N., Kagerer S., Johren O., Lehnert H., Malendowicz L.K. *et al.* (2013) QRFP induces aldosterone production via PKC and T-type calcium channel-mediated pathways in human adrenocortical cells: Evidence for a novel role of GPR103. *Am. J. Physiol. Endocrinol. Metab.*, **305**, E1049-58.

Ramirez-Bermudez J. (2012) Alzheimer's disease: Critical notes on the history of a medical concept. *Arch. Med. Res.*, **43**, 595-599.

Randeva H.S., Karteris E., Grammatopoulos D. and Hillhouse E.W. (2001) Expression of orexin-A and functional orexin type 2 receptors in the human adult adrenals: Implications for adrenal function and energy homeostasis. *J. Clin. Endocrinol. Metab.*, **86**, 4808-4813.

Reddy P.H. and Beal M.F. (2008) Amyloid beta, mitochondrial dysfunction and synaptic damage: Implications for cognitive decline in aging and Alzheimer's disease. *Trends Mol. Med.*, **14**, 45-53.

Reilly J.F., Games D., Rydel R.E., Freedman S., Schenk D., Young W.G., Morrison J.H. and Bloom F.E. (2003) Amyloid deposition in the hippocampus and entorhinal cortex: Quantitative analysis of a transgenic mouse model. *Proc. Natl. Acad. Sci. U. S. A.*, **100**, 4837-4842.

Roux P.P. and Blenis J. (2004) ERK and p38 MAPK-activated protein kinases: A family of protein kinases with diverse biological functions. *Microbiol. Mol. Biol. Rev.*, **68**, 320-344.

Russell S.H., Kim M.S., Small C.J., Abbott C.R., Morgan D.G., Taheri S., Murphy K.G., Todd J.F., Ghatei M.A. and Bloom S.R. (2000) Central administration of orexin A suppresses basal and domperidone stimulated plasma prolactin. *J. Neuroendocrinol.*, **12**, 1213-1218.

Rylett R.J., Ball M.J. and Colhoun E.H. (1983) Evidence for high affinity choline transport in synaptosomes prepared from hippocampus and neocortex of patients with alzheimer's disease. *Brain Res.*, **289**, 169-175.

Saab B.J., Georgiou J., Nath A., Lee F.J., Wang M., Michalon A., Liu F., Mansuy I.M. and Roder J.C. (2009) NCS-1 in the dentate gyrus promotes exploration, synaptic plasticity, and rapid acquisition of spatial memory. *Neuron,* **63**, 643-656.

Sagare A.P., Bell R.D., Zhao Z., Ma Q., Winkler E.A., Ramanathan A. and Zlokovic B.V. (2013) Pericyte loss influences Alzheimer-like neurodegeneration in mice. *Nat. Commun.*, **4**, 2932.

Sakamoto K., Karelina K. and Obrietan K. (2011) CREB: A multifaceted regulator of neuronal plasticity and protection. *J. Neurochem.,* **116**, 1-9.

Sakurai T. (2007) The neural circuit of orexin (hypocretin): Maintaining sleep and wakefulness. *Nat. Rev. Neurosci.,* **8**, 171-181.

Sakurai T. (2006) Roles of orexins and orexin receptors in central regulation of feeding behavior and energy homeostasis. *CNS Neurol. Disord. Drug Targets,* **5**, 313-325.

Sakurai T., Amemiya A., Ishii M., Matsuzaki I., Chemelli R.M., Tanaka H., Williams S.C., Richarson J.A., Kozlowski G.P., Wilson S. *et al.* (1998) Orexins and orexin receptors: A family of hypothalamic neuropeptides and G protein-coupled receptors that regulate feeding behavior. *Cell,* **92**, 1 page following 696.

Sakurai T., Moriguchi T., Furuya K., Kajiwara N., Nakamura T., Yanagisawa M. and Goto K. (1999) Structure and function of human prepro-orexin gene. *J. Biol. Chem.,* **274**, 17771-17776.

Satoh A., Brace C.S., Ben-Josef G., West T., Wozniak D.F., Holtzman D.M., Herzog E.D. and Imai S. (2010) SIRT1 promotes the central adaptive response to diet restriction through activation of the dorsomedial and lateral nuclei of the hypothalamus. *J. Neurosci.,* **30**, 10220-10232.

Saura C.A., Choi S.Y., Beglopoulos V., Malkani S., Zhang D., Shankaranarayana Rao B.S., Chattarji S., Kelleher R.J.,3rd, Kandel E.R., Duff K. *et al.* (2004) Loss of presenilin function causes impairments of memory and synaptic plasticity followed by age-dependent neurodegeneration. *Neuron,* **42**, 23-36.

Sawai N., Ueta Y., Nakazato M. and Ozawa H. (2010) Developmental and aging change of orexin-A and -B immunoreactive neurons in the male rat hypothalamus. *Neurosci. Lett.,* **468**, 51-55.

Scahill R.I., Frost C., Jenkins R., Whitwell J.L., Rossor M.N. and Fox N.C. (2003) A longitudinal study of brain volume changes in normal aging using serial registered magnetic resonance imaging. *Arch. Neurol.,* **60**, 989-994.

Scales T.M., Derkinderen P., Leung K.Y., Byers H.L., Ward M.A., Price C., Bird I.N., Perera T., Kellie S., Williamson R. *et al.* (2011) Tyrosine phosphorylation of tau by the SRC family kinases lck and fyn. *Mol. Neurodegener,* **6**, 12-1326-6-12.

Scammell T.E. and Winrow C.J. (2011) Orexin receptors: Pharmacology and therapeutic opportunities. *Annu. Rev. Pharmacol. Toxicol.,* **51**, 243-266.

Scammell T.E., Matheson J.K., Honda M., Thannickal T.C. and Siegel J.M. (2012) Coexistence of narcolepsy and alzheimer's disease. *Neurobiol. Aging,* **33**, 1318-1319.

Scheibe R.J., Ginty D.D. and Wagner J.A. (1991) Retinoic acid stimulates the differentiation of PC12 cells that are deficient in cAMP-dependent protein kinase. *J. Cell Biol.,* **113**, 1173-1182.

Schmidt F.M., Kratzsch J., Gertz H.J., Tittmann M., Jahn I., Pietsch U.C., Kaisers U.X., Thiery J., Hegerl U. and Schonknecht P. (2013) Cerebrospinal fluid melanin-concentrating hormone (MCH) and hypocretin-1 (HCRT-1, orexin-A) in alzheimer's disease. *PLoS One,* **8**, e63136.

Schuff N., Woerner N., Boreta L., Kornfield T., Shaw L.M., Trojanowski J.Q., Thompson P.M., Jack C.R.,Jr, Weiner M.W. and Alzheimer's Disease Neuroimaging Initiative (2009) MRI of hippocampal volume loss in early alzheimer's disease in relation to ApoE genotype and biomarkers. *Brain,* **132**, 1067-1077.

Sellayah D., Bharaj P. and Sikder D. (2011) Orexin is required for brown adipose tissue development, differentiation, and function. *Cell. Metab.,* **14**, 478-490.

Senechal Y., Larmet Y. and Dev K.K. (2006) Unraveling in vivo functions of amyloid precursor protein: Insights from knockout and knockdown studies. *Neurodegener Dis.,* **3**, 134-147.

Shaftel S.S., Griffin W.S. and O'Banion M.K. (2008) The role of interleukin-1 in neuroinflammation and alzheimer disease: An evolving perspective. *J. Neuroinflammation,* **5**, 7-2094-5-7.

Shah S., Lee S.F., Tabuchi K., Hao Y.H., Yu C., LaPlant Q., Ball H., Dann C.E.,3rd, Sudhof T. and Yu G. (2005) Nicastrin functions as a gamma-secretase-substrate receptor. *Cell,* **122**, 435-447.

Shan X. and Lin C.L. (2006) Quantification of oxidized RNAs in alzheimer's disease. *Neurobiol. Aging,* **27**, 657-662.

Sharf R., Sarhan M. and Dileone R.J. (2010) Role of orexin/hypocretin in dependence and addiction. *Brain Res.,* **1314**, 130-138.

Sharova L.V., Sharov A.A., Nedorezov T., Piao Y., Shaik N. and Ko M.S. (2009) Database for mRNA half-life of 19 977 genes obtained by DNA microarray analysis of Shaw S., Bencherif M. and Marrero M.B. (2003) Angiotensin II blocks nicotine-mediated neuroprotection against beta-amyloid (1-42) via activation of the tyrosine phosphatase SHP-1. *J. Neurosci.,* **23**, 11224-11228.

Sheng L., Zhou Y., Chen Z., Ren D., Cho K.W., Jiang L., Shen H., Sasaki Y. and Rui L. (2012) NF-kappaB-inducing kinase (NIK) promotes hyperglycemia and glucose intolerance in obesity by augmenting glucagon action. *Nat. Med.,* **18**, 943-949.

Shi W., Wang H., Pan G., Geng Y., Guo Y. and Pei D. (2006) Regulation of the pluripotency marker rex-1 by nanog and Sox2. *J. Biol. Chem.,* **281**, 23319-23325.

Shibata M., Yamada S., Kumar S.R., Calero M., Bading J., Frangione B., Holtzman D.M., Miller C.A., Strickland D.K., Ghiso J. *et al.* (2000) Clearance of alzheimer's amyloid-ss(1-40) peptide from brain by LDL receptor-related protein-1 at the blood-brain barrier. *J. Clin. Invest.,* **106**, 1489-1499.

Shirasaka T., Nakazato M., Matsukura S., Takasaki M. and Kannan H. (1999) Sympathetic and cardiovascular actions of orexins in conscious rats. *Am. J. Physiol.,* **277**, R1780-5.

Shu Q., Hu Z.L., Huang C., Yu X.W., Fan H., Yang J.W., Fang P., Ni L., Chen J.G. and Wang F. (2014) Orexin-A promotes cell migration in cultured rat astrocytes via Ca2+-dependent PKCalpha and ERK1/2 signals. *PLoS One,* **9**, e95259.

Siehler S. (2009) Regulation of RhoGEF proteins by G12/13-coupled receptors. *Br. J. Pharmacol.,* **158**, 41-49.

Sikder D. and Kodadek T. (2007) The neurohormone orexin stimulates hypoxia-inducible factor-1 activity. *Genes Dev.,* **21**, 2995-3005.

Silva J., Beckedorf A. and Bieberich E. (2003) Osteoblast-derived oxysterol is a migration-inducing factor for human breast cancer cells. *J. Biol. Chem.,* **278**, 25376-25385.

Silverberg G.D., Mayo M., Saul T., Rubenstein E. and McGuire D. (2003) Alzheimer's disease, normal-pressure hydrocephalus, and senescent changes in CSF circulatory physiology: A hypothesis. *Lancet Neurol.,* **2**, 506-511.

Singer C.A., Figueroa-Masot X.A., Batchelor R.H. and Dorsa D.M. (1999) The mitogen-activated protein kinase pathway mediates estrogen neuroprotection after glutamate toxicity in primary cortical neurons. *J. Neurosci.,* **19**, 2455-2463.

Sisodia S. (2007) *Alzheimer's Disease: Advances in Genetics, Molecular and Cellular Biology.* Springer Science, New York, USA.

Sisodia S.S. (1999) Alzheimer's disease: Perspectives for the new millennium. *J. Clin. Invest.,* **104**, 1169-1170.

Smart D., Jerman J.C., Brough S.J., Rushton S.L., Murdock P.R., Jewitt F., Elshourbagy N.A., Ellis C.E., Middlemiss D.N. and Brown F. (1999) Characterization of

recombinant human orexin receptor pharmacology in a chinese hamster ovary cell-line using FLIPR. *Br. J. Pharmacol.,* **128**, 1-3.

Smith M.A., Zhu X., Tabaton M., Liu G., McKeel D.W.,Jr, Cohen M.L., Wang X., Siedlak S.L., Dwyer B.E., Hayashi T. *et al.* (2010) Increased iron and free radical generation in preclinical alzheimer disease and mild cognitive impairment. *J. Alzheimers Dis.,* **19**, 363-372.

Smith P.M., Connolly B.C. and Ferguson A.V. (2002) Microinjection of orexin into the rat nucleus tractus solitarius causes increases in blood pressure. *Brain Res.,* **950**, 261-267.

Smrcka A.V. (2008) G protein betagamma subunits: Central mediators of G protein-coupled receptor signaling. *Cell Mol. Life Sci.,* **65**, 2191-2214.

Sokolowska P., Urbanska A., Bieganska K., Wagner W., Ciszewski W., Namiecinska M. and Zawilska J.B. (2014) Orexins protect neuronal cell cultures against hypoxic stress: An involvement of akt signaling. *J. Mol. Neurosci.,* **52**, 48-55.

Sommer B. (2002) Alzheimer's disease and the amyloid cascade hypothesis: Ten years on. *Curr. Opin. Pharmacol.,* **2**, 87-92.

Song M., Xiong J.X., Wang Y.Y., Tang J., Zhang B. and Bai Y. (2012) VIP enhances phagocytosis of fibrillar beta-amyloid by microglia and attenuates amyloid deposition in the brain of APP/PS1 mice. *PLoS One,* **7**, e29790.

Sonnen J.A., Breitner J.C., Lovell M.A., Markesbery W.R., Quinn J.F. and Montine T.J. (2008) Free radical-mediated damage to brain in alzheimer's disease and its transgenic mouse models. *Free Radic. Biol. Med.,* **45**, 219-230.

Soucek T., Cumming R., Dargusch R., Maher P. and Schubert D. (2003) The regulation of glucose metabolism by HIF-1 mediates a neuroprotective response to amyloid beta peptide. *Neuron,* **39**, 43-56.

Spilman P., Podlutskaya N., Hart M.J., Debnath J., Gorostiza O., Bredesen D., Richardson A., Strong R. and Galvan V. (2010) Inhibition of mTOR by rapamycin abolishes cognitive deficits and reduces amyloid-beta levels in a mouse model of Alzheimer's disease. *PLoS One,* **5**, e9979.

Spinazzi R., Andreis P.G., Rossi G.P. and Nussdorfer G.G. (2006) Orexins in the regulation of the hypothalamic-pituitary-adrenal axis. *Pharmacol. Rev.,* **58**, 46-57.

Squire L.R. (2009) The legacy of patient H.M. for neuroscience. *Neuron,* **61**, 6-9.

Stanciu M., Wang Y., Kentor R., Burke N., Watkins S., Kress G., Reynolds I., Klann E., Angiolieri M.R., Johnson J.W. *et al.* (2000) Persistent activation of ERK contributes to

glutamate-induced oxidative toxicity in a neuronal cell line and primary cortical neuron cultures. *J. Biol. Chem.,* **275**, 12200-12206.

Stanley E.M. and Fadel J. (2012) Aging-related deficits in orexin/hypocretin modulation of the septohippocampal cholinergic system. *Synapse*, **66**, 445-452.

Steinerman J.R., Irizarry M., Scarmeas N., Raju S., Brandt J., Albert M., Blacker D., Hyman B. and Stern Y. (2008) Distinct pools of beta-amyloid in alzheimer disease-affected brain: A clinicopathologic study. *Arch. Neurol.*, **65**, 906-912.

Stiess M. and Bradke F. (2010) Neuronal polarization: The cytoskeleton leads the way. *Dev. Neurobiol.*, .

Strittmatter W.J. and Roses A.D. (1996) Apolipoprotein E and alzheimer's disease. *Annu. Rev. Neurosci.*, **19**, 53-77.

Suh S.W., Jensen K.B., Jensen M.S., Silva D.S., Kesslak P.J., Danscher G. and Frederickson C.J. (2000) Histochemically-reactive zinc in amyloid plaques, angiopathy, and degenerating neurons of alzheimer's diseased brains. *Brain Res.*, **852**, 274-278.

Supnet C., Noonan C., Richard K., Bradley J. and Mayne M. (2010) Up-regulation of the type 3 ryanodine receptor is neuroprotective in the TgCRND8 mouse model of alzheimer's disease. *J. Neurochem.*, **112**, 356-365.

Svennerholm L., Bostrom K. and Jungbjer B. (1997) Changes in weight and compositions of major membrane components of human brain during the span of adult human life of swedes. *Acta Neuropathol.*, **94**, 345-352.

Szafran K., Faron-Gorecka A., Kolasa M., Kusmider M., Solich J., Zurawek D. and Dziedzicka-Wasylewska M. (2013) Potential role of G protein-coupled receptor (GPCR) heterodimerization in neuropsychiatric disorders: A focus on depression. *Pharmacol. Rep.*, **65**, 1498-1505.

Tabuchi A., Sakaya H., Kisukeda T., Fushiki H. and Tsuda M. (2002) Involvement of an upstream stimulatory factor as well as cAMP-responsive element-binding protein in the activation of brain-derived neurotrophic factor gene promoter I. *J. Biol. Chem.*, **277**, 35920-35931.

Taheri S., Mahmoodi M., Opacka-Juffry J., Ghatei M.A. and Bloom S.R. (1999) Distribution and quantification of immunoreactive orexin A in rat tissues. *FEBS Lett.*, **457**, 157-161.

Takami M., Nagashima Y., Sano Y., Ishihara S., Morishima-Kawashima M., Funamoto S. and Ihara Y. (2009) Gamma-secretase: Successive tripeptide and tetrapeptide release from the transmembrane domain of beta-carboxyl terminal fragment. *J. Neurosci.*, **29**, 13042-13052.

Takayasu S., Sakurai T., Iwasaki S., Teranishi H., Yamanaka A., Williams S.C., Iguchi H., Kawasawa Y.I., Ikeda Y., Sakakibara I. *et al.* (2006) A neuropeptide ligand of the G protein-coupled receptor GPR103 regulates feeding, behavioral arousal, and blood pressure in mice. *Proc. Natl. Acad. Sci. U. S. A.*, **103**, 7438-7443.

Tandon A. and Fraser P. (2002) The presenilins. *Genome Biol.*, **3**, reviews3014.

Tang J., Chen J., Ramanjaneya M., Punn A., Conner A.C. and Randeva H.S. (2008) The signalling profile of recombinant human orexin-2 receptor. *Cell. Signal.*, **20**, 1651-1661.

Taussig R., Iniguez-Lluhi J.A. and Gilman A.G. (1993) Inhibition of adenylyl cyclase by gi alpha. *Science*, **261**, 218-221.

Terao A., Apte-Deshpande A., Morairty S., Freund Y.R. and Kilduff T.S. (2002) Age-related decline in hypocretin (orexin) receptor 2 messenger RNA levels in the mouse brain. *Neurosci. Lett.*, **332**, 190-194.

Thapa N. and Anderson R.A. (2012) PIP2 signaling, an integrator of cell polarity and vesicle trafficking in directionally migrating cells. *Cell. Adh Migr.*, **6**, 409-412.

Tharp W.G. and Sarkar I.N. (2013) Origins of amyloid-beta. *BMC Genomics*, **14**, 290-2164-14-290.

Thilakawardhana S., Everett D.M., Murdock P.R., Dingwall C. and Owen J.S. (2005) Quantification of apolipoprotein E receptors in human brain-derived cell lines by real-time polymerase chain reaction. *Neurobiol. Aging*, **26**, 813-823.

Thinakaran G., Borchelt D.R., Lee M.K., Slunt H.H., Spitzer L., Kim G., Ratovitsky T., Davenport F., Nordstedt C., Seeger M. *et al.* (1996) Endoproteolysis of presenilin 1 and accumulation of processed derivatives in vivo. *Neuron*, **17**, 181-190.

Thomas S.K., Messam C.A., Spengler B.A., Biedler J.L. and Ross R.A. (2004) Nestin is a potential mediator of malignancy in human neuroblastoma cells. *J. Biol. Chem.*, **279**, 27994-27999.

Thomas S.M., Hartley C.L. and Mason H.J. (1991) Effects of neurotoxins on neurone-specific enolase and lactate dehydrogenase activity and leakage in neuroblastoma cells. *Toxicol. In. Vitro.*, **5**, 439-442.

Ting J.T., Kelley B.G., Lambert T.J., Cook D.G. and Sullivan J.M. (2007) Amyloid precursor protein overexpression depresses excitatory transmission through both presynaptic and postsynaptic mechanisms. *Proc. Natl. Acad. Sci. U. S. A.*, **104**, 353-358.

Togo T., Katsuse O. and Iseki E. (2004) Nitric oxide pathways in alzheimer's disease and other neurodegenerative dementias. *Neurol. Res.*, **26**, 563-566.

Trivedi P., Yu H., MacNeil D.J., Van der Ploeg L.H. and Guan X.M. (1998) Distribution of orexin receptor mRNA in the rat brain. *FEBS Lett.,* **438**, 71-75.

Tsujino N. and Sakurai T. (2009) Orexin/hypocretin: A neuropeptide at the interface of sleep, energy homeostasis, and reward system. *Pharmacol. Rev.,* **61**, 162-176.

Tsuneki H., Wada T. and Sasaoka T. (2012) Role of orexin in the central regulation of glucose and energy homeostasis. *Endocr. J.,* **59**, 365-374.

Tucker J.B., Mathews S.A., Hendry K.A., Mackie J.B. and Roche D.L. (1985) Spindle microtubule differentiation and deployment during micronuclear mitosis in paramecium. *J. Cell Biol.,* **101**, 1966-1976.

Tumilowicz J.J., Nichols W.W., Cholon J.J. and Greene A.E. (1970) Definition of a continuous human cell line derived from neuroblastoma. *Cancer Res.,* **30**, 2110-2118.

Ukena K., Vaudry H., Leprince J. and Tsutsui K. (2011) Molecular evolution and functional characterization of the orexigenic peptide 26RFa and its receptor in vertebrates. *Cell Tissue Res.,* **343**, 475-481.

van Blitterswijk W.J. and Houssa B. (2000) Properties and functions of diacylglycerol kinases. *Cell. Signal.,* **12**, 595-605.

Van Den Pol A.N., Patrylo P.R., Ghosh P.K. and Gao X.B. (2001) Lateral hypothalamus: Early developmental expression and response to hypocretin (orexin). *J. Comp. Neurol.,* **433**, 349-363.

van Marum R.J. (2009) Update on the use of memantine in alzheimer's disease. *Neuropsychiatr. Dis. Treat.,* **5**, 237-247.

van Someren E.J., Hagebeuk E.E., Lijzenga C., Scheltens P., de Rooij S.E., Jonker C., Pot A.M., Mirmiran M. and Swaab D.F. (1996) Circadian rest-activity rhythm disturbances in alzheimer's disease. *Biol. Psychiatry,* **40**, 259-270.

Vereecke L., Beyaert R. and van Loo G. (2009) The ubiquitin-editing enzyme A20 (TNFAIP3) is a central regulator of immunopathology. *Trends Immunol.,* **30**, 383-391.

Verhaeghen P. and Cerella J. (2002) Aging, executive control, and attention: A review of meta-analyses. *Neurosci. Biobehav. Rev.,* **26**, 849-857.

Vijayan S., El-Akkad E., Grundke-Iqbal I. and Iqbal K. (2001) A pool of beta-tubulin is hyperphosphorylated at serine residues in alzheimer disease brain. *FEBS Lett.,* **509**, 375-381.

Vina J., Borras C. and Miquel J. (2007) Theories of ageing. *IUBMB Life,* **59**, 249-254.

Volkoff H. and Peter R.E. (2001) Interactions between orexin A, NPY and galanin in the control of food intake of the goldfish, carassius auratus. *Regul. Pept.,* **101**, 59-72.

von Heijne G. (1986) A new method for predicting signal sequence cleavage sites. *Nucleic Acids Res.,* **14**, 4683-4690.

Walker E.S., Martinez M., Brunkan A.L. and Goate A. (2005) Presenilin 2 familial alzheimer's disease mutations result in partial loss of function and dramatic changes in abeta 42/40 ratios. *J. Neurochem.,* **92**, 294-301.

Wang C., Pan Y., Zhang R., Bai B., Chen J. and Randeva H.S. (2013) Heterodimerization of mouse orexin type 2 receptor variants and the effects on signal transduction. *Biochim. Biophys. Acta*, **1843**, 652-663.

Wang J., Dickson D.W., Trojanowski J.Q. and Lee V.M. (1999) The levels of soluble versus insoluble brain abeta distinguish alzheimer's disease from normal and pathologic aging. *Exp. Neurol.,* **158**, 328-337.

Wang J., Tanila H., Puolivali J., Kadish I. and van Groen T. (2003) Gender differences in the amount and deposition of amyloidbeta in APPswe and PS1 double transgenic mice. *Neurobiol. Dis.,* **14**, 318-327.

Wenzel J., Grabinski N., Knopp C.A., Dendorfer A., Ramanjaneya M., Randeva H.S., Ehrhart-Bornstein M., Dominiak P. and Johren O. (2009) Hypocretin/orexin increases the expression of steroidogenic enzymes in human adrenocortical NCI H295R cells. *Am. J. Physiol. Regul. Integr. Comp. Physiol.,* **297**, R1601-9.

Wess J. (1997) G-protein-coupled receptors: Molecular mechanisms involved in receptor activation and selectivity of G-protein recognition. *FASEB J.,* **11**, 346-354.

Wettschureck N. and Offermanns S. (2005) Mammalian G proteins and their cell type specific functions. *Physiol. Rev.,* **85**, 1159-1204.

Whitehouse P.J., Price D.L., Struble R.G., Clark A.W., Coyle J.T. and Delon M.R. (1982) Alzheimer's disease and senile dementia: Loss of neurons in the basal forebrain. *Science*, **215**, 1237-1239.

Wilhelmsen K.C., Lynch T., Pavlou E., Higgins M. and Nygaard T.G. (1994) Localization of disinhibition-dementia-parkinsonism-amyotrophy complex to 17q21-22. *Am. J. Hum. Genet.,* **55**, 1159-1165.

Willie J.T., Chemelli R.M., Sinton C.M., Tokita S., Williams S.C., Kisanuki Y.Y., Marcus J.N., Lee C., Elmquist J.K., Kohlmeier K.A. *et al.* (2003) Distinct narcolepsy syndromes in orexin receptor-2 and orexin null mice: Molecular genetic dissection of non-REM and REM sleep regulatory processes. *Neuron,* **38**, 715-730.

Willie J.T., Chemelli R.M., Sinton C.M. and Yanagisawa M. (2001) To eat or to sleep? orexin in the regulation of feeding and wakefulness. *Annu. Rev. Neurosci.,* **24**, 429-458.

Winblad B., Engedal K., Soininen H., Verhey F., Waldemar G., Wimo A., Wetterholm A.L., Zhang R., Haglund A., Subbiah P. *et al.* (2001) A 1-year, randomized, placebo-controlled study of donepezil in patients with mild to moderate AD. *Neurology,* **57**, 489-495.

Xavier G.F. and Costa V.C. (2009) Dentate gyrus and spatial behaviour. *Prog. Neuropsychopharmacol. Biol. Psychiatry,* **33**, 762-773.

Xia Z., Dickens M., Raingeaud J., Davis R.J. and Greenberg M.E. (1995) Opposing effects of ERK and JNK-p38 MAP kinases on apoptosis. *Science,* **270**, 1326-1331.

Xie H.R., Hu L.S. and Li G.Y. (2010) SH-SY5Y human neuroblastoma cell line: In vitro cell model of dopaminergic neurons in parkinson's disease. *Chin. Med. J. (Engl),* **123**, 1086-1092.

Xu T.R., Ward R.J., Pediani J.D. and Milligan G. (2011) The orexin OX(1) receptor exists predominantly as a homodimer in the basal state: Potential regulation of receptor organization by both agonist and antagonist ligands. *Biochem. J.,* **439**, 171-183.

Yagishita S., Futai E. and Ishiura S. (2008) In vitro reconstitution of gamma-secretase activity using yeast microsomes. *Biochem. Biophys. Res. Commun.,* **377**, 141-145.

Yamada N., Katsuura G., Tatsuno I., Kawahara S., Ebihara K., Saito Y. and Nakao K. (2009) Orexins increase mRNA expressions of neurotrophin-3 in rat primary cortical neuron cultures. *Neurosci. Lett.,* **450**, 132-135.

Yamamoto T., Miyazaki R. and Yamada T. (2009) Intracerebroventricular administration of 26RFa produces an analgesic effect in the rat formalin test. *Peptides,* **30**, 1683-1688.

Yamanaka A., Beuckmann C.T., Willie J.T., Hara J., Tsujino N., Mieda M., Tominaga M., Yagami K., Sugiyama F., Goto K. *et al.* (2003) Hypothalamic orexin neurons regulate arousal according to energy balance in mice. *Neuron,* **38**, 701-713.

Yamanaka A., Tsujino N., Funahashi H., Honda K., Guan J.L., Wang Q.P., Tominaga M., Goto K., Shioda S. and Sakurai T. (2002) Orexins activate histaminergic neurons via the orexin 2 receptor. *Biochem. Biophys. Res. Commun.,* **290**, 1237-1245.

Yan J.A., Ge L., Huang W., Song B., Chen X.W. and Yu Z.P. (2008) Orexin affects dorsal root ganglion neurons: A mechanism for regulating the spinal nociceptive processing. *Physiol. Res.,* **57**, 797-800.

Yan S.D., Chen X., Fu J., Chen M., Zhu H., Roher A., Slattery T., Zhao L., Nagashima M., Morser J. *et al.* (1996) RAGE and amyloid-beta peptide neurotoxicity in alzheimer's disease. *Nature,* **382**, 685-691.

Yang B. and Ferguson A.V. (2002) Orexin-A depolarizes dissociated rat area postrema neurons through activation of a nonselective cationic conductance. *J. Neurosci.,* **22**, 6303-6308.

Yang S.N., Hsieh W.Y., Liu D.D., Tsai L.M., Tung C.S. and Wu J.N. (1998) The involvement of nitric oxide in synergistic neuronal damage induced by beta-amyloid peptide and glutamate in primary rat cortical neurons. *Chin. J. Physiol.*, **41**, 175-179.

Yano M., Toyooka S., Tsukuda K., Dote H., Ouchida M., Hanabata T., Aoe M., Date H., Gazdar A.F. and Shimizu N. (2005) Aberrant promoter methylation of human DAB2 interactive protein (hDAB2IP) gene in lung cancers. *Int. J. Cancer,* **113**, 59-66.

Yonemura Y., Futai E., Yagishita S., Suo S., Tomita T., Iwatsubo T. and Ishiura S. (2011) Comparison of presenilin 1 and presenilin 2 gamma-secretase activities using a yeast reconstitution system. *J. Biol. Chem.*, **286**, 44569-44575.

Yuan L.B., Dong H.L., Zhang H.P., Zhao R.N., Gong G., Chen X.M., Zhang L.N. and Xiong L. (2011) Neuroprotective effect of orexin-A is mediated by an increase of hypoxia-inducible factor-1 activity in rat. *Anesthesiology,* **114**, 340-354.

Zamzow D.R., Elias V., Shumaker M., Larson C. and Magnusson K.R. (2013) An increase in the association of GluN2B containing NMDA receptors with membrane scaffolding proteins was related to memory declines during aging. *J. Neurosci.,* **33**, 12300-12305.

Zandi P.P., Anthony J.C., Khachaturian A.S., Stone S.V., Gustafson D., Tschanz J.T., Norton M.C., Welsh-Bohmer K.A., Breitner J.C. and Cache County Study Group (2004) Reduced risk of alzheimer disease in users of antioxidant vitamin supplements: The cache county study. *Arch. Neurol.,* **61**, 82-88.

Zawilska J.B., Urbanska A. and Sokolowska P. (2013) Orexins/hypocretins stimulate accumulation of inositol phosphate in primary cultures of rat cortical neurons. *Pharmacol. Rep.,* **65**, 513-516.

Zhang B., Maiti A., Shively S., Lakhani F., McDonald-Jones G., Bruce J., Lee E.B., Xie S.X., Joyce S., Li C. *et al.* (2005) Microtubule-binding drugs offset tau sequestration by stabilizing microtubules and reversing fast axonal transport deficits in a tauopathy model. *Proc. Natl. Acad. Sci. U. S. A.,* **102**, 227-231.

Zhang Q., Qiu P., Arreaza M.G., Simon J.S., Golovko A., Laverty M., Vassileva G., Gustafson E.L., Rojas-Triana A., Bober L.A. *et al.* (2007) P518/Qrfp sequence polymorphisms in SAMP6 osteopenic mouse. *Genomics,* **90**, 629-635.

Zhang Y.W., Luo W.J., Wang H., Lin P., Vetrivel K.S., Liao F., Li F., Wong P.C., Farquhar M.G., Thinakaran G. *et al.* (2005) Nicastrin is critical for stability and trafficking but not association of other presenilin/gamma-secretase components. *J. Biol. Chem.*, **280**, 17020-17026.

Zhang Z., Yan J., Chang Y., ShiDu Yan S. and Shi H. (2011) Hypoxia inducible factor-1 as a target for neurodegenerative diseases. *Curr. Med. Chem.*, **18**, 4335-4343.

Zhen G., Kim Y.T., Li R.C., Yocum J., Kapoor N., Langer J., Dobrowolski P., Maruyama T., Narumiya S. and Dore S. (2012) PGE2 EP1 receptor exacerbated neurotoxicity in a mouse model of cerebral ischemia and alzheimer's disease. *Neurobiol. Aging*, **33**, 2215-2219.

Zhong Y., Yao H., Deng L., Cheng Y. and Zhou X. (2007) Promotion of neurite outgrowth and protective effect of erythropoietin on the retinal neurons of rats. *Graefes Arch. Clin. Exp. Ophthalmol.*, **245**, 1859-1867.

Zhu Y., Miwa Y., Yamanaka A., Yada T., Shibahara M., Abe Y., Sakurai T. and Goto K. (2003) Orexin receptor type-1 couples exclusively to pertussis toxin-insensitive G-proteins, while orexin receptor type-2 couples to both pertussis toxin-sensitive and -insensitive G-proteins. *J. Pharmacol. Sci.*, **92**, 259-266.

Ziello J.E., Jovin I.S. and Huang Y. (2007) Hypoxia-inducible factor (HIF)-1 regulatory pathway and its potential for therapeutic intervention in malignancy and ischemia. *Yale J. Biol. Med.*, **80**, 51-60.

Zilka N. and Novak M. (2006) The tangled story of alois alzheimer. *Bratisl. Lek. Listy*, **107**, 343-345.

Zink D., Sadoni N. and Stelzer E. (2003) Visualizing chromatin and chromosomes in living cells. *Methods*, **29**, 42-50.